UNIVERSIDADE FEDERAL DE MINAS GERAIS
Instituto de Ciências Biológicas
Programa de Pós-Graduação em Zoologia

Caroline Batistim Oswald

Diversificação de Anuros Endêmicos da Porção Mineira da Serra do Espinhaço

Belo Horizonte
2021

Caroline Batistim Oswald

Diversificação de Anuros Endêmicos da Porção Mineira da Serra do Espinhaço

Versão final

Tese apresentada ao programa de Pós-Graduação em Zoologia da Universidade Federal de Minas Gerais, como requisito parcial à obtenção do título de Doutora em Zoologia.

Orientador: Prof. Dr. Rafael F. de Magalhães
Coorientador: Prof. Dr. Paulo C. de A. Garcia

Belo Horizonte
2021

043 Oswald, Caroline Batistim.
Diversificação de anuros endêmicos da porção mineira da Serra do Espinhaço [manuscrito] / Caroline Batistim Oswald. – 2021.
268 f. : il. ; 29,5 cm.

Orientador: Prof. Dr. Rafael Félix de Magalhães. Coorientador: Prof. Dr. Paulo Cristiano de Anchietta Garcia.
Tese (doutorado) – Universidade Federal de Minas Gerais, Instituto de Ciências Biológicas. Programa de Pós-Graduação em Zoologia.

1. Zoologia. 2. Filogeografia. 3. Evolução Biológica. 4. Anfíbios. 5. Anuros. I. Magalhães, Rafael Félix de. II. Garcia, Paulo Cristiano de Anchietta. III. Universidade Federal de Minas Gerais. Instituto de Ciências Biológicas. IV. Título.

CDU: 591

Ficha catalografica elaborada pela bibliotecária Fabiane C. M. Reis – CRB: 6/2680

UNIVERSIDADE FEDERAL DE MINAS GERAIS
INSTITUTO DE CIÊNCIAS BIOLÓGICAS
PÓS-GRADUAÇÃO EM ZOOLOGIA

FOLHA DE APROVAÇÃO DE TESE

DIVERSIFICAÇÃO DE ANUROS ENDÊMICOS DA PORÇÃO MINEIRA DA SERRA DO ESPINHAÇO

CAROLINE BATISTIM OSWALD

Esta tese foi apresentada em sessão pública e submetida a avaliação em 30 de novembro de 2021, sendo aprovada pela Banca Examinadora composta pelos seguintes membros:

Prof. Dr. Arley Camargo Bentaberry (Membro / Universidad de La Republica)

Profa. Dra. Cecília Fonseca Fiorini (Membro / UFMG)

Profa. Dra. Fernanda de Pinho Werneck (Membro / INPA)

Prof. Dr. Fernando Augusto de Oliveira e Silveira (Membro / UFMG)

Prof. Dr. Rafael Félix de Magalhães (Orientador / UFSJ)

Belo Horizonte, 30 de novembro de 2021

Documento assinado eletronicamente por **Arley Camargo Bentaberry**, **Usuário Externo**, em 03/12/2021, às 11:55, conforme horário oficial de Brasília, com fundamento no art. 5º do Decreto nº 10.543, de 13 de novembro de 2020.

Documento assinado eletronicamente por **Fernanda de Pinho Werneck**, **Usuário Externo**, em 03/12/2021, às 17:03, conforme horário oficial de Brasília, com fundamento no art. 5º do Decreto nº 10.543, de 13 de novembro de 2020.

Documento assinado eletronicamente por **Rafael Félix de Magalhães**, **Usuário Externo**, em 06/12/2021, às 10:10, conforme horário oficial de Brasília, com fundamento no art. 5º do Decreto nº 10.543, de 13 de novembro de 2020.

Documento assinado eletronicamente por **Fernando Augusto de Oliveira e Silveira**, **Professor do Magistério Superior**, em 10/09/2022, às 05:46, conforme horário oficial de Brasília, com fundamento no art. 5º do Decreto nº 10.543, de 13 de novembro de 2020.

Documento assinado eletronicamente por **Cecilia Fonseca Fiorini**, **Usuário Externo**, em 16/09/2022, às 10:26, conforme horário oficial de Brasília, com fundamento no art. 5º do Decreto nº 10.543, de 13 de novembro de 2020.

A autenticidade deste documento pode ser conferida no site https://sei.ufmg.br/sei/controlador_externo.php?acao=documento_conferir&id_orgao_acesso_externo=0, informando o código verificador **1126026** e o código CRC **3EB3BFA9**.

Agradecimentos

Ao longo do doutorado diversas pessoas contribuíram tanto para o meu crescimento como pessoa e pesquisadora, quanto para o desenvolvimento da tese e não poderia deixar de agradecê-las.

Primeiramente, agradeço ao meu orientador Rafael Félix de Magalhães, por todas oportunidades e ensinamentos ao longo destes anos, incluindo a de desenvolver essa tese. Pela amizade, orientação e colaborações, por me apresentar e me fazer encantar com a Serra do Espinhaço e por sempre acreditar em mim.

Ao Paulo Garcia, pelo incentivo para ingressar no doutorado, por todas as conversas e por todo suporte ao longo deste tempo.

À minha família, por todo o apoio e compreensão, desde a decisão de seguir na academia, da escolha do objeto de estudo, e estar sempre presente mesmo longe fisicamente.

Ao André, pelo companheirismo e carinho por todos esses anos. Obrigada pelos tantos incentivos necessários e compreensão nesta reta final.

À Gisele, Rachel, Paula, Carla, Bárbara e Lica pelo acolhimento e amizade em um importante momento deste último ano. Por perceberam e ajudarem mesmo com minhas relutâncias.

Agradeço ao Grupo de Mulheres na Ciência do ICB/UFMG pelas conversas, apoio e amizade neste ano difícil para todos. A retomada dos encontros, mesmo que virtuais, foram essenciais para passar por esse isolamento.

Ao pessoal Laboratório de Herpetologia, Igor, Dani, Babi, Tiago, Brenda, Raíla, Dhara e Igor Brendo, pela agradável convivência, pelos ótimos momentos aglomerados em volta de uma cafeteira, enquanto isso foi possível.

Ao Laboratório de Biodiversidade e Evolução Molecular, principalmente ao professor Fabrício, pela infraestrutura, colaboração e por possibilitar atividades para o desenvolvimento da tese.

Às meninas do basquete da UFMG e da Biologia pela amizade, escape essencial e ótimas partidas.

A todo o corpo docente da Pós-Graduação em Zoologia pela hospitalidade e agradável convívio em todos esses anos que estou na UFMG, pelos conhecimentos científicos e técnicos, e pelas valiosas discussões.

Ao pessoal do canal Herpeto Sem Fronteiras, pelos assuntos e conhecimentos variados e enriquecedores, e principalmente por me fazerem enfrentar as câmeras e perder um pouco do medo envolvido nisso.

Ao Jean pela convivência, e por estar sempre pronto para ajudar com problemas computacionais, que não foram poucos ao longo do doutorado.

A todos os autores dos trabalhos desenvolvidos, pela colaboração, em especial à Priscila, Tetê e Marcelo pelas valiosas discussões e ao Felipe pelo convite para participar do capítulo de livro sobre o Espinhaço.

À banca examinadora desta tese, Dra. Cecília Fiorini, Dra. Fernanda de P. Werneck, Dr. Arley Camargo, Dr. Fernando A. O. Silveira e Dr. Almir R. Pepato, por aceitarem prontamente o convite para participar da defesa e por todas as considerações e avaliações, contribuindo para o enriquecimento dos trabalhos.

À Fundação de Amparo à Pesquisa do Estado de Minas Gerais (FAPEMIG) pelas bolsas no primeiro ano de doutorado e pelo financiamento de projetos do grupo de pesquisa na Serra do Espinhaço; e à Coordenação de Aperfeiçoamento de Pessoal de Nível Superior (CAPES) pelas bolsas nos anos finais de doutorado.

Muito obrigada!

Resumo

Fatores bióticos e abióticos, e suas interações, desempenham um papel importante na formação da história evolutiva das espécies, bem como nos padrões de distribuição e composição da diversidade em uma determinada área. A filogeografia é uma disciplina importante para auxiliar na reconstrução da história evolutiva de um grupo taxonômico no espaço e tempo. Apesar dos grandes esforços para conhecer os anuros da Serra do Espinhaço, muitas questões relacionadas aos padrões de riqueza, composição, endemismo, aspectos biológicos e processos envolvidos na diversificação ainda permanecem sem resposta. Assim, esta tese teve como objetivos apresentar uma atualização do conhecimento sobre os anuros endêmicos da Serra do Espinhaço, e investigar a distribuição genética na paisagem em diferentes escalas, à nível intraespecífico e de uma assembleia de anuros endêmicos. A maior riqueza de endemismos da Serra do Espinhaço está concentrada no sul da Serra do Espinhaço em Minas Gerais, ao longo da Serra do Cipó. Girinos e vocalizações são conhecidos para a maioria das espécies endêmicas da Serra do Espinhaço, bem como o relacionamento filogenético destas com espécies congêneres. Entretanto, dados de comportamento e história natural são escassos para a maioria delas. Muitos dos estudos são incipientes, revelando a necessidade e oportunidades para futuras investigações científicas, como estudos sobre os efeitos de gradientes ambientais e adaptações das espécies endêmicas às condições ambientais do campo rupestre. Diferentes processos como hibridização, colonização, e fragmentação impactaram a evolução de biota da Serra do Espinhaço, e flutuações climáticas passadas parecem ter sido importantes para a diversificação e distribuição das espécies endêmicas. A história evolutiva da Serra do Espinhaço é complexa, e precisamos considerar a multiplicidade de processos e fatores associados a diversificação de biota. Novos estudos filogeográficos com a inclusão de dados nucleares, novas espécies endêmicas da Serra do Espinhaço e dados sobre a biologia das espécies bem como dados do ambiente, analisados sob a ótica da filogeografia comparativa, podem nos ajudar a entender melhor os diferentes pulsos de diversificação ocorrentes na Serra do Espinhaço ao longo do tempo.

Palavras-chave: Campo rupestre, filogeografia, evolução, anfíbios, delimitação de espécie

Abstract

Biotic and abiotic factors, and their interactions, play an important role in shaping the evolutionary history of species, as well as in patterns of distribution and composition of diversity in an area. Phylogeography is an important discipline to assist in the reconstruction of the evolutionary history of a taxonomic group in space and time. Despite the great efforts to know the anurans of Serra do Espinhaço, many questions related to patterns of richness, composition, endemism, biological aspects, and processes involved in diversification still remain unanswered. Thus, this thesis aimed to present an update of the knowledge about the endemic frogs of Serra do Espinhaço, and to investigate the genetic distribution in the landscape at different scales, at the intraspecific level and in an assemblage of endemic frogs. The greatest wealth of endemisms in Serra do Espinhaço is concentrated in the south of Serra do Espinhaço in Minas Gerais, along the Serra do Cipó. Tadpoles and vocalizations are well known for most endemic species of Serra do Espinhaço, as well as their phylogenetic relationship with congener species. However, behavioral and natural history data are scarce for most of them. Many of the studies are incipient, revealing the need and opportunities for future scientific investigations, such as studies on the effects of environmental gradients and adaptations of endemic species to the environmental conditions of the rupestrian field. Different processes such as hybridization, colonization, and fragmentation impacted the evolution of the Serra do Espinhaço biota, and past climatic fluctuations seem to have been important for the diversification and distribution of endemic species. The evolutionary history of Serra do Espinhaço is complex, and we need to consider the multiplicity of processes and factors associated with biota diversification. New phylogeographic studies with the inclusion of nuclear data, other endemic species to Serra do Espinhaço, biology data of species as well as environmental data, analyzed from the perspective of comparative phylogeography, can help us to better understand the different pulses of diversification that occur in Serra do Espinhaço over time.

Keywords: *Campo rupestre*, phylogeography, evolution, amphibians, species delimitation

Lista de Figuras

<u>Capítulo1:</u> Status do Conhecimento Sobre os Anfíbios Anuros Endêmicos da Serra do Espinhaço

Figura 1. Mapa da Serra do Espinhaço e as diferentes regiões considerando-se assembleias de anuros endêmicos: Chapada Diamantina ao norte delimitada em azul, Espinhaço Mineiro ao centro delimitado de vermelho, e Quadrilátero Ferrífero ao sul delimitado de verde. 1 = Depressão Couto de Magalhães; 2 = Serra do Cabral. Altitudes a cima de 800 m em cinza escuro 28

Figura 2. Ambiente de reprodução de anuros no Quadrilátero Ferrífero (A); Macho (B), Fêmea (C) e girino (D) de *Bokermannohyla martinsi*. Fotos: A - Lucas Perillo; B, C, D - Tiago L. Pezzuti 29

Figura 3. Paisagem no Espinhaço Mineiro, ao norte de Minas Gerais (A); *Pleurodema alium* (B); Adulto (C) e girino (D) de *Bokermannohyla alvarengai*. Fotos: Tiago L. Pezzuti . 33

Figura 4. Paisagem na Serra do Cabral, Minas Gerais (A); *Bokermannohyla saxicola* (B); *Scinax cabralensis* (C); e *Thoropa megatympanum* (D). Fotos: Tiago L. Pezzuti 34

Figura 5. Paisagem na Chapada Diamantina, Bahia (A); *Pristimantis rupicola* (B); *Haddadus aramunha* (C); e *Rupirana cardosoi* (D). Fotos: A - Tiago L. Pezzuti; B, C, D - Leandro Drummond 35

Figura 6. Diagrama de Venn-Euler indicando a contagem de espécies endêmicas exclusivas e compartilhadas em cada porção da Serra do Espinhaço, no leste do Brasil. Os números centrais nos círculos indicam a contagem de espécies exclusivas de cada área (CD = Chapada Diamantina (azul), EM = Espinhaço Mineiro (vermelho), QFe = Quadrilátero Ferrífero (verde)) e os números nas interseções indicam a contagem de espécies endêmicas compartilhadas por cada região delimitada 39

Figura 7. Mapa de endemismo de anuros na Serra do Espinhaço em quadriculas de 0.3° x 0.3°, baseado nos pontos de ocorrência das espécies. Altitudes a cima de 850 m em cinza escuro 40

Figura 8. Ambiente de reprodução de anuros em Itacambira/MG, no Espinhaço Mineiro (A); *Scinax curicica* (B); Adulto (C) e girino (D) de *Pithecopus megacephalus*. Fotos: Tiago L. Pezzuti 43

Figura 9. Ambiente de reprodução na Chapada Diamantina, Bahia (A); *Bokermannohyla flavopicta* (B); *B. itapoty* (C); desova de *Bokermannohyla*. Fotos: A, B: Leandro Drummond; C, D: Tiago L. Pezzuti 51

<u>Capítulo 2:</u> Colonization rather than fragmentation explains the geographic distribution and diversification of treefrogs endemic to Brazilian shield sky islands

Figure 1 (a) View of the Serra Azul in Serranópolis de Minas (location 3), showing the contrast between lowland (seasonal semideciduous forest) and high-altitude environments (campo rupestre); (b) Map of Brazilian Shield highlands and its location in South America (inset), with Espinhaço Mineiro (EM) highlighted and enlarged in (c). Espinhaço Baiano (EB) is the upland region north of EM, outside the red box; (c) Localities of Bokermannohyla saxicola in EM, including records of genetic and morphometric data. Coloured circles correspond to delimited lineages (yellow = Northern, blue = Central, green = Southern, red = Cabral; see Section 3), and numbers correspond to locations, from north to south: (1) Santo Antônio do Retiro; (2) Rio Pardo de Minas; (3) Serranópolis de Minas; (4) Padre Carvalho; (5) Grão Mogol; (6) Itacambira; (7) Botumirim; (8) Turmalina; (9) Buenópolis (Parque Nacional das Sempre Vivas); (10) Diamantina; (11) São Gonçalo do Rio Preto; (12) Rio Vermelho; (13) Itamarandiba; (14) Serra Azul de Minas; (15) Santo Antônio do Itambé; (16) Augusto de Lima (Águas de Santa Bárbara); (17) Presidente Kubitschek; (18) Serro; (19) Santana de Pirapama; (20) Alvorada de Minas; (21) Congonhas do Norte; (22) Conceição do Mato Dentro; (23) Santana do Riacho; (24) Morro do Pilar; (25) São Sebastião do Rio Preto; (26) Barão de Cocais; (27) Santa Bárbara; (28) Francisco Dumont; (29) Joaquim Felício; (30) Buenópolis; (31) Lassance; (32) Augusto de Lima. Region denominated as Diamantina plateau correspond to the locations (9–11) and (14–18), Quadrilátero Ferrífero to (26–27), and Serra do Cabral to (28–32). For details on georeferenced sampling points, see Table S1 89

Figure 2 Evolutionary scenarios tested using DIYABC for *Bokermannohyla saxicola* in Espinhaço Range. Vicariance process: (1) Constant populations size over time, (2) Southern lineage expansion and (3) Southern linage stable and other retraction; Diffusion: (4) Constant populations size over time, (5) Southern expansion and other stable, (6) Southern lineage stable and other retraction; and (7) Jump dispersal. We assumed one first ancestral population not sampled, with effective size Na, in black in all scenarios. Time and effective population size in scenarios are not in scale 90

Figure 3 Multiple lineages and time framework of *Bokermannohyla saxicola* in the Espinhaço Range. The same colours represent the observed lineages. (a) Q-plot at K = 4, showing each individual as a bar and membership probabilities as different colours; (b) Multilocus nuclear Neighbor-net representation. Scale bar represents standardized genetic distances for the net. Different shades of green represent the two subclades found by Nascimento et al. (2018) and GMYC. Adult and tadpole photographs by Tiago Leite Pezzuti. The photographs do not respect real proportion and were taken from Cabral lineages; (c) Left: Time-calibrated species tree. Node bars correspond to the 95% High Posterior Density (HPD) time. Values on branches correspond to posterior probabilities above and average time in million years below. Right: Distribution range of each lineage in the Espinhaço Range.....91

Figure 4 Distribution models for *Bokermannohyla saxicola* that represent the relative climatic suitability areas over time. The map of stability areas represents the sum of maps in all periods for *B. saxicola*. The colour scales represent the suitability or stability for the maps, from areas with low (0) to high (1) values. The grey shape represents the limits modified from Fernandes et al. (2014) of the campo rupestre, the predominant ecosystem in Espinhaço Range. The time slice abbreviations correspond to: BA, abrupt warming at the onset of the BøllingAllerød; EH, early-Holocene; HS1, Heinrich Event 1; LGM, Last Glacial Maximum; LH, late-Holocene; LIG, Last Interglacial past; M2, Marine Isotope Stage in the late Pliocene; MH, mid-Holocene; MIS19, Marine Isotope Stage in the Pleistocene; mPWP, mid-Pliocene Warm Period; YD, rapid cooling at the onset of the Younger Dryas 92

Figure 5 (a)–(d) Snapshots of the spatial–temporal dynamics of *Bokermannohyla saxicola* in Espinhaço Range. Circles R, 1 and 2 represent the estimated root location and subsequent cladogenetic events, respectively. Grey polygons represent 80% Highest Posterior Density (HPD) interval of uncertainty in the location of ancestral branches. Coloured polygons represent the current distribution of distinct lineages; (e) Diffusion rate through time. The grey shape represents the limits modified from Fernandes et al. (2014) of the campo rupestre, the predominant ecosystem in the Espinhaço Range.....93

<u>Capítulo 3:</u> Comparative Phylogeography of anurans endemic to Espinhaço Mountain Range, the second largest mountain range in Neotropics

Fig 1 Mitochondrial trees, on the bottom left, sampled anurans photographs on the top left, and the minimum convex polygon of the distribution of each population, on the right, for a) *Bokermannohyla alvarengai*; b) *Bokermannohyla saxicola*; c) *Leptodactylus camaquara*; d) *Pithecopus megacephalus*; e) *Scinax curicica*; and f) *Thoropa megatympanum*. * on branches correspond to posterior probability higher than 0.90 and ** higher than 0.95. Blue represents the northern population and pink southern population in all species. Yellow represents the far north population of *Bokermannohyla saxicola*, and green represent Cabral populations in *B. saxicola*, and *P. megacephalus*, *T. megatympanum*. The terminals of the mtDNA tree were collapsed through the cartoon option in FigTree v. 1.4.4 (Rambaut, 2018) and the minimum convex polygon was drawn from sampling coordinates in QGis v. 3.20.3 (QGIS Development Team, 2021). Photographs: a, c-f: Tiago L. Pezzuti; b: André Yves 122

Fig 2 Illustrated dataset of endemic species sampled of Espinhaço Range; a) *Bokermannohyla alvarengai*; b) *Bokermannohyla saxicola*; c) *Leptodactylus camaquara*; d) *Pithecopus megacephalus*; e) *Scinax curicica*; and f) *Thoropa megatympanum*; g) Map of Brazilian Shield highlands and its location in South America (inset), with Espinhaço Mineiro and Quadrilátero Ferrífero highlighted and enlarged in (h); h) Phylogeographic barriers found in each species. Numbers correspond to locations, 1: Itacambira and 2: Botumirim. The colors surrounding the photographs match the barriers in the large map (h). Photographs: a, c-f: Tiago L. Pezzuti; b: André Yves 123

Fig 3 Mean and 95% HPD coalescence times (estimated in BEAST) between populations north and south of the central barrier. The geological time scale on the right corresponds to the y-axis time 124

Lista de Tabelas

<u>Capítulo1:</u> Status do Conhecimento Sobre os Anfíbios Anuros Endêmicos da Serra do Espinhaço

Tabela 1. Anuros endêmicos da Serra do Espinhaço. Distribuição: CD = Chapada Diamantina, EM = Espinhaço Mineiro, QFe = Quadrilátero Ferrífero; ambiente reprodutivo: R = afloramento rochoso, LA= lâmina d'água em rocha úmida, LP = lagoas, poças e brejos permanentes, RP = riachos permanentes, RT = riachos temporários, AT = alagadiços rasos temporários, LT = lagoas, poças e brejos temporários, BR = bromélias); e modo reprodutivo (*sensu* Haddad & Prado, 2005): ? = desconhecido, 1 = ovos e girinos exotróficos em corpos d'água lênticos, 2 = ovos e girinos exotróficos em corpos d'água lóticos, 3 = ovos e estágios larvais iniciais em câmaras subaquáticas construídas; girinos exotróficos em riachos, 4 = ovos e estágios larvais iniciais em bacias naturais ou construídas; após a inundação, girinos exotróficos em lagoas ou riachos, 5 = ovos e estágios larvais iniciais em ninhos subterrâneos construídos; após a inundação, girinos exotróficos em lagoas ou riachos, 11 = ninho de espuma flutuando em poças; girinos exotróficos em poças. 19 = ovos em rochas úmidas; girinos exotróficos semiterrestres vivendo em lâmina de água, sobre rochas na interface água-terra, 21 = ovos eclodindo em girinos endotróficos que completam seu desenvolvimento no ninho, 25 = ovos eclodindo em girinos exotróficos que caem de folhas suspensas em corpos d'água lóticos, 26 = ovos eclodindo em girinos exotróficos que se desenvolvem em cavidades cheias de água em bromélias, 28 = ninho de espuma no solo úmido; após a inundação, girinos exotróficos em poças, 30 = ninho de espuma com ovos e estágios larvais iniciais em ninhos subterrâneos construídos; após a inundação, girinos exotróficos em poças. 36

Tabela 2. Espécies endêmicas, categorias de ameaça nas últimas avaliações da IUCN (2021) e Brasileira (MMA 2014), e ocorrência dentro de Unidades de Conservação de proteção integral. Categorias de ameaça: LC = Menos preocupante, NE = Não avaliada, NT = Quase ameaçada, EN = Em perigo, CR = Criticamente em perigo, DD = Dados deficientes. Unidades de Conservação: 1 – Parque Nacional (PARNA) da Serra do Gandarela, 2 – PARNA da Serra do Cipó, 3 – PARNA das Sempre-Vivas, 4 – PARNA da Chapada Diamantina; MG: 1 – Parque Estadual (PE) da Serra do Ouro Branco, 2 – Monumento Natural Estadual (MONA) do Itatiaia, 3 – PE do Itacolomi, 4 – Estação Ecológica (EE) do Tripuí, 5 – MONA da Serra da Moeda, 6 – EE de Arêdes, 7 – EE dos

Fechos, 8 – PE da Serra do Rola Moça, 9 – EE do Cercadinho, 10 – PE do Limoeiro, 11 – PE da Serra do Intendente, 12 – MONA da Várzea do Lageado, 13 – PE do Pico do Itambé, 14 – PE do Rio Preto, 15 – PE Biribiri, 16 – PE da Serra do Cabral, 17 – PE da Serra Negra, 18 – PE de Botumirim, 19 – EE de Acauã, 20 – PE de Grão Mogol, 21 – PE de Serra Nova e Talhado, 22 – PE de Montezuma, 23 - EE Mata dos Ausentes; BA: 24 – PE do Morro do Chapéu, 25 – PE das Sete Passagens, 26 – MONA da Cachoeira do Ferro Doido, 27 – PE Caminho das Gerais, 28 – PE da Serra dos Montes Altos.....52

Capítulo 2: Colonization rather than fragmentation explains the geographic distribution and diversification of treefrogs endemic to Brazilian shield sky islands

Table 1 Results of permutational multivariate analysis of variance (PERMANOVA) showing differences in morphometric data from lineages of *Bokermannohyla saxicola* in Espinhaço Range. *P < 0.05 in pairwise PERMANOVA 88

Capítulo 3: Comparative Phylogeography of anurans endemic to Espinhaço Mountain Range, the largest extra-Andean Mountain chain in South America

Table 1 – Species sampled, outgroup, mtDNA fragment, and the number of individuals sampled. COI = Citochrome oxidase, subunit I; Cyt-b = Citochrome B; 16S = Ribossomal gene encoding 16S rRNA.....120

Table 2 – Summary of the alternative models with $\Delta AIC \leq 2$ selection by PHRAPL. Values of Akaike Information Criterion (AIC); composite likelihood (lnL); the number of parameters of the model (params.K); the difference between AIC values of each model (ΔAIC); and Akaike Information Criterion weights (wAIC) of each taxon. Model numbers refer to the schematic models defined in Tale S2. 121

Sumário

Apresentação 18
Introdução geral 20
Referências 21
Capítulo 1 24
Status do Conhecimento Sobre os Anfíbios Anuros Endêmicos da Serra do Espinhaço 25
Introdução 26
Um breve histórico 30
Conhecimento taxonômico e padrões de distribuição 32
Ecologia, comportamento e história natural 41
Evolução e biogeografia 44
Conservação 48
Conclusão 54
Referências Bibliográficas 54
Capítulo 2 68
Introduction 70
Material and Methods 73
Results 81
Discussion 83
References 94
Capítulo 3 107
Comparative Phylogeography of anurans endemic to Espinhaço Mountain Range, the largest extra-Andean Mountain chain in South America 108
Introduction 109
Material and Methods 111
Results 116
Discussion 117
References 124
Considerações finais 133
Referências 134

Apêndice 135

I) Material Suplementar – Capítulo 2 135

a) Supporting information 135

b) Supplementary figures 141

c) Supplementary tables 147

II) Material Suplementar – Capítulo 3 223

a) Supplementary figures 223

b) Supplementary tables 231

Anexo 252

Evidence of introgression in endemic frogs from the *campo rupestre* contradicts the reduced hybridization hypothesis 253

Apresentação

Esta tese de doutorado compreende um trabalho desenvolvido na Pós-Graduação em Zoologia da Universidade Federal de Minas Gerais sob orientação do Professor Dr. Rafael Félix de Magalhães e coorientação do Professor Dr. Paulo Christiano de Anchietta Garcia. Ela é parte de projetos ainda em andamento na porção mineira da Serra do Espinhaço e a compilação destes resultados visa contribuir para o entendimento da dinâmica evolutiva da anurofauna endêmica da Serra do Espinhaço. Em vista do interesse econômico e importância biológica da Serra do Espinhaço (Fernandes et al., 2014; Silveira et al., 2016), é importante aumentarmos nossa compreensão sobre a dinâmica evolutiva de sua biota, pois essas informações podem ajudar futuramente na avaliação de áreas críticas para a conservação, na identificação de áreas de endemismo e de linhagens evolutivas únicas.

Para melhor apresentação do conteúdo, a tese seguiu o modelo de divisão em capítulos, correspondentes a artigos/trabalhos, que é atualmente aceito pelo programa de Pós-Graduação em Zoologia. Ela está organizada em cinco partes, consistindo em uma introdução geral bem como os objetivos da tese, três capítulos que correspondem à três trabalhos científicos gerados a partir dos resultados obtidos e ao final, uma seção com as considerações finais. A norma bibliográfica e idioma em cada capítulo seguiu, para os dois primeiros, o formato da revista/publicação nas quais foram submetidos, e para o terceiro, seguiu a norma da revista planejada para sua submissão. As demais partes textuais da tese, introdução geral e considerações finais, seguiram formatação padrão própria e estão em português.

O primeiro capítulo é intitulado “Status do Conhecimento Sobre os Anfíbios Anuros Endêmicos da Serra do Espinhaço”, e está submetido ao livro “Ecologia e Sustentabilidade no campo rupestre”, editorado pelo Dr. Geraldo W. A. Fernandes, com previsão de publicação para o ano de 2022. O capítulo traz um panorama geral do conhecimento atual sobre os anuros endêmicos da Serra do Espinhaço, incluindo um breve histórico do conhecimento dos anuros da Serra do Espinhaço, o conhecimento atual sobre taxonomia, padrões de distribuição, história natural, evolução, biogeografia e conservação. O segundo capítulo tem como foco a filogeografia *multilocus* de *Bokermannohyla saxicola*, uma perereca endêmica da Serra do Espinhaço. O manuscrito intitulado “*Colonization rather than fragmentation explains the geographic distribution and diversification of treefrogs endemic to Brazilian shield sky islands”* foi aceito para publicação no periódico *Journal of Biogeography* no dia 09 de novembro de 2021. O terceiro capítulo está centrado no Espinhaço, e traz uma filogeografia

comparativa de seis espécies de anuros endêmicos da formação. O capítulo intitulado "*Comparative Phylogeography of anurans endemic to Espinhaço Mountain Range, the largest extra-Andean Mountain chain in South America*" será submetido ao periódico *Organisms diversity and Evolution.*

Por fim, anexo a tese, apresento uma produção relacionada a esta tese, liderada pelo meu orientador Dr. Rafael Félix de Magalhães, na qual tive a oportunidade de colaborar, juntamente com outros pesquisadores. No artigo publicado em 2021 no periódico *Biological Journal of the Linnaen Society*, apresentamos evidência de introgressão entre espécies não irmãs (*Pithecopus ayeaye* e *P. megacephalus*).

Introdução geral

Nos últimos anos, o entendimento de alguns processos tem sido inferido através da filogeografia, disciplina que visa compreender as relações filogenéticas de um grupo taxonômico projetando-as no espaço e tempo (Avise, 2009). Através de um conjunto de metodologias, estudos filogeográficos podem identificar, através de informações sobre processos históricos de demografia e migração, fatores biogeográficos responsáveis pela estrutura populacional de espécies (Avise, 2009; Knowles, 2009). Com a incorporação de diferentes ferramentas estatísticas baseadas na teoria da coalescência e conjunto de dados *multilocus*, estudos filogeográficos se tornaram importantes para a investigação de padrões históricos envolvidos na diversificação de linhagens e no reconhecimento de unidades taxonômicas de regiões com elevada diversidade genética e centros de origem e dispersão (Avise et al., 1987; Knowles & Maddison, 2002; Kuhner, 2008; Knowles, 2009). Informações essas, de grande importância para os planos de conservação da biodiversidade (Avise, 2009).

Comparar padrões filogeográficos de diferentes espécies codistribuídas nos ajuda a compreender as influências de eventos históricos sobre a comunidade biológica e, assim, a importância deles nos padrões de diversidade observados em uma determinada área (Hickerson *et al.*, 2010). A filogeografia comparada auxilia no reconhecimento de áreas historicamente estáveis (ou refúgios ecológicos), e na compreensão das influências de eventos da trajetória da Terra sobre múltiplas espécies codistribuídas (Hickerson *et al.*, 2010). Os padrões filogeográficos compartilhados por diferentes espécies podem ser resultado de processos evolutivos dependentes, devido a um evento histórico comum, revelando a história biogeográfica de uma região (Bell *et al.*, 2012).

Os padrões de distribuição e composição de diversidade respondem a vários fatores bióticos e abióticos, como heterogeneidade topográfica, processo geológico, mudanças climáticas cíclicas, capacidade de dispersão e interações de espécies (ex.: predação e mutualismo) (Antonelli et al., 2018; Sandel et al., 2011; Wisz et al., 2013). Essas mudanças e interações desempenham um papel importante na formação da história evolutiva das espécies, afetando a variabilidade genética entre as paisagens (Guedes et al., 2020). Com alta heterogeneidade topográfica e diferentes gradientes ambientais, montanhas são ambientes que abrigam uma biodiversidade excepcional, com alta concentração da população humana (Körner et al., 2017). Mas, apesar dos inúmeros estudos recentes, a alta diversidade nas montanhas continua sendo um dos maiores desafios para a compreensão dos padrões de diversificação de

espécies (Rahbek et al., 2019; Perrigo et al., 2020). Assim, montanhas representam um ótimo ambiente para estudos de especiação e diversificação genética devido ao possível isolamento genético/reprodutivo gerado pela alopatria em relação às populações-irmãs.

Anfíbios geralmente tem baixa capacidade de dispersão, e por isso, tendem a apresentar um elevado grau de diferenciação genética interpopulacional (Johns & Avise, 1998), tornando-se excelentes modelos em estudos filogeográficos (Zeisset & Beebee 2008). Espécies de anfíbios que possuem distribuição geográfica restritas a determinados ambientes, como montanhas, constituem alvos ideais para a investigação dos processos de diversificação ocorridos da região.

Os anuros estão presentes nos diferentes ambientes da Serra do Espinhaço, e uma compilação antiga identificou alta diversidade e endemismo na região (Leite et al., 2008). A Serra do Espinhaço é a maior cadeia de montanhas do Brasil e faz parte do Complexo de Ilhas de Altitude do Escudo Brasileiro (sensu Warshall, 1994). Entretanto, apesar da elevada diversidade de anuros na Serra (Leite et al., 2008) e inúmeros estudos taxonômicos na região (e.g., Leal et al., 2020; Taucce et al., 2020), pouco se sabe sobre a diversidade genética das populações e menos ainda sobre os padrões e processos envolvidos na sua diversidade.

Assim, esta tese teve como objetivo sintetizar o conhecimento dos anuros endêmicos da Serra do Espinhaço, estudar a distribuição da variabilidade genética de *Bokermannohyla saxicola* em toda sua área de ocorrência, e comparar os padrões filogeográficos de seis espécies de anuros endêmicos codistribuídas na Serra do Espinhaço em Minas Gerais.

Referências

Antonelli, A., Kissling, W.D., Flantua, S.G.A., Bermúdez, M.A., Mulch, A., Muellner-Riehl, A.N., ... Hoorn, C. (2018). Geological and climatic influences on mountain biodiversity. *Nature Geoscience 11*, 718–725. https://doi.org/10.1038/s41561-018-0236-z

Avise, J.C., Arnold, J., Ball, R.M.; Bermingham, E.; Lamb, T.; Neigel, J.E.; Reeb, C.A.; Saunders, N.C. (1987). Intraspecific phylogeography: the mitochondrial DNA bridge between population genetics and systematics. *Annual Review of Ecology and Systematics 18*, 489–522. http://www.jstor.org/stable/2097141

Avise, J.C. (2009). Phylogeography: retrospect and prospect. *Journal of Biogeography 36*, 3-15. https://doi.org/10.1111/j.1365-2699.2008.02032.x

Bell, R.C., MacKenzie, J.B., Hickerson, M.J., Chavarría, K.L., Cunningham, M., Williams, S., Moritz, C. (2012). Comparative multi-locus phylogeography confirms multiple vicariance events in co-distributed rainforest frogs. *Proceedings of the Royal Society B: Biological Sciences 279*, 991–999. https://doi.org/10.1098/rspb.2011.1229

Guedes, T.B., Azevedo, J.A.R., Bacon, C.D., Provete, D.B., Antonelli, A. (2020). Diversity, Endemism, and Evolutionary History of Montane Biotas Outside the Andean Region. In: Rull, V., Carnaval, A. C. (eds) *Neotropical Diversification: Patterns and Process*. Springer International Publishing, pp 299-328.

Hickerson, M.J., Carstens, B.C., Cavender-Bares, J., Crandall, K.A., Graham, C.H., Johnson, J.B., … Yoder, A.D. (2010). Phylogeography's past, present, and future: 10 years after Avise, 2000. *Molecular Phylogenetics and Evolution 54*, 291–301. https://doi.org/10.1016/j.ympev.2009.09.016

Johns, G.C., Avise, J.C. (1998). A comparative summary of genetic distances in the vertebrates from the mitochondrial cytochrome b gene. *Molecular Biology and Evolution 15*, 1481–1490. https://doi.org/10.1093/oxfordjournals.molbev.a025875

Knowles, L.L. (2009). Statistical phylogeography. *Annual Review of Ecology, Evolution, and Systematics 40*, 593–612.

Knowles, L.L., Maddison, W.P. (2002). Statistical phylogeography. *Molecular Ecology 11*, 2623–2635.

Körner, C., Jetz, W., Paulsen, J., Payne, D., Rudmann-Maurer, K., Spehn, E.M. (2017). A global inventory of mountains for bio-geographical applications. *Alpine Botany 127*, 1-15. https://doi.org/10.1007/s00035-016-0182-6

Kuhner, M.K. (2008). Coalescent genealogy samplers: windows into population history. *Trends in Ecology and Evolution 24*, 86–93.

Leal, F., Leite, F.S.F., Costa, W.P., Nascimento, L.B., Lourenço, L.B., Garcia, P.C.A. (2020). Amphibians from Serra do Cipó, Minas Gerais, Brasil. VI: A New Species of the *Physalemus deimaticus* Group (Anura, Leptodactylidae). *Zootoxa 4766*, 306-330. https://doi.org/10.11646/zootaxa.4766.2.3

Leite, F.S.F., Juncá, F.A., Eterovick, P.C. (2008). Status do conhecimento, endemismo e conservação de anfíbios anuros da Cadeia do Espinhaço, Brasil. *Megadiversidade 4*, 158–176.

Perrigo, A., Hoorn, C., Antonelli, A. (2020). Why mountains matter for biodiversity. *Journal of Biogeography 47*(2), 315–325. https://doi.org/10.1111/jbi.13731

Rahbek, C., Borregaard, M.K., Colwell, R.K., Dalsgaard, B., Holt, B.G., Morueta Holme, N., … Fjeldså, J. (2019). Humboldt's enigma: What causes global patterns of mountain biodiversity? *Science 365*(6458), 1108–1113. https://doi.org/10.1126/science.aax0149

Sandel, B., Arge, L., Dalsgaard, B., Davies, R.G., Gaston, K.J., Sutherland, W.J., Svenning, J.C. (2011). The influence of late quaternary climate-change velocity on species endemism. *Science 334*, 660–664. https://doi.org/10.1126/science.1210173

Taucce, P.P.G., Nascimento, J.S., Trevisan, C.C., Leite, F.S.F., Santana, D.J., Haddad, C.F.B, Napoli, M.F. (2020). A new rupicolous species of the *Pristimantis conspicillatus* group (Anura: Brachycephaloidea: Craugastoridae) from central Bahia, Brazil. *Journal of Herpetology 54*, 245–257.

Warshall, P. (1994). The Madrean sky island archipelago: a planetary overview. In: DeBano, L.F., Ffolliott, P.F., Ortega-Rubio, A., Gottfried, G.J., Hamre, R.H., Edminster, C.B. (tech. cords.) Biodiversity and management of the Madrean Archipelago: the sky islands of southwestern United States and northwestern Mexico. United States Department of Agriculture, pp. 6-18.

Wisz, M.S., Pottier, J., Kissling, W.D., Pellissier, L., Lenoir, J., Damgaard, C.F., … Svenning, J.C. (2013). The role of biotic interactions in shaping distributions and realized assemblages of species: Implications for species distribution modelling. *Biological Reviews 88*, 15–30.

Zeisset, I., Beebee, T. (2008). Amphibian phylogeography: a model for understanding historical aspects of species distributions. *Heredity 101*, 109–119. https://doi.org/10.1038/hdy.2008.30%20

Capítulo 1

Status do Conhecimento Sobre os Anfíbios Anuros Endêmicos da Serra do Espinhaço

Submetido ao livro *Ecologia e Sustentabilidade no campo rupestre* editorado pelo Prof. Dr. Geraldo W. A. Fernandes (Universidade Federal de Minas Gerais), com previsão de publicação para 2022.

Status do Conhecimento Sobre os Anfíbios Anuros Endêmicos da Serra do Espinhaço

Título abreviado: *Anuros endêmicos da Serra do Espinhaço*

Autores: Caroline Batistim Oswald[1a], Rafael Félix de Magalhães[1,2], Tiago Leite Pezzuti[1b], Felipe Sá Fortes Leite[3]

[1]Programa de Pós-Graduação em Zoologia, Departamento de Zoologia, Universidade Federal de Minas Gerais. Avenida Presidente Antônio Carlos, 6627. Pampulha, Belo Horizonte, MG, Brasil. E-mail: [a]carolbatistim@gmail.com, [b]tlpezzuti@gmail.com

[2]Departamento de Ciências Naturais, campus Dom Bosco, Universidade Federal de São João del-Rei. Praça Dom Helvécio, 74. Dom Bosco, São João del-Rei, MG, Brasil. E-mail: rafaelmagalhaes@ufsj.edu.br

[3]Instituto de Ciências Biológicas e da Saúde, campus Florestal, Universidade Federal de Viçosa. Rodovia LMG 818, km 06. Florestal, MG, Brasil. E-mail: fsfleite@gmail.com

Abstract

Espinhaço Range's frogs have attracted attention since the middle of the 20th century. Despite great efforts to understand the taxonomy, patterns of distribution and biology of the anurans of this mountain range, many questions still remain. In this chapter, we update the knowledge about the endemic anurans of Espinhaço Range, including information on species ecology, behavior, natural history, evolution, biogeography and conservation. Approximately one third of the species of anurans distributed in the Espinhaço range are endemic, and this number may still be underestimated, since almost every year new endemic species are discovered and described, such as *Pristimantis rupicola* (2020) and *Corythomantis botoque* (2021). The greatest richness of endemism in the Espinhaço range is concentrated in its southern portion, along Serra do Cipó. Tadpoles and vocalizations are known for most of the endemic species, as well as their phylogenetic relationship within genera. However, data on behavior and natural history are scarce for most of them. Many of the studies are incipient, revealing the need and opportunities for future scientific investigations, such as studies on the effects of environmental gradients and adaptations of endemic species to the environmental conditions of the *campo rupestre*.

Resumo

A Serra do Espinhaço desperta atenção em relação à anurofauna desde meados do século 20. Apesar dos grandes esforços para conhecer os anuros da serra, muitas questões relacionadas aos padrões de riqueza, composição, endemismo e aspectos biológicos ainda permanecem sem resposta. Neste capítulo, apresentamos uma atualização do conhecimento sobre os anuros endêmicos da Serra do Espinhaço, incluindo uma lista de espécies atualizada e dados sobre ecologia, comportamento, história natural, evolução, biogeografia e conservação. Aproximadamente um terço das espécies de anuros distribuídas na cadeia do Espinhaço são endêmicas, e esse número pode estar subestimado, visto que quase todos os anos novas espécies endêmicas são descobertas e descritas, como por exemplo *Pristimantis rupícola* (2020 e *Corythomantis botoque* (2021). A maior riqueza de endemismos da Serra do Espinhaço está concentrada no sul do Espinhaço Mineiro, ao longo da Serra do Cipó. Girinos e vocalizações são conhecidos para a maioria das espécies endêmicas da Serra do Espinhaço, bem como o relacionamento filogenético destas com espécies congêneres. Entretanto, dados de comportamento e história natural são escassos para a maioria delas. Muitos dos estudos são incipientes, revelando a necessidade e oportunidades para futuras investigações científicas, como estudos sobre os efeitos de gradientes ambientais e adaptações das espécies endêmicas às condições ambientais do campo rupestre.

Termos para Indexação

Campo rupestre, Caatinga, Cerrado, Mata Atlântica, Biogeografia, Ecologia, Conservação, Sistemática, História Natural, Modos Reprodutivos, Guildas Ecomorfológicas, Relicto Biogeográfico.

Introdução

O Brasil é o país com a maior riqueza conhecida de anuros do mundo, com cerca de 15.5% das 7340 espécies viventes (Segalla et al. 2021, Frost 2021). Esses animais são conhecidos por sua baixa capacidade de dispersão e necessidade de habitats específicos (Smith & Green 2005). A pequena vagilidade dos anuros favorece a diferenciação alopátrica das linhagens, podendo levar à especiação (Valero et al. 2019). A especificidade de habitat, por sua vez, está atrelada às particularidades reprodutivas de cada espécie. Neste contexto, os anuros são o grupo de tetrápodes com a maior diversidade de modos reprodutivos (Haddad & Prado 2005), com 42 modos registrados no mundo e 32 na região Neotropical (Malagoli et al.

2021). A combinação dos locais de postura de ovos, características dos ovos e das desovas, padrões de desenvolvimento e tipo de cuidado parental são responsáveis por esta diversidade (Haddad & Prado 2005). Como os modos reprodutivos estão vinculados a diferentes sítios de oviposição, regiões com alta heterogeneidade de habitat tendem a sustentar uma maior diversidade desses modos e uma maior riqueza de espécies (Eterovick & Barata 2006, Bickford et al. 2010). Rodríguez e colaboradores (2015) encontraram uma relação direta entre o efeito da complexidade topográfica e a diferenciação genética de anuros tropicais. Segundo os autores, o aumento da complexidade resulta em uma maior riqueza de microhabitats, o que sustenta uma alta diversidade de espécies. Cada tipo de microhabitat, por sua vez, tende a ser raro e apresentar distribuição espacial aleatória, favorecendo o isolamento entre subpopulações que dependem de habitats específicos, podendo resultar em diferenciação genética.

Cadeias de montanhas são os ambientes com maior complexidade topográfica (Körner et al. 2017) e, não por acaso, apresentam alta riqueza de anfíbios, sendo importantes centros de endemismo (e.g., Rödder et al. 2010, Silva et al. 2018, Guedes et al. 2020). A riqueza de anfíbios em montanhas está inversamente correlacionada com a latitude, com as maiores riquezas encontradas nos trópicos (García-Rodríguez et al. 2021). Fatores bióticos e abióticos desempenham um importante papel na história evolutiva das espécies, afetando a variabilidade biológica nas paisagens (Guedes et al. 2020). Assim, além da topografia e da capacidade de dispersão, mudanças climáticas e interações entre espécies podem influenciar a distribuição e composição da diversidade local (Antonelli et al. 2018, Sandel et al. 2011, Wisz et al. 2013).

Neste cenário, destaca-se a Serra do Espinhaço, a segunda maior cadeia de montanhas da América do Sul (Guedes et al. 2020). O Espinhaço se estende na direção Norte-Sul, ao longo de 1.200km no leste do Brasil, da Bahia a Minas Gerais (Fernandes et al. 2014). Considerando-se as assembleias de anuros endêmicos, a cadeia pode ser dividida latitudinalmente em três regiões: Quadrilátero Ferrífero (QFe), no extremo sul (Figs. 1,2a); Espinhaço Mineiro (EM), que se inicia ao norte do QFe, em Minas Gerais e se estende até o sudoeste da Bahia, incluindo a Serra do Cabral, uma unidade disjunta a oeste do espigão principal (Figs. 1,3a,4a); e Chapada Diamantina (CD), que se inicia na região da Serra das Almas, e segue a nordeste, até o norte da Bahia (Figs. 1,5a; Leite et al. 2008a). As áreas de altitude (i.e., acima de 800 m) são dominadas pelo campo rupestre, um ecossistema caracterizado por um mosaico de vegetação campestre e arbustiva que cresce em afloramentos rochosos ou solos pobres, arenosos e rasos, ao qual estão associadas a maioria das espécies endêmicas de plantas e animais (Silveira et al. 2016). O Espinhaço funciona como uma fronteira entre os domínios da Caatinga, Cerrado e Mata

Atlântica, sendo influenciada por suas biotas, principalmente nas encostas (Silveira et al. 2016).

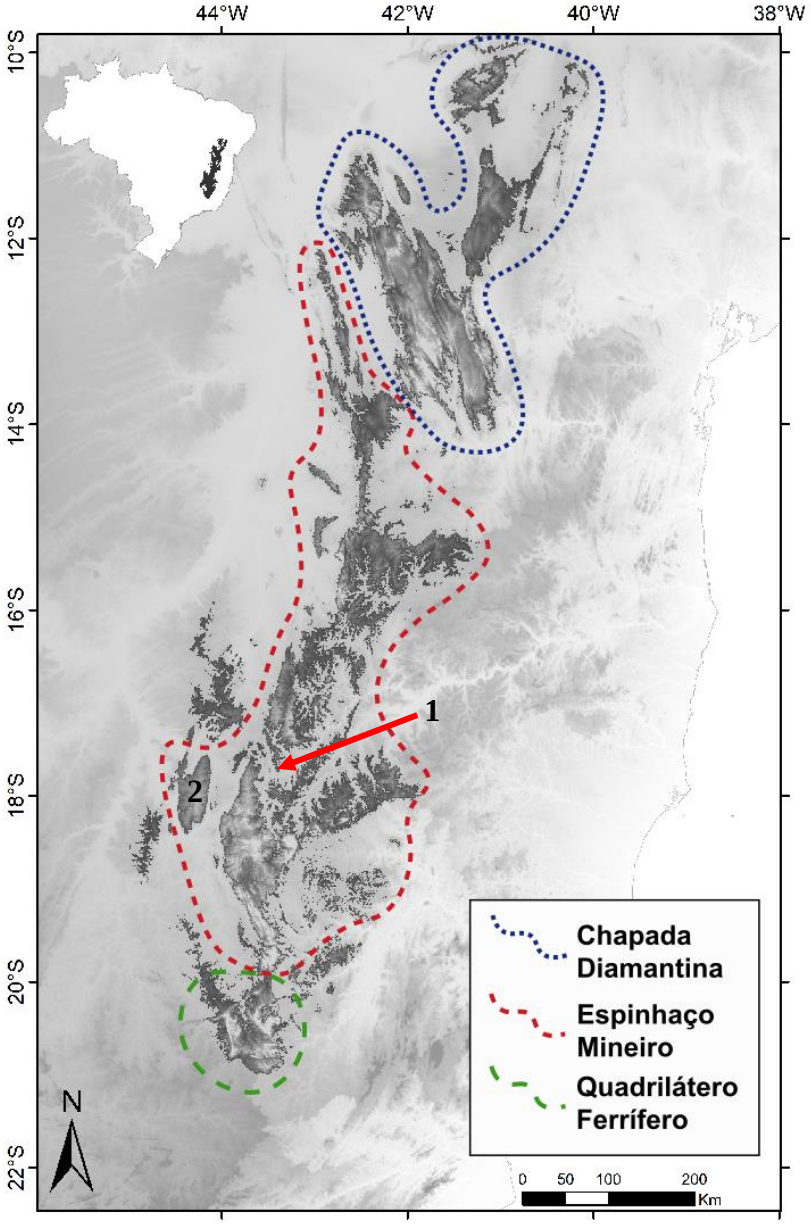

Figura 1. Mapa da Serra do Espinhaço e as diferentes regiões considerando-se assembleias de anuros endêmicos: Chapada Diamantina ao norte delimitada em azul, Espinhaço Mineiro ao centro delimitado de vermelho, e Quadrilátero Ferrífero ao sul delimitado de verde. 1 = Depressão Couto de Magalhães; 2 = Serra do Cabral. Altitudes a cima de 800 m em cinza escuro

A Serra do Espinhaço abriga uma grande diversidade de fauna, flora e funga, com várias espécies e alguns gêneros endêmicos (e.g., Pardiñas et al. 2014, Coutinho et al. 2015, Scatigna et al. 2020). No Cerrado, o Espinhaço Mineiro é a área de endemismo mais rica para a

herpetofauna, com 31 espécies restritas a ele, sendo 20 anuros (Azevedo et al. 2016). Já na Caatinga, 16 das 21 espécies de anfíbios endêmicas do domínio têm distribuição restrita à Chapada Diamantina (Marques et al. 2021). Além disso, grande parte da riqueza e endemismo de anuros de Minas Gerais está distribuída na Cadeia do Espinhaço (Leite et al. 2008a), destacando a serra como uma importante área para a preservação da biodiversidade regional. Por sua peculiaridade e relevância ambiental, econômica e social, a Serra do Espinhaço foi considerada Reserva da Biosfera em 2005 (UNESCO 2021).

Figura 2. Ambiente de reprodução de anuros no Quadrilátero Ferrífero (A); Macho (B), Fêmea (C) e girino (D) de *Bokermannohyla martinsi*. Fotos: A - Lucas Perillo; B, C, D - Tiago L. Pezzuti

A extensão latitudinal do Espinhaço, aliada a variações altitudinais, geológicas e edáficas, resultam em uma pronunciada heterogeneidade ambiental (Silveira et al. 2016, Miola et al. 2021), fornecendo um amplo espectro de habitats para a reprodução de anuros (Eterovick & Barata 2006). Não obstante, ambientes aquáticos de altitude parecem desempenhar um papel

importante na composição da anurofauna, abrigando uma ampla diversidade filogenética de espécies endêmicas (e.g., espécies dos gêneros *Bokermannohyla* (Hylidae), *Hylodes* (Hylodidae), *Phasmahyla* (Phyllomedusidae), *Physalaemus* (Leptodactylidae), *Proceratophrys* (Odontophrynidae) e *Thoropa* (Cycloramphidae); Heyer 1999, Eterovick & Barata 2006, Oliveira & Eterovick 2010).

O campo rupestre está entre as fisionomias com maior diversidade biológica do mundo e, mesmo com o recente aumento dos estudos locais (Miola et al. 2021), informações básicas sobre endemismo, riqueza e composição de espécies ainda são escassas ou incompletas. Para anuros, quase todos os anos novas espécies são descobertas e descritas para a região (e.g., Taucce et al. 2020, Pinheiro et al. 2021), mas o último levantamento regional data de mais de uma década (Leite et al. 2008a). Com o objetivo de fornecer informações que possam auxiliar no planejamento da conservação, na elaboração de planos de manejo e outros estudos, revisitamos o trabalho de Leite e colaboradores (2008a), atualizando o status do conhecimento sobre os anuros endêmicos da Serra do Espinhaço.

Um breve histórico

Os estudos sobre a anurofauna da Serra do Espinhaço começaram na década de 1950, com os esforços dos naturalistas Werner Bokermann e Ivan Sazima para descrever diversas espécies restritas à região e aspectos observacionais de suas biologias (e.g., Bokermann 1956, 1964, 1967; Bokermann & Sazima 1973a, b, 1978; Sazima & Bokermann 1978, 1982). Uma série de cinco artigos científicos intitulados “Anfíbios da Serra do Cipó” foi resultado do esforço de ambos, nos quais foram descritas seis espécies de anuros de três diferentes famílias, além de observações sobre a história natural de *Bokermannohyla alvarengai* (Bokermann & Sazima 1973a, b, 1978; Sazima & Bokermann 1977, 1982). Contudo, esses primeiros trabalhos foram descritivos, ainda que importantes para minimizar o déficit de conhecimento Linneano no Espinhaço (ver Hortal et al. 2015 sobre déficits da biodiversidade).

Heyer (1999) foi o primeiro autor a sugerir que a fragmentação natural da Serra do Espinhaço, sua posição geográfica entre a Caatinga, o Cerrado e a Mata Atlântica, além das particularidades paisagísticas do campo rupestre, poderiam estar associados aos endemismos de anuros da região. Segundo o autor, diversas espécies de anuros restritas ao Espinhaço seriam possivelmente derivadas de ancestrais da Mata Atlântica, já que gêneros como *Hylodes* (Hylodidae), *Phasmahyla* (Phyllomedusidae) e *Thoropa* (Cycloramphidae), por exemplo, são quase inteiramente endêmicos desse domínio, com exceção das espécies disjuntas na Serra do

Espinhaço. Heyer (1999) apontou que uma das explicações para esse fenômeno é que poucas espécies de anuros do Cerrado possuem adaptações para a reprodução e o desenvolvimento em ambientes lóticos, ao contrário do que se observa na Mata Atlântica. A Serra do Espinhaço apresenta abundância desses corpos d'água, o que ofereceu oportunidades para a ocupação da região pelos ancestrais florestais de muitas das espécies endêmicas. Apesar disso, espécies campestres de ambientes lênticos como *Leptodactylus camaquara* e *L. cunicularius* (Leptodactylidae), seriam derivadas de ancestrais do Cerrado (Heyer 1999). Por fim, o autor indicou que todos os endemismos de anuros da Serra do Espinhaço eram a nível específico, com exceção de *Rupirana cardosoi* (Fig. 5d), um gênero endêmico da área, descrito naquele mesmo trabalho. Como hipóteses alternativas, Heyer sugeriu que (i) esse gênero seria um relicto biogeográfico, (ii) estaria mais amplamente distribuído do que apenas no Espinhaço ou (iii) representaria um erro de definição taxonômica. Mais de uma década depois, a primeira das hipóteses do Heyer (1999) foi corroborada por Fouquet e colaboradores (2013) e por Santos e colaboradores (2020b). Esses achados evidenciam a importância da posição geográfica da Serra do Espinhaço e de sua história evolutiva na diversificação da anurofauna endêmica a ela.

Em anos subsequentes, além de trabalhos de taxonomia, alguns estudos de ecologia e história natural foram realizados pela pesquisadora Paula Eterovick e colaboradores. Nestes estudos, os pesquisadores avaliaram como fatores abióticos (e.g., parâmetros temporais, espaciais) e bióticos (e.g., predação e competição) influenciam a composição das assembleias de anuros em diferentes regiões do Espinhaço, como o Quadrilátero Ferrífero (Kopp & Eterovick 2006; Afonso & Eterovick 2007a, b) e o Espinhaço Mineiro (Eterovick & Fernandes 2001; Eterovick 2003; Oliveira & Eterovick 2009, 2010). O grupo de pesquisa também realizou diversos estudos de história natural de espécies endêmicas do Espinhaço, com abordagens que foram desde biologia reprodutiva, demografia e desenvolvimento larval (Leite et al. 2008b, Oliveira et al. 2012) até experimentos comportamentais envolvendo estratégias de defesa de girinos e estudos de dieta (Gontijo et al. 2018, Kloh et al. 2018). O conhecimento da história natural dessas espécies tem fornecido informações para a conservação e a avaliação de impactos antrópicos sobre as suas populações (Eterovick et al. 2015, Mascarenhas et al. 2016, Lima et al. 2019).

Leite e colaboradores (2008a) compilaram os anfíbios endêmicos do Espinhaço e identificaram 28 espécies com distribuição restrita ao complexo serrano. Alguns trabalhos com escopo similar, mas restritos a áreas específicas da Serra do Espinhaço, foram publicados posteriormente, incluindo livros (Pimenta et al. 2014, Silveira et al. 2019, Eterovick et al. 2020)

e recursos digitais (Leite et al. 2019a). O livro “Anfíbios: Alvorada de Minas - Conceição do Mato Dentro - Dom Joaquim - Minas Gerais” contemplou 58 espécies com informações sobre taxonomia, morfologia, hábitos, reprodução, vocalização, girinos e conservação, além de chaves de identificação (Pimenta et al. 2014). Já o livro "Anfíbios do Quadrilátero Ferrífero (Minas Gerais)" apresentou uma lista comentada com fotos e mapas de ocorrência de 92 espécies, com dados compiladas através de amostragens de campo, revisões bibliográficas e de coleções científicas (Silveira et al. 2019). Leite e colaboradores (2019a) disponibilizaram ferramentas para a identificação das espécies, como chaves de identificação de adultos e girinos (Pezzuti et al. 2019a, b), guias de vocalizações e mapas com a distribuição das espécies do Quadrilátero Ferrífero (Leite et al. 2019a). O livro “Anfíbios da Serra do Cipó, Minas Gerais - Brasil” trouxe uma lista com 58 espécies da região, bem como informações sobre reprodução, tipos de desovas e girinos, entre outras. Uma chave ilustrada para a identificação dos anfíbios anuros da Serra do Cipó também foi apresentada (Eterovick et al. 2020). O número de espécies de anfíbios descritas para a Cadeia do Espinhaço aumentou, seguindo a tendência nacional e mundial de descrições de novos táxons (Guerra et al. 2020, Moura & Jetz 2021). Assim, a atualização do estado do conhecimento faz-se necessária. Neste capítulo, os dados de distribuição e biologia das espécies foram compilados por meio da literatura científica publicada desde o levantamento previamente realizado por Leite e colaboradores (2008a).

Conhecimento taxonômico e padrões de distribuição

Vinte novas espécies com distribuição restrita ao Espinhaço foram descritas após o estudo de Leite e colaboradores (2008a) [i.e., *Boana botumirim* (Caramaschi et al. 2009), *Bokermannohyla juiju* Faivovich et al. 2009, *Pleurodema alium* Maciel & Nunes 2010 (Fig. 3b), *Physalaemus orophilus* Cassini et al. 2010, *Bokermannohyla sagarana* Leite et al. 2011, *Proceratophrys minuta* Napoli et al. 2011, *Bokermannohyla flavopicta* Leite et al. 2012, *Nyctimantis galeata* (Pombal et al. 2012), *Proceratophrys redacta* Teixeira et al. 2012, *Leptodactylus oreomantis* Carvalho et al. 2013, *Crossodactylodes itambe* Barata et al. 2013, *Sphaenorhyncus canga* Araujo-Vieira et al. 2015, *Scinax montivagus* Juncá et al. 2015, *Odontophrynus Juquinha* Rocha et al. 2017, *Physalaemus claptoni* Leal et al. 2020, *Pristimantis rupícola* Taucce et al. 2020, *Aplastodiscus heterophonicus* Pinheiro et al. 2021, *Corythomantis botoque* Marques et al. 2021, *Leptodactylus avivoca* Carvalho et al. 2021].

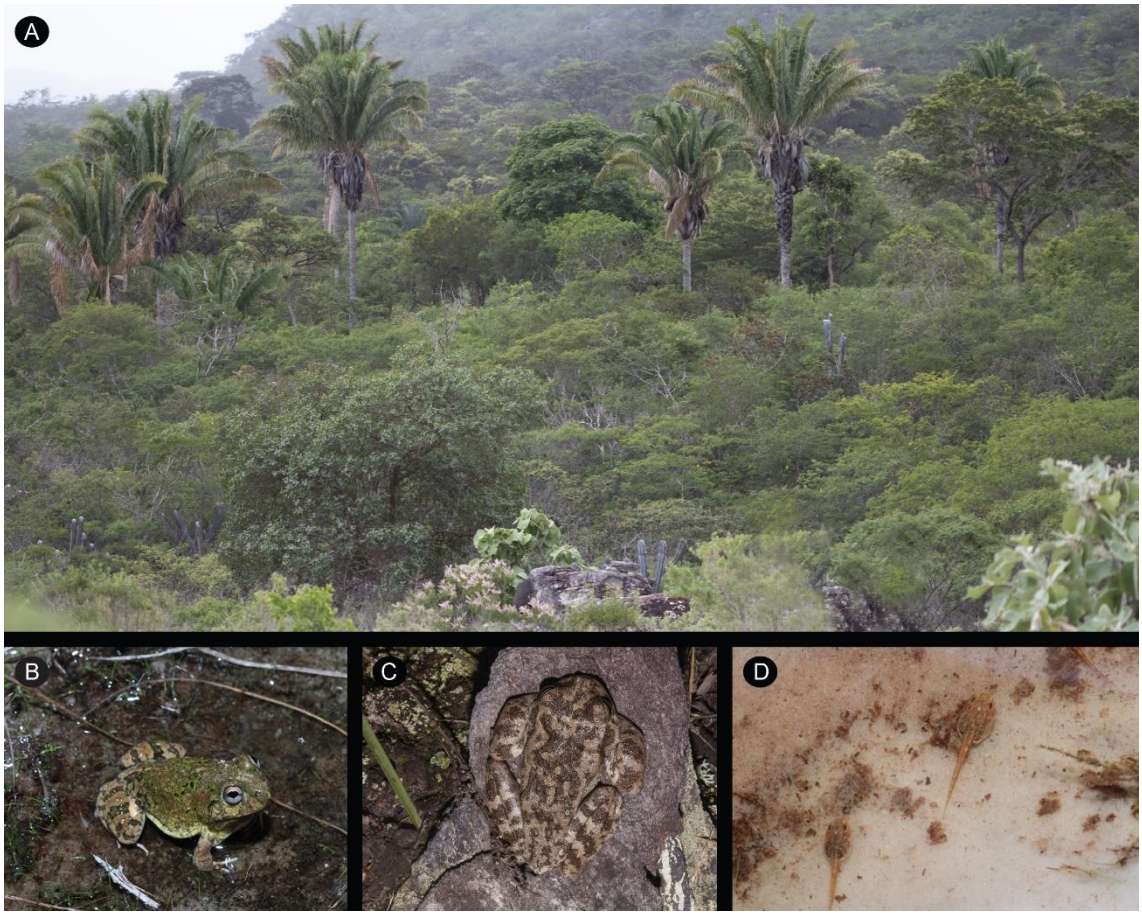

Figura 3. Paisagem no Espinhaço Mineiro, ao norte de Minas Gerais (A); *Pleurodema alium* (B); Adulto (C) e girino (D) de *Bokermannohyla alvarengai*. Fotos: Tiago L. Pezzuti

Além disso, novos registros das espécies já conhecidas foram acumulados ao longo de mais de uma década desde a última compilação. Três espécies consideradas de distribuição restrita ao Espinhaço perderam o *status* de endêmicas. Baêta e colaboradores (2009) demonstraram que *Pithecopus itacolomi*, antes restrita ao Quadrilátero Ferrífero, é sinônimo júnior de *Pithecopus ayeaye* e, portanto, deixou de ser endêmica do Espinhaço, uma vez que *P. ayeaye* também ocorre em outras regiões serranas do sudeste brasileiro (Magalhães et al. 2017). Taucce e colaboradores (2012) ampliaram a distribuição geográfica de *Ischnocnema izecksohni* e Silva e colaboradores (2013) ampliaram a distribuição de *Scinax tripui* para fora dos limites da Serra do Espinhaço, assim as espécies também deixaram de ser consideradas endêmicas da região. *Bokermannohyla nanuzae* também poderia ser incluída no grupo das espécies supracitadas, uma vez que foi sinonimizada a *Bokermannohyla feioi*, espécie distribuída na Serra da Mantiqueira (Walker et al. 2015). Entretanto, apesar da sobreposição morfológica nas características que diagnosticam as espécies (Walker et al. 2015), dados

moleculares indicam que *Bokermannohyla nanuzae* e *B. feioi* são espécies distintas (Taucce et al. em preparação, Faivovich et al. em preparação). Sendo assim, nós mantivemos *B. nanuzae* como espécie endêmica do Espinhaço.

Figura 4. Paisagem na Serra do Cabral, Minas Gerais (A); *Bokermannohyla saxicola* (B); *Scinax cabralensis* (C); e *Thoropa megatympanum* (D). Fotos: Tiago L. Pezzuti

Assim, dentre as 143 espécies de anuros registradas na Serra do Espinhaço [i.e., 130 spp. inventariadas por Leite (2012), 12 espécies endêmicas descritas após esse trabalho e uma espécie descrita com ocorrência no Espinhaço (Andrade et al. 2018)], 44 delas podem ser consideradas endêmicas da região (Tabela 1), representando cerca de 31% da riqueza total. As espécies endêmicas da Serra do Espinhaço estão distribuídas em 22 gêneros alocados em sete famílias, sendo Hylidae a família com o maior número de endêmicas (20 espécies). A segunda família com mais representantes foi Leptodactylidae (12 espécies), seguida por Odontophrynidae (5 espécies), Hylodidae (3 espécies), Phyllomedusidae (2 espécies), Craugastoridae (2 espécies) e Cycloramphidae (1 espécie). Dentre as espécies endêmicas,

Scinax curicica é a única amplamente distribuída nas três porções da Serra do Espinhaço, enquanto a maioria, está restrita à apenas uma das porções (Tabela 1).

Figura 5. Paisagem na Chapada Diamantina, Bahia (A); *Pristimantis rupicola* (B); *Haddadus aramunha* (C); e *Rupirana cardosoi* (D). Fotos: A - Tiago L. Pezzuti; B, C, D - Leandro Drummond

Tabela 1. Anuros endêmicos da Serra do Espinhaço. Distribuição: CD = Chapada Diamantina, EM = Espinhaço Mineiro, QFe = Quadrilátero Ferrífero; ambiente reprodutivo: R = afloramento rochoso, LA= lâmina d'água em rocha úmida, LP = lagoas, poças e brejos permanentes, RP = riachos permanentes, RT = riachos temporários, AT = alagadiços rasos temporários, LT = lagoas, poças e brejos temporários, BR = bromélias); e modo reprodutivo (*sensu* Haddad & Prado, 2005): ? = desconhecido, 1 = ovos e girinos exotróficos em corpos d'água lênticos, 2 = ovos e girinos exotróficos em corpos d'água lóticos, 3 = ovos e estágios larvais iniciais em câmaras subaquáticas construídas; girinos exotróficos em riachos, 4 = ovos e estágios larvais iniciais em bacias naturais ou construídas; após a inundação, girinos exotróficos em lagoas ou riachos, 5 = ovos e estágios larvais iniciais em ninhos subterrâneos construídos; após a inundação, girinos exotróficos em lagoas ou riachos, 11 = ninho de espuma flutuando em poças; girinos exotróficos em poças. 19 = ovos em rochas úmidas; girinos exotróficos semiterrestres vivendo em lâmina de água, sobre rochas na interface água-terra, 21 = ovos eclodindo em girinos endotróficos que completam seu desenvolvimento no ninho, 25 = ovos eclodindo em girinos exotróficos que caem de folhas suspensas em corpos d'água lóticos, 26 = ovos eclodindo em girinos exotróficos que se desenvolvem em cavidades cheias de água em bromélias, 28 = ninho de espuma no solo úmido; após a inundação, girinos exotróficos em poças, 30 = ninho de espuma com ovos e estágios larvais iniciais em ninhos subterrâneos construídos; após a inundação, girinos exotróficos em poças.

Táxon	**Distribuição**	**Ambiente reprodutivo**		**Modo Reprodutivo**
		Área aberta	**Matas de galeria e florestas de encosta**	
Craugastoridae				
Haddadus aramunha	CD	AR		23
Pristimantis rupicola	CD	AR		23
Cycloramphidae				
Thoropa megatympanum	QFe, EM	LA		19
Hylidae				
Aplastodiscus heterophonicus	EM		LP, RP	5
Boana botumirim	EM	RP, LP		2
Boana cipoensis	EM	RP, LP		2
Bokermannohyla alvarengai	QFe, EM	RT		2
Bokermannohyla diamantina	EM, CD	AT		4
Bokermannohyla flavopicta	CD	RP	RP	2
Bokermannohyla itapoty	CD	RP		2
Bokermannohyla juiju	CD	RT	RP	?
Bokermannohyla martinsi	QFe		RP	2
Bokermannohyla nanuzae	EM		RP	2
Bokermannohyla oxente	CD	RP	RP	2

Bokermannohyla sagarana	EM	RT, RP		?
Bokermannohyla saxicola	QFe, EM	RP	RP	2
Corythomantis botoque	EM, CD	RP		?
Nyctimantis galeata	CD	RP, LT		?
Scinax cabralensis	EM	LT		1, 2
Scinax curicica	QFe, EM, CD	LT, LP, RP, RT		1, 2
Scinax machadoi	EM, CD	RP		2
Scinax montivagus	CD	LT, LP, RP, RT	LT, LP, RP, RT	1
Sphaenorhynchus canga	QFe	LP, LT		1
Phyllomedusidae				
Phasmahyla jandaia	QFe, EM		RP	25
Pithecopus megacephalus	EM	RT		25
Hylodidae				
Crossodactylus trachystomus	QFe, EM		RP	3
Hylodes otavioi	EM		RP	3
Hylodes uai	QFe		RP	3
Leptodactylidae				
Crossodactylodes itambe	EM	BR		26
Leptodactylus avivoca	EM	AT, RT		?
Leptodactylus camaquara	QFe, EM	AT, RT		30
Leptodactylus oreomantis	CD	AT, RT		?
Physalaemus claptoni	EM		LT	?
Physalaemus deimaticus	EM	RT		?
Physalaemus erythros	QFe	RT		28
Physalaemus evangelistai	QFe, EM	LT		28
Physalaemus orophilus	QFe, EM		LP, LT	28
Pleurodema alium	EM, CD	LT		11
Pseudopaludicola mineira	EM	AT, LT		1
Rupirana cardosoi	CD	AT, RT, RP		1
Odontophrynidae				
Odontophrynus juquinha	EM, CD	LT		1
Proceratophrys cururu	EM	RT, RP		2
Proceratophrys minuta	CD		RP	2
Proceratophrys redacta	CD	RT, RP		2

Apesar do aumento de estudos que resultaram em novas descrições de espécies, a anurofauna do Espinhaço ainda não é totalmente conhecida. O Brasil é o país com o maior potencial para futuras descobertas de espécies, incluindo de anfíbios (Moura & Jetz 2021) e há indícios de que o Espinhaço pode ser uma região de grande interesse e relevância neste sentido. Estudos apontaram a existência de espécies possivelmente novas e endêmicas, que ainda carecem de uma descrição formal. Dentre estas, inclui-se duas espécies do gênero *Ischnocnema* (Silveira et al. 2019), *Aplastodiscus* aff. *arildae* (Silveira et al. 2019), *Scinax* aff. *machadoi* (Leite et al. 2019b), *Proceratophrys* sp. (Mângia et al. em preparação), *Crossodactylodes* sp. (Santos et al. 2020b, 2021) e três espécies com afinidade à *Bokermannohyla saxicola* (Nascimento et al. 2018).

Além da descrição da morfologia dos anuros na fase adulta, dados bioacústicos e larvais também fornecem importantes caracteres para a taxonomia destes animais (Grosjean 2005, Köhler et al. 2017). Os girinos das espécies endêmicas com desenvolvimento indireto são relativamente bem conhecidos e apenas nove deles não foram descritos (i.e., *Boana botumirim, Bokermannohyla juiju, B. sagarana, Scinax cabralensis, Leptodactylus avivoca, Physalaemus claptoni, P. deimaticus, Pleurodema alium* e *Proceratophrys redacta*. Quanto à bioacústica, apenas quatro espécies não têm o canto descrito (i.e., *Boana cipoensis*, *Bokermannohyla sagarana*, *Physalaemus deimaticus* e *Pleurodema alium*).

Das 44 espécies endêmicas, 14 estão restritas ao Espinhaço Mineiro, 12 à Chapada Diamantina e quatro ao Quadrilátero Ferrífero (Tabela 1; Fig. 6). Oito espécies são compartilhadas entre o Espinhaço Mineiro e o Quadrilátero Ferrífero e cinco entre o Espinhaço Mineiro e a Chapada Diamantina (Tabela 1; Fig. 6). Apenas *Scinax curicica* ocorre nas três regiões (Tabela 1; Fig. 6, desde o Quadrilátero Ferrífero até o sul da Chapada Diamantina, na região do Pico da Almas.

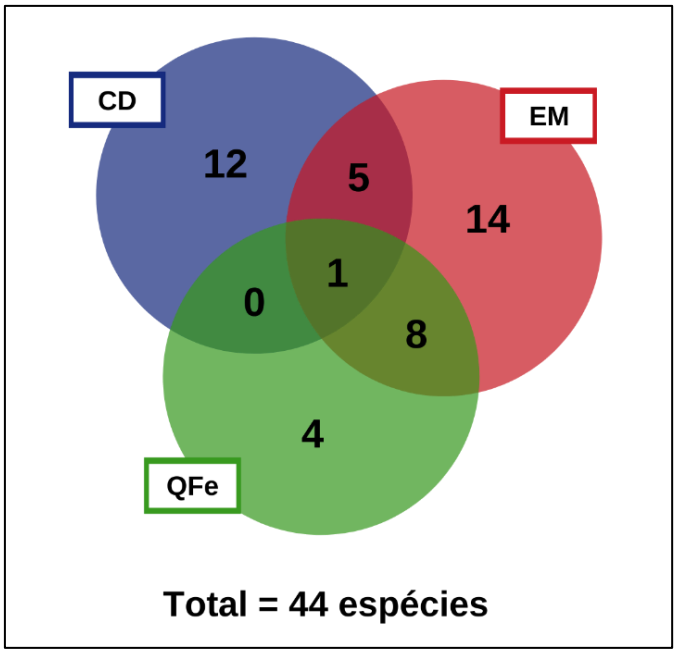

Figura 6. Diagrama de Venn-Euler indicando a contagem de espécies endêmicas exclusivas e compartilhadas em cada porção da Serra do Espinhaço, no leste do Brasil. Os números centrais nos círculos indicam a contagem de espécies exclusivas de cada área (CD = Chapada Diamantina (azul), EM = Espinhaço Mineiro (vermelho), QFe = Quadrilátero Ferrífero (verde)) e os números nas interseções indicam a contagem de espécies endêmicas compartilhadas por cada região delimitada

Com base nas localidades disponíveis na literatura e na Coleção Herpetológica do Centro de Coleções Taxonômicas da Universidade Federal de Minas Gerais (CCT-UFMG), avaliamos a riqueza de endemismos ao longo da Serra do Espinhaço. Para isto, sobrepusemos a distribuição conhecida de todas as espécies endêmicas em um único mapa com resolução espacial de grade de célula 0,3° usando o software ArcGis™. As maiores riquezas de endemismo estão localizadas no sul do Espinhaço Mineiro, em áreas que correspondem à Serra do Cipó, onde uma única quadrícula pode abrigar até 20 espécies endêmicas (Fig. 7). A região central da Chapada Diamantina apresenta endemismo intermediário, com diminuição em direção ao norte da Bahia. O mesmo acontece com a região central do Espinhaço Mineiro (Botumirim), que apresenta valores moderados de riqueza de endemismo. Essa riqueza diminui em direção ao norte de Minas Gerais, exceto pela região de Rio Pardo de Minas que apresenta um alto valor para este índice (Fig. 7). A Serra do Cabral também apresenta endemismo moderado. Diferenças no número de espécies endêmicas podem estar relacionadas ao menor esforço de amostragem realizado no norte do Espinhaço Mineiro e Chapada

Diamantina em relação ao sul do Espinhaço Mineiro e Quadrilátero Ferrífero (Leite et al. 2012). Entretanto, o maior endemismo no Espinhaço Mineiro pode não ser apenas um artefato amostral, e estar relacionado com as afinidades geográficas desta área com a Mata Atlântica, a região com a anurofauna mais rica do país (Rossa-Feres et al. 2017).

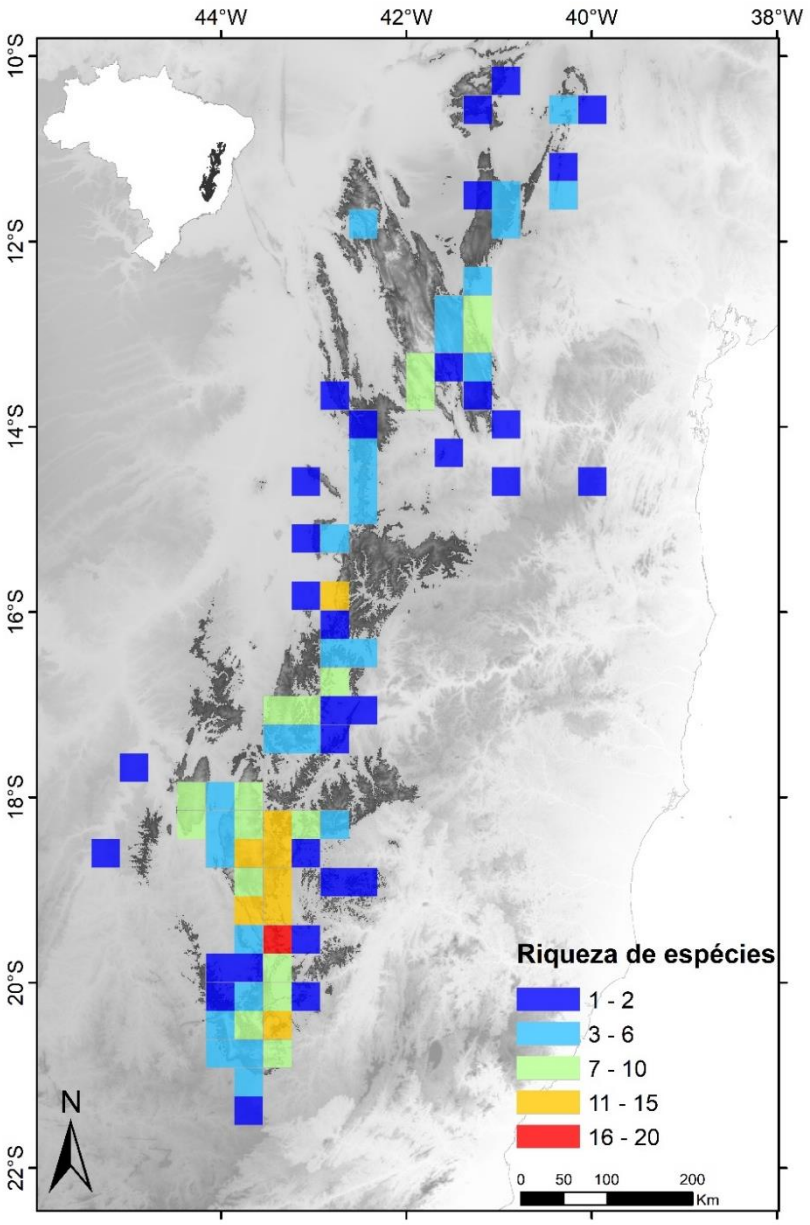

Figura 7. Mapa de endemismo de anuros na Serra do Espinhaço em quadriculas de 0.3° x 0.3°, baseado nos pontos de ocorrência das espécies. Altitudes a cima de 850 m em cinza escuro

Ecologia, comportamento e história natural

A diversidade de modos reprodutivos dos anuros está relacionada a uma combinação de aspectos ecológicos, comportamentais e morfofisiológicos das diferentes espécies, como: 1) locais escolhidos para oviposição (aquáticos, terrestres ou arbóreos); 2) tipos de desenvolvimento larval (indireto – com larvas exotróficas, ou direto – larvas endotróficas); 3) tipos de corpos d'água (lênticos – brejos, poças e lagoas; lóticos – córregos e riachos); 4) especificidades de micro-habitat em que as desovas são depositadas (e.g., cavidades subterrâneas, câmaras subaquáticas, cavidades de plantas, rochas úmidas); 5) características do ninho (e.g., ninhos de espumas ou bolhas); 6) presença de cuidado parental, dentre outros (Haddad & Prado 2005, Malagoli et al. 2021).

Os anuros endêmicos da Serra do Espinhaço estão presentes em áreas abertas ou em matas de galeria e florestas de encosta (Tabela 1). Nestes ambientes, eles apresentam pelo menos 12 diferentes modos reprodutivos, sendo que para algumas das espécies não são conhecidos aspectos reprodutivos que permitam a classificação segundo Haddad & Prado (2005). Oito modos reprodutivos reportados para os anuros da Serra do Espinhaço são típicos de linhagens da Mata Atlântica (modos 2, 3, 5, 19, 21, 25, 26, 28) e os demais podem ser observados tanto em linhagens de áreas abertas quanto florestais (modos 1, 4, 11, 30; Haddad & Prado 2005). Apenas duas espécies (*Haddadus aramunha* e *Pristimantis rupicola*; Figs. 4b,c) apresentam desenvolvimento direto, ou seja, têm o estágio larval suprimido. Todas as demais espécies necessitam de corpos d'água para reprodução (Tabela 1).

Uma alta diversidade funcional de anuros tem sido registrada para a Serra do Espinhaço também como reflexo da riqueza de ambientes reprodutivos e da diversidade filogenética. Pezzuti e colaboradores (2019), estudaram a morfologia e aspectos ecológicos de girinos de 67 espécies de anuros do Quadrilátero Ferrífero. Os girinos estudados representam 12 das 15 guildas ecomorfológicas de girinos exotróficos conhecidos para o mundo (McDiarmid & Altig 1999). Essa diversidade é consideravelmente maior se comparada à fauna de girinos em outras regiões brasileiras, tanto da Mata Atlântica (Fatorelli et al. 2018, Dubeux et al. 2020) quanto do Cerrado (Rossa-Feres & Nomura 2006).

Riachos e córregos são corpos d'água abundantes no campo rupestre e diversas espécies endêmicas os utilizam para a reprodução e desenvolvimento larval (Eterovick & Barata 2006, Pezzuti et al. 2019). O volume do riacho, o número de predadores de girinos, a diversidade de microhabitats e a cobertura relativa da vegetação arbórea marginal são características importantes que determinam a composição das assembleias larvais (Eterovick &

Barata 2006). Diversas espécies utilizam poços com baixo fluxo de água nos riachos para oviposição e/ou para o desenvolvimento larval (Eterovick et al. 2020). Como este recurso é limitado, é comum que os machos das espécies que os utilizam defendam esses territórios. Fidelidade de habitats reprodutivos em ambientes lóticos (Figs. 2a,8a,9a) foi reportada para machos de *B. alvarengai* (Fig. 3c; Centeno et al. 2015b) e *P. megacephalus* (Fig. 8c; Oliveira et al. 2012). Machos de *B. alvarengai* são maiores do que as fêmeas, apresentam pré-pólex e membros anteriores hipertrofiados, não se agregam espacialmente, e muitos deles apresentam cicatrizes de luta no dorso (Sazima & Bokermann 1977, Centeno et al. 2015b, Centeno et al. 2021), o que reforça a hipótese da territorialidade. Um padrão similar foi observado para *B. martinsi* (Figs. 2b,c,d), além do relato de luta entre machos (Magalhães et al. 2018). Portanto, é possível que a territorialidade seja um aspecto comportamental comum em espécies de riacho do Espinhaço, já que estes habitats são essenciais para a reprodução de muitas das espécies endêmicas (Tabela 1).

Adaptações morfofisiológicas de anfíbios às condições ambientais da Serra do Espinhaço, como altos índices de radiação solar e condições extremas de calor e frio são pouco conhecidas. Um estudo recente investigou a morfologia e aspectos bioquímicos das secreções lipídicas da pele de *B. alvarengai*, espécie frequentemente encontrada repousando sob luz solar por longos períodos do dia (Centeno et al. 2015a). Esse comportamento, que auxilia na termorregulação da espécie, envolve mudanças na coloração da pele que auxiliam na refletância de luz (Eterovick et al. 2006; Centeno et al. 2015a). Além disso, uma camada extra-epidérmica, formada por compostos lipídicos, sobre superfície dorsal do animal e dobras cutâneas bem desenvolvidas na região ventral e uma extensa hipervascularização, podem desempenhar um papel importante na prevenção de perda excessiva e reabsorção de água (Centeno et al. 2015a). Estratégias adaptativas similares parecem ser mais comuns em espécies que ocorrem em regiões relativamente altas (Vences et al., 2002). O comportamento de exposição ao sol já foi relatado para outras espécies do gênero associadas a afloramentos rochosos (Brandão et al. 2012) e, no Espinhaço, também foi observado em *B. sagarana* (T.L. Pezzuti, observação pessoal), o que sugere que a exposição ao sol seja comum nas espécies rupícolas do gênero.

Estudos comportamentais com girinos de espécies endêmicas do Espinhaço têm demostrado o valor adaptativo dos padrões de coloração em relação ao potencial críptico e estratégias de defesa à predadores visualmente orientados. Girinos de *B. alvarengai* (Fig. 3d) e *S. machadoi*, apresentam colorações disruptivas, pela presença de manchas douradas e listras que quebram o contorno do corpo, e ao se sentirem ameaçados escolhem áreas do riacho

que maximizam sua camuflagem ao substrato (Espanha et al. 2016, Eterovick et al. 2018). Entretanto, tal comportamento não foi observado para girinos de outras espécies, como *B. martinsi* (Fig. 2d) e *B. saxicola* (Fig. 4b; Espanha et al. 2016, Eterovick et al. 2018). Outros fatores como a alta incidência solar ou sombreamento dos corpos d'água, podem estar relacionados a seleção dos padrões de coloração, como os padrões melânicos encontrados em girinos de *B. martinsi* e *B. nanuzae* (Leite & Eterovick 2010), assim como hipotetizado para algumas linhagens de áreas montanhosas (Faivovich et al. 2013). Essas e outras correlações entre uso de habitat e estratégias adaptativas de girinos de campos rupestres, como morfologias especializadas à riachos de corredeiras e tipos de desenvolvimento em ambientes frios, permanecem por ser investigados.

Figura 8. Ambiente de reprodução de anuros em Itacambira/MG, no Espinhaço Mineiro (A); *Scinax curicica* (B); Adulto (C) e girino (D) de *Pithecopus megacephalus*. Fotos: Tiago L. Pezzuti

Evolução e biogeografia

Entre as 44 espécies endêmicas da Serra do Espinhaço (Tabela 1), 26 já foram incluídas em análises filogenéticas amplas, que abrangeram a maioria das espécies do grupo e que apresentaram topologias sólidas, bem resolvidas e com nós suportados. Apesar de poucos destes trabalhos terem reconstruído a biogeografia dos grupos amostrais (Carvalho et al. 2021, Vasconcellos et al. 2021), é possível sugerir a origem das espécies endêmicas, baseando-se na distribuição geográfica das espécies irmãs, em cladogramas taxonômicos de áreas (i.e., substituindo as espécies pelas áreas onde elas ocorrem) e no mapeamento destas áreas através da parcimônia. Note que aqui, nós não pretendemos reconstruir a biogeografia das espécies endêmicas nem inferir as suas origens de maneira definitiva. O objetivo é apenas avaliar as filogenias superficialmente e gerar hipóteses testáveis para posteriores investigações biogeográficas. Desta maneira, foram identificadas quatro possíveis origens principais para a anurofauna endêmica do Espinhaço. Na primeira delas, os endêmicos são espécies derivadas que fazem parte de clados compostos majoritariamente ou exclusivamente por espécies da Mata Atlântica. Estão incluídos neste grupo *Aplastodiscus heterophonicus* (Pinheiro et al. 2021), *Crossodactylodes itambe* (Santos et al. 2020a, b), *Thoropa megatympanum* (Fig. 4d; Sabbag et al. 2018), *Sphaenorhynchus canga* (Araujo-Vieira et al. 2019), *Physalaemus evangelistai* (Lourenço et al. 2015), *Proceratophrys cururu* (Magalhães et al. 2020, Mângia et al., 2020) e *Phasmahyla jandaia* (Faivovich et al. 2010). A origem de *Pseudopaludicola mineira* parece ser o resultado da ocupação do Espinhaço por um ancestral de savanas do Cerrado (Veiga-Menoncello 2014). *Pleurodema alium*, por sua vez, originou-se de um ancestral da Caatinga (Faivovich et al. 2012, Thomé & Carstens 2016). Por fim, *Rupirana cardosoi* corresponde a um gênero endêmico originado *in situ*, sendo considerado um relicto biogeográfico (Fouquet et al. 2013, Santos et al. 2020b).

Em alguns gêneros, existem clados compostos exclusivamente por espécies endêmicas do campo rupestre, sejam elas restritas ao Espinhaço ou não. É o caso dos *Physalaemus* do clado de *P. deimaticus*, um grupo monofilético que inclui *P. claptoni*, *P. deimaticus*, *P. erythros* e *P. rupestris*, sendo os três primeiros restritos ao Espinhaço e o último endêmico de disjunções do campo rupestre no complexo serrano da Mantiqueira (Lourenço et al. 2015, Leal et al. 2020). Outro exemplo inclui *Boana botumirim* e *B. cipoensis*, espécies irmãs que compartilham um ancestral do Cerrado e especiaram-se *in situ* (Vasconcellos et al. 2021). Como as duas espécies habitam o campo rupestre *lato sensu* (Caramaschi et al. 2009, Eterovick et al. 2020), deduz-se que o seu ancestral comum também habitava este tipo de ambiente no domínio. É possível que a

especiação *in situ* também tenha sido responsável pela origem de *Proceratophrys minuta* e *P. redacta*, um clado monofilético e endêmico da Chapada Diamantina (Magalhães et al. 2020, Mângia et al. 2020).

Carvalho e colaboradores (2021) reconstruíram a filogenia e a biogeografia do clado de *Leptodactylus plaumanni,* que possui nove espécies e inclui *L. avivoca*, *L. camaquara* e *L. oreomantis*, endêmicas da Serra do Espinhaço. Segundo os autores, o clado surgiu no Espinhaço durante o Mioceno (~6,4 Ma; 95% HDP = 10,0–3,6 Ma), com *L. camaquara* sendo o primeiro a divergir das demais espécies. Apesar das três espécies não constituírem um clado, a reconstrução das áreas dos ancestrais de *L. avivoca* e *L. oreomantis* indicam que a linhagem continuou se diversificando na Serra do Espinhaço concomitantemente à colonização de novas áreas de montanha do Brasil, como a Serra da Mantiqueira, Chapada dos Veadeiros e Planalto Central, assim como de áreas baixas da Mata Atlântica (e.g., *L. marambaiae*, que ocorre em restingas).

O clado das pererecas-macaco de altitude do gênero *Pithecopus* é composto por seis espécies, sendo *P. rohdei* endêmica da Mata Atlântica (Ramos et al. 2019), *P. rusticus* restrita a campos naturais em áreas altas da Serra Geral, em Santa Catarina (Bruschi et al. 2014) e *P. ayeaye*, *P. centralis*, *P. megacephalus* e *P. oreades* endêmicas do campo rupestre (Faivovich et al. 2010, Magalhaes et al. 2017, Magalhães et al. 2018, Ramos et al. 2018). *Pithecopus megacephalus*, a única destas espécies endêmica da Serra do Espinhaço (Tabela 1), é mais aparentada com a espécie de Mata Atlântica do que com as demais espécies rupícolas, que formam um clado monofilético (Faivovich et al. 2010). Duas hipóteses biogeográficas poderiam explicar este padrão: (i) o clado possui um ancestral rupícola e linhagens derivadas se expandiram para a Mata Atlântica e para os campos da Serra Geral ou (ii) a ocupação do campo rupestre ocorreu através de dois eventos independentes, com um ancestral originário da Mata Atlântica e as demais espécies originadas *in situ*. É notável que, apesar de não serem irmãs, estas espécies de *Pithecopus* endêmicas do campo rupestre apresentam uma série de convergências, incluindo o padrão de coloração reticulado, o modo reprodutivo (*sensu* Haddad & Prado 2005; Tabela 1) e seleção reprodutiva *K* ao invés de *r*, que é a mais comum nas outras espécies do gênero (Faivovich et al. 2010, Oliveira 2017).

Corythomantis e *Haddadus* possuem origens biogeográficas ambíguas, já que ambos possuem apenas duas espécies descritas e que ocupam habitats distintos (Amaro et al. 2013, Marques et al. 2021). *Haddadus aramunha* é endêmica do campo rupestre na Chapada Diamantina e é um dos únicos craugastorídeos que ocupam áreas abertas, já que a maioria do

grupo habita florestas, incluindo a espécie irmã *H. binotatus* (Cassimiro et al. 2008, Amaro et al. 2013). Sendo assim, tanto um ancestral florestal quanto um campestre são alternativas igualmente parcimoniosas para a origem do gênero. Contudo, a distribuição majoritariamente florestal da família (Cassimiro et al. 2008) favorece a primeira hipótese. *Corythomantis botoque* é uma espécie recém descrita e endêmica do Espinhaço Mineiro e Chapada Diamantina (Marques et al 2021). A outra espécie do gênero, *C. greeningi*, possui ampla distribuição na Caatinga e em áreas de transição entre este domínio e o Cerrado (Silva et al. 2014, Marques et al. 2021). Assim como em *Haddadus*, a origem do ancestral de *Corythomantis* na Caatinga ou no campo rupestre são hipóteses igualmente plausíveis.

Pode-se dizer também que há incertezas biogeográficas quanto à origem de *Nyctimantis galeata.* A perereca faz parte de um gênero com sete espécies, a maioria delas florestais (Blotto et al. 2021, Frost 2021). Apesar disso, ela integra um clado com uma espécie que se distribui no Chaco e nos Pampas na Argentina, Paraguai e Uruguai (i.e., *N. siemersi*; Cajade et al. 2010, Lajmanovích et al. 2012), uma na Amazônia Ocidental (i.e., *N. rugiceps*), duas espécies da Mata Atlântica (i.e., *N. bokermanni* e *N. pomba*) e uma com distribuição em matas do Cerrado (i.e., *Nyctimantis* sp., R.A. Brandão, informação pessoal), sendo irmã de um clado formado por esta última mais *N. pomba* (Blotto et al. 2021). Neste caso, é possível que a linhagem ancestral de *N. galeata* ocupasse o Espinhaço e tenha se expandido subsequentemente para o Cerrado e a Mata Atlântica ou que ela tenha colonizado o campo rupestre a partir de um destes domínios. Apesar de aspectos da história natural de *N. galeata* serem pouco conhecidos, estudos recentes apontam que a espécie apresenta preferência por áreas abertas (Dias et al. 2020, Magalhães et al. 2021), característica compartilhada, em parte, apenas com *N. siemersi* (Lajmanovích et al. 2012).

Odontophrynus juquinha é irmã de uma espécie não descrita, afim de *O. americanus*, distribuída em áreas altas da Serra da Mantiqueira (Rosset et al. 2021). Estes dois sapos compõem um clado que inclui táxons majoritariamente distribuídos em áreas abertas subtropicais da América do Sul (Rosset et al. 2006). Este padrão de relacionamento entre a Serra do Espinhaço e domínios subtropicias, como os Pampas ou o Chaco, já foi observado para linhagens de *Scinax pinimus* (Baldo et al. 2019) e *S. squalirostris* (Abreu-Jardim et al. 2021). Contudo, não se sabe quais processos resultaram na ocupação destes ambientes por estas espécies.

Pristimantis rupicola representa um enigma biogeográfico. A espécie é irmã de *P. gaigei*, uma rã-de-folhiço distribuída em florestas tropicais da Costa Rica, Panamá e Colômbia

(Taucce et al. 2020, Frost 2021). A única outra espécie rupestre do gênero, *P. hoogmoedi*, não parece proximamente relacionada à *P. rupicola*, assim como as outras espécies que habitam o Brasil (Taucce et al. 2020). Portanto, entender a ocupação da Serra do Espinhaço por *P. rupícola* é essencial para a elucidação das origens e dos processos que resultaram na diversificação da anurofauna endêmica da região.

Bokermannohyla é um gênero composto por 30 espécies (Frost 2021), sendo o mais diversificado da Serra do Espinhaço, com 10 espécies endêmicas (Tabela 1). Curiosamente, o relacionamento filogenético destas espécies ainda não foi testado, mas é possível que a região seja um centro de diversificação para o gênero. Os representantes da família Hylodidae endêmicos do Espinhaço (Tabela 1) também não foram incluídos em filogenias abrangentes. A despeito disto, como a maioria dos membros desta família são encontrados na Mata Atlântica (Frost 2021), é provável que os ancestrais de *Crossodactylus trachystomus*, *Hylodes uai* e *H. otavioi* sejam originários deste domínio (Heyer 1999). Além dessas espécies, o posicionamento filogenético de *Physalaemus orophilus*, *Scinax cabralensis* (Fig. 4c), *S. curicica* (Fig. 8b), *S. machadoi* e *S. montivagus* também não foram avaliados.

A origem dos anuros endêmicos não foi concomitante ao surgimento da Serra do Espinhaço. A região tem origem Pré-Cambriana e atualmente experimenta estabilidade geológica (Silveira et al. 2016). Poucos estudos investigaram o tempo de diversificação das espécies endêmicas, entretanto, estes estimaram datas relativamente recentes, entre o Mioceno e o Pleistoceno (e.g., Sabbag et al. 2018, Santos et al. 2020b, Carvalho et al. 2021, Oliveira et al. 2021). O número de estudos filogeográficos tem crescido nos últimos anos (e.g., Ramos et al. 2018, Oliveira et al. 2021, Magalhães et al. 2021). Apesar disso, eles ainda são escassos e faltam muitas evidências para a melhoria do entendimento dos processos de diversificação que levaram ao elevado número de endemismos na Serra do Espinhaço (Miola et al. 2021). Processos distintos e independentes têm sido relatados como importantes para a diversificação e evolução da anurofauna do Espinhaço, sugerindo diferentes pulsos de diversificação ao longo da história. A colonização de novas áreas, por exemplo, foi o principal processo evocado para explicar a distribuição geográfica atual da diversidade genética de *Bokermannohyla alvarengai* (Oliveira et al. 2021). Já a fragmentação, um importante processo para a evolução de diversas espécies de plantas (Silveira et al. 2020), também está envolvida na diversificação de *Crossodactylodes itambe* e *Rupirana cardosoi* (Santos et al. 2020b). Por outro lado, o fluxo gênico, entre diferentes linhagens ou com espécies não endêmicas, também parece influenciar a

diversidade atual, tendo sido identificado entre *Pleurodema alium* e *P. diplolister* (Thomé et al. 2016) e entre *Pithecopus megacephalus* e *P. ayeaye* (Magalhães et al. 2021).

Embora os processos envolvidos na diversificação e os eventos cladogenicos aparentemente não serem coincidentes entre as diferentes espécies endêmicas, alguns padrões espaciais têm sido recuperados em trabalhos filogeográficos recentes (e.g., Nascimento et al. 2018, Ramos et al. 2018, Sabbag et al. 2018, Oliveira et al. 2021). A mais recorrente dessas quebras filogeográficas é a depressão entre o planalto de Diamantina e a Serra de Itacambira (16S e 42W), no Espinhaço Mineiro, conhecida como Depressão de Couto de Magalhães (Fig. 1; Saadi, 1995). Esta barreira foi observada em *Pithecopus megacephalus* e em *Thoropa megatympanum* (Ramos et al., 2018; Sabbag et al., 2018). Apesar de *Bokermannohyla saxicola* e *B. alvarengai* apresentarem estruturação nesta mesma região, a localização exata da barreira não é idêntica entre estas espécies (Nascimento et al. 2018, Oliveira et al. 2021). Aspectos biológicos e história natural das espécies podem estar relacionados com essas diferenças, mas a região e as espécies devem ser melhor investigadas para entendermos a evolução no local.

As áreas baixas entre a Serra do Cabral e o espigão central do Espinhaço Mineiro (Fig. 1), podem ter atuado como uma barreira contínua entre diferentes populações e espécies. Ela parece ser um importante limite para a distribuição de algumas espécies de anuros ao longo do Espinhaço. *Bokermannohyla sagarana* e *Scinax cabralensis*, por exemplo, estão restritas a Serra do Cabral, enquanto *B. alvarengai*, não ocorre nesta serra (Oliveira et al. 2021). Apesar de outras espécies, como *B. saxicola* e *T. megatympanum*, estarem amplamente distribuídas na Serra do Cabral e no espigão central do Espinhaço Mineiro, elas apresentam estruturação genética entre essas áreas (Sabbag 2013, Nascimento et al. 2018).

Conservação

Os anfíbios são espécies indicadoras e sensíveis às mudanças ambientais (Hopkins 2007). Suas estratégias de reprodução, comportamento e fisiologia os tornam vulneráveis a diversas ameaçadas nos diferentes estágios de vida (Bolochio et al. 2020). Como consequência, aproximadamente 41% das espécies de anfíbios do mundo estão sob algum grau de ameaça (IUCN 2021a). Na cadeia do Espinhaço, entre as espécies endêmicas apenas *Crossodactylodes itambe* e *Bokermannohyla sagarana* estão categorizadas em algum nível de ameaça de extinção (Tabela 2; IUCN 2021b). Outras três, *B. martinsi, H. otavioi* e *N. galeata*, estão categorizadas como quase ameaçadas (Tabela 2; IUCN 2021b). Um dos possíveis motivos para a baixa taxa

de espécies ameaçadas é que a Serra do Espinhaço possui uma ampla rede de unidades de conservação (UCs) de proteção integral (categorias I-IV da IUCN; Brasil 2000), tais como parques nacionais e estaduais, monumentos naturais e estações ecológicas.

A perda e fragmentação de habitat são as principais ameaças à distribuição e persistência de anfíbios (Baillie 2004). As ameaças à integridade e qualidade dos habitats e persistência dos anuros endêmicos da cadeia do Espinhaço podem variar em fonte e intensidade, de acordo com particularidades dos locais em que estão distribuídos. O campo rupestre sofre grande pressão de atividades como a mineração, silvicultura, agricultura e urbanização (Fernandes et al. 2018), atividades prejudiciais à qualidade de habitats dos anuros ali distribuídos. A Serra do Cabral, por exemplo, sofre intenso uso do solo para cultivo de *Eucalyptus* e *Pinus.* Mesmo com o Parque Estadual na região, estas atividades estão alterando de maneira significativa as paisagens e foram identificadas como as principais ameaças às populações de *B. sagarana* (Leite et al. 2011). De maneira similar, as atividades antrópicas na Serra do Cabral podem estar ameaçando as demais espécies distribuídas na área, incluindo a diversidade genética de espécies distribuídas em outras regiões do Espinhaço (e.g., Sabbag 2013, Nascimento et al. 2018) e outras restritas, como *Scinax cabralensis* (Drummond et al. 2007). Espécies fitotelmatas, como *Crossodactylodes itambe*, sofrem ameaças adicionais à extensão e qualidade do seu habitat à medida que as plantas às quais elas estão associadas (i.e, bromélias) sofrem impactos naturais ou antrópicos isolados. O fogo e a remoção seletiva de plantas com valor comercial podem dizimar os microhabitats onde a espécie vive e se reproduz (Barata et al. 2013, Santos et al. 2020a). Apesar do fogo ser apontado como uma ameaça para algumas espécies de anuros do campo rupestre, Drummond e colaboradores (2018), ao analisaram uma área do Parque Estadual do Itacolomi, encontraram um aumento na riqueza total da assembleia de anuros após um evento de incêndio. Os autores sugerem que espécies generalistas ocuparam as áreas pós-queimada e que a heterogeneidade do campo rupestre pode proporcionar diferentes ambientes para os anuros locais se protegerem dos incêndios (Drummond et al. 2018). Entretanto, esta é uma observação pontual e o mesmo pode não se aplicar para espécies não generalistas, e outros locais e assembleias da Serra do Espinhaço.

Paisagens de beleza cênica e riachos encachoeirados distribuídos ao longo da Cadeia do Espinhaço atraem inúmeras pessoas anualmente. Entretanto, o turismo desordenado e desregulado pode impactar negativamente os habitats de espécies do campo rupestre, como identificado para *Bokermannohyla juiju* (Taucce et al. 2015) e *B. flavopicta* (Fig. 9b; Leite et al. 2012). O fungo quitrídeo [*Batrachochytrium dendrobatidis (Bd*)], responsável por causar

grandes declínios em populações de anuros ao redor do globo (Berger et al. 2016), soma-se à lista de ameaças identificados aos anuros endêmicos do Espinhaço. Amorim e colaboradores (2019) encontraram amostras positivas para o fungo na Chapada Diamantina, em *Rhinella rubescens* e em girino de uma *Bokermannohyla* não identificada. Contudo, pouco se sabe sobre a distribuição do *Bd* ao longo da cadeia e como ele está afetando as espécies endêmicas. Somada a essas ameaças diretas, as mudanças climáticas poderão ter um papel crucial para perda do campo rupestre até 2070, com uma estimativa de retração de 68% das áreas atuais climaticamente adequadas para o ecossistema (Fernandes et al. 2018), causando fragmentação e perda do habitat dos anuros endêmicos da cadeia do Espinhaço.

Espécies com distribuição restrita são mais vulneráveis a ações antrópicas e naturais adversas (Sodhi et al. 2008, González-del-Pliego 2019), e por isso, ações de conservação são necessárias. Diante da diversidade da herpetofauna, lacunas de conhecimento e elevada ameaça, um Plano de Ação Nacional (PAN para a conservação dos répteis e anfíbios ameaçados de extinção na Serra do Espinhaço) foi proposto em 2012 para aumentar o conhecimento sobre espécies-alvo e minimizar o efeito das ações antrópicas sobre elas (ICMBio 2012). O primeiro ciclo do PAN Herpetofauna do Espinhaço Mineiro se encerrou em 2017 com 55% das ações concluídas, assim, em 2018, foi aprovado um segundo ciclo, com o objetivo de implementar medidas que favoreçam a conservação das espécies e de seus habitats (ICMBio 2018).

Uma das maneiras de minimizar as ameaças e garantir a conservação da biodiversidade tem sido a criação de UCs. Ao todo, 32 UCs de Proteção Integral estão distribuídas ao longo da Serra do Espinhaço (considerando um limite altitudinal acima de 800 m), sendo 4 federais e 28 estaduais (MMA 2021a). A porção do Espinhaço em Minas Gerais (i.e., Espinhaço Mineiro e Quadrilátero Ferrífero) conta com três UCs federais e 23 estaduais, enquanto a porção na Bahia conta com apenas uma UC federal e cinco estaduais (Tabela 2). Diante do conjunto de UCs da Cadeia do Espinhaço, mosaicos foram propostos com o objetivo de criar uma gestão integrada entre gestores das UCs e população local, para compatibilizar, integrar e otimizar atividades desenvolvidas nas UCs, pensando na manutenção da biodiversidade, da sociodiversidade e desenvolvimento sustentável regional (MMA 2021b). Três mosaicos foram reconhecidos pelo Ministério do Meio Ambiente para a área da Cadeia do Espinhaço: O Mosaico do Espinhaço – Alto Jequitinhonha – Serra do Cabral pela portaria n° 444 (MMA 2010); o Mosaico da Serra do Cipó pela portaria n° 368 (MMA 2018a) e Mosaico da Serra do Espinhaço – Quadrilátero Ferrífero, através da portaria n° 473 (MMA 2018b). Apesar do alto número de UCs, poucas espécies foram avaliadas quanto a distribuição em seus limites (e.g., Barata et al. 2016, Ramos

et al. 2018). Entre as espécies restritas a cadeia do Espinhaço, apenas seis não foram amostradas em nenhuma UC de proteção integral, enquanto 10 espécies foram amostradas em apenas uma (Tabela 2). Contudo, a presença em UCs não garante, isoladamente, a proteção efetiva das espécies que nelas ocorrem, especialmente em áreas não florestais como o campo rupestre (Françoso et al. 2015, Geldmann et al. 2019). A atividade mineradora, por exemplo, está presente em várias áreas-chave para a conservação da biodiversidade e UCs do Espinhaço, contaminando corpos d'água cronicamente através da deposição continuada de rejeitos (Kamino et al. 2020).

Pesquisas centradas na conservação de espécies endêmicas de anfíbios do Espinhaço têm emergido nos últimos anos, incluindo investigações sobre genética da conservação (Eterovick et al. 2016, Ramos et al. 2018) e efeitos de estressores ambientais sobre a ontogenia de adultos e girinos (Eterovick et al. 2016, Lima et al. 2019), mas ainda são escassos.

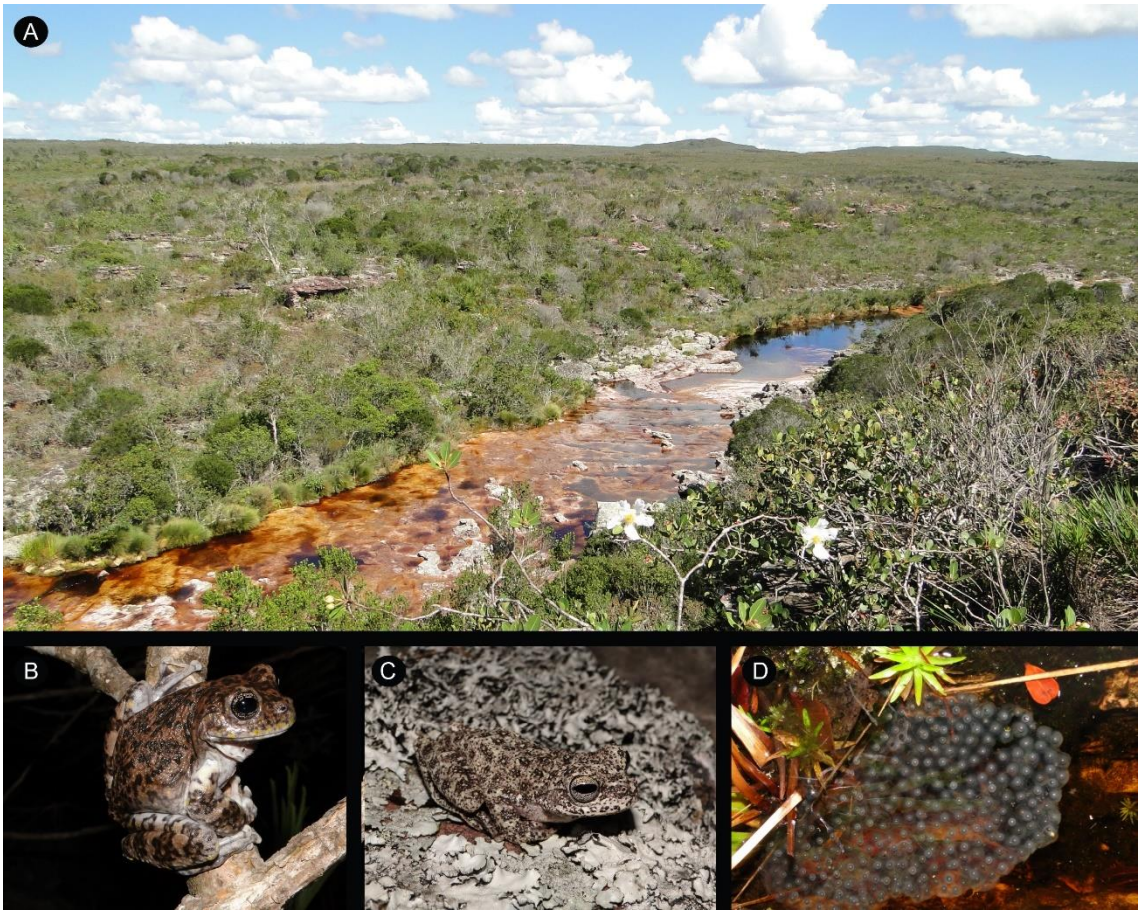

Figura 9. Ambiente de reprodução na Chapada Diamantina, Bahia (A); *Bokermannohyla flavopicta* (B); *B. itapoty* (C); desova de *Bokermannohyla*. Fotos: A, B: Leandro Drummond; C, D: Tiago L. Pezzuti

Tabela 2. Espécies endêmicas, categorias de ameaça nas últimas avaliações da IUCN (2021) e Brasileira (MMA 2014), e ocorrência dentro de Unidades de Conservação de proteção integral. Categorias de ameaça: LC = Menos preocupante, NE = Não avaliada, NT = Quase ameaçada, EN = Em perigo, CR = Criticamente em perigo, DD = Dados deficientes. Unidades de Conservação: 1 – Parque Nacional (PARNA) da Serra do Gandarela, 2 – PARNA da Serra do Cipó, 3 – PARNA das Sempre-Vivas, 4 – PARNA da Chapada Diamantina; MG: 1 – Parque Estadual (PE) da Serra do Ouro Branco, 2 – Monumento Natural Estadual (MONA) do Itatiaia, 3 – PE do Itacolomi, 4 – Estação Ecológica (EE) do Tripuí, 5 – MONA da Serra da Moeda, 6 – EE de Arêdes, 7 – EE dos Fechos, 8 – PE da Serra do Rola Moça, 9 – EE do Cercadinho, 10 – PE do Limoeiro, 11 – PE da Serra do Intendente, 12 – MONA da Várzea do Lageado, 13 – PE do Pico do Itambé, 14 – PE do Rio Preto, 15 – PE Biribiri, 16 – PE da Serra do Cabral, 17 – PE da Serra Negra, 18 – PE de Botumirim, 19 – EE de Acauã, 20 – PE de Grão Mogol, 21 – PE de Serra Nova e Talhado, 22 – PE de Montezuma, 23 - EE Mata dos Ausentes; BA: 24 – PE do Morro do Chapéu, 25 – PE das Sete Passagens, 26 – MONA da Cachoeira do Ferro Doido, 27 – PE Caminho das Gerais, 28 – PE da Serra dos Montes Altos.

Táxon	**Lista Vermelha**		**Presença em UC Integral**	
	IUCN 2021	**Brasil 2014**	**Federal**	**Estadual**
Craugastoridae				
Haddadus aramunha	LC	NE	4	25
Pristimantis rupícola	NE	NE	-	-
Cycloramphidae				
Thoropa megatympanum	LC	NE	2, 3	11, 13, 14, 16, 17, 18, 20, 21
Hylidae				
Aplastodiscus heterophonicus	NE	NE	-	-
Boana botumirim	LC	NE	3	13, 14 16, 18, 21
Boana cipoensis	LC	NE	2	11
Bokermannohyla alvarengai	LC	NE	1, 2, 3	1, 11, 13, 14, 18, 20, 21, 27
Bokermannohyla diamantina	LC	DD	-	21, 28
Bokermannohyla flavopicta	LC	NE	-	-
Bokermannohyla itapoty	LC	NE	4	-
Bokermannohyla juiju	LC	DD	4	-
Bokermannohyla martinsi	NT	NT	1	1, 2, 3, 5
Bokermannohyla nanuzae	LC	NE	2, 3	11, 13, 14, 17
Bokermannohyla oxente	LC	NE	4	25

Bokermannohyla sagarana	EN	NE	-	16
Bokermannohyla saxicola	LC	NE	1, 2, 3	11, 13, 14, 15, 16, 17, 18, 19, 20, 21
Corythomantis botoque	NE	NE	-	16
Nyctimantis galeata	NT	NE	-	26
Scinax cabralensis	LC	DD	-	16
Scinax curicica	LC	NE	1, 2, 3, 4	1, 2, 3, 11, 13, 14
Scinax machadoi	LC	NE		11, 13, 14, 16, 17, 18, 20, 21
Scinax montivagus	NE	NE	4	25, 26
Sphaenorhynchus canga	LC	NE	-	-
Phyllomedusidae				
Phasmahyla jandaia	LC	NE	1	1
Pithecopus megacephalus	LC	NE	2, 3	11, 14, 18, 20, 21
Hylodidae				
Crossodactylus trachystomus	LC	NE	2, 3	1, 13, 14, 21
Hylodes otavioi	NT	DD	-	11
Hylodes uai	LC	NE	-	3
Leptodactylidae				
Crossodactylodes itambe	CR	DD	-	13
Leptodactylus avivoca	NE	NE	3	21
Leptodactylus camaquara	LC	NE	2, 3	11, 13, 14, 18, 20, 21
Leptodactylus oreomantis	LC	NE	4	-
Physalaemus claptoni	DD	NE	-	-
Physalaemus deimaticus	LC	DD	2	13
Physalaemus erythros	LC	DD	1	3
Physalaemus evangelistai	LC	NE	1, 2	1, 3, 11, 14
Physalaemus orophilus	LC	NE	-	10, 11, 13
Pleurodema alium	LC	NE	-	-
Pseudopaludicola mineira	LC	NE	2, 3	11, 13, 14, 16
Rupirana cardosoi	LC	NE	4	24, 26
Odontophrynidae				
Odontophrynus juquinha	LC	NE	-	11, 18, 21
Proceratophrys cururu	LC	NE	2, 3	11, 13, 14
Proceratophrys minuta	LC	NE	4	25
Proceratophrys redacta	LC	NE	-	24, 26

Conclusão

A Serra do Espinhaço é considerada um laboratório natural para pesquisas de ecologia e evolução (Silveira et al. 2016, Miola et al. 2021). Apesar disto, o conhecimento sobre aspectos biológicos das espécies de anuros endêmicas da área ainda é escasso. Muitos dos estudos sobre ecologia, evolução, biogeografia e conservação são incipientes, revelando a necessidade e oportunidades de investigações científicas. Ainda não existem estudos sobre os efeitos de gradientes ambientais (e.g., altitudinais e latitudinais) sobre a diversidade de anfíbios da região, por exemplo. Também há uma grande carência de pesquisas sobre adaptações das espécies endêmicas às condições ambientais do campo rupestre (Miola et al. 2021). A falta de dados básicos da biologia das espécies endêmicas bem como espécies endêmicas não descritas são um fator preocupante para a conservação e manutenção da fauna local. Com este capítulo nós ressaltamos a importância de compilações periódicas para atualização do estado do conhecimento das espécies endêmicas da Serra do Espinhaço, e esperamos facilitar e incentivar a realização de novos estudos na região.

Agradecimentos

Nós agradecemos a Marcus Thadeu T. Santos pela revisão e contribuições ao texto. CBO agradece à FAPEMIG e à CAPES por suas bolsas de doutorado. TLP agradece à CAPES pela bolsa PNPD (88887.468027/2019-00). FSFL agradece à FAPEMIG e Fundação Vale (FAPEMIG/VALE: RDP-00004-17) e FAPEMIG (APQ-01796-15; APQ-00413-16).

Referências Bibliográficas

Abreu-Jardim TPF, Jardim L, Ballesteros-Mejia L, Maciel NM, Collevatti RG (2021) Predicting impacts of global climatic change on genetic and phylogeographical diversity of a Neotropical treefrog. Diversity and Distributions 27:1519-1535.

Afonso LG, Eterovick PC (2007a) Microhabitat choice and differential use by anurans in forest streams in southeastern Brazil', Journal of Natural History 41:937-948.

Afonso LG, Eterovick PC (2007b) Spatial and temporal distribution of breeding anurans in streams in southeastern Brazil. Journal of Natural History 41:949-963.

Amorim FO, Pimentel LA, Machado LF, Cavalcanti ADC, Napoli MF, Juncá FA (2019) New records of *Batrachochytrium dendrobatidis* in the state of Bahia, Brazil: histological analysis in anuran amphibian collections. Diseases of Aquatic organisms 136:147-155.

Antonelli A, Kissling WD, Flantua SGA, Bermúdez MA, Mulch A, Muellner-Riehl AN, Kreft H, Linder HP, Badgley C, Fjeldså J, Fritz SA, Rahbek C, Herman F, Hooghiemstra H, Hoorn C (2018) Geological and climatic influences on mountain biodiversity. Nature Geoscience 11:718-725.

Araujo-Vieira K, Blotto BL, Caramaschi U, Haddad CFB, Faivovich J, Grant T (2019) A total evidence analysis of the phylogeny of hatchet-faced treefrogs (Anura: Hylidae: *Sphaenorhynchus*). Cladistics 35:469-486.

Araujo-Vieira K, Lacerda JVA, Pezzuti TL, Leite FSF, Assis CL, Cruz CAG (2015) A new species of Hatchet-faced Treefrog *Sphaenorhynchus* Tschudi (Anura: Hylidae) from Quadrilátero Ferrífero, Minas Gerais, southeastern Brazil. Zootaxa 4059:96-114.

Azevedo JAR, Valdujo PH, Nogueira CC (2016) Biogeography of anurans and squamates in the Cerrado hotspot: coincident endemism patterns in the richest and most impacted savanna on the globe. Journal of Biogeography 43:2454-2464

Baêta D, Caramaschi U, Cruz CAG, Pombal Jr. JP (2009) *Phyllomedusa itacolomi* Caramaschi, Cruz & Feio, 2006, a junior synonym of *Phyllomedusa ayeaye* (B. Lutz, 1966) (Hylidae, Phyllomedusinae). Zootaxa 2226:58-65.

Baillie JEM, Hilton-Taylor C, Stuart SN (2004) 2004 IUCN Red List of Threatened Species: A Global Species Assessment. IUCN, Gland, Switzerland and Cambridge. xxiv+191pp.

Baldo D, Araujo-Vieira K, Cardozo D, Borteiro C, Leal F, Pereyra MO, Kolenc F, Lyra ML, Garcia PCA, Haddad CFB, Faivovich J (2019) A review of the elusive bicolored iris Snouted Treefrogs (Anura: Hylidae: *Scinax uruguayus* group). PLoS ONE 14:1-45.

Barata IM, Santos MTT, Leite FSF, Garcia PCA (2013) A new species of *Crossodactylodes* (Anura: Leptodactylidae) from Minas Gerais, Brazil: first record of genus within the Espinhaço Mountain Range. Zootaxa 3731:552-560.

Barata IM, Uhlig VM, Silva GH, Ferreira GB (2016) Downscaling the gap: Protected areas, scientific knowledge and the conservation of amphibian species in Minas Gerais, Southeastern Brazil. South American Journal of Herpetology 11:34-45.

Berger L, Roberts AA, Voyles J, Longcore JE, Murray KA, Skerratt LF (2016) History and recent progress on chytridiomycosis in amphibians. Fungal Ecology 19:89-99.

Bickford D, Ng TH, Qie L, Kudavidanage EP, Bradshaw CJA (2010) Forest Fragment and Breeding Habitat Characteristics Explain Frog Diversity and Abundance in Singapore. Biotropica 42:119-125.

Bokermann WCA (1956) Sobre uma espécie de *Hyla* do Estado de Minas Gerais, Brasil. Papéis Avulsos de Zoologia 12:357-362.

Bokermann WCA (1964) Dos nuevas especies de *Hyla* de Minas Gerais y notas sobre *Hyla alvarengai* Bok. (Amphibia, Salientia, Hylidae). Neotropica 10:67-76.

Bokermann WCA (1967) Trés novas espécies de *Physalaemus* do sudeste brasileiro (Amphibia, Leptodactylidae). Revista Brasileira de Biologia 27:135-143.

Bokermann WCA, Sazima I (1973a) Anfíbios da Serra do Cipó, Minas Gerais, Brasil. – Espécies novas de *Hyla* (Anura, Hylidae). Revista Brasileira de Biologia 33:329-336.

Bokermann WCA, Sazima I (1973b) Anfíbios da Serra do Cipó, Minas Gerais, Brasil. II: Duas espécies novas de *Hyla* (Anura, Hylidae). Revista Brasileira de Biologia 33:521-528.

Bokermann WCA, Sazima I (1978) Anfíbios da Serra do Cipó, Minas Gerais, Brasil. 4: Descrição de *Phyllomedusa jandaia* sp. n. (Anura, Hylidae). Rev. Brasileira de Biologia 38:927-930.

Bolochio BE, Lescano JN, Cordier JM, Loyola R, Nori J (2020) A functional perspective for global amphibian conservation. Biological Conservation 245:1-9.

Brandão RA, Magalhães RF, Garda AA, Campos LA, Sebben A, Maciel NM (2012) A new species of *Bokermannohyla* (Anura: Hylidae) from highlands of Central Brazil. Zootaxa 3527:28-42.

Brasil (2000) Lei n° 9.985, de 18 de julho de 2000. Diário Oficial da União. Brasília, Brasil.

Cajade R, Schaefer EF, Duré MI, Kehr AI, Marangoni F (2010) Reproductive biology of *Argenteohyla siemersi pederseni* Williams and Bosso, 1994 (Anura: Hylidae) in northeastern Argentina. Journal of Natural History 44:1953-1978.

Caramaschi U, Cruz CAG, Nascimento LB (2009) A New Species of *Hypsiboas* of the *H. polytaenius* Clade from Southeastern Brazil (Anura: Hylidae). South American Journal of Herpetology 4:210-216.

Carvalho TR, Leite FSF, Pezzuti TL (2013) A new species of *Leptodactylus* Fitzinger (Anura, Leptodactylidae, Leptodactylinae) from montane rock fields of the Chapada Diamantina, northeastern Brazil. Zootaxa 3701:349-364.

Carvalho TR, Seger KR, Magalhães FM, Lourenço LB, Haddad CFB (2021) Systematics and cryptic diversification of *Leptodactylus* frogs in the Brazilian *campo rupestre*. Zoologica Scripta 50:300-317.

Cassini CS, Cruz CAG, Caramaschi U (2010) Taxonomic review of *Physalaemus olfersii* (Lichtenstein & Martens, 1856) with revalidation of *Physalaemus lateristriga*

(Steindachner, 1864) and description of two new related species (Anura: Leiuperidae). Zootaxa 2491:1-33.

Centeno FC, Antoniazzi MM, Andrade DV, Kodama RT, Sciani JM, Pimenta DC, Jared C (2015a) Anuran skin and basking behavior: The case of the treefrog *Bokermannohyla alvarengai* (Bokermann, 1956). Journal of Morphology 276:1172-1182.

Centeno FC, Pinheiro PDP, Andrade DV (2015b) Courtship behavior of *Bokermannohyla alvarengai*, a waltzing anuran. Herpetological Review 46:166-168.

Centeno FC, Vivancos A, Andrade DV (2021) Reproductive Biology and Sexual Dimorphism in *Bokermannohyla alvarengai* (Anura: Hylidae). Herpetologica 77:14-23.

Coutinho ES, Fernandes GW, Berbara RLL, Valério HM, Goto BT (2015) Variation of arbuscular mycorrhizal fungal communities along an altitudinal gradient in rupestrian grasslands in Brazil. Mycorrhiza 25:627-638.

Dias IR, Silva GT, Solé M, Mira-Mendes CV (2020) The advertisement call of the rare casque-headed frog *Nyctimantis galeata* (Anura: Hylidae) from its type locality, Morro do Chapéu, Bahia, Brazil. Zootaxa 4853:447-450.

Drummond LO, Baêta D, Pires MRS (2007) A new species of *Scinax* (Anura, Hylidae) of the *S. ruber* clade from Minas Gerais, Brazil. Zootaxa 1612:45-53.

Drummond LO, Moura FR, Pires MRS (2018) Impact of fire on anurans of rupestrian grasslands (campos rupestres): a case study in the Serra do Espinhaço, Brazil. Salamandra 54:1-10.

Dubeux MJM, Nascimento FAC, Lima LR, Magalhães FM, Silva IRS, Gonçalves U, Almeida JPF, Correia LL, Garda AA, Mesquita DO, Rossa-Feres DC, Mott T (2020) Morphological characterization and taxonomic key of tadpoles (Amphibia: Anura) from the northern region of the Atlantic Forest. Biota Neotropica 20.

Espanha J, Vasconcelos MF, Eterovick PC (2016) The role of tadpole coloration against visually oriented predators. Behavioral Ecology and Sociobiology 70:255–267.

Eterovick PC (2003) Distribution of anuran species among montane streams in south-eastern Brazil. Journal of Tropical Ecology 19:219-228.

Eterovick PC, Bar LFF, Souza JB, Castro JFM, Leite FSF, Alford RA (2015) Testing the Relationship between Human Occupancy in the Landscape and Tadpole Developmental Stress. PLoS ONE 10:1-15.

Eterovick PC, Barata IM (2006) Distribution of tadpoles within and among Brazilian streams: The influence of predators, habitat size and heterogeneity. Herpetologica 62:365-377.

Eterovick PC, Fernandes GW (2001) Tadpole distribution within montane meadow streams at the Serra do Cipó, southeastern Brazil: ecological or phylogenetic constraints? Journal of Tropical Ecology 17:683-693.

Eterovick PC, Mendes IS, Kloh JS, Pinheiro LT, Václav ABHP, Santos T, Gontijo ASB (2018) Tadpoles respond to background colour under threat. Scientific Reports 8:1-8.

Eterovick, PC, Sloss BL, Scalzo JAM, Alford RA (2016) Isolated frogs in a crowded world: Effects of human-caused habitat loss on frog heterozygosity and fluctuating asymmetry. Biological Conservation, 195:52-59.

Eterovick PC, Souza AM, Sazima I (2020) Anfíbios da Serra do Cipó, Minas Gerais. 1ª ed. Belo Horizonte, 292p.

Faivovich J, Lugli L, Lourenço ACC, Haddad CFB (2009) A New Species of the *Bokermannohyla martinsi* Group from Central Bahia, Brazil with Comments on *Bokermannohyla* (Anura: Hylidae). Herpetologica 65:303-310.

Faivovich J, McDiarmid RW, Myers CW (2013) Two new species of *Myersiohyla* (Anura: Hylidae) from Cerro de la Neblina, Venezuela, with comments on other species of the genus. American Museum Novitates 3792:1-63.

Fatorelli P, Nogueira-Costa P, Rocha CFD (2018) Characterization of tadpoles of the southward portion (oceanic face) of Ilha Grande, Rio de Janeiro, Brazil, with a proposal for identification key. North-Western Journal of Zoology 14:171-184.

Fernandes GW, Barbosa NPU, Alberton B, Barbieri A, Dirzo R, Goulart F, Guerra TJ, Morellato LPC, Solar RRC (2018) The deadly route to collapse and the uncertain fate of Brazilian rupestrian grasslands. Biodiversity and Conservation 27:2587-2603.

Fernandes GW, Barbosa NPU, Negreiros D, Paglia AP (2014) Challenges for the conservation of vanishing megadiverse rupestrian grasslands. Natureza & Conservação 2:162-165.

Fouquet A, Blotto BL, Moronna MM, Verdade VK, Juncá FA, de Sá R, Rodrigues MT (2013) Unexpected phylogenetic positions of the genera *Rupirana* and *Crossodactylodes* reveal insights into the biogeography and reproductive evolution of leptodactylid frogs. Molecular Phylogenetics and Evolution 67:445-457.

Françoso RD, Brandão R, Nogueira CC, Salmona YB, Machado RB, Colli GR (2015) Habitat loss and the effectiveness of protected areas in the Cerrado Biodiversity Hotspot. Natureza & Conservação 13:35-40.

Frost DR (2021) Amphibian Species of the World: an Online Reference v. 6.1. (03 de maio de 2021). Acessível em: https://amphibiansoftheworld.amnh.org/index.php.

Furness A, Capellini I (2019) The evolution of parental care diversity in amphibians. Nature Communications 10:1-12.

García-Rodríguez A, Parra-Olea G, Velasco JA, Villalobos F (2021) Effects of evolutionary time, speciation rates and local abiotic conditions on the origin and maintenance of amphibian montane diversity. Global Ecology and Biogeography 30:674-684.

Geldmann J, Manica A, Burgess ND, Coad L, Balmford A (2019) A global-level assessment of the effectiveness of protected areas at resisting anthropogenic pressures. PNAS 116:23209-23215.

Gontijo ASB, Espanha J, Eterovick PC (2018) Is tadpole coloration adaptive against birdpredation? acta ethologica 21:69–79.

González-del-Pliego P, Freckleton RP, Edwards DP, Koo MS, Scheffers BR, Pyron RA, Jetz W (2019) Phylogenetic and Trait-Based Prediction of Extinction Risk for Data-Deficient Amphibians. Current Biology 29:1557-1563.

Grosjean S (2005) The choice of external morphological characters and developmental stages for tadpole-based anuran taxonomy: a case study in *Rana* (*Sylvirana*) *nigrovittata* (Blyth, 1855) (Amphibia, Anura, Ranidae). Contributions to Zoology 74:61-76.

Guedes TB, Azevedo JAR, Bacon CD, Provete DB, Antonelli A (2020) Diversity, Endemism, and Evolutionary History of Montane Biotas Outside the Andean Region. In: Rull V, Carnaval AC (eds) Neotropical Diversification: Patterns and Process. Springer International Publishing, pp 299-328.

Guerra V, Jardim L, Llusia D, Márquez R, Bastos RP (2020) Knowledge status and trends in description of amphibian species in Brazil. Ecological Indicators 118.

Haddad CFB, Prado CPA (2005) Reproductive Modes in Frogs and Their Unexpected Diversity in the Atlantic Forest of Brazil. BioScience 55:207-217.

Heyer W (1999) A new genus and species of frog from Bahia, Brazil (Amphibia: Anura: Leptodactylidae) with comments on the zoogeography of the Brazilian *campos rupestres*. Proceedings of the Biological Society of Washington 112:19-39.

Hortal J, Bello F, Diniz-Filho AF, Lewinsohn TM, Lobo JM, Ladle RJ (2015) Seven Shortfalls that Beset Large-Scale Knowledge of Biodiversity. Annual Review of Ecology, Evolution, and Systematics 46:523-549.

Hopkins WA (2007) Amphibians as Models for Studying Environmental Change. ILAR Journal 48:270-277.

ICMBio – Instituto Chico Mendes de Conservação a Biodiversidade (2012) Sumário Executivo: Plano de Ação Nacional para a Conservação dos Répteis e Anfíbios Ameaçados de Extinção na Serra do Espinhaço. Acessível em: https://www.gov.br/icmbio/pt-br/assuntos/biodiversidade/pan/pan-herpetofauna-do-espinhaco/1-ciclo/pan-herpetofauna-do-espinhaco-sumario.pdf

ICMBio – Instituto Chico Mendes de Conservação da Biodiversidade (2018) Plano de Ação Nacional para Conservação da Herpetofauna da Serra do Espinhaço em Minas Gerais. (03 de maio de 2021). Acessível em: https://www.icmbio.gov.br/portal/faunabrasileira/plano-de-acao-nacional-lista/2465-pan-da-herpetofauna-da-serra-do-espinhaco

IUCN - International Union for Conservation of Nature and Natural Resources (2021a) The IUCN Red List of Threatened Species v. 2021-1. (25 de abril de 2021). Acessível em: https://www.iucnredlist.org/

IUCN - International Union for Conservation of Nature and Natural Resources (2021b) Brazilian Red List Assessment Workshop.

Juncá FA, Napoli MF, Nunes I, Mercês EA, Abreu RO (2015) A new species of the *Scinax ruber* clade (Anura, Hylidae) from the Espinhaço Range, northeastern Brazil. Herpetologica 71:299–309.

Kamino LHY, Pereira EO, Carmo FF (2020) Conservation paradox: Large-scale mining waste in protected areas in two global hotspots, southeastern Brazil. Ambio 49:1629-1638.

Kloh JS, Figueredo CC, Eterovick PC (2018) You are what, where, and when you eat: seasonal and ontogenetic changes in a tropical tadpole's diet. Amphibia-Reptilia 39:445-456.

Köhler J, Jansen M, Rodríguez A, Kok PJR, Toledo FL, Emmrich M, Glaw F, Haddad CFB, Rödel MO, Vences M (2017) The use of bioacoustics in anuran: theory, terminology, methods and recommendations for best practice. Zootaxa 4251:1-124.

Kopp K, Eterovick PC (2006) Factors influencing spatial and temporal structure of frog assemblages at ponds in southeastern Brazil. Journal of Natural History 40:1813-1830.

Körner C, Jetz W, Paulsen J, Payne D, Rudmann-Maurer K, Spehn EM (2017) A global inventory of mountains for bio-geographical applications. Alpine Botany 127:1-15.

Lajmanovích RC, Peltzer PP, Attademo AM, Cabagna MC, Junges CM, Basso A (2012) Amphibia, Anura, Hylidae, *Argenteohyla siemersi pederseni* (Williams and Bosso, 1994): first record and some hematological data in Santa Fe Province, Argentina. Check List 8:790-791.

Leal F, Leite FSF, Costa WP, Nascimento LB, Lourenço LB, Garcia PCA (2020) Amphibians from Serra do Cipó, Minas Gerais, Brasil. VI: A New Species of the *Physalemus deimaticus* Group (Anura, Leptodactylidae). Zootoxa 4766:306-330.

Leite FSF (2012) Taxonomia, biogeografia e conservação de anfíbios da Serra do Espinhaço. 2012. Tese de doutorado, Universidade Federal de Minas Gerais, Belo Horizonte, Brasil.

Leite FSF, Juncá FA, Eterovick PC (2008a) Status do conhecimento, endemismo e conservação de anfíbios anuros da Cadeia do Espinhaço, Brasil. Megadiversidade 4:158-176.

Leite FSF, Pacheco BG, Eterovick, PC (2008b) Development and demography of *Phasmahyla jandaia* (Bokermann and Sazima, 1978) (Anura, Hylidae) tadpoles in an Atlantic Forest site, southeastern Brazil'. Journal of Natural History 42:2777-2791.

Leite FSF, Pezzuti TL, Drummond LO (2011) A New Species of *Bokermannohyla* from the Espinhaço Range, State of Minas Gerais, Southeastern Brazil. Herpetologica 67:440-448.

Leite FSF, Pezzuti TL, Garcia PCA (2012) A New Species of the *Bokermannohyla pseudopseudis* Group from the Espinhaço Range, Central Bahia, Brazil (Anura: Hylidae). Herpetologica 68:401-409.

Leite FSF, Pezzuti TL, Garcia PCA (2019a) Anfíbios anuros do Quadrilátero Ferrífero. (03 de maio de 2021). Acessível em: http://saglab.ufv.br/aqf/

Leite FSF, Pezzuti TL, Garcia PCA (2019b) Anfíbios anuros do Quadrilátero Ferrífero: Lista de Espécies. (03 de maio de 2021). Acessível em: http://saglab.ufv.br/aqf/lista/

Lima NGS, Oliveira U, Souza RCC, Eterovick PC (2019) Dynamic and diverse amphibian assemblages: Can we differentiate natural processes from human induced changes? PLoS ONE 14:1-21.

Maciel DB, Nunes I (2010) A new species of four-eyed frog genus *Pleurodema* Tschudi, 1838 (Anura: Leiuperidae) from the rock meadows of Espinhaço range, Brazil. Zootaxa 2640:53-61.

Magalhães FM, Brandão RA, Garda AA, Mângia S (2020) Revisiting the generic position and acoustic diagnosis of *Odontophrynus salvatori* (Anura: Odontophrynidae). Herpetological Journal 30:189-196

Magalhães FM, Marques R, Santos DF, Magalhães RF, Pezzuti TL (2021) Tadpole of *Nyctimantis galeata* (Anura: Hylidae: Lophyohylini), a narrow endemic casque-headed frog from Bahia, Brazil. Zootaxa 4948:295-300.

Magalhães RF, Lacerda JVA, Reis LP, Garcia PCA, Pinheiro PDP (2018) Sexual Dimorphism in *Bokermannohyla martinsi* (Bokermann, 1964) (Anura, Hylidae) with a Report of Male–Male Combat. South American Journal of Herpetology 13:202-209.

Magalhães RF, Lemes P, Camargo A, Oliveira U, Brandão RA, Thomassen H, Garcia PCA, Leite FSF, Santos FR (2017) Evolutionarily significant units of the critically endangered leaf frog *Pithecopus ayeaye* (Anura, Phyllomedusidae) are not effectively preserved by the Brazilian protected areas network. Ecology and Evolution 7:8812-8828.

Magalhães RF, Lemes P, Santos MTT, Mol RM, Ramos EKS, Oswald CB, Pezzuti TL, Santos FR, Brandão RA, Garcia PCA (2021) Evidence of introgression in endemic frogs from the *campo rupestre* contradicts the reduced hybridization hypothesis. Biological Journal of the Linnean Society 133:561-576.

Magalhães RF, Rocha PC, Santos FR, Strüssmann C, Giaretta AA (2018) Integrative taxonomy helps to assess the extinction risk of anuran species. J. for Nature Conservation 45:1-10.

Malagoli LR, Pezzuti TL, Bang DL, Faivovich J, Lyra ML, Giovanelli JGR, Garcia PCA, Sawaya RJ, Haddad CFB (2021) A new reproductive mode in anurans: Natural history of *Bokermannohyla astartea* (Anura: Hylidae) with the description of its tadpole and vocal repertoire. PLoS ONE 16:1-30.

Marques RB, Haddad CFB, Garda AA (2021) There and back again from monotypy: A new species of the casque-headed *Corythomantis* Boulenger 1896 (Anura, Hylidae) from the Espinhaço mountain range, Brazil. Herpetologica 77: 56-71.

Mascarenhas L, Tiso C, Linares AM, de Moura CFO, Pezzuti TL, Leite FSF, Eterovick PC (2015) Improved local inventory and regional contextualization for anuran (Amphibia) diversity assessment at an endangered habitat in southeastern Brazil. Journal of Natural History 50:1265-1281.

Miola DTB, Ramos VDV, Silveira FAO (2021) A brief history of research in *campo rupestre*: identifying research priorities and revisiting the geographical distribution of an ancient, widespread Neotropical biome. Biol. J. of the Linnean Society 133:464-4840.

MMA – Ministério do Meio Ambiente (2010). Portaria n° 444, de 26 de novembro de 2010. Diário Oficial da União. Brasília, Brasil.

MMA – Ministério do Meio Ambiente (2018a) Portaria n° 368, de 18 de setembro de 2018. Diário Oficial da União. Brasília, Brasil.

MMA – Ministério do Meio Ambiente (2018b) Portaria n° 473, de 28 de dezembro de 2018. Diário Oficial da União. Brasília, Brasil.

MMA – Ministério do Meio Ambiente (2021a) Mapas de Áreas Especiais. (26 de abril de 2021). Acessível em: http://mapas.mma.gov.br/i3geo/datadownload.htm#.

MMA – Ministério do Meio Ambiente (2021b) Mosaicos. (03 de maio de 2021). Acessível em: https://antigo.mma.gov.br/acesso-a-informacao/item/52.html

Moura MR, Jetz W (2021) Shortfalls and opportunities in terrestrial vertebrate species discovery. Nature Ecology and Evolution 5:631-639.

Napoli MF, Cruz CAG, Abreu RO, Del-Grande ML (2011) A new species of *Proceratophrys* Miranda-Ribeiro (Amphibia: Anura: Cycloramphidae) from the Chapada Diamantina, State of Bahia, northeastern Brazil. Zootaxa 3133:37-49.

Nascimento AC, Chaves AV, Leite FSF, Eterovick PC, Santos FR (2018) Past vicariance promoting deep genetic divergence in an endemic frog species of the Espinhaço Range in Brazil: The historical biogeography of *Bokermannohyla saxicola* (Hylidae). PLoS ONE 13:1-19.

Oliveira FFR (2017) Mating behaviour, territoriality and natural history notes of *Phyllomedusa ayeaye* Lutz, 1966 (Hylidae: Phyllomedusinae) in southeastern Brazil. Journal of Natural History 51:657-675.

Oliveira FFR, Eterovick PC (2009) The role of river longitudinal gradients, local and regional attributes in shaping frog assemblages. Acta Oecologica 35:727-738.

Oliveira FFR, Eterovick PC (2010) Patterns of spatial distribution and microhabitat use by syntopic anuran species along permanent lotic ecosystems in the Cerrado of southeastern Brazil. Herpetologica 66:159-171.

Oliveira FFR, Nogueira PAG, Eterovick PC (2012) Natural history of *Phyllomedusa megacephala* (Miranda-Ribeiro, 1926) (Anura: Hylidae) in southeastern Brazil, with descriptions of its breeding biology and male territorial behaviour. Journal of Natural History 46:117-129.

Pardiñas UFJ, Lessa G, Teta P, Salazar-Bravo J, Câmara EMVC (2014) A new genus of sigmodontine rodent from eastern Brazil and the origin of the tribe Phyllotini. Journal of Mammalogy 95:201–215.

Pezzuti TL, Leite FSF, Garcia PCA (2019) Chave de identificação interativa para os girinos do Quadrilátero Ferrífero, Minas Gerais, Sudeste do Brasil. Versão 1.0 (03 de maio de 2021). Acessível em: http://biodiversus.com.br/saglab/aqf/chave/girinos/

Pimenta B, Costa D, Murta-Fonseca R, Pezzuti T (2014) Anfíbios: Alvorada de Minas, Conceição do Mato Dentro, Dom Joaquim - Minas Gerais. Bicho do Mato Editora: 196pp.

Pinheiro PDP, Pezzuti TL, Berneck BM, Lyra ML, Lima RCL, Leite FSF (2021) A new cryptic species of the *Aplastodiscus albosignatus* group (Anura: Hylidae). Salamandra 57:27-43.

Pombal JPJr, Menezes VA, Fontes AF, Nunes I, Rocha CFD, Sluys MV (2012) A second species of the casque-headed frog genus *Corythomantis* (Anura: Hylidae) from northeastern Brazil, the distribution of *C. greeningi*, and comments on the genus. Boletim do Museu Nacional 530:1-14.

Rocha PC, Sena LMF, Pezzuti TL, Leite FSF, Svartman M, Rosset SD, Baldo D, Garcia PCA (2017) A new diploid species belonging to the *Odontophrynus americanus* species group (Anura: Odontophrynidae) from the Espinhaço range, Brazil. Zootaxa 4329:327-350.

Rödder D, Schlüter A, Lötters S (2010) Is the 'Lost World' Lost? High Endemism of Aphibians [sic] and Reptiles on South American Tepuís in a Changing Climate. In: Habel JC, Assmann T (eds) Relict Species. Springer, Berlin, Heidelberg.

Rodríguez A, Börner M, Pabijan M, Gehara M, Haddad CFB, Vences M (2015) Genetic divergence in tropical anurans: deeper phylogeographic structure in forest specialists and in topographically complex regions. Evolutionary Ecology 29:765-785.

Rossa-Feres DC, Garey MV, Caramaschi U, Napoli MF, Nomura F, Bispo AA, Brasileiro CA, Thomé MTC, Sawaya RJ, Conte CE, Cruz CAG, Nascimento LB, Gasparini JL, Almeida AP, Haddad CFB (2017) Anfíbios da Mata Atlântica: Lista de espécies, histórico dos estudos, biologia e conservação. In: Conte CE, Monteiro-Filho ELA (eds) Revisões de Zoologia: Mata Atlântica. Editora UFPR: Curitiba, p 237-314.

Rossa-Feres DC, Nomura F (2006) Characterization and taxonomic key for tadpoles (Amphibia: Anura) from the northwestern region of São Paulo State, Brazil. Biota Neotropica 6.

Rosset SD, Baldo D, Lanzone C, Basso NG (2006) Review of the Geographic Distribution of Diploid and Tetraploid Populations of the *Odontophrynus americanus* Species Complex (Anura: Leptodactylidae). Journal of Herpetology 40:465-477.

Rosset SD, Fadel RM, Guimarães CS, Carvalho PS, Ceron K, Pedrozo M, Serejo R, Souza RS, Baldo D, Mângia S (2021) A New Burrowing Frog of the *Odontophrynus americanus* Species Group (Anura, Odontophrynidae) from Subtropical Regions of Argentina, Brazil, and Paraguay. Ichthyology & Herpetology 109:228-244.

Saadi A (1995) A geomorfologia da Serra do Espinhaço em Minas Gerais e de suas margens. Geonomos 3:41-63.

Sabbag AF (2013) Filogeografia de *Thoropa* grupo *miliaris* (Anura: Cycloramphidae). 2013. Dissertação de mestrado, Universidade Estadual Paulista “Júlio de Mesquita Filho, São José do Rio Preto, Brasil.

Sabbag AF, Lyra ML, Zamudio KR, Haddad CFB, Feio RN, Leite FSF, Gasparini JL, Brasileiro CA (2018) Molecular phylogeny of Neotropical rock frogs reveals a long history of vicariant diversification in the Atlantic Forest. Molecular Phylogenetics and Evolution 122:142-156.

Sandel B, Arge L, Dalsgaard B, Davies RG, Gaston KJ, Sutherland WJ, Svenning JC (2011) The influence of late quaternary climate-change velocity on species endemism. Science 334:660-664.

Santos MTT, Barata IM, Ferreira RB, Haddad CFB, Gridi-Papp M, Carvalho TR (2021) Complex acoustic signals in *Crossodactylodes* (Leptodactylidae, Paratelmatobiinae): a frog genus historically regarded as voiceless. Bioacoustics 31:175-190.

Santos MTT, Magalhães RF, Ferreira RB, Vittorazzi SE, Dias IR, Leite FSF, Lourenço LB, Santos FR, Haddad CFB, Garcia PCA (2020a) Systematic revision of the rare bromeligenous genus *Crossodactylodes* Cochran 1938 (Anura: Leptodactylidae: Paratelmatobiinae). Herpetological Monographs 34:1-38.

Santos MTT, Magalhães RF, Lyra ML, Santos FR, Zaher H, Giasson LOM, Garcia PCA, Carnaval AC, Haddad CFB (2020b) Multilocus phylogeny of Paratelmatobiinae (Anura: Leptodactylidae) reveals strong spatial structure and previously unknown diversity in the Atlantic Forest hotspot. Molecular Phylogenetics and Evolution 148:1-18.

Sazima I, Bokermann WCA (1977) Anfíbios da Serra do Cipó, Minas Gerais, Brasil. 3: Observações sobre a biologia de *Hyla alvarengai* Bok. (Anura, Hylidae). Rev. Brasileira de Biologia 57:413-417.

Sazima I, Bokermann WCA (1978) Cinco novas espécies de *Leptodactylus* do centro e sudeste Brasileiro (Amphibia, Anura, Leptodactylidae). Rev. Brasileira de Biologia 38:899-912.

Sazima I, Bokermann WCA (1983 "1982"). Anfíbios da Serra do Cipó, Minas Gerais, Brasil. 5: *Hylodes otavioi* sp. n. (Anura, Leptodactylidae). Rev. Bras. de Biologia 42:767-771.

Scatigna AV, Souza VC, Machado RM, Simões AO (2020) *Lapaea* (Plantaginaceae, Gratioleae), a new genus endemic to the Espinhaço Range (Brazil) with a remarkable red-flowered new species. Systematics and Biodiversity 18:739-756.

Segalla MV, Berneck B, Canedo C, Caramaschi U, Cruz CAG, Garcia PCA, Grant T, Haddad CFB, Lourenço ACC, Mângia S, Mott T, Nascimento LB, Toledo LF, Werneck FP, Langone JA (2021) List of Brazilian Amphibians. Herpetologia Brasileira 10:121-216.

Silva ET, Peixoto MAA, Leite FSF, Feio RN, Garcia PCA (2018) Anuran Distribution in a Highly Diverse Region of the Atlantic Forest: The Mantiqueira Mountain Range in Southeastern Brazil. Herpetologica 74:294-305.

Silva G, Hepp F, Luna-Dias C, Silva S (2013) First record of *Scinax tripui* Lourenço, Nascimento and Pires, 2010 (Amphibia: Anura: Hylidae) from Espírito Santo state, Brazil. Check List 9:645-646.

Silva LA, Hoffmann MC, Santana DJ (2014) New record of *Corythomantis greening* Boulenger, 1896 (Amphibia, Hylidae) in the Cerrado domain, state of Tocantins, central Brazil. Herpetology Notes 7:717-720.

Silveira AL, Ribeiro LSVB, Fernandes TN, Dornas TT (2019) Anfíbios do Quadrilátero Ferrífero (Minas Gerais): atualização do conhecimento, lista comentada e guia fotográfico. 1. ed. Belo Horizonte: Rupestre. 448p.

Silveira FAO, Negreiros D, Barbosa NPU, Buisson E, Carmo FF, Carstensen DW, Conceição AA, Cornelissen TG, Echternacht L, Fernandes GW, Garcia QS, Guerra TJ, Jacobi CM, Lemos-Filho JP, Le Stradic S, Morellato LPC, Neves FS, Oliveira RS, Schaefer CE, Viana PL, Lambers H (2016) Ecology and Evolution of plant diversity in the endangered *campo rupestre*: a neglected conservation priority. Plant and Soil 403:129-152.

Smith MA, Green DM (2005) Dispersal and the metapopulation paradigm in amphibian ecology and conservation: are all amphibian populations metapopulations? Ecography 28:110-128.

Sodhi NS, Bickford D, Diesmos AC, Lee TM, Koh LP, Brook BW, Sekercioglu CH, Bradshaw CJA (2008) Measuring the Meltdown: Drivers of Global Amphibian Extinction and Decline. PLoS ONE 3:1-8.

Taucce PPG, Leite FSF, Santos PS, Feio RN, Garcia PCA (2012) The advertisement call, color patterns and distribution of *Ischnocnema izecksohni* (Caramaschi and Kisteumacher, 1989) (Anura, Brachycephalidae). Papéis Avulsos de Zoologia 52:112-120.

Taucce PPG, Nascimento JS, Trevisan CC, Leite FSF, Santana DJ, Haddad CFB, Napoli MF (2020) A new rupicolous species of the *Pristimantis conspicillatus* group (Anura:

Brachycephaloidea: Craugastoridae) from central Bahia, Brazil. Journal of Herpetology 54:245-257.

Taucce PPG, Pinheiro PDP, Leite FSF, Garcia PCA (2015) Advertisement call and morphological variation of the poorly known and endemic *Bokermannohyla juiju* Faivovich, Lugli, Lourenço and Haddad, 2009 (Anura: Hylidae) from Central Bahia, Brazil. Zootaxa 3915:99-110.

Teixeira MJr, Amaro RC, Recoder RS, Vechio FD, Rodrigues MT (2012) A new dwarf species of *Proceratophrys* Miranda-Ribeiro, 1920 (Anura, Cycloramphidae) from the highlands of Chapada Diamantina, Bahia, Brazil. Zootaxa 3551:25-42.

UNESCO – United Nations Educational, Scientific and Cultural Organization (2021) Biosphere reserves in Latin America and the Caribbean. (03 de maio de 2021).

Vági B, Végvári Z, Liker A, Freckleton RP, Székely T (2019) Parental care and the evolution of terrestriality in frogs. Proceedings of Royal Society B 286: 20182737.

Valero KCW, Marshall JC, Bastiaans E, Caccone A, Camargo A, Morando M, Niemiller ML, Pabijan M, Russello MA, Sinervo B, Werneck FP, Sites Jr JW, Wiens JJ, Steinfartz S (2019) Patterns, Mechanisms and Genetics of Speciation in Reptiles and Amphibians. Genes 10:646.

Vasconcellos MM, Colli GR, Cannatella DC (2021) Paleotemperatures and recurrent habitat shifts drive diversification of treefrogs across distinct biodiversity hotspots in sub-Amazonian South America. Journal of Biogeography 48:305-320.

Vences M, Galan P, Vieites DR, Puente M, Oetter K, Wanke S (2002) Field body temperatures and heating rates in a montane frog population: The importance of black dorsal pattern for thermoregulation. Annales Zoologici Fennici 39:209-220.

Walker M, Lourenço ACC, Pimenta BVS, Nascimento LB (2015) Morphological variation, advertisement call, and tadpoles of *Bokermannohyla nanuzae* (Bokermann, 1973), and taxonomic status of *B. feioi* (Napoli & Caramaschi, 2004) (Anura, Hylidae, Cophomantini). Zootaxa 3937:161-178.

Wisz MS, Pottier J, Kissling WD, Pellissier L, Lenoir J, Damgaard CF, Dormann CF, Forchhammer MC, Grytnes JA, Guisan A, Heikkinen RK, Høye TT, Kühn I, Luoto M, Maiorano L, Nilsson MC, Normand S, Öckinger E, Schmidt NM, Termansen M, Tiemmermann A, Wardle DA, Aastrup P, Svenning JC (2013) The role of biotic interactions in shaping distributions and realized assemblages of species: Implications for species distribution modelling. Biological Reviews 88:15-30.

Capítulo 2

Colonization rather than fragmentation explains the geographic distribution and diversification of treefrogs endemic to Brazilian shield sky islands

Aceito para publicação dia 9 de novembro de 2021 no periódico *Journal of Biogeography*.

Colonization rather than fragmentation explains the geographic distribution and diversification of treefrogs endemic to Brazilian shield sky islands

Phylogeography of the ledge treefrog

Caroline Batistim Oswald [1, *] – *carolbatistim@gmail.com
Priscila Lemes[2]
Maria Tereza C. Thomé[3]
Tiago Leite Pezzuti[1]
Fabricio Rodrigues Santos[1,4]
Paulo Christiano de Anchietta Garcia[1,5]
Felipe Sá Fortes Leite[1,6]
Rafael Félix de Magalhães[1,7,*] – *rafaelmagalhaes@ufsj.edu.br

[1]Programa de Pós-Graduação em Zoologia, Universidade Federal de Minas Gerais. Avenida Presidente Antônio Carlos, 6627. Pampulha, Belo Horizonte, MG 31270-901, Brazil
[2]Laboratório de Ecologia e Conservação, Departamento de Botânica e Ecologia, Instituto de Biociências, Universidade Federal do Mato Grosso, Cuiabá, Mato Grosso, Brazil
[3] Department of Evolution, Ecology and Organismal Biology, The Ohio State University, Columbus, OH, USA
[4] Departamento de Genética, Ecologia e Evolução, Universidade Federal de Minas Gerais. Avenida Presidente Antônio Carlos, 6627. Pampulha, Belo Horizonte, MG 31270-901, Brazil
[5]Departamento de Zoologia, Universidade Federal de Minas Gerais. Avenida Presidente Antônio Carlos, 6627. Pampulha, Belo Horizonte, MG 31270-901, Brazil
[6]Instituto de Ciências Biológicas e da Saúde, *campus* Florestal, Universidade Federal de Viçosa. Rodovia LMG 818, km 06. Florestal, MG 35690-000, Brazil
[7]Departamento de Ciências Naturais, *campus* Dom Bosco, Universidade Federal de São João del-Rei. Praça Dom Helvécio, 74. Dom Bosco, São João del-Rei, MG 36301-160, Brazil
*Corresponding author

Acknowledgments

We thank Elisa Ramos for providing computational resources and valuable discussion of iBPP, Nubia Marques and Vitor Carvalho-Rocha for enriching discussion on statistics, and Pedro Taucce for the valuable suggestion for some BEAST analyses. CBO thanks Fundação de Amparo à Pesquisa do Estado de Minas Gerais (FAPEMIG) and Coordenação de Aperfeiçoamento de Pessoal de Nível Superior (CAPES) for her PhD fellowships. TLP thanks CAPES for his PNPD fellowship (88887.468027/2019-00). PCAG and FRS thank Conselho Nacional de Desenvolvimento Científico e Tecnológico (CNPq) for their research fellowships.

We thank FAPEMIG and Fundação Vale (FAPEMIG/VALE: RDP-00004-17) and FAPEMIG (APQ-01796-15; APQ-00413-16; APQ-01120-16).

Abstract

Aim: Geographical patterns of montane biodiversity worldwide are related to biotic and abiotic factors, such as historical climate dynamics and species dispersal capabilities, which affect the biota from population to community levels. Understanding of processes related to population diversification in extra-Andean Neotropical mountains remains largely unknown. Here, we tested how colonization of new areas as opposed to fragmentation of geographical ranges influenced the distribution and diversification of frogs from Brazilian mountains.

Location: Espinhaço Range, the largest extra-Andean mountain range in South America.

Taxon: Ledge treefrog *Bokermannohyla saxicola*.

Methods: We used multilocus DNA and morphometric data throughout the species' distribution to delimit lineages, infer phylogenetic relationships and estimate divergence times. We used ecological niche modelling (ENM) and approximate Bayesian computation (ABC) to reconstruct changes of geographical distribution and population sizes for testing alternative hypotheses of diversification concerning fragmentation and colonization.

Results: We found four evolutionary significant lineages that diverged from the Pliocene to the Early Pleistocene. All lineages were validated by DNA and morphometric data by independent and joint analyses. ENM showed that climatic fluctuations might have influenced the species' distribution, whereas ABC model selection further supports associated demographic changes. Taken together, a Pleistocene jump-dispersal scenario best explains the diversification of the *Bokermannohyla saxicola* lineages.

Main conclusions: Endemism in the Espinhaço Range is usually explained by ancient diversification, associated with long-term isolation of climatic stable areas following climate-driven habitat fragmentation. Our results challenge this general view, indicating recent diversification, habitat expansion and colonization of new areas as important processes explaining the current distribution and genetic diversity of *B. saxicola*.

K E Y W O R D S

Approximate Bayesian computation, *Bokermannohyla saxicola*, *campo rupestre*, ecological niche modelling, Espinhaço Range, flickering connectivity system, OCBIL, species delimitation

Introduction

Mountains host exceptional biodiversity (Körner et al., 2017). They make up to approximately a quarter of the Earth's land area, but hold about 87% of the world's vertebrate

species, many of which present endemic distributions (Rahbek et al., 2019). Geographical patterns of diversity in these areas are related to several biotic and abiotic factors, such as topographic heterogeneity, geological dynamics, historical climate changes, dispersion capacities and species interactions (Antonelli et al., 2018; Sandel et al., 2011; Wisz et al., 2013). Despite numerous recent studies (Flantua et al., 2019; Kok et al., 2018; Muellner-Riehl et al., 2019), the understanding of processes related to the diversification of mountain biotas remains largely unknown (Perrigo et al., 2020; Rahbek et al., 2019).

Models to explain patterns of diversification in mountains have recently emerged. Among these, two deserve attention concerning mountains: the 'flickering connectivity system' (FCS; (Flantua & Hooghiemstra, 2018) and the 'old, climatically buffered, infertile landscapes' theory (OCBILs; (Hopper, 2009; Hopper et al., 2016). The FCS postulates that altitudinal changes in climate during the Pleistocene may have influenced alpine diversification through fragmentation of geographical distributions, intermixing between formerly isolated biotas, colonization of new areas, and hybridization between previously allopatric populations and species (Flantua et al., 2019; Flantua & Hooghiemstra, 2018). On the other hand, the OCBILs posit that some environments (including mountains) are so ancient and climatically stable that Pleistocene climate changes had little or no influence on the diversification of their biotas (Hopper, 2009). In this case, diversification would be explained by long-term population isolation and adaptation to local conditions and specific microhabitats (Hopper, 2009; Hopper et al., 2016). In short, while OCBILs predict old biotas in ancient and stable environments, FCS proposes biotas reacting to Pleistocene environmental shifts. This dichotomy between young and old diversification is a consuetude discussion in literature, and evidence indicates that both may contribute to the formation of current Neotropical montane biotas (Rull, 2011; Turchetto-Zolet et al., 2013).

The Espinhaço Range (ER) is a mountain belt in eastern Brazil that extends over 1200 km in the South–North direction, Minas Gerais (MG) to Bahia (BA) states (latitudes 20S and 11S; Figure 1), and is the largest mountain range in South America after the Andes (Fernandes et al., 2014; Guedes et al., 2020). Its formation dates to the Precambrian, about 640 Ma, and it now experiences long-term geological stability (Alkmin, 2012; Saadi, 1995), currently separating the Cerrado, Caatinga and Atlantic Forest dominions. The ER is divided latitudinally in two main provinces: Chapada Diamantina and Southern Espinhaço (SE; Colli-Silva et al., 2019). The SE is also divided into several isolated mountains all the way to Quadrilátero Ferrífero at its southern end (Colli-Silva et al., 2019). The ER is home to an outstanding

diversity of animals, plants and fungi, with several endemic species (Salazar et al., 2019; Santos et al., 2020).

The predominant montane ecosystem (occurring mostly over 900 m above sea level) consists of the *campo rupestre*, assumed as an OCBIL and defined as grassy-shrubby vegetation mosaics associated with rock outcrops (i.e. quartzite, arenite or ironstone), white sands, stony soils and/or seasonally flooded areas (Miola et al., 2021; Silveira et al., 2016). *Campo rupestre* is distributed as a sky islands system, where elevated areas are separated by 'seas' of lowlands with distinct environments (Silveira et al., 2016). Most plants and animals endemic to the ER are associated with *campo rupestre* ecosystem (Guedes et al., 2020).

Despite the growing interest in ecology and evolution of the ER biota in recent years (Silveira et al., 2016, 2020), little is known about the processes involved in its diversification, especially for animals (Miola et al., 2021). For anurans, the ER houses more than 160 species, of which 30% are endemic (Leite, 2012) and often associated with *campo rupestre* (Leite, 2012; Leite et al., 2008). Only seven studies have examined the evolutionary history of these endemics at the phylogeographical level (Carvalho et al., 2021; de Oliveira et al., 2021; Magalhães et al., 2021; Nascimento et al., 2018; Ramos et al., 2018; Thomé et al., 2016; Thomé & Carstens, 2016).

One of these investigations focused on the mitochondrial phylogeography of the ledge treefrog *Bokermannohyla saxicola* (Bokermann, 1964) (Nascimento et al., 2018), a species associated with permanent rocky streams (Eterovick & Brandão, 2001). Nascimento et al. (2018) found that the species may constitute a complex of four allopatric lineages, possibly undescribed species, whose cladogenetic events occurred since the Miocene Period. Because of the timeframe, Nascimento et al. (2018) also hypothesized that past vicariance caused by warming climate events since the Late Pliocene isolated these lineages on mountain tops, thus following the rationale expected for OCBIL-associated diversification.

Recent research has shown that the Pleistocene climate dynamics' influence on the ER biota diversification may be more widespread than expected by the OCBIL theory (de Oliveira et al., 2021; Magalhães et al., 2021; Vasconcelos et al., 2020). Given that (i) species delimitation based solely on one genetic marker can be misleading (Camargo & Sites, 2013; Knowles & Carstens, 2007), (ii) mtDNA-based molecular dating tends to overestimate divergence times in phylogeny reconstruction (McCormack et al., 2011; Smith et al., 2013), and (iii) the descriptive nature of the work of Nascimento et al. (2018), it is necessary to add data under a question-driven framework to formally test theirs and other diversification hypotheses in *B. saxicola*. By adding morphometric data, six nuclear markers and a rigorous statistical framework, we here

tested the hypothesis of multiple species under the *B. saxicola* name and addressed multiple diversification hypotheses in which Pleistocene climate changes (FCS model), palaeogeographical stability since Neogene (as expected by OCBIL theory), or both, influenced genetic divergence and demographic history in this taxon.

Material and Methods

Sampling strategy

Genetic data

The samples in this study were those used by Nascimento et al. (2018), plus new samples for an additional population (Turmalina/MG, number 8 in Figure 1c; Table S1), thus covering the entire known distribution of the species. We sub-sampled 50 individuals representing all populations for which we sequenced six additional nuclear DNA markers (nDNA; Table S1). The nDNA loci were fragments of the following genes: intron 7 of the Beta-fibrinogen (*β*-fib); Beta-crystallin (*β*-cry), Disulphide Isomerase A6 Precursor, intron 6 (DIA6); Protooncogene cellular myelotomatosis (c-*myc*); Proopiomelanocortin A (POMC); SWI/SNF related, matrix associated, actin-dependent regulator of chromatin, subfamily b, member 1 (SmarcB1) (Table S2). We sampled one individual of *Bokermannohyla nanuzae* as outgroup due to phylogenetic proximity (J. Faivovich, pers. comm.). Details of laboratory procedures are available in Appendix S1.

We assembled, checked and edited sequence fluorograms in SeqScape 2.6 software (Applied Biosystems™). We aligned edited sequences using Muscle (Edgar, 2004) as implemented in AliView 1.26 (Larsson, 2014) under default parameters. We phased heterozygous nuclear sequences using PHASE 2.1.1 (Stephens et al., 2001) under a threshold of 0.7 posterior probability (PP). For insertions/deletions in DIA6, we phased sequences in the Indelligent 1.2 web tool (Dmitriev & Rakitov, 2008a, 2008b).

Morphometric data

We examined 469 adults and 133 tadpoles' specimens from 32 locations representing the known species' distribution (Figure 1c). Specimens are housed in the Herpetological collection of Centro de Coleções Taxonômicas—Universidade Federal de Minas Gerais (CCT-UFMG; Table S1). For adults, we determined sex according to external characters and took 21 body measurements (Table S3) using a digital calliper with an accuracy of 0.01 mm. For tadpoles (stages of development between 25 and 40; (Gosner, 1960), we obtained 24 body

measurements (Table S4) from photos with ImageJ 1.53a (Schneider et al., 2012). We photographed the individuals using an adjustable platform to support tadpoles immersed in water (Schacht & McBrayer, 2009) and a Canon® EOS 60D Digital camera with a 60 mm lens.

Testing for multiple species

Exploring genetic structure

Considering the premises of coalescent-based analyses, we conducted a ϕ-test for recombination in SplitsTree 4.14.8 (Bruen et al., 2006; Huson & Bryant, 2006) and the Tajima's D neutrality test with the R package 'pegas' 0.13 in R 3.5.3 (Paradis, 2010; R Core Team, 2019; Tajima, 1989). We estimated number of haplotypes, haplotype and nucleotide diversity, with the R package 'pegas' 0.13, and segregating sites with the R packages 'ape' 5.0 (Paradis, 2010; Paradis & Schliep, 2019).

We combined mtDNA and nDNA to determine the number of populations (K) and individual assignment coefficients using the R package 'Geneland' 4.0.6, with the spatial model and uncorrelated allele frequencies (Table S1; (Guillot, Estoup, et al., 2005; Guillot, Mortier, et al., 2005). For this, we coded haplotypes as alleles for nDNA fragments. We performed 10 parallel runs with K ranging from 1 to 11, consisting of 1×10^7 iterations and thinning of 1×10^3. To select a priori range of the population for this analysis, we ran an exploratory mtDNA species delimitation using a Generalized Mixed Yule Coalescent (GMYC) model (Pons et al., 2006). We used the maximum value of ML entities' credibility as the maximum number of clusters (K) and we set the minimum K as 1 to include the null hypothesis of a single species. After determining the optimal K, we performed an analysis with this value fixed to obtain more accurate individual assignment coefficients (Guillot, Estoup, et al., 2005).

We constructed haplotype networks of each fragment independently with Haploviewer (Salzburger et al., 2011). We first estimated a maximum likelihood gene tree with RAxML 8.2.10 under the GTRGAMMA model using the new rapid hill-climbing algorithm (Stamatakis, 2014; Stamatakis et al., 2007), with 100 independent searches for the best gene trees. Assuming that each indel must be the result of a single mutational event, we represented the long indels in DIA6 (i.e. >one bp) as one-bp indels. Additionally, we inferred a nuclear multilocus distance matrix to check the concordance between nDNA and mtDNA data for *B. saxicola*. We calculated this matrix using the genpofad algorithm implemented in POFAD 1.07, with the additive method enabled to infer missing nucleotides and sequences (Joly et al., 2015; Joly & Bruneau, 2006). Then, we converted the resultant pairwise distance matrix into a network in

SplitsTree 4.14.8, using the NeighborNet algorithm (Bryant & Moulton, 2004; Huson & Bryant, 2006).

Molecular species delimitation

To validate the discovered lineages, we performed an analysis in STACEY 1.2.5 implemented in BEAST 2.6.2 (Bouckaert et al., 2019; Jones, 2017). We assigned individuals a priori to a group/lineage according to the Geneland result. We set the collapse height prior to 1×10^{-3} and estimated collapse weight from a beta distribution, with a minimum of 1×10^{-2} and a maximum of 1 (Jones et al., 2015). We set the β-cry substitution rate at one, and estimated those of the others relative to this (Jones et al., 2015). We conducted the analysis in two replicates, with 2.5×10^{8} generations, 1×10^{3} thinning and 10% burn-in. After the congruence checking between runs, we combined the results using LogCombiner 2.6.2 (Bouckaert et al., 2019). We used the SpeciesDelimitationAnalyzer (SpeciesDA (Jones et al., 2015) to summarize the STACEY result, using simcutoff 1 and collapse height 1×10^{-4}.

Morphological species delimitation

Since we found female-biased sexual dimorphism (see Appendix S1; Table S5), we made adult morphometric analyses only with male data. We first removed the allometric size effect from all morphometric data (males and tadpoles), following Lleonart et al. (2000). Initially, we log10-transformed all variables, and then we used a Principal Component Analysis (PCA) to find a proxy for body size (i.e. the variable with the highest loading value from the first principal component). We obtained the eigenvectors of the variance–covariance matrix using the prcomp function in the R package 'stats' (R Core Team, 2019). We selected the variable UAL (Table S3) as a proxy for adult males and TMH (Table S4) for tadpoles. We used the residuals of the regression of the variables against proxies instead of the original variables for subsequent analyses using morphometric data (Lleonart et al., 2000). We then calculated variance inflation factors (VIF) among variables to remove multicollinearity, using the function vif in the R package 'car' 3.0–10 (Fox & Weisberg, 2019). Only variables with VIF smaller than five were retained for subsequent analyses (Akinwande et al., 2015). As a result, we eliminated three variables (SVL, TL and FL; Table S3) from the final males' matrix and five (BWE, ESD, BL, BWN and MTH; Table S4) from the final tadpoles' matrix.

To verify the morphometric differentiation between the validated molecular lineages, we conducted a permutational analysis of variance (PERMANOVA) for adult male and tadpole

morphometric data independently in the R package 'vegan' 2.5–6 (Oksanen et al., 2019), using Euclidian distance and 1 × 104 permutations. We implemented a post hoc pairwise test for each dataset, employing Bonferroni p-adjustment and Euclidean distance.

Integrative species delimitation

We performed an integrative delimitation with genetic and morphometric data in integrated BPP 2.1.3 (iBPP; Solís-Lemus et al., 2015). As iBPP analysis required a fixed tree, we ran each analysis twice, using distinct species trees generated by STACEY and StarBEAST2 (see below) as input to check the delimitation's robustness. We performed two sets of analyses for each tree, one with molecular data plus adults' morphometry and another plus tadpoles' morphometry, both with the same configuration of priors. We used four distinct combinations of gamma prior (theta [θ] and tau [τ] parameters) to evaluate whether the result was sensitive to the prior settings: (1) large ancestral population sizes and deep divergence (θ ~ G (2, 100), τ ~ G (2, 200)); (2) small ancestral population size and shallow divergences (θ ~ G (2, 1000), τ ~ G (2, 2000)); (3) small ancestral population sizes and deep divergences (θ ~ G (2, 1000), τ ~ G (2, 200)); and (4) large ancestral population sizes and shallow divergences (θ ~ G (2, 100), τ ~ G (2, 2000)). We assigned the other parameters to automatic adjustment by algorithm. We conducted all analyses with 2×10^6 generations, 10 thinning and 0.1% burn-in.

Testing for diversification scenarios

Estimating a temporal framework

We first estimated a temporal window for diversification using a dated species tree in StarBEAST2 0.15.5, implemented in BEAST 2.6.2 (Bouckaert et al., 2019; Ogilvie et al., 2017), using the species validated by STACEY. For this, we set a birth–death tree prior, uncorrelated log-normal clock, and we rooted the tree using *B. nanuzae* (Gernhard, 2008). We used 'bModelTest' 1.2.1 (Bouckaert & Drummond, 2017) to co-estimate nucleotide substitution models for all genes during the runs. To calibrate the clock, we truncated the substitution rate for cyt-*b* between the general substitution rate for vertebrates (mean of 10^{-2} substitutions per lineage per million years) (Johns & Avise, 1998) and 1.61×10^{-2} substitutions per lineage per million years as obtained by Stöck et al. (2012), with a uniform distribution. We used default priors for most parameters, except for clock rates of nDNA fragments and COI, for which we used a broad prior with 1/x distribution, and the algorithm co-estimated the substitution rates. We ran two replicates with 2×10^8 generations, 10% burn-in and thinning of

5×10^3 each. We combined the results of both runs using LogCombiner 2.6.2, and we annotated the MCC tree using TreeAnnotator 2.6.2 (Bouckaert et al., 2019) and visualized using FigTree 1.4.4 (Rambaut, 2018).

Past distribution of climatic niches

To assess climate-driven fluctuations in *B. saxicola*'s range, we generated maps of past distributions of climatic niches using ecological niche modelling (ENM). We critically reviewed the species dataset by deleting ambiguous, duplicate or unreliable records, and removing those whose geographical location or taxonomic Information were not precisely defined using a suite of coord_ functions from the R package 'scrubr' (Chamberlain, 2016). After this data cleaning, we spatially thinned the occurrence localities by 20 km to minimize clustering of records due to biased sampling using thin() available in the R package 'spThin' (Aiello-Lammens et al., 2015). We reached a dataset containing 30 unique and not clustered occurrence records (Table S1).

We used 14 bioclimatic variables as current candidate predictors with a spatial resolution of 0.08333° (~10 km) from the global dataset of PaleoClim (Brown et al., 2018). To avoid problems associated with multicollinearity, we selected the candidate predictors by VIF (Zuur et al., 2010), and we retained only variables with VIF smaller than 10 (Dormann et al., 2013) using the function vifstep from the R package 'usdm' (Naimi et al., 2014). As a result, we retained five variables — Mean Temperature of Driest Quarter (bio_9), Annual precipitation (bio_12), Precipitation of Wettest Month (bio_13), Precipitation of Driest Quarter (bio_17) and Precipitation of Warmest Quarter (bio_18) — in our final environmental dataset. We used the same environmental dataset for calibration and projection in the past climates. To characterize past climate conditions, we used the same current environmental dataset projected to the Marine Isotope Stage (MIS) in the Late Pliocene (M2, ca. 3.3 Ma), the mid-Pliocene Warm Period (mPWP, ~3.264–3.025 Ma), the Marine Isotope Stage 19 in the Pleistocene (MIS19; ~787 ka), the Last Interglacial past (LIG; ~130 ka), the Last Glacial Maximum (LGM; ~21 ka), the Heinrich Event 1 (HS1; ~17.0–14.7 ka), the abrupt warming at the onset of the Bølling–Allerød (BA; 14.7–12.9 ka), the rapid cooling at the onset of the Younger Dryas (YD; 12.9–11.6 ka), the early-Holocene (EH; 11.7–8.326 ka), the mid-Holocene (MH; 8.326–4.2 ka) and the Late Holocene (LH; ~4.2–0.3 ka). All global climate slices are available on PaleoClim (Brown et al., 2018). We check for the presence of non-analogous conditions in all scenarios of projection using the MESS (multivariate environmental similarity surface) analysis. We considered each

grid cell and compared our subset of bioclimatic variables in the projection of the past range with that of the calibration range (Elith et al., 2010). If the grid cells have a positive value, they indicate a similar environment between the past and current ranges. The environmental dissimilarity is indicated by negative values. We used the R package 'ecospat' 3.1 (Broennimann et al., 2020; Di Cola et al., 2017) to compute the MESS analysis for identifying how similar the past and current range projections are.

To characterize environmental conditions experienced by *B. saxicola* to predict its model of ecological niche, we associated the spatial distribution records with climate data. We used the R package 'sdm' (Naimi & Araújo, 2016) to develop the ensemble forecasting (Araújo & New, 2007) of ENM (Peterson & Soberón, 2012), and we combined the output models to generate a single prediction. We used seven methods including 'brt' (boosted regression trees; (Friedman, 2001), 'svm' (support vector machine; (Vapnik, 1995), 'maxent' (maximum entropy; Phillips et al., 2006), 'maxlike' (likelihood-based estimator adopted for presenceonly data; Royle et al., 2012), 'glm' (generalized linear models; McCullagh & Nelder, 1989), 'gam' (generalized additive models; Hastie & Tibshirani, 1990) and 'mad' (mixture discriminant analyses; Hastie & Tibshirani, 1996). Besides considering different types of data (presence-only and presence-background), these methods together consider a variety of statistical techniques (Rangel & Loyola, 2012) desirable for more robust ensemble forecasts (Araújo & New, 2007). We generated a random sample of 1×10^4 sites similar to absence, and we performed the analysis using 30 runs of subsampling replication methods by splitting into training and test dataset (70:30). We built and calibrated the model within a polygon (xmin: −79.47263; xmax: −27.53447; ymin: −35.13761; ymax: −0.19551). Ensemble models were parameterizing using weighted averaging based on TSS statistic.

We used the area under the curve (AUC) of the receiver operating characteristic (ROC) to assess the accuracy of ENM (Fielding & Bell, 1997). AUC values of 0.7–0.9 indicate good accuracy, while values above 0.9, high accuracy (Swets, 1988). We also used the true skill statistic (TSS), which considers both model sensitivity and specificity (Allouche et al., 2006). We generated 210 individually calibrated models, and we used the TSS to create a weighted average of each prediction model. We generated ensemble forecasting using the output models for each time slice. We classified continuous predictions into presence and absence maps based on maximizing the TSS (Allouche et al., 2006). Furthermore, we assembled the binary maps by simple mean values from single methods under current and past climate conditions. Also, we evaluated the variable importance (Murray & Conner, 2009) and plotted the predicted response

curve (Elith et al., 2005) for inferring the relationship between the environmental variables and predicted habitat suitability. Finally, we used the binary maps for each time slice to establish the climatic stability surfaces.

Demographic model selection

To test hypotheses of lineages diversification in our focal species, we conducted coalescent simulations under seven competing scenarios (Figure 2) to select those that best fit the data using approximate Bayesian computation (ABC) framework, as implemented in DIYABC 2.1 (Cornuet et al., 2014). Following the results on species delimitation, all scenarios included four lineages and had 14.29% a priori probability each. These scenarios represent three groups of diversification models: fragmentation, diffusion and jump dispersal (Lomolino et al., 2010), with scenario 1 fitting all the premises of the model proposed by Nascimento et al. (2018) following OCBIL theory (i.e. long-term fragmentation and climatic stability). For fragmentation scenarios (1–3), we set population sizes of descendent populations always smaller than ancestral ones. In diffusion scenarios (4–6), we set up an increase in ancestral population size before each cladogenetic event. In the jump-dispersal scenario (7), the settings were similar to diffusion scenarios for ancestral populations, whereas the colonization took place after a period with a substantial size reduction (i.e. founder effect). Moreover, we tested scenarios with no demographic changes (1, 4), with an expansion of the Southern lineage (2, 5), or with bottlenecks of Cabral, Central and Northern lineages (3, 6), taking relative θ between lineages into account. The relative θ parameters were estimated in Migrate-n 3.7.2 (Appendix S1; Beerli, 2006, 2007, 2009).

We assumed a generation time of 1 year, using a Jukes–Cantor evolution model for each group of markers (mtDNA and nDNA), and the nucleotide substitution rate (per site per generation) as the same as StarBeast2 for mtDNA and between 1×10^{-9} and 1×10^{-10} for nDNA. We used 95% highest posterior density (HPD) of the species tree's nodes as priors for the time of divergence. The priors for bottleneck or expansion (scenarios 2–6) varied between the last cladogenetic event and the transition between the Pleistocene and Holocene (i.e. 11.7 ka), keeping divergence time older than time for contraction/expansion as a condition. In scenario 7, we conditioned the maximum time for the expansion after the founder effect to the time of the subsequent cladogenetic event for the first two diverging lineages (i.e. Northern and Cabral). For Central and Southern lineages, the maximum value for this prior was the Pleistocene and Holocene's transition. Priors for population size varied from 1×10^5 to 1×10^6,

population size during contraction and founder effect varied from 1×10^3 to 1×10^5, and population sizes expansion in Southern lineage (scenarios 2 and 5) varied from 1×10^6 to 1×10^8. All ancestral populations varied from 1×10^3 to 1×10^8. We assumed a uniform distribution for all priors.

To select adequate summary statistics, we did runs (1×10^5 generations for each scenario) performing the rejection step with each summary statistic individually (i.e. number of haplotypes, number of segregating sites, mean of pairwise differences, variance of pairwise differences, Tajima's D, private segregating sites, mean of numbers of the rarest nucleotide at segregating sites, variance of numbers of the rarest nucleotide at segregating sites). We used the total posterior predictive error over 100 pseudo-observed datasets, keeping all other values in their default configurations and the 'evaluate confidence in scenario choice' function to select summary statistics with a posterior error lower than 0.4. Finally, we simulated 1×10^5 generations for each scenario and computed posterior probabilities for each model with a tolerance of 0.1% using the direct and 1% logistic approach. We determined the best model with a Bayes factor (i.e. the probability of the best model divided by the probability of the second best model), and checked the model with PCA based on the 1% genealogies closest to the observed data.

Historical diffusion reconstruction

As a dispersion model best fit our data (see Section 3), we estimated the historical dispersion routes and the ancestral distribution of each node in the tree through a species tree diffusion approach based on Relaxed Random Walk (RRW) algorithm implemented in BEAST 1.10.4 (Nylinder et al., 2014; Suchard et al., 2018). The species trees used as input were the posterior sampling generated in the StarBEAST2 analysis above. To represent each lineage's geographical distribution, we constructed minimum convex polygons (MCP) with 10 km buffer for the geographical records in Qgis 3.14.1 Pi (QGIS Development Team, 2020). We used the script made available by Nylinder et al. (2014) to configure the input analysis from species trees and MCPs. We ran the analysis per se assuming a log-normal RRW, with two replicates of 5×10^7 generations, 5×10^3 thinning and 5% burn-in. We combined the results of both runs using LogCombiner 1.10.4, and annotated the MCC tree with TreeAnnotator 1.10.4 (Suchard et al., 2018). We generated the visual representation of the spatial diffusion in SPREAD 1.0.7 (Bielejec et al., 2011), and summarized the variation of diffusion rate over time using the TimeSlicer tool (Lemey et al., 2010). We ran all BEAST (1.10.4 or 2.6.2) analyses using the

online CIPRES Science Gateway Portal (Miller et al., 2010), and checked the stationarity and convergence using Tracer 1.7.1 (Rambaut et al., 2018) through a visual inspection of adequate minimum effective sample sizes (ESS > 200) of the estimated parameters.

Results

Testing for multiple species

Exploring genetic structure

All loci are neutral, with a non-significant value of Tajima's D, and two fragments, *β*-fib and c-*myc*, showed evidence for recombination in ϕ-tests (Table S6). Because of this, both were removed from all coalescent analyses.

GMYC identified two lineages in the Southern distribution (Figure S1). The Geneland analysis returned four clusters (K = 4), with an average frequency above 54% among MCMC iterations, after a burn-in of 1.5×10^3 initial generations (Figure S2). All individuals had a 100% probability of belonging to their own population (Figure 3a).

The multilocus nDNA network showed a clear differentiation between the four lineages delimited by Geneland, with no mixed individuals between them (Figure 3b). The GMYC subclades were not recovered in the nDNA data, and a mixture can be seen between individuals from the two mtDNA clades (Figure 3b). Only the nDNA fragments β-fib and DIA6 showed reciprocally exclusive haplotypes concerning the lineages discovered by Geneland (Figure S3). However, none of the nDNA fragments showed exclusive and well-differentiated haplogroups (Figure S3). Despite the haplotype sharing, there is no evidence of recent hybridization between any pair of lineages, as revealed by the absence of mixed individuals in the Q-plot and the lack of individuals represented in the ‘torso’ of the multilocus network (Figure 3a,b).

Molecular species delimitation

The four distinct lineages of *Bokermannohyla saxicola* in SE were validated in STACEY, with PP = 99.76%. In the STACEY tree, Cabral is the sister lineage of all the other ones (i.e. (Cabral, (Northern, (Central, Southern)))). However, the Northern-Central-Southern clade is poorly supported (PP = 0.39).

Morphological species delimitation

PERMANOVA results showed significant divergence between the adult males and tadpoles traits of different lineages. There is a subtle pairwise difference in males, ranging from

2.71% between Southern and Central to 7.94% between Northern and Central (Table 1). In tadpoles, despite the significant result, not all pairs of lineages differed. Only Cabral lineage is morphometrically distinct from the others, ranging from 8.34% (Southern) to 20.73% (Central) of pairwise lineage divergences (Table 1).

Integrative species delimitation

iBPP results were congruent, and both confirmed the four lineages as species with high statistic support (PP > 0.99), regardless of θ and τ combinations and initial tree (Table S7).

Testing for diversification scenarios

Estimating a temporal framework

The StarBEAST2 species tree showed a distinct topology (Figure 3c). The Northern lineage was the first to diverge in the Pliocene, about ~3.19 Ma (95% HPD: 2.29–4.33 Ma). Cabral is the sister lineage of Southern + Central, and this cladogenetic event occurred in the Early Pleistocene, about ~2.11 Ma (95% HPD: 1.47–2.86 Ma). Central and Southern lineages also diverged in the Pleistocene, dating ~1.03 Ma (95% HPD: 0.72–1.39 Ma; Figure 3c). Because the strong node support in this analysis (PP = 1), we consider this topology in further analyses (i.e. ABC and RRW).

Past distribution of climatic niches

Our models showed high predictive accuracies with an AUC of 0.981 (SD = 0.014). The response curves showed that the probability of occurrence of *B. saxicola* is fundamentally limited by precipitation (Figures S4 and S5), the precipitation of wettest month (bio_13) and precipitation of warmest quarter (bio_18) have high relative importance among predictors. Using the consensual maps (TSS = 0.953, SD = 0.026), the models of ecological niche showed that for *B. saxicola* there was cyclic contraction and expansion of suitable climate over time. For example, in the most distant past, between M2 and mPWP (~3.3–3.025 Ma), a contraction in area is predicted to have occurred (Figure 4). On the other hand, LGM shows the climatic suitable area for *B. saxicola* is greatly increased in a northerly direction (Figure 4). From the HS1, there was an altitudinal change in models from higher to lower altitude regions. High climate suitability in lowlands was observed in HS1 and BA (Figure 4) times. With the climate becoming warmer in the mid-Holocene, the suitable areas underwent an expansion, with areas being maintained until current time in EM, mainly at high altitudes (Figure 4). The areas of

greatest climate stability for *B. saxicola* coincide with the limits of *campo rupestre* plus the marginal areas from the southwestern of the SE (Figure 4). The MESS analysis revealed that past and current climatic niches of *B. saxicola* are similar over time (Figure S6).

Demographic model selection

The evaluation of summary statistics in DIYABC resulted in eliminating four of them as non-informative for distinguishing among the seven alternative demographic scenarios. Thus, we conducted the analysis by considering the mean of pairwise differences, Tajima's D, private segregating sites and mean of numbers of the rarest nucleotide at segregating sites. ABC identified the jump dispersal (scenario 7) as the most likely model to explain the current geographical distributions and effective sizes of *Bokermannohyla saxicola* lineages (Table S8). According to the direct and logistic approach, the Bayes factor provided strong and substantial support for the best selected model (Bayes factordirect = 37.75, Bayes factorlogistic = 5.55; *sensu* (Jeffreys, 1961). The PCA showed model fit and adequacy, with the observed data within the posterior distribution (Figure S7).

Historical diffusion reconstruction

We inferred the dynamics of *B. saxicola* spread occurred in a centrifugal dispersion pattern. According to RRW, the most likely region for onset of diversification of *B. saxicola* was located between the current geographical distributions of the Central and Southern lineages. The first colonization event occurred from this region to the north (current distribution of Northern lineage) (Figure 5a). The second event occurred from the ancestral location towards the southwest (current distribution of Cabral lineage) and east (Figure 5b,c). Finally, the Southern and Central lineages' ancestor spread to their current distribution areas (Figure 5d). The diffusion rate was slow and constant through time, with a mean diffusion rate of ~70.771 km per million years (=0.071 m/year; 95% HPD: 0.022–0.142 m/year; Figure 5e).

Discussion

Our results support the hypothesis of multiple putative species in the ledge treefrog within the EM. We also found support that the diversification of these lineages was influenced by climate changes that have occurred since the late Pliocene, leading to the colonization of the region. Therefore, our results differ in several temporal and biogeographical patterns and

processes from those presented and interpreted by Nascimento et al. (2018) and from OCBIL theory premises (Hopper, 2009; Hopper et al., 2016).

Although the mitochondrial data show two distinct clades in the Southern lineage, as pointed by Nascimento et al. (2018), they are not supported by our multilocus analysis. This apparent mitochondrial structure is likely an isolation by distance (IBD) effect, as previously reported (Nascimento et al., 2018), leading to an overestimation of K (Frantz et al., 2009; Perez et al., 2018). All other lineages proposed by Nascimento et al. (2018) were strongly supported by multigenic and morphological data. Because there is a significant morphometric overlap between lineages in both adults and larvae, we suggest that the *B. saxicola* species complex must be revised in a taxonomic investigation that includes other types of phenotypic traits such as calls and other aspects of behaviour.

The four delimited lineages are currently allopatric, and there may exist geographical barriers restricting gene flow among them (Nascimento et al., 2018). The depression between the Diamantina plateau (i.e. north of the continuous core of the Southern lineage; Figure 1) and Serra de Itacambira (the distribution of the Central lineage; Figure 1) is a putative barrier as it corresponds to phylogeographical breaks also in other taxa. It was observed to delimit distributions in the large-headed leaf frog (*Pithecopus megacephalus*) and the large-eared rock frog (*Thoropa megatympanum*) (Ramos et al., 2018; Sabbag et al., 2018), and also, for at least one species of cactus (*Pilosocereus aurisetus*; Perez et al., 2016). Although the populations of *B. saxicola* from Turmalina and Botumirim (locations 7 and 8, respectively; Figure 1) group genetically with the Southern lineage, they are geographically closer to the Central region. Conversely, in the other abovementioned anurans, the Botumirim samples group with lineages located north of the depression. This may be related to species-specific natural histories and dispersal abilities, as well as to their idiosyncratic responses to biogeographical events (Flantua et al., 2020). Note that none of the other species have been registered in Turmalina (R.F.M., pers. obs.), a marginal ER area with a strong influence of semi-deciduous Atlantic Forest. The Pleistocene's climate dynamics may have favoured the connectivity between the *campo rupestre* of the Espinhaço core and these marginal areas. These changes were favourable for forming climatically suitable corridors in lowlands mainly in HS1 and BA time slice (Figure 4). The displacement of the suitable climate may have maintained connectivity between the Diamantina plateau populations and the lower areas of the Turmalina region, favouring the colonization of Botumirim by the Southern lineage. Botumirim and Turmalina, for example, are approximately in the same longitude and are only 46.5 km apart (Figure 1).

Although the geographical structure is not completely identical as in other co-distributed species, some barriers seem recurrent. The low-latitude borders of Serra do Cabral, a disjunct montane unit west of ER (Figure 1), experienced high climatic instability and low suitability through time and may have acted as a continuous climatic barrier for taxa in the region. A corresponding genetic break is observed in the ledge treefrog (between the Cabral and the other lineages), as well as in other species such as the Alvarenga's treefrog (*Bokermannohyla alvarengai*), which does not occur in Serra do Cabral (de Oliveira et al., 2021), and the large eared rock frog, which has similar genetic structure to *B. saxicola* (Sabbag, 2013). In addition, the phylogeographical break between the central portion and the northern sky islands of SE was also observed for the large-headed frog (Ramos et al., 2018). From those results, major geographical patterns in ER emerge, and their concordance at community level may be further tested in comparative phylogeographical studies (e.g. Bell et al., 2012).

Even though some similar spatial barriers can be highlighted among co-distributed taxa in ER, they may not be related to the same temporal events associated with the diversification of *B. saxicola*. The congeneric Alvarenga's treefrog has a more recent diversification, with the northern and southern lineages diverging around 340 ka (de Oliveira et al., 2021). On the other hand, structure in the large-eared rock frog coalesced in times comparable to our study, around 3 Ma (Sabbag et al., 2018). Thus, it is likely that the high biotic diversity and endemism observed in ER may result from multiple pulses of diversification throughout its history. Our results suggest that the diversification of *B. saxicola* started in late Pliocene, with credibility intervals including the Pleistocene, supporting more recent diversification events than those reported by Nascimento et al. (2018). This difference is likely related to the addition of nuclear markers since mtDNA genes have higher mutation rates and a quarter of the effective population size of nuclear ones, which usually results in an overestimation of divergence time when this type of data is used alone (Allio et al., 2017; Hickerson et al., 2010; Hoelzer, 1997; McCormack et al., 2011). The multilocus unlinked genes can better accommodate coalescent stochasticity and improve the accuracy and precision of phylogenetic inferences and divergence time estimates (Beheregaray, 2008; McCormack et al., 2011). Although we did not use anuran fossil for species tree calibration, the mutation rates of the cyt-b mtDNA (Johns & Avise, 1998; Stöck et al., 2012) have been used to calibrations in anurans and appear reliable (Dufresnes et al., 2016; Ramos et al., 2019). Furthermore, Nascimento et al. (2018) used a very similar calibration method, making our results directly comparable. Despite the discrepancy in

divergence times, our species tree showed the same topology as the tree of Nascimento et al. (2018).

Eterovick et al. (2016) used microsatellite markers to describe the spatial genetic diversity of *B. saxicola* and suggested the centre of diversification of the species to be in the EM's southern region. Their conclusions were based on the greater genetic diversity observed for the lineage in this region. Our results disagree with this hypothesis, suggesting an origin for the species at the centre of its distribution followed by a centrifugal colonization pattern. Two factors can explain the greater genetic diversity of the Southern lineage. First, this lineage occupies the largest continuous area of *campo rupestre* in EM. The greater carrying capacity of this continuous core plus the genetic variants that arose on the small isolated sky island nearby could explain the Southern lineage's greater genetic diversity, since this metric is directly correlated with area and isolation among sites (Vellend, 2003). Second, changes in effective population sizes mediated by Pleistocene climate fluctuations may have been softer in this region. The best scenario selected by ABC accommodate population expansion for all lineages after a founder effect, which implies recent growth. However, the posterior estimates in the ABC show that the population size in the Southern lineage is greater than that of the other lineages, and this may be a result of the lineage growth along with increases in the climatically favourable areas for the lineage. Changes in effective population size associated with Pleistocene climate regimes in the SE have also been reported for the Alvarenga's treefrog (de Oliveira et al., 2021) and for the cactus *P. aurisetus* (Bonatelli et al., 2014; Perez et al., 2016). This indicates that, even for some plants, the OCBIL premise of climatic buffering for the *campo rupestre* may be unrealistic (Magalhães et al., 2021).

The phylogeography of *B. saxicola* also disagrees with the longterm fragmentation premise of OCBIL theory (Hopper, 2009; Hopper et al., 2016). Our data contradict the hypothesis that this species occurred continuously in SE and that genetic structure was mainly caused by the historical fragmentation of an ancestral population (e.g. vicariance), as suggested by Nascimento et al. (2018). Instead, we show that the species' current distribution and diversity were achieved by crossing barriers and colonizing new areas, thus, an evolutionary history dominated by dispersion. Pleistocene climate fluctuations may have facilitated this colonization, although none of the ENM time slices projections coincides in time with lineages cladogeneses, the vertical displacement of suitable areas in different times led us to hypothesize that early Pleistocene climate changes allowed *B. saxicola* to cross barriers (i.e. lowlands) and to expand its geographical range through successive founder events. While the

palaeopalynologic data are scant for the ER (Barbosa & Fernandes, 2016), at least one study reported that lowlands today dominated by tropical semi-deciduous forests and savannahs have replaced subtropical grasslands ecosystems that predominated during cold periods over the past 48 ka in SE (Behling & Lichte, 1997). This record offers independent support for our hypothesis of altitudinal climatic displacements in ER throughout the Pleistocene.

Colonization of new areas is recovered as an important process for the evolution of the *campo rupestre* biota. This process also explains the contemporary geographical distribution of the genetic diversity in *Vellozia auriculata* bushes (Fiorini et al., 2019) and in the Alvarenga's treefrog (de Oliveira et al., 2021). Introgressive hybridization has also been reported for two *Pithecopus* monkey-frogs (Magalhães et al., 2021). da Silva et al. (2018), in turn, demonstrated that many species endemic to Brazilian highlands are shared between Quadrilátero Ferrífero in ER and Mantiqueira mountains (located south of the ER). This may indicate past intermixing between these mountain ranges. Therefore, the ER's mountain fingerprint is more complex than that expected solely by the OCBIL theory (Flantua & Hooghiemstra, 2018; Hopper et al., 2016). That does not mean that fragmentation is not a relevant process shaping the ER diversity for other taxa. Silveira et al. (2020) reviewed the phylogeographical and population genetic studies published with endemic plants to the *campo rupestre*. The authors reported that most of the genetic structure was correlated with geographical fragmentation. This process was also important for at least the frogs in the genera *Crossodactylodes* and *Rupirana* (Santos et al., 2020). Therefore, other processes than fragmentation in FCS model (Flantua & Hooghiemstra, 2018) are at least as good of an explanation, with both being probably complementary to describe the *campo rupestre* mountain fingerprint.

The ER's endemic plants' phylogeography has been relatively well explored (Silveira et al., 2020). However, there are still several shortfalls in the ecology and evolution of animals (Miola et al., 2021), even with the recent improvement in studies of anurofauna (e.g. de Oliveira et al., 2021; Magalhães et al., 2021). Our study adds one more piece to understanding the patterns and processes responsible for generating the ER's diversity and endemism. Our results add further evidence that the diversification scenario of the *campo rupestre* is more complex than predicted by the OCBIL theory, whose popularity has grown since the last decade (Hopper et al., 2016; Miola et al., 2021; Silveira et al., 2016). Future comparative and interdisciplinary approaches at the community level may help us better understand which temporal and spatial mechanisms have driven the current distribution of the co-distributed lineages in the ER and *campo rupestre* (Bell et al., 2012; Flantua & Hooghiemstra, 2018).

Tables

Table 1 Results of permutational multivariate analysis of variance (PERMANOVA) showing differences in morphometric data from lineages of *Bokermannohyla saxicola* in Espinhaço Range. *P < 0.05 in pairwise PERMANOVA

	Adult males (n = 402)						**Tadpoles (n = 133)**					
	Df	**Sum sqs**	**Mean sqs**	**F model**	**R2**	**P (>F)**	**Df**	**Sum sqs**	**Mean sqs**	**F model**	**R2**	**P (>F)**
Lineages	3	0.878	0.298	13.618	0.093	9.99×10^{-5}	3	1.321	0.440	5.155	0.107	9.99×10^{-5}
Residuals	398	8.556	0.022		0.907		129	11.015	0.085		0.893	
Total	401	9.434			1		132	12.336			1	
Pairwise PERMANOVA: R^2 value (F model)												
	Cabral	**Central**	**Northern**	**Southern**			**Cabral**	**Central**	**Northern**	**Southern**		
Cabral	-						-					
Central	0.076* (6.221)	-					0.208* (11.504)	-				
Northern	0.072* (4.641)	0.079* (4.832)	-				0.104* (3.954)	0.054 (1.378)	-			
Southern	0.050* (18.113)	0.027* (9.425)	0.054* (18.382)	-			0.083* (9.550)	0.225 (2.186)	0.030 (2.669)	-		

Figures

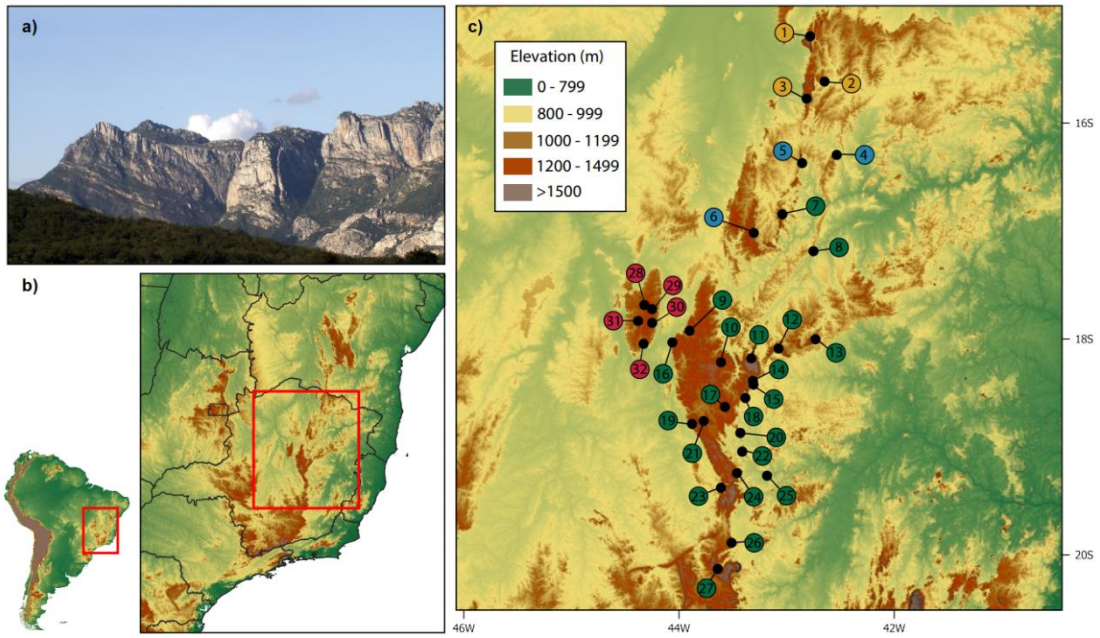

Figure 1 (a) View of the Serra Azul in Serranópolis de Minas (location 3), showing the contrast between lowland (seasonal semideciduous forest) and high-altitude environments (*campo rupestre*); (b) Map of Brazilian Shield highlands and its location in South America (inset), with Espinhaço Mineiro (EM) highlighted and enlarged in (c). Espinhaço Baiano (EB) is the upland region north of EM, outside the red box; (c) Localities of *Bokermannohyla saxicola* in EM, including records of genetic and morphometric data. Coloured circles correspond to delimited lineages (yellow = Northern, blue = Central, green = Southern, red = Cabral; see Section 3), and numbers correspond to locations, from north to south: (1) Santo Antônio do Retiro; (2) Rio Pardo de Minas; (3) Serranópolis de Minas; (4) Padre Carvalho; (5) Grão Mogol; (6) Itacambira; (7) Botumirim; (8) Turmalina; (9) Buenópolis (Parque Nacional das Sempre Vivas); (10) Diamantina; (11) São Gonçalo do Rio Preto; (12) Rio Vermelho; (13) Itamarandiba; (14) Serra Azul de Minas; (15) Santo Antônio do Itambé; (16) Augusto de Lima (Águas de Santa Bárbara); (17) Presidente Kubitschek; (18) Serro; (19) Santana de Pirapama; (20) Alvorada de Minas; (21) Congonhas do Norte; (22) Conceição do Mato Dentro; (23) Santana do Riacho; (24) Morro do Pilar; (25) São Sebastião do Rio Preto; (26) Barão de Cocais; (27) Santa Bárbara; (28) Francisco Dumont; (29) Joaquim Felício; (30) Buenópolis; (31) Lassance; (32) Augusto de Lima. Region denominated as Diamantina plateau correspond to the locations (9–11) and (14–18), Quadrilátero Ferrífero to (26–27), and Serra do Cabral to (28–32). For details on georeferenced sampling points, see Table S1

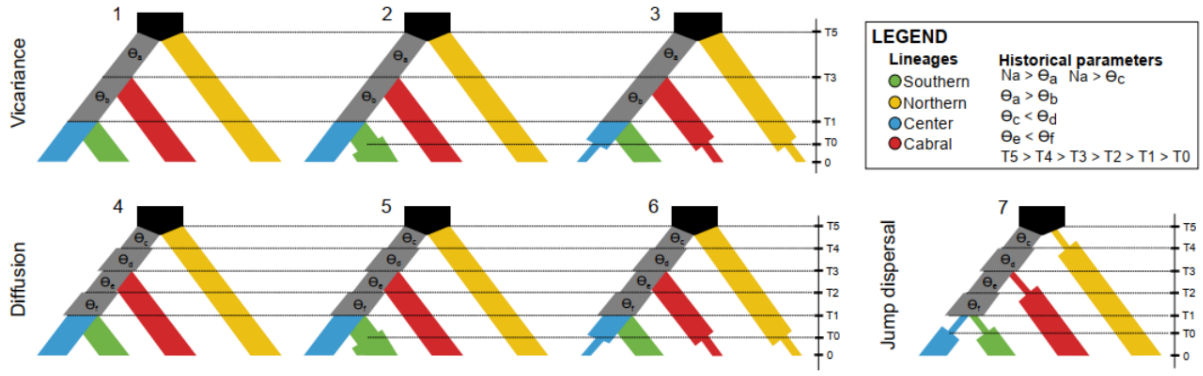

Figure 2 Evolutionary scenarios tested using DIYABC for *Bokermannohyla saxicola* in Espinhaço Range. Vicariance process: (1) Constant populations size over time, (2) Southern lineage expansion and (3) Southern linage stable and other retraction; Diffusion: (4) Constant populations size over time, (5) Southern expansion and other stable, (6) Southern lineage stable and other retraction; and (7) Jump dispersal. We assumed one first ancestral population not sampled, with effective size Na, in black in all scenarios. Time and effective population size in scenarios are not in scale

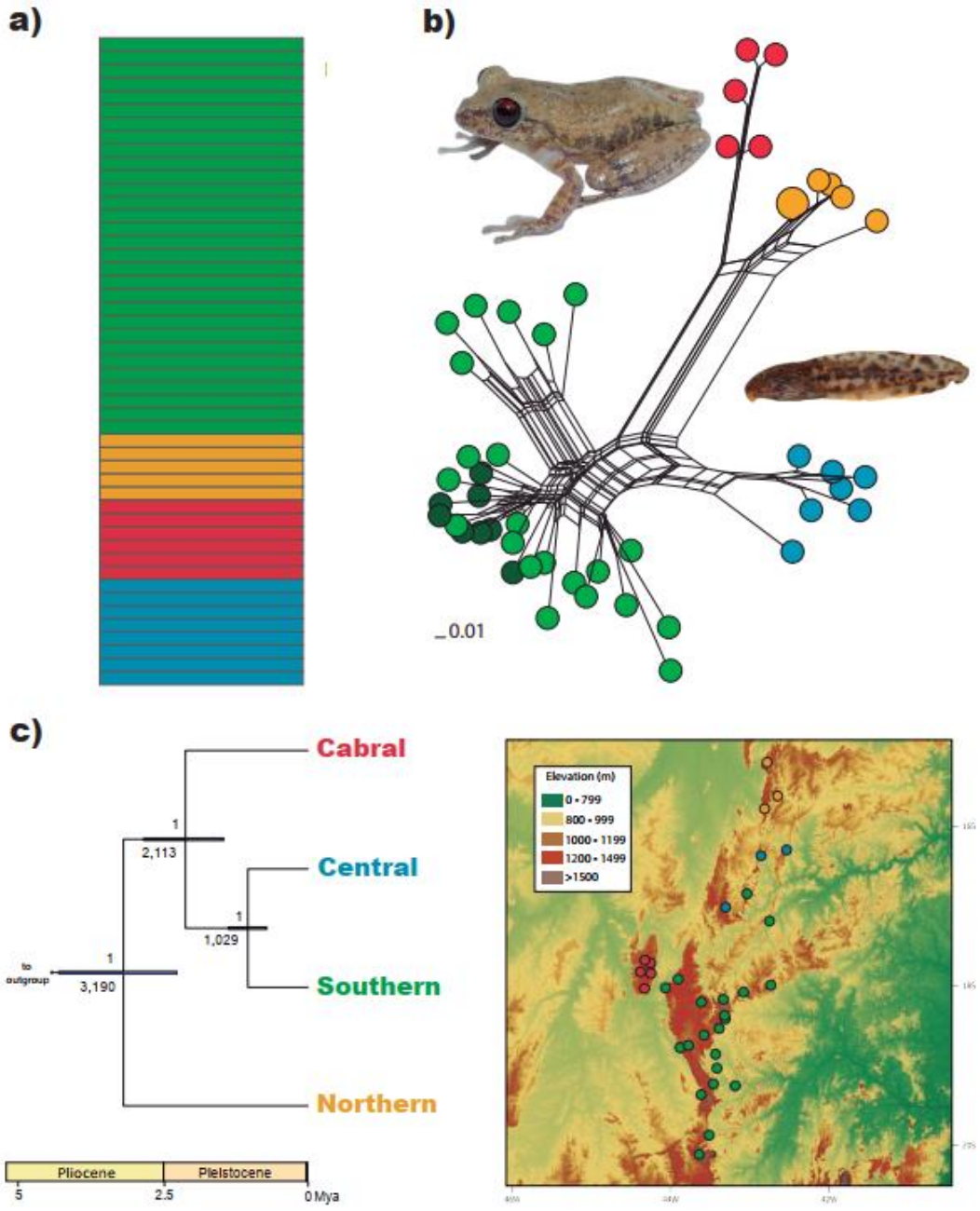

Figure 3 Multiple lineages and time framework of *Bokermannohyla saxicola* in the Espinhaço Range. The same colours represent the observed lineages. (a) Q-plot at K = 4, showing each individual as a bar and membership probabilities as different colours; (b) Multilocus nuclear Neighbor-net representation. Scale bar represents standardized genetic distances for the net. Different shades of green represent the two subclades found by Nascimento et al. (2018) and GMYC. Adult and tadpole photographs by Tiago Leite Pezzuti. The photographs do not respect real proportion and were taken from Cabral lineages; (c) Left: Time-calibrated species tree. Node bars correspond to the 95% High Posterior Density (HPD) time. Values on branches correspond to posterior probabilities above and average time in million years below. Right: Distribution range of each lineage in the Espinhaço Range

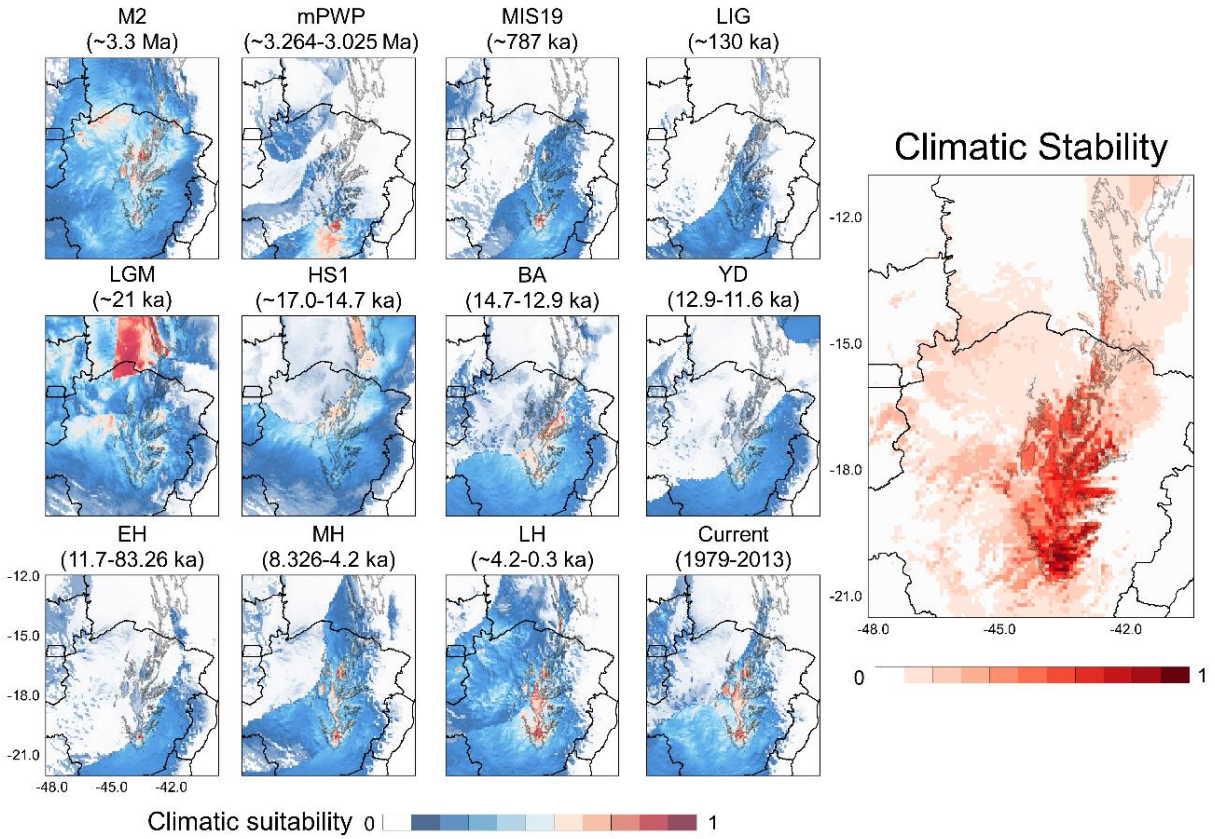

Figure 4 Distribution models for *Bokermannohyla saxicola* that represent the relative climatic suitability areas over time. The map of stability areas represents the sum of maps in all periods for *B. saxicola*. The colour scales represent the suitability or stability for the maps, from areas with low (0) to high (1) values. The grey shape represents the limits modified from Fernandes et al. (2014) of the *campo rupestre*, the predominant ecosystem in Espinhaço Range. The time slice abbreviations correspond to: BA, abrupt warming at the onset of the BøllingAllerød; EH, early-Holocene; HS1, Heinrich Event 1; LGM, Last Glacial Maximum; LH, late-Holocene; LIG, Last Interglacial past; M2, Marine Isotope Stage in the late Pliocene; MH, mid-Holocene; MIS19, Marine Isotope Stage in the Pleistocene; mPWP, mid-Pliocene Warm Period; YD, rapid cooling at the onset of the Younger Dryas

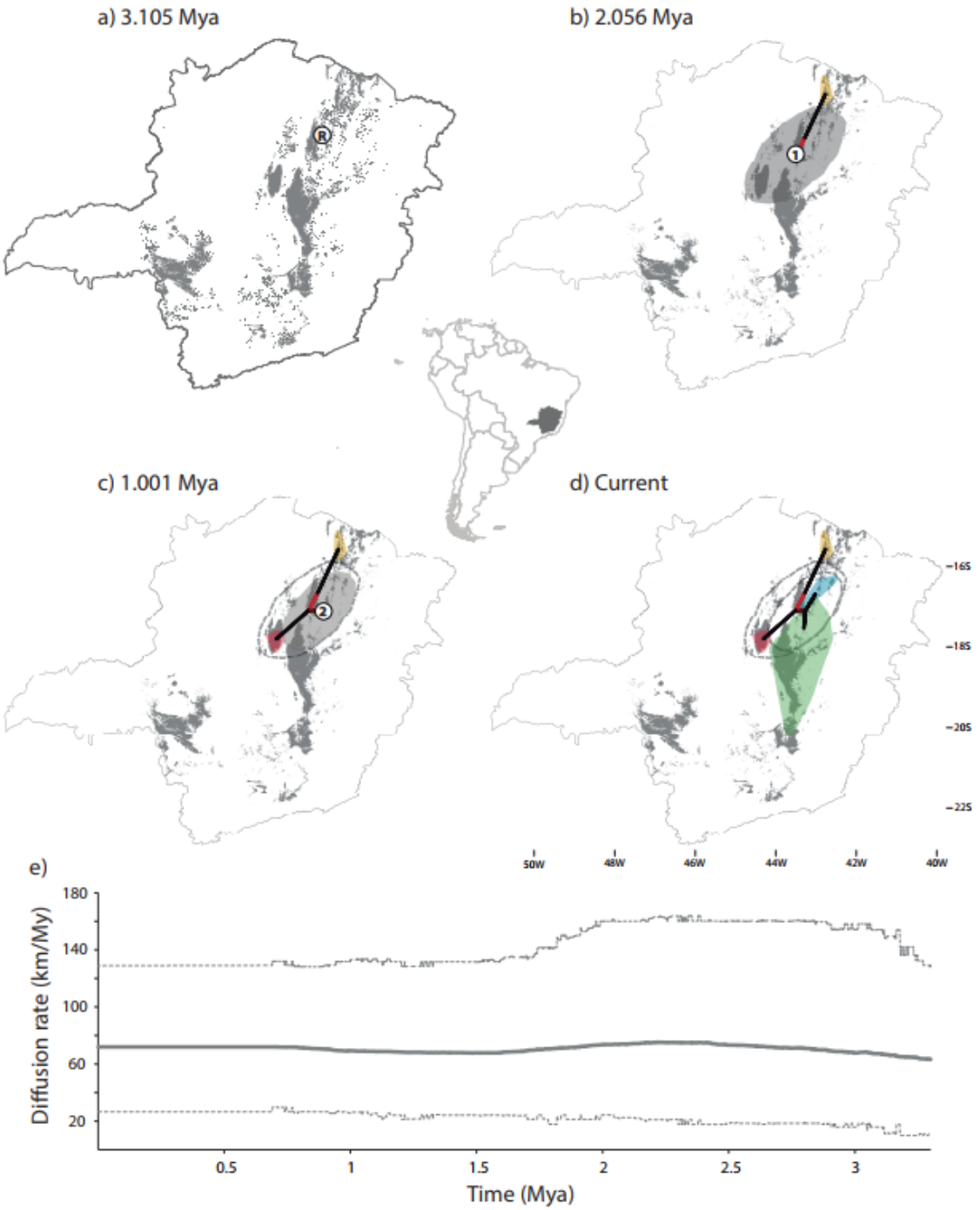

Figure 5 (a)–(d) Snapshots of the spatial–temporal dynamics of *Bokermannohyla saxicola* in Espinhaço Range. Circles R, 1 and 2 represent the estimated root location and subsequent cladogenetic events, respectively. Grey polygons represent 80% Highest Posterior Density (HPD) interval of uncertainty in the location of ancestral branches. Coloured polygons represent the current distribution of distinct lineages; (e) Diffusion rate through time. The grey shape represents the limits modified from Fernandes et al. (2014) of the *campo rupestre*, the predominant ecosystem in the Espinhaço Range

Data Availability Statement

Gene sequences are available at GenBank (accession numbers: OL672838-OL672842, OL653177-OL653182, OL661345-OL661352, OL943989-OL944005, OL653183-OL653194, OL653230-OL653295, OL653195-OL653221, OL653222-OL653229; Table S1). Geographical and morphometric data are available in Tables S1, S3 and S4.

References

Aiello-Lammens, M. E., Boria, R. A., Radosavljevic, A., Vilela, B., & Anderson, R. P. (2015). spThin: An R package for spatial thinning of species occurrence records for use in ecological niche models. *Ecography, 38*(5), 541–545. https://doi.org/10.1111/ecog.01132

Akinwande, M. O., Dikko, H. G., & Samson, A. (2015). Variance Inflation Factor: As a Condition for the Inclusion of Suppressor Variable(s) in Regression Analysis. *Open Journal of Statistics, 05*(07), 754–767. https://doi.org/10.4236/ojs.2015.57075

Allio, R., Donega, S., Galtier, N., & Nabholz, B. (2017). Large variation in the ratio of mitochondrial to nuclear mutation rate across animals: Implications for genetic diversity and the use of mitochondrial DNA as a molecular marker. *Molecular Biology and Evolution, 34*(11), 2762–2772. https://doi.org/10.1093/molbev/msx197

Allouche, O., Tsoar, A., & Kadmon, R. (2006). Assessing the accuracy of species distribution models: Prevalence, kappa and the true skill statistic (TSS). *Journal of Applied Ecology, 43*(6), 1223–1232. https://doi.org/10.1111/j.1365-2664.2006.01214.x

Antonelli, A., Kissling, W. D., Flantua, S. G. A., Bermúdez, M. A., Mulch, A., Muellner-Riehl, A. N., Kreft, H., Linder, H. P., Badgley, C., Fjeldså, J., Fritz, S. A., Rahbek, C., Herman, F., Hooghiemstra, H., & Hoorn, C. (2018). Geological and climatic influences on mountain biodiversity. Nature Geoscience, 11(10), 718–725. https://doi.org/10.1038/s41561-018-0236-z

Araújo, M. B., & New, M. (2007). Ensemble forecasting of species distributions. Trends in Ecology and Evolution, 22(1), 42–47. https://doi.org/10.1016/j.tree.2006.09.010

Barbosa, N. P. U., & Fernandes, G. W. (2016). Rupestrian grassland: Past, present and future distribution. In G. W. Fernandes (Ed.), *Ecology and conservation of mountaintop grasslands in Brazil* (pp. 531–544). Springer International Publishing.

Beerli, P. (2006). Comparison of Bayesian and maximum-likelihood inference of population genetic parameters. *Bioinformatics, 22*(3), 341–345. https://doi.org/10.1093/bioinformatics/bti803

Beerli, P. (2007). Estimation of the population scaled mutation rate from microsatellite data. *Genetics, 177*(3), 1967–1968. https://doi.org/10.1534/genetics.107.078931

Beerli, P. (2009). How to use MIGRATE or why are Markov chain Monte Carlo programs difficult to use? In G. Bertorelle, M. W. Bruford, H. C. Hauffe, A. Rizzoli, & C. Vernesi (Eds.), *Population Genetics for Animal Conservation* (pp. 42–79). Cambridge University Press. https://doi.org/10.1017/CBO9780511626920.004

Beheregaray, L. B. (2008). Twenty years of phylogeography: The state of the field and the challenges for the Southern Hemisphere. *Molecular Ecology, 17*(17), 3754–3774. https://doi.org/10.1111/j.1365-294X.2008.03857.x

Behling, H., & Lichte, M. (1997). Evidence of Dry and Cold Climatic Conditions at Glacial Times in Tropical Southeastern Brazil. *Quaternary Research, 48*(3), 348–358. https://doi.org/10.1006/qres.1997.1932

Bell, R. C., MacKenzie, J. B., Hickerson, M. J., Chavarría, K. L., Cunningham, M., Williams, S., & Moritz, C. (2012). Comparative multi-locus phylogeography confirms multiple vicariance events in co-distributed rainforest frogs. *Proceedings of the Royal Society B: Biological Sciences, 279*(1730), 991–999. https://doi.org/10.1098/rspb.2011.1229

Bielejec, F., Rambaut, A., Suchard, M. A., & Lemey, P. (2011). SPREAD: Spatial phylogenetic reconstruction of evolutionary dynamics. *Bioinformatics, 27*(20), 2910–2912. https://doi.org/10.1093/bioinformatics/btr481

Bokermann, W. C. A. (1964). Dos nuevas especies de Hylade Minas Gerais y notas sobre *Hyla alvarengai* Bok. (Amphibia, Salientia, Hylidae). *Neotropica (La Plata), 10*, 67–76

Bonatelli, I. A. S., Perez, M. F., Peterson, A. T., Taylor, N. P., Zappi, D. C., Machado, M. C., Koch, I., Pires, A. H. C., & Moraes, E. M. (2014). Interglacial microrefugia and diversification of a cactus species complex: Phylogeography and palaeodistributional reconstructions for *Pilosocereus aurisetus* and allies. *Molecular Ecology, 23*(12), 3044–3063. https://doi.org/10.1111/mec.12780

Bouckaert, R. R., & Drummond, A. J. (2017). bModelTest: Bayesian phylogenetic site model averaging and model comparison. *BMC Evolutionary Biology, 17*(1), 1–11. https://doi.org/10.1186/s12862-017-0890-6

Bouckaert, R. R., Vaughan, T. G., Barido-Sottani, J., Duchêne, S., Fourment, M., Gavryushkina, A., Heled, J., Jones, G., Kühnert, D., de Maio, N., Matschiner, M., Mendes, F. K., Müller, N. F., Ogilvie, H. A., du Plessis, L., Popinga, A., Rambaut, A., Rasmussen, D., Siveroni, I., … Drummond, A. J. (2019). BEAST 2.5: An advanced software platform for Bayesian evolutionary analysis. *PLoS Computational Biology, 15*(4), 1–28. https://doi.org/10.1371/journal.pcbi.1006650

Broennimann, O., Di Cola, V., & Guisan, A. (2020). *ecospat: Spatial ecology miscellaneous methods.* R package version 3.1.

Brown, J. L., Hill, D. J., Dolan, A. M., Carnaval, A. C., & Haywood, A. M. (2018). Paleoclim, high spatial resolution paleoclimate surfaces for global land areas. *Scientific Data, 5*, 1–9. https://doi.org/10.1038/sdata.2018.254

Bruen, T. C., Philippe, H., & Bryant, D. (2006). A simple and robust statistical test for detecting the presence of recombination. *Genetics, 172*(4), 2665–2681. https://doi.org/10.1534/genetics.105.048975

Bryant, D., & Moulton, V. (2004). Neighbor-Net: An Agglomerative Method for the Construction of Phylogenetic Networks. *Molecular Biology and Evolution, 21*(2), 255–265. https://doi.org/10.1093/molbev/msh018

Camargo, A., & Sites, J. (2013). Species Delimitation: A Decade After the Renaissance. In I. Pavlinov (Ed.), *The Species Problem* - Ongoing Issues. Moscow State University. https://doi.org/10.5772/52664

Carvalho, T. R., Seger, K. R., Magalhães, F. M., Lourenço, L. B., & Haddad, C. F. B. (2021). Systematics and cryptic diversification of *Leptodactylus* frogs in the Brazilian *campo rupestre*. *Zoologica Scripta, 50*, 300–317. https://doi.org/10.1111/zsc.12470

Chamberlain, S. (2016). *sCrubr: Clean biological occurrence records (0.1).*

Colli-Silva, M., Vasconcelos, T. N. C., & Pirani, J. R. (2019). Outstanding plant endemism levels strongly support the recognition of *campo rupestre* provinces in mountaintops of eastern South America. *Journal of Biogeography, 46*(8), 1723–1733. https://doi.org/10.1111/jbi.13585

Cornuet, J. M., Pudlo, P., Veyssier, J., Dehne-Garcia, A., Gautier, M., Leblois, R., Marin, J. M., & Estoup, A. (2014). DIYABC v2.0: A software to make approximate Bayesian computation inferences about population history using single nucleotide polymorphism, DNA sequence and microsatellite data. *Bioinformatics, 30*(8), 1187–1189. https://doi.org/10.1093/bioinformatics/btt763

da Silva, E. T. da, Peixoto, M. A. A., Leite, F. S. F., Feio, R. N., & Garcia, P. C. A. (2018). Anuran Distribution in a Highly Diverse Region of the Atlantic Forest: The Mantiqueira Mountain Range in Southeastern Brazil. *Herpetologica, 74*(4), 294–305. https://doi.org/10.1655/herpetologica-d-17-00025.1

de Oliveira, F. R. de, Gehara, M., Solé, M., Lyra, M., Haddad, C. F. B., Silva, D. P., Magalhães, R. F. de, Leite, F. S. F., & Burbrink, F. T. (2021). Quaternary climatic fluctuations influence the

demographic history of two species of sky-island endemic amphibians in the Neotropics. *Molecular Phylogenetics and Evolution, 160*. https://doi.org/10.1016/j.ympev.2021.107113

Di Cola, V., Broennimann, O., Petitpierre, B., Breiner, F. T., D'Amen, M., Randin, C., … Guisan, A. (2017). ecospat: An R package to supportspatial analyses and modeling of species niches and distributions. *Ecography*, *40*(6), 774–787. https://doi.org/10.1111/ecog.02671

Dmitriev, D. A., & Rakitov, R. A. (2008a). Decoding of superimposed traces produced by direct sequencing of heterozygous indels. *PLoS Computational Biology, 4*(7). https://doi.org/10.1371/journal.pcbi.1000113

Dmitriev, D. A., & Rakitov, R. A. (2008b). *Indelligent v.1.2*.

Dormann, C. F., Elith, J., Bacher, S., Buchmann, C., Carl, G., Carré, G., Marquéz, J. R. G., Gruber, B., Lafourcade, B., Leitão, P. J., Münkemüller, T., Mcclean, C., Osborne, P. E., Reineking, B., Schröder, B., Skidmore, A. K., Zurell, D., & Lautenbach, S. (2013). Collinearity: A review of methods to deal with it and a simulation study evaluating their performance. *Ecography*, *36*(1), 27–46. https://doi.org/10.1111/j.1600-0587.2012.07348.x

Dufresnes, C., Litvinchuk, S. N., Leuenberger, J., Ghali, K., Zinenko, O., Stöck, M., & Perrin, N. (2016). Evolutionary melting pots: a biodiversity hotspot shaped by ring diversifications around the Black Sea in the Eastern tree frog (*Hyla orientalis*). *Molecular Ecology, 25*(17), 4285–4300. https://doi.org/10.1111/mec.13706

Edgar, R. C. (2004). MUSCLE: Multiple sequence alignment with high accuracy and high throughput. Nucleic Acids Research, 32(5), 1792–1797. https://doi.org/10.1093/nar/gkh340

Elith, J., Ferrier, S., Huettmann, F., & Leathwick, J. (2005). The evaluation strip: A new and robust method for plotting predicted responses from species distribution models. *Ecological Modelling, 186*(3), 280–289. https://doi.org/10.1016/j.ecolmodel.2004.12.007

Eterovick, P. C., & Brandão, R. A. (2001). A description of the tadpoles and advertisement calls of members of the *Hyla pseudopseudis* group. *Journal of Herpetology, 35*(3), 442–450. https://doi.org/10.2307/1565962

Eterovick, P. C., Sloss, B. L., Scalzo, J. A. M., & Alford, R. A. (2016). Isolated frogs in a crowded world: Effects of human-caused habitat loss on frog heterozygosity and fluctuating asymmetry. *Biological Conservation, 195*, 52–59. https://doi.org/10.1016/j.biocon.2015.12.036

Fernandes, G. W., Barbosa, N. P. U., Negreiros, D., & Paglia, A. P. (2014). Challenges for the conservation of vanishing megadiverse rupestrian grasslands. *Natureza & Conservação, 2*(2), 162–165. https://doi.org/10.1016/j.ncon.2014.08.003

Fielding, A. H., & Bell, J. F. (1997). A review of methods for the assessment of prediction errors in conservation presence/absence models. *Environmental Conservation*, *24*(1), 38–49. https://doi.org/10.1017/S0376892997000088

Fiorini, C. F., Miranda, M. D., Silva-Pereira, V., Barbosa, A. R., Oliveira, U. De, Kamino, L. H. Y., Mota, N. F. D. O., Viana, P. L., & Borba, E. L. (2019). The phylogeography of *Vellozia auriculata* (Velloziaceae) supports low zygotic gene flow and local population persistence in the *campo rupestre*, a Neotropical OCBIL. *Botanical Journal of the Linnean Society*, *191*(3), 381–398. https://doi.org/10.1093/botlinnean/boz051

Flantua, S. G. A., & Hooghiemstra, H. (2018). Historical connectivity and mountain biodiversity. In C. Hoorn, Perrigo Allison, & A. Antonelli (Eds.), *Mountains, Climate and Biodiversity* (1st ed., Issue March 2019, pp. 171–185). John Wiley & Sons Ltda.

Flantua, S. G. A., O'Dea, A., Onstein, R. E., Giraldo, C., & Hooghiemstra, H. (2019). The flickering connectivity system of the north Andean páramos. *Journal of Biogeography*, *46*(8), 1808–1825. https://doi.org/10.1111/jbi.13607

Flantua, S. G. A., Payne, D., Borregaard, M. K., Beierkuhnlein, C., Steinbauer, M. J., Dullinger, S., Essl, F., Irl, S. D. H., Kienle, D., Kreft, H., Lenzner, B., Norder, S. J., Rijsdijk, K. F., Rumpf, S. B., Weigelt, P., & Field, R. (2020). Snapshot isolation and isolation history challenge the analogy between mountains and islands used to understand endemism. *Global Ecology and Biogeography*, *29*(10), 1651–1673. https://doi.org/10.1111/geb.13155

Fox, J., & Weisberg, S. (2019). *An {R} Companion to Applied Regression* (4th ed.). Sage Publications, Inc.

Frantz, A. C., Cellina, S., Krier, A., Schley, L., & Burke, T. (2009). Using spatial Bayesian methods to determine the genetic structure of a continuously distributed population: clusters or isolation by distance? *Journal of Applied Ecology*, *46*(2), 493–505. https://doi.org/10.1111/j.1365-2664.2008.01606.x

Friedman, J. H. (2001). Greedy Function Approximation: A Gradient Boosting Machine. *The Annals of Statistics*, *29*(5), 1189–1232.

Gernhard, T. (2008). The conditioned reconstructed process. *Journal of Theoretical Biology*, *253*(4), 769–778. https://doi.org/10.1016/j.jtbi.2008.04.005

Gosner, K. L. (1960). A Simplified Table for Staging Anuran Embryos and Larvae with Notes on Identification. *Herpetologica*, *16*(3), 183–190.

Guedes, T. B., Azevedo, J. A. R., Bacon, C. D., Provete, D. B., & Antonelli, A. (2020). Diversity, Endemism, and Evolutionary History of Montane Biotas Outside the Andean Region. In V.

Rull & A. C. Carnaval (Eds.), *Neotropical Diversification: Patterns and Process* (pp. 299–328). Springer International Publishing. https://doi.org/10.1007/978-3-030-31167-4

Guillot, G., Estoup, A., Mortier, F., & Cosson, J. F. (2005). A spatial statistical model for landscape genetics. *Genetics*, *170*(3), 1261–1280. https://doi.org/10.1534/genetics.104.033803

Guillot, G., Mortier, F., & Estoup, A. (2005). GENELAND: A computer package for landscape genetics. *Molecular Ecology Notes*, *5*(3), 712–715. https://doi.org/10.1111/j.1471-8286.2005.01031.x

Hastie, T., & Tibshirani, R. (1990). *Generalized Additive Models* (1st ed.). Chapman and Hall. https://doi.org/10.1201/9780203753781

Hastie, T., & Tibshirani, R. (1996). Discriminant Analysis by Gaussian Mixtures. *Journal of the Royal Statistical Society: Series B (Methodological)*, *58*(1), 155–176. https://doi.org/10.1111/j.2517-6161.1996.tb02073.x

Hickerson, M. J., Carstens, B. C., Cavender-Bares, J., Crandall, K. A., Graham, C. H., Johnson, J. B., Rissler, L., Victoriano, P. F., & Yoder, A. D. (2010). Phylogeography's past, present, and future: 10 years after Avise, 2000. *Molecular Phylogenetics and Evolution*, *54*(1), 291–301. https://doi.org/10.1016/j.ympev.2009.09.016

Hoelzer, G. A. (1997). Inferring Phylogenies From mtDNA Variation: Mitochondrial-Gene Trees Versus Nuclear-Gene Trees Revisited. *Evolution*, *51*(2), 622–626.

Hopper, S. D. (2009). OCBIL theory: Towards an integrated understanding of the evolution, ecology and conservation of biodiversity on old, climatically buffered, infertile landscapes. *Plant and Soil*, *322*(1), 49–86. https://doi.org/10.1007/s11104-009-0068-0

Hopper, S. D., Silveira, F. A. O., & Fiedler, P. L. (2016). Biodiversity hotspots and OCBIL theory. *Plant and Soil*, *403*(1–2), 167–216. https://doi.org/10.1007/s11104-015-2764-2

Huson, D. H., & Bryant, D. (2006). Application of phylogenetic networks in evolutionary studies. Molecular Biology and Evolution, 23(2), 254–267. https://doi.org/10.1093/molbev/msj030

Jeffreys, H. (1961). *Theory of Probability* (3rd ed.). Clarendon Press. https://doi.org/10.2307/2582798

Johns, G. C., & Avise, J. C. (1998). A comparative summary of genetic distances in the vertebrates from the mitochondrial cytochrome b gene. *Molecular Biology and Evolution and Evolution*, *15*(11), 1481–1490. https://doi.org/10.1093/oxfordjournals.molbev.a025875

Joly, S., & Bruneau, A. (2006). Incorporating allelic variation for reconstructing the evolutionary history of organisms from multiple genes: An example from Rosa in North America. *Systematic Biology*, *55*(4), 623–636. https://doi.org/10.1080/10635150600863109

Joly, S., Bryant, D., & Lockhart, P. J. (2015). Flexible methods for estimating genetic distances from single nucleotide polymorphisms. *Methods in Ecology and Evolution, 6*(8), 938–948. https://doi.org/10.1111/2041-210X.12343

Jones, G. (2017). Algorithmic improvements to species delimitation and phylogeny estimation under the multispecies coalescent. *Journal of Mathematical Biology, 74*(1–2), 447–467. https://doi.org/10.1007/s00285-016-1034-0

Jones, G., Aydin, Z., & Oxelman, B. (2015). DISSECT: An assignment-free Bayesian discovery method for species delimitation under the multispecies coalescent. *Bioinformatics, 31*(7), 991–998. https://doi.org/10.1093/bioinformatics/btu770

Knowles, L. L., & Carstens, B. C. (2007). Delimiting species without monophyletic sene trees. *Systematic Biology, 56*(6), 887–895. https://doi.org/10.1080/10635150701701091

Kok, P. J. R., Ratz, S., MacCulloch, R. D., Lathrop, A., Dezfoulian, R., Aubret, F., & Means, D. B. (2018). Historical biogeography of the palaeoendemic toad genus *Oreophrynella* (Amphibia: Bufonidae) sheds a new light on the origin of the Pantepui endemic terrestrial biota. *Journal of Biogeography, 45*(1), 26–36. https://doi.org/10.1111/jbi.13093

Körner, C., Jetz, W., Paulsen, J., Payne, D., Rudmann-Maurer, K., & Spehn, E. M. (2017). A global inventory of mountains for bio-geographical applications. *Alpine Botany, 127*(1), 1–15. https://doi.org/10.1007/s00035-016-0182-6

Larsson, A. (2014). AliView: A fast and lightweight alignment viewer and editor for large datasets. *Bioinformatics, 30*(22), 3276–3278. https://doi.org/10.1093/bioinformatics/btu531

Leite, F. S. F. (2012). Taxonomia, biogeografia e conservação dos anfíbios da Serra do Espinhaço [Universidade Federal de Minas Gerais]. https://repositorio.ufmg.br/handle/1843/BUOS-96VGWR

Leite, F. S. F., Juncá, F. A., & Eterovick, P. C. (2008). Status do conhecimento, endemismo e conservação de anfíbios anuros da Cadeia do Espinhaço, Brasil. *Megadiversidade, 4*(1–2), 158–176.

Lemey, P., Rambaut, A., Welch, J. J., & Suchard, M. A. (2010). Phylogeography takes a relaxed random walk in continuous space and time. *Molecular Biology and Evolution, 27*(8), 1877–1885. https://doi.org/10.1093/molbev/msq067

Lleonart, J., Salat, J., & Torres, G. J. (2000). Removing allometric effects of body size in morphological analysis. *Journal of Theoretical Biology, 205*(1), 85–93. https://doi.org/10.1006/jtbi.2000.2043

Lomolino, M. V., Riddle, B. R., Whittaker, R. J., & Brown, J. H. (2010). Dispersal and Immigration. In M. V. Lomolino, B. R. Riddle, R. J. Whittaker, & J. H. Brown (Eds.), *Biogeography* (4th ed., p. 764). Sinauer Associates, Inc.

Magalhães, R. F., Lemes, P., Santos, M. T. T., Mol, R. M., Ramos, E. K. S., Oswald, C. B., Pezzuti, T. L., Santos, F. R., Brandão, R. A., & Garcia, P. C. A. (2021). Evidence of introgression in endemic frogs from the *campo rupestre* contradicts the reduced hybridization hypothesis. Biological *Journal of the Linnean Society*, *138*, 561–576. https://doi.org/10.1093/biolinnean/blaa142

McCormack, J. E., Heled, J., Delaney, K. S., Peterson, A. T., & Knowles, L. L. (2011). Calibrating divergence times on species trees versus gene trees: Implications for speciation history of *Aphelocoma jays*. *Evolution*, *65*(1), 184–202. https://doi.org/10.1111/j.1558-5646.2010.01097.x

McCullagh, P., & Nelder, J. A. (1989). Generalized Linear Models (2nd ed.). Chapman and Hall. https://doi.org/10.2307/2347392

Miller, M. A., Pfeiffer, W., & Schwartz, T. (2010). Creating the CIPRES Science Gateway for inference of large phylogenetic trees. *2010 Gateway Computing Environments Workshop (GCE)*. https://doi.org/10.1109/GCE.2010.5676129

Miola, D. T. B., Ramos, V. D. v, & Silveira, F. A. O. (2021). A brief history of research in *campo rupestre*: identifying research priorities and revisiting the geographical distribution of an ancient, widespread Neotropical biome. *Biological Journal of the Linnean Society, 133*(2), 464–480. https://doi.org/10.1093/biolinnean/blaa175

Muellner-Riehl, A. N., Schnitzler, J., Kissling, W. D., Mosbrugger, V., Rijsdijk, K. F., Seijmonsbergen, A. C., Versteegh, H., & Favre, A. (2019). Origins of global mountain plant biodiversity: Testing the 'mountain-geobiodiversity hypothesis.' *Journal of Biogeography, 46*(12), 2826–2838. https://doi.org/10.1111/jbi.13715

Murray, K., & Conner, M. M. (2009). Methods to quantify variable importance: implications for the analysis of noisy ecological data. *Ecology*, *90*, 348–355. https://doi.org/10.1890/0012-9658-90.5.1425

Naimi, B., & Araújo, M. B. (2016). sdm: A reproducible and extensible R platform for species distribution modelling. *Ecography, 39*(4), 368–375. https://doi.org/10.1111/ecog.01881

Naimi, B., Hamm, N. A. S., Groen, T. A., Skidmore, A. K., & Toxopeus, A. G. (2014). Where is positional uncertainty a problem for species distribution modelling? *Ecography, 37*(2), 191–203. https://doi.org/10.1111/j.1600-0587.2013.00205.x

Nascimento, A. C., Chaves, A. V., Leite, F. S. F., Eterovick, P. C., & Santos, F. R. (2018). Past vicariance promoting deep genetic divergence in an endemic frog species of the Espinhaço Range in Brazil: The historical biogeography of *Bokermannohyla saxicola* (Hylidae). *PLoS ONE*, *13*(11), 1–19. https://doi.org/10.1371/journal.pone.0206732

Nylinder, S., Lemey, P., De Bruyn, M., Suchard, M. A., Pfeil, B. E., Walsh, N., & Anderberg, A. A. (2014). On the biogeography of centipeda: A species-tree diffusion approach. *Systematic Biology*, *63*(2), 178–191. https://doi.org/10.1093/sysbio/syt102

Ogilvie, H. A., Bouckaert, R. R., & Drummond, A. J. (2017). StarBEAST2 brings faster species tree inference and accurate estimates of substitution rates. *Molecular Biology and Evolution*, *34*(8), 2101–2114. https://doi.org/10.1093/molbev/msx126

Oksanen, J., Blanchet, F. G., Friendly, M., Kindt, R., Legendre, P., McGlinn, D., Minchin, P. R., O'Hara, R. B., Simpson, G. L., Solymos, P., Stevens, M. H. H., Szoecs, E., & Wagner, H. (2019). *vegan: Community Ecology Package (2.5-6).*

Paradis, E. (2010). Pegas: An R package for population genetics with an integrated-modular approach. Bioinformatics, 26(3), 419–420. https://doi.org/10.1093/bioinformatics/btp696

Paradis, E., & Schliep, K. (2019). Ape 5.0: An environment for modern phylogenetics and evolutionary analyses in R. *Bioinformatics*, *35*(3), 526–528. https://doi.org/10.1093/bioinformatics/bty633

Perez, M. F., Bonatelli, I. A. S., Moraes, E. M., & Carstens, B. C. (2016). Model-based analysis supports interglacial refugia over long-dispersal events in the diversification of two South American cactus species. *Heredity*, *116*(6), 550–557. https://doi.org/10.1038/hdy.2016.17

Perez, M. F., Franco, F. F., Bombonato, J. R., Bonatelli, I. A. S., Khan, G., Romeiro-Brito, M., Fegies, A. C., Ribeiro, P. M., Silva, G. A. R., & Moraes, E. M. (2018). Assessing population structure in the face of isolation by distance: Are we neglecting the problem? *Diversity and Distributions*, *24*(12), 1883–1889. https://doi.org/10.1111/ddi.12816

Perrigo, A., Hoorn, C., & Antonelli, A. (2020). Why mountains matter for biodiversity. *Journal of Biogeography*, *47*(2), 315–325. https://doi.org/10.1111/jbi.13731

Peterson, A. T., & Soberón, J. (2012). Species distribution modeling and ecological niche modeling: Getting the Concepts Right. *Natureza & Conservação*, *10*(2), 102–107. https://doi.org/10.4322/natcon.2012.019

Phillips, S. J., Anderson, R. P., & Schapire, R. E. (2006). Maximum entropy modeling of species geographic distributions. *Ecological Modelling*, *190*(3–4), 231–259. https://doi.org/https://doi.org/10.1016/j.ecolmodel.2005.03.026

Pons, J., Barraclough, T. G., Gomez-Zurita, J., Cardoso, A., Duran, D. P., Hazell, S., Kamoun, S., Sumlin, W. D., & Vogler, A. P. (2006). Sequence-based species delimitation for the DNA taxonomy of undescribed insects. *Systematic Biology, 55*(4), 595–609. https://doi.org/10.1080/10635150600852011

QGIS Development Team. (2020). *QGIS: A Free and Open Source Geographic Information System (3.14.1 Pi)*. Open Source Geospatial Foundation Project.

R Core Team. (2019). *R: A language and environment for statistical computing (3.5.3)*. R Foundation for Statistical Computing. https://doi.org/https://www.r-project.org/

Rahbek, C., Borregaard, M. K., Colwell, R. K., Dalsgaard, B., Holt, B. G., Morueta-Holme, N., Nogues-Bravo, D., Whittaker, R. J., & Fjeldså, J. (2019). Humboldt's enigma: What causes global patterns of mountain biodiversity? *Science, 365*(6458), 1108–1113. https://doi.org/10.1126/science.aax0149

Rambaut, A. (2018). *FigTree*. http://tree.bio.ed.ac.uk/software/figtree/

Rambaut, A., Drummond, A. J., Xie, D., Baele, G., & Suchard, M. A. (2018). Posterior summarization in Bayesian phylogenetics using Tracer 1.7. *Systematic Biology, 67*(5), 901–904. https://doi.org/10.1093/sysbio/syy032

Ramos, E. K. S., de Magalhães, R. F., Sari, E. H. R., Rosa, A. H. B., Garcia, P. C. A., & Santos, F. R. (2018). Population genetics and distribution data reveal conservation concerns to the sky island endemic *Pithecopus megacephalus* (Anura, Phyllomedusidae). *Conservation Genetics, 19*(1), 99–110. https://doi.org/10.1007/s10592-017-1013-z

Ramos, E. K. S., Magalhães, R. F. de, Marques, N. C. S., Baêta, D., Garcia, P. C. A., & Santos, F. R. (2019). Cryptic diversity in Brazilian endemic monkey frogs (Hylidae, Phyllomedusinae, *Pithecopus*) revealed by multispecies coalescent and integrative approaches. *Molecular Phylogenetics and Evolution, 132*, 105–116. https://doi.org/10.1016/j.ympev.2018.11.022

Rangel, T. F., & Loyola, R. D. (2012). Labeling ecological niche models. *Natureza & Conservação, 10*(2), 119–126. https://doi.org/10.4322/natcon.2012.030

Royle, J. A., Chandler, R. B., Yackulic, C., & Nichols, J. D. (2012). Likelihood analysis of species occurrence probability from presence-only data for modelling species distributions. *Methods in Ecology and Evolution, 3*(3), 545–554. https://doi.org/10.1111/j.2041-210X.2011.00182.x

Rull, V. (2011). Neotropical biodiversity: Timing and potential drivers. *Trends in Ecology and Evolution, 26*(10), 508–513. https://doi.org/10.1016/j.tree.2011.05.011

Saadi, A. (1995). A geomorfologia da Serra do Espinhaço em Minas Gerais e de suas margens. *Geonomos, 3*, 41–63.

Sabbag, A. F. (2013). Filogeografia de *Thoropa* grupo *miliaris* (Anura: Cycloramphidae) [Universidade Estadual Paulista "Júlio de Mesquita Filho]. https://repositorio.unesp.br/handle/11449/87555

Sabbag, A. F., Lyra, M. L., Zamudio, K. R., Haddad, C. F. B., Feio, R. N., Leite, F. S. F., Gasparini, J. L., & Brasileiro, C. A. (2018). Molecular phylogeny of Neotropical rock frogs reveals a long history of vicariant diversification in the Atlantic Forest. *Molecular Phylogenetics and Evolution, 122*, 142–156. https://doi.org/10.1016/j.ympev.2018.01.017

Salazar, G. A., Batista, J. A. N., Meneguzzo, T. E. C., Cabrera, L. I., Figueroa, C., Calvillo-Canadell, L., Vale, A. A. D., & Jiménez-Machorro, R. (2019). Polyphyly of *Mesadenus* (Orchidaceae, Spiranthinae) and a New Genus from the Espinhaço Range, Southeastern Brazil. *Systematic Botany*, *44*(2), 282–296. https://doi.org/10.1600/036364419X15562054132974

Salzburger, W., Ewings, G. B., & Haeseler, A. von. (2011). The performance of phylogenetic algorithms in estimating haplotype genealogies with migration. *Molecular Ecology, 20*, 1952–1963. https://doi.org/10.1111/j.1365-294X.2011.05066.x

Sandel, B., Arge, L., Dalsgaard, B., Davies, R. G., Gaston, K. J., Sutherland, W. J., & Svenning, J. C. (2011). The influence of late quaternary climate-change velocity on species endemism. *Science, 334*(6056), 660–664. https://doi.org/10.1126/science.1210173

Santos, M. T. T., de Magalhães, R. F., Lyra, M. L., Santos, F. R., Zaher, H., Giasson, L. O. M., Garcia, P. C. A., Carnaval, A. C., & Haddad, C. F. B. (2020). Multilocus phylogeny of Paratelmatobiinae (Anura: Leptodactylidae) reveals strong spatial structure and previously unknown diversity in the Atlantic Forest hotspot. *Molecular Phylogenetics and Evolution, 148*, 106819. https://doi.org/10.1016/j.ympev.2020.106819

Schacht, M. C., & McBrayer, L. D. (2009). A Method for Constructing an Adjustable Platform to Obtain Lateral Photographs of Larval Anurans. *Herpetological Review, 40*(3), 303–304.

Schneider, C. A., Rasband, W. S., & Eliceiri, K. W. (2012). NIH Image to ImageJ: 25 years of image analysis. *Nature Methods, 9*(7), 671–675. https://doi.org/10.1038/nmeth.2089

Silveira, F. A. O., Dayrell, R. L. C., Fiorini, C. F., Negreiros, D., & Borba, E. L. (2020). Diversification in Ancient and Nutrient-Poor Neotropical Ecosystems: How Geological and Climate Buffering Shaped Plant Diversity in Some of the World's Neglected Hotspots. In V. Rull & A. C. Carnaval (Eds.), *Neotropical Diversification: Patterns and Process* (pp. 329–368). Springer International Publishing. https://doi.org/10.1007/978-3-030-31167-4

Silveira, F. A. O., Negreiros, D., Barbosa, N. P. U., Buisson, E., Carmo, F. F., Carstensen, D. W., Conceição, A. A., Cornelissen, T. G., Echternacht, L., Fernandes, G. W., Garcia, Q. S., Guerra,

T. J., Jacobi, C. M., Lemos-Filho, J. P., le Stradic, S., Morellato, L. P. C., Neves, F. S., Oliveira, R. S., Schaefer, C. E., … Lambers, H. (2016). Ecology and evolution of plant diversity in the endangered *campo rupestre*: a neglected conservation priority. *Plant and Soil, 403*(1–2), 129–152. https://doi.org/10.1007/s11104-015-2637-8

Smith, B. T., Ribas, C. C., Whitney, B. M., Hernández-Baños, B. E., & Klicka, J. (2013). Identifying biases at different spatial and temporal scales of diversification: A case study in the Neotropical parrotlet genus *Forpus*. *Molecular Ecology, 22*(2), 483–494. https://doi.org/10.1111/mec.12118

Solís-Lemus, C., Knowles, L. L., & Ané, C. (2015). Bayesian species delimitation combining multiple genes and traits in a unified framework. *Evolution, 69*(2), 492–507. https://doi.org/10.1111/evo.12582

Stamatakis, A. (2014). RAxML version 8: A tool for phylogenetic analysis and post-analysis of large phylogenies. *Bioinformatics*, *30*(9), 1312–1313. https://doi.org/10.1093/bioinformatics/btu033

Stamatakis, A., Blagojevic, F., Nikolopoulos, D. S., & Antonopoulos, C. D. (2007). Exploring New Search Algorithms and Hardware for Phylogenetics: RAxML Meets the IBM Cell. *Journal of VLSI Signal Processing*, *48*(3), 271–286. https://doi.org/10.1007/s11265-007-0067-4

Stephens, M., Smith, N. J., & Donnelly, P. (2001). A New Statistical Method for Haplotype Reconstruction from Population Data. American Journal of Human *Genetics*, *68*, 978–989. https://doi.org/10.1086/319501

Stöck, M., Dufresnes, C., Litvinchuk, S. N., Lymberakis, P., Biollay, S., Berroneau, M., Borzée, A., Ghali, K., Ogielska, M., & Perrin, N. (2012). Cryptic diversity among Western Palearctic tree frogs: Postglacial range expansion, range limits, and secondary contacts of three European tree frog lineages (*Hyla arborea* group). *Molecular Phylogenetics and Evolution, 65*, 1–9. https://doi.org/10.1016/j.ympev.2012.05.014

Suchard, M. A., Lemey, P., Baele, G., Ayres, D. L., Drummond, A. J., & Rambaut, A. (2018). Bayesian phylogenetic and phylodynamic data integration using BEAST 1.10. *Virus Evolution, 4*(1), 1–5. https://doi.org/10.1093/ve/vey016

Swets, J. A. (1988). Measuring the Accuracy of Diagnostic Information. *Science, 240*(4857), 1285–1293. https://doi.org/10.1002/9781118341544.ch5

Tajima, F. (1989). Statistical Method for Testing the Neutral Mutation Hypothesis by DNA Polymorphism. *Genetics*, *123*(3), 585–595.

Thomé, M. T. C., & Carstens, B. C. (2016). Phylogeographic model selection leads to insight into the evolutionary history of four-eyed frogs. *Proceedings of the National Academy of Sciences of the United States of America, 113*(29), 8010–8017. https://doi.org/10.1073/pnas.1601064113

Thomé, M. T. C., Sequeira, F., Brusquetti, F., Carstens, B., Haddad, C. F. B., Rodrigues, M. T., & Alexandrino, J. (2016). Recurrent connections between Amazon and Atlantic forests shaped diversity in Caatinga four-eyed frogs. *Journal of Biogeography, 43*(5), 1045–1056. https://doi.org/10.1111/jbi.12685

Turchetto-Zolet, A. C., Pinheiro, F., Salgueiro, F., & Palma-Silva, C. (2013). Phylogeographical patterns shed light on evolutionary process in South America. *Molecular Ecology, 22*(5), 1193–1213. https://doi.org/10.1111/mec.12164

Vapnik, V. N. (1995). *The Nature of Statistical Learning Theory* (1st ed.). Springer. https://doi.org/10.1007/978-1-4757-2440-0

Vasconcelos, T. N. C., Alcantara, S., Andrino, C. O., Forest, F., Reginato, M., Simon, M. F., & Pirani, J. R. (2020). Fast diversification through a mosaic of evolutionary histories characterizes the endemic flora of ancient Neotropical mountains. *Proceedings of the Royal Society B: Biological Sciences, 287*(1923). https://doi.org/10.1098/rspb.2019.2933

Vellend, M. (2003). Island Biogeography of Genes and Species. *American Naturalist, 162*(3), 358–365. https://doi.org/10.1086/377189

Wisz, M. S., Pottier, J., Kissling, W. D., Pellissier, L., Lenoir, J., Damgaard, C. F., Dormann, C. F., Forchhammer, M. C., Grytnes, J. A., Guisan, A., Heikkinen, R. K., Høye, T. T., Kühn, I., Luoto, M., Maiorano, L., Nilsson, M. C., Normand, S., Öckinger, E., Schmidt, N. M., … Svenning, J. C. (2013). The role of biotic interactions in shaping distributions and realised assemblages of species: Implications for species distribution modelling. *Biological Reviews, 88*(1), 15–30. https://doi.org/10.1111/j.1469-185X.2012.00235.x

Zuur, A. F., Ieno, E. N., & Elphick, C. S. (2010). A protocol for data exploration to avoid common statistical problems. *Methods in Ecology and Evolution, 1*(1), 3–14. https://doi.org/10.1111/j.2041-210x.2009.00001.x

Capítulo 3

Comparative Phylogeography of anurans endemic to Espinhaço Mountain Range, the largest extra-Andean Mountain chain in South America

A ser submetido ao periódico *Organisms Diversity and Evolution*.

Atenção: as análises e resultados do capítulo ainda são preliminares e devem ser avaliados com cautela pelo leitor.

Comparative Phylogeography of anurans endemic to Espinhaço Mountain Range, the largest extra-Andean Mountain chain in South America

Caroline Batistim Oswald [1], Marcelo Coelho Miguel Gehara[2], Ariadne Fares Sabbag[3], Francisco Fonseca Ribeiro de Oliveira[4], Thiago Ribeiro de Carvalho[3], Diego José Santana[5], Fabricio Rodrigues Santos[1,6], Felipe Sá Fortes Leite[1,7], Rafael Félix de Magalhães[1,8]*

[1]Programa de Pós-Graduação em Zoologia, Universidade Federal de Minas Gerais. Avenida Presidente Antônio Carlos, 6627. Pampulha, Belo Horizonte, MG 31270-901, Brazil

[2]Department of Earth and Environmental Sciences, Rutgers University-Newark. 195 University Ave, Newark, NJ 07102, USA

[3]Instituto de Biociências, Universidade Estadual Paulista Júlio de Mesquita Filho. Avenida 24 A, 1515. Jardim Bela Vista, Rio Claro, SP 13506-900, Brazil

[4]Programa de Pós-Graduação em Ecologia e Conservação da Biodiversidade, Universidade Estadual de Santa Cruz, Ilhéus, BA 45662-900, Brazil

[5]Instituto de Biociências, Universidade Federal de Mato Grosso do Sul. Avenida Costa e Silva, sn. Universitário, Campo Grande, MS 79070-900, Brazil

[6]Departamento de Genética, Ecologia e Evolução, Universidade Federal de Minas Gerais. Avenida Presidente Antônio Carlos, 6627. Pampulha, Belo Horizonte, MG 31270-901, Brazil

[7]Instituto de Ciências Biológicas e da Saúde, *campus* Florestal, Universidade Federal de Viçosa. Rodovia LMG 818, km 06. Florestal, MG 35690-000, Brazil

[8]Departamento de Ciências Naturais, *campus* Dom Bosco, Universidade Federal de São João del-Rei. Praça Dom Helvécio, 74. Dom Bosco, São João del-Rei, MG 36301-160, Brazil

*Corresponding author: rafaelmagalhaes@ufsj.edu.br

Abstract

Biotic and abiotic interactions are expected to affect multiple co-distributed species in a landscape. Located in Brazil, Espinhaço Range (ER) is topographically and ecologically complex, providing opportunities for genetic differentiation of its biota. Some phylogeographic studies have shown similar signatures of spatially-related population divergence, potentially revealing important regional barriers. Comparative studies of an assemblage can help to provide insights into the current and historical role of valleys, depressions, or climate acting as barriers to gene flow of co-distributed mountain species. Understanding the role of topography and

associated patterns of diversification within communities is important to conservation efforts in Espinhaço Range, a threatened region. We assessed patterns of geographically-related genetic structure within six endemic anuran species of Espinhaço Mineiro and Quadrilátero Ferrífero, subregions of the ER. We estimated mitochondrial gene trees for the species to assess spatially structured monophyletic clades. Then, we used these trees to test hypotheses about demographic changes. Finally, to evaluate the congruence in divergence times among populations across the most common biogeographic break (i.e., a central barrier between Planalto de Diamantina and Grão Mogol regions), we ran a hierarchical Approximate Bayesian Computation. Our results show spatial and demographic concordance between the species; however, there are multiple divergences events associated to the same barrier. Therefore, the hypothesis of idiosyncratic histories of diversification was corroborated in this study.

Keywords: Phylogeographic barrier, Espinhaço Range, demographic changes, mountain diversification, *campo rupestre*, Hierarchical Approximate Bayesian computation.

Acknowledgments

We thank Michael J. Hickerson for providing recommendations for running MTML-msBayes. We also thank Tiago L. Pezzuti and André Yves for species photographs. CBO thanks Fundação de Amparo à Pesquisa do Estado de Minas Gerais (FAPEMIG) and Coordenação de Aperfeiçoamento de Pessoal de Nível Superior (CAPES) for her PhD fellowships. FRS thanks Conselho Nacional de Desenvolvimento Científico e Tecnológico (CNPq) for his research fellowship. We thank FAPEMIG and Fundação Vale (FAPEMIG/VALE: RDP-00004-17) and FAPEMIG (APQ-01796-15; APQ-00413-16; APQ-01120-16).

DATA AVAILABILITY STATEMENT: Gene sequences used in the present study will be deposited and available at GenBank upon manuscript acceptance.

Introduction

Mountains host high biodiversity, acting as cradles of diversification of new lineages (Fiorini et al., 2019; Perrigo et al., 2020). Past climate changes, river avulsions, uplifts, habitat fragmentation, changes in other environmental conditions, and their interactions with distinct life histories can play important roles in the genetic structure of species (Paz et al., 2015; Sánchez-Montes et al., 20118; Myers et al., 2019; García-Rodríguez et al., 2021). Additionally,

topographical heterogeneity also provides a diversity of microhabitats that can work like local islands, facilitating allopatric diversification (Rodríguez et al., 2015; Steinbauer et al., 2016; Nali et al., 2020). These microhabitats can also act as microrefugia, amortizing the impacts of climate changes on populations (Bonatelli et al., 2014). When distinct factors and events occur across landscapes, they are expected to affect multiple co-distributed species (Oaks et al., 2020).

In Brazil, the Espinhaço Mountain Range (ER) comprises a Precambrian, geologically stable mountain belt, that extends latitudinally for 1,200 km, through two states, and three phytogeographic domains (i.e., Cerrado, Caatinga and Atlantic Forest) in the east of the country (Saadi, 1995; Alkmin, 2012). This mountain range is topographically and ecologically complex, which provides opportunities for genetic differentiation of its biota. Espinhaço range has several sky island archipelagos and can be divided into two main provinces: Chapada Diamantina (CD) (between latitudes 11S and 14S), entirely in the Caatinga dominion; and Southern Espinhaço (SE) (between latitudes 12S and 19S), bounded to the north by the Caatinga, to the east by the Atlantic Forest, and to the west by Cerrado (Colli-Silva et al., 2019). The highest altitudes (i.e., above 800 m) of the Espinhaço Range are covered by *campo rupestre*, a mountain top ecosystem characterized by grassy-shrubby vegetation mosaics associated with quartzite, sandstone, or ironstone outcrops and poor soils (Silveira et al., 2016; Miola et al., 2021).

Despite the accumulation of knowledge about Espinhaço Mountain biota in last decades (Miola et al., 2021), studies involving the genetic structure of populations are incipient. Some single-species phylogeographic studies have shown that several organisms have similar signatures of spatially-related population divergence, potentially revealing important regional barriers (e.g., Perez et al., 2016; Oliveira et al., 2021; Oswald et al., in press). Serra do Cabral, for example, is an isolated sky island west of SE that was recovered as a distinct unit for the distribution of some species. In this plateau, there is absence of some species widely distributed in SE, some restrict endemic, and populations deeply structured (Leite et al., 2011; Oliveira et al., 2021; Oswald et al., in press). Another region pointed out as a possible barrier in different studies is the region between the municipality of Grão Mogol and Diamantina plateau, in the center of SE. With small variations concerning the exact depression that acts as a barrier, this region has already been identified as a phylogeographic break for a species of cactus, *Pilosocereus aurisetus* (Perez et al., 2016), and for some anurans, like *Bokermannohyla alvarengai* (Oliveira et al., 2021), *B. saxicola* (Oswald et al., in press), *Pithecopus megacephalus* (Ramos et al., 2018), and *Thoropa megatympanum* (Sabbag et al., 2018). It is also an important milestone for the differentiation in the floristic composition of

Melastomataceae (Pacifico et al., 2021) and other vascular plants (Echternacht et al., 2011) along the range, being their northern and southern regions delimitated as distinct districts of Southern Espinhaço Province (Colli-Silva et al., 2019).

Even with the growth of anuran phylogeographic studies in the ER (e.g., Thomé et al., 2016; Ramos et al., 2018; Magalhães et al., 2021; Oliveira et al., 2021), the spatial patterns of genetic diversity have not been examined in a comparative framework. Which leaves a gap in our understanding of how these patterns have been established, becoming a research priority (Miola et al., 2021). Comparative studies within an assemblage or community can help to provide insights into the current and historical role of valleys, depressions, or climate in the formation of barriers to gene flow in co-distributed species. Understanding the role of topography and associated patterns of diversification within communities is important to conservation efforts in this important and threatened region (Fernandes et al., 2014; Silveira et al., 2016).

Thus, to better explain the evolution of the Espinhaço Range anurofauna, we first identified potential barriers to gene flow for some endemic anuran species to Southern Espinhaço. Then, we checked alternative diversification models for each species concerning changes in effective population sizes through time. Finally, we tested three distinct diversification scenarios and demographic patterns through comparative phylogeography: i) all focal species have a concordant and ancient, pre-Quaternary divergence, in agreement with the 'old, climatically buffered, infertile landscapes' theory (OCBIL; Hopper, 2009, 2021; Hopper et al., 2016), that predicts long-term fragmentation in ancient landscapes' biotas; ii) all species have a concordant and recent divergence, with their populations diverged during the climatic events of the Pleistocene, in agreement with the Pleistocene refugia hypothesis (Haffer, 1969; Flantua & Hooghiemstra, 2018); iii) the tempo of divergence is idiosyncratic, thus evidencing multiple pulses of diversification along Espinhaço Range (Rull, 2011).

Material and Methods

Taxon sampling

We sampled six endemic species from four distinct anuran families, that are co-distributed in Southern Espinhaço, southeastern Brazil. The most representative family in the study, and also with the largest number of endemic species in Espinhaço Range is Hylidae (Oswald et al. in revision), from which we sampled the treefrogs *Bokermannohyla alvarengai* (Bokermann, 1956), *B. saxicola* (Bokermann, 1964), and *Scinax curicica* Pugliese, Pombal, &

Sazima, 2004. The families Cycloramphidae, Leptodactylidae, and Phyllomedusidae are represented by one species each, being they *Thoropa megatympanum* (Caranaschi & Sazima, 1984), *Leptodactylus camaquara* (Sazima & Bokermann, 1978), and *Pithecopus megacephalus* (Miranda-Ribeiro, 1926), respectively. These species are associated with *campo rupestre* and, although co-distributed in this ecosystem, they exhibit distinct life-strategies. All species show indirect development and exotrophic tadpoles, but differ in microhabitat used for reproduction and tadpole development (i.e., lotic or lentic water bodies, or semi-terrestrial), and adult body size (Eterovick et al., 2020).

Bokermannohyla alvarengai (Alvarenga's Treefrog) is the largest species sampled, with adult males having an average size of 141 mm (Eterovick et al., 2020). This treefrog reproduces in temporary streams with rocky or sandy bottoms in open areas (Sazima & Bokermann, 1977). The species can be found along SE Province, except in Serra do Cabral (Oliveira et al., 2021). Its tadpoles can select microhabitats that better match their lightness and color, increasing their cryptic potential (Eterovick et al., 2010), possibly being an adaptation to live and survive in rock environments common in *campo rupestre* (Oswald et al., in revision).

The congeneric species *B. saxicola* (Ledge Treefrog) is a medium-sized treefrog, with an average of 54 mm in adult males (Eterovick et al., 2020). It breeds in permanent streams and, more rarely, can be found in temporary ones (Eterovick et al., 2020). Usually, the species is preferentially associated with riparian forests but may also occur in open areas, especially in large waterfalls (Eterovick et al., 2020; Oswald et al., in revision). *Bokermannohyla saxicola* is widely distributed in SE (Oswald et al., in press). The tadpoles are nocturnal and mostly found associated to the rocky bottom of streams (Eterovick & Brandão, 2001). Adults of *B. alvarengai* and *B. saxicola* are nocturnal and terrestrial, inhabiting rocky habitats (Eterovick et al., 2020). The phylogenetic position of these species is not known; however, ER may be the center of diversification for *Bokermannohyla*, due to the high richness and endemism of the genus in the region (Oswald et al., in revision).

Scinax curicica (Lanceback Treefrog) has a small size, with approximately 28 mm in adult males, is nocturnal and arboreal (Pugliese et al., 2004). It inhabits open areas and reproduces in temporary puddles, ponds, swamps, and backwaters of streams surrounded by shrubby or arboreal vegetation (Pugliese et al., 2014). *Scinax curicica* is the only endemic anuran which is distributed in the two provinces of ER, except in Serra do Cabral (Oswald et al., in revision). The tadpoles are diurnal and develop in places with abundant aquatic vegetation

(Eterovick et al., 2020). Like the other members of the Hylidae family in this study, the phylogenetic placement of *S. curicica* is still unresolved (Oswald et al., in revision).

Thoropa megatympanum (Large-eared Rock Frog) are nocturnal and territorial, and inhabits rocky environments, such as the species of *Bokermannohyla*. Its tadpole is semi-terrestrial, being found at moist surfaces of rocks of temporary streams surrounded by herbaceous and shrubby vegetation (Caramschi & Sazima, 1984; Eterovick et al., 2020). The species is a medium-sized frog, with adult males measuring 43 mm on average. Adults have a dark tone, homochromic with the rocky substrate, proving good camouflage (Caramaschi & Sazima, 1984). *Thoropa megatympanum* is widely distributed in SE, being the only species of the genus that occupies *campo rupestre* environments (Sabbag et al., 2018).

Leptodactylus camaquara (Digger Foam Frog) has a small size, with 30 mm on average, is diurnal, and occupies wet soils (Sazima & Bokermann, 1978; Eterovick et al., 2020). It reproduces at flooded areas with herbaceous vegetation, depositing the egg clutches wrapped in foam in burrows under the rocks (Sazima & Bokermann, 1978). The tadpoles develop in swamp areas (Eterovick et al., 2020). The species is distributed in SE, except in Serra do Cabral (Carvalho et al., 2021). Unlike *T. megatympanum*, *L. camaquara* is recovered within a clade with species endemic to *campo rupestre* ecosystem (Sabbag et al., 2018; Carvalho et al., 2021).

Pithecopus megacephalus (Large-headed leaf-frog) is a medium-sized monkey frog, with adult males measuring 39 mm on average, nocturnal, territorial and arboreal species (Caramaschi, 2006; Oliveira et al., 2012). It is associated to temporary streams with rocky or sandy bottoms, surrounded by herbaceous or shrubby vegetation (Eterovick et al., 2020). The eggs are deposited on leaves hanging above the water and the yellowish tadpoles slide through the leaf and fall into the water after hatching (Oliveira et al., 2012; Eterovick et al., 2020). The species is widely distributed in Espinhaço Mineiro and do not occur in Quadrilátero Ferrífero district, south of the SE Province (Brandão et al., 2012; Ramos et al., 2018). *Pithecopus rohdei*, the sister-species of *P. megacephalus*, is distributed in the Atlantic Forest (Faivovich et al., 2010; Ramos et al., 2019), raising the doubt if the most recent common ancestor of these species was distributed in the Atlantic Forest or *campo rupestre* (Oswald et al., in revision).

DNA sampling

We sampled a total of 505 distinct mitochondrial sequences (mtDNA), including six from the outgroups (Tables 1, S1). We obtained most of the mtDNA sequences from previous unpublished studies, which will be made available upon acceptance of the manuscript, and some

of them from GenBank (Table S1; Clark et al., 2016). We sequenced individuals from new localities for *P. megacephalus* through a Sanger automatized sequencer ABI 3130XL (Applied Biosystems™) (Table S1). We performed the new genomic extraction following a standard phenol-chloroform protocol (Sambrook & Russel, 2001). For the amplification and sequencing procedures, we followed Ramos et al. (2018). We aligned sequences using Muscle (Edgar, 2004) as implemented in AliView 1.26 (Larsson, 2014) under default parameters.

Mitochondrial DNA gene trees and barrier inference

We estimated mtDNA gene trees for each species in BEAST v. 2.6.6, assuming a strict molecular clock (Bouckaert et al., 2019). Due to the lack of taxa-specific evidence, we estimated the substitution rate based on rates published for anurans, with the set range variating according to the mitochondrial marker. For 16S (in *L. camaquara, S. curicica,* and *T. megatympanum*), we set the rate between 2.77×10^{-3} and 5.42×10^{-3} substitutions per lineage per million years (Lemmon et al., 2007; Fouquet et al., 2012). For Cyt-*b* (in *B. saxicola* and *P. megacephalus*), we set the rate between 1×10^{-2} and 1.61×10^{-2} substitutions per lineage per million years (Johns & Avise, 1998; Stöck et al., 2012). For COI (in *B. alvarengai* and *B. saxicola*), we set the substitution rate between 7.45×10^{-3} and 1.63×10^{-2} substitutions per lineage per million years, corresponding to the 95% high posterior density (HPD) interval estimated by Oswald et al. (in press) for *Bokermannohyla saxicola*. In all these cases, the parameter's prior distributions were set as uniform. For *B. saxicola,* we link the gene tree from both fragment available (COI and Cyt-*b*).

We set a Yule tree process and rooted the tree using MRCA prior (Gernhard, 2008) with the respective outgroup of each species (Table 1). We choose outgroups based on availability in GenBank and phylogenetic proximity to our focal species. We used the 'bModelTest' v. 1.2.1 package to co-estimate nucleotide substitution models during the runs (Bouckaert & Drummond, 2017). We used default priors for all other parameters and analysed them in three replicates with 5×10^7 generations, 5% burn-in, and 5×10^3 thinning each. We checked the stationarity and convergence of all runs using Tracer v. 1.7.2 (Rambaut et al., 2018) and combined the results of the replicates using LogCombiner v. 2.6.6 (Bouckaert et al., 2019). We annotated the tree with maximum clade credibility (MCC) using TreeAnnotator v. 2.6.6 (Bouckaert et al., 2019). The trees were visualized using FigTree v. 1.4.4 (Rambaut, 2018).

After BEAST results, we constructed distribution maps in QGis v. 3.20.3 (QGIS Development Team, 2021) for all linages and, we considered as putative barriers the area

between the geographic ranges of reciprocally monophyletic and geographically structured clades of gene trees.

Demographic modeling

To assess hypotheses about demographic changes (expansion, retraction, or stability) in distinct lineages of each species, we choose the best demographic model that fits our data through PHRAPL v. 0.6.5 (Jackson et al., 2017). Because the Espinhaço range was not structured equally in all focal species, with distinct structuring patterns in some species, we included only northern and southern populations of the most common barrier (see Results), evaluating the possible common demographic processes between them. We constructed and tested different demographic models with the same parameters for each species except for *Pithecopus megacephalus*, which was removed from this analysis due to the lack of geographically structured clades in the previous step (see Results). All tested models were categorized as isolation only, with a single coalescent event and no migration. Additionally, we set matrices for demographic changes of one, both, or none populations. Thereby, we tested the best model among all 10 possible demographic scenarios (Table S2). As input, we used the mtDNA gene trees generated in the previous step. We ran PHRAPL by taking four samples per population, 1000 subtrees, and 25 subsample replicates for each species. For *Leptodactylus camaquara*, we took only three samples per population, due to their sample size being less than four in one of its populations. We identified the best model ranking the models by Akaike weights (wAIC).

Testing for synchronous population divergences

To evaluate the congruence in divergence times among populations across the genetic break in landscape, we ran a hierarchical Approximate Bayesian Computation (hABC) approach implemented by MTML-msBayes v. 20170510 (Hickerson et al., 2007; Huang et al., 2011). In this analysis, *P. megacephalus* was removed for the same reason mentioned above. We set the same mutation model to all mtDNA markers as HKY and set τ (i.e., the prior for the divergence times) as 1.1 and the upper limit of ancestral population size prior as 1. We performed 1×10^6 simulations and estimated 1×10^3 accepted draws of them. The Ψ hyperparameter (i.e., the number of divergence times) was obtained by a final step acceptance/rejection through local multinomial logistic regression and simple rejection.

Following the previous analysis, and in order not to violate the MTML-msBayes premises (Huang et al., 2011), we only included the north and south populations (see Results).

Results

Mitochondrial DNA gene tree and barrier inference

The mitochondrial gene trees of five species, except of *P. megacephalus*, revealed at least two distinct geographic populations, 'northern' and 'southern' (Figs 1; S1 – S6). Samples from Serra do Cabral were recovered as phylogenetically distinct lineages for *B. saxicola* and *T. megatympanum*. For *Pithecopus megacephalus*, although Cabral samples were grouped in a clade, they are nested with southern samples in a clade poorly supported (Fig. 1).

The most common genetic break in landscape, called from here on as 'central barrier', is similar in all available species but *P. megacephalus,* with some variation in its exact location concerning the surroundings of Botumirim and Itacambira regions (Fig. 2). There is a structuring trend between northern and southern individuals of *P. megacephalus,* but its gene tree show low node supports, and individuals from Rio Pardo de Minas, a northern locality, were grouped in different clades of the tree (Fig. 1). Individuals from Botumirim grouped with the northern population in almost all species (i.e., *Leptodactylus camaquara*, *Scinax curicica*, and *Thoropa megatympanum*), implying a phylogeographic break in the depression southern of this region (Fig. 1). However, the two species of *Bokermannohyla* show a different location from the central barrier. In *Bokermannohyla alvarengai*, Botumirim, and Itacambira samples grouped with the southern population, resulting in a northern-shifted central break (Fig. 2). In *B. saxicola*, Botumirim samples clustered with the southern clade while Itacambira samples clustered with the northern clade, resulting in an eastern-shifted central break (Fig. 2).

Demographic modeling

The PHRAPL revealed higher support for a model of no demographic changes for all populations, indicating concordant demographic stability between the different species. In all species, but *B. alvarengai*, the model that best fit the data was around 2.72 times better than the second. (Table 2; S3). In *B. alvarengai*, the best model was only slightly better than the other substantially supported (i.e., $\Delta AIC \leq 2$) models (Burnham & Anderson, 2002, 2004) (Table 2).

Testing for synchronous population divergences

MTML-msBayes analysis rejects synchronous divergence for the anuran endemic species of the Espinhaço Mountain range, with three distinct divergence times between north and south lineage in the assemblage ($\Psi = 3$ for both local multinomial logistic regression and simple rejection). *Bokermannohyla saxicola*, and *T. megatympanum* probably co-diverged, with average coalescences of 2.38 Ma (95% HPD: 1.6 - 3.28 Ma) and 2.31 Ma (95% HPD: 1.26 - 3.58 Ma), respectively. *Bokermannohyla alvarengai* populations diverged more recently, at 1.47 Ma (95% HPD: 0.77 - 2.38 Ma), while *L. camaquara* and *S. curicica* lineages had the oldest coalescence time, at 2.90 Ma (95% HPD: 1.62 - 4.49 Ma) and 3.29 Ma (95% HPD: 1.76 - 5.15 Ma), respectively (Fig. 3).

Discussion

Although multiple environmental factors can act synchronously and spatially in all species of an assemblage, it seems not the case in Espinhaço Mountain Range, at least in Quadrilátero Ferrífero and Espinhaço Mineiro portions. Our study supports a history of shared temporal co-divergence only for two pairs of the five species investigated, suggesting at least three pulses of diversification associated with the central barrier. However, it is worth mentioning that there is overlap in the confidence intervals of divergence time. Additionally, we cannot discard a fourth independent divergence, since *P. megacephalus* presents an evolutionary history much more recent than that of the other investigated species (Ramos et al., 2019). Instead, our comparative results suggest that specific traits and colonization histories for each species can be important in the diversification of the anuran assemblages from the Espinhaço Range. We showed that, although there is a spatial and demographic concordance between the species, the divergence was not caused by the same diversification event. Therefore, the hypothesis of idiosyncratic histories of diversification was corroborated in this study.

All species were composed of no less than two different monophyletic and spatially structured lineages with correspondent ranges, similar to that found by the species-focused phylogeographic studies (Nascimento et al., 2018; Oliveira er al., 2021; Oswald et al., in press). The only exception was *P. megacephalus,* whose mtDNA gene tree show low supports and spatial mixing. Despite the tendency to geographic divergence, observed in the mtDNA haplotype network (Ramos et al., 2018), it is possible that the spatially structured populations of experienced gene flow, evidenced by the presence of samples from Rio Pardo de Minas

nested with southern ones. This would not be surprising, since gene flow is a common process in the evolution of phylomedusids, and there is even evidence of interspecific introgression involving the species (Magalhães et al., 2021). Despite that, Ramos et al. (2018) used a distinct methodology to access spatially structured populations, finding the same central barrier evidenced in this work. Therefore, for a better understanding of the processes that generate biodiversity in the Espinhaço Range, the gene flow must be taken into account in future assessments of geographic structure and phylogeographic relationships of *P. megacephalus* demes.

Oliveira et al. (2021) and Oswald et al. (in press) found evidence of demographic changes for *B. alvarengai* and *B. saxicola*, in disagreement with our PHRAPL results. It is important to note that these investigations used mitonuclear datasets, that more adequately capture the demographic processes experienced by species (Felsenstein, 2006; Gill et al., 2013). Our results, in turn, just reconstruct the demography of the mitochondrial genome of these frogs. However, although the scenario without demographic changes is the best fit for all species, scenarios 2, 3, 4, and 6 showed $\Delta AIC \leq 2$, being substantially supported (Burnham & Anderson, 2002, 2004). Scenarios 2 and 3, involved demographic changes in one population, northern or southern, at a time. Scenario 4 covers demographic changes in both populations, while scenario 6 represent no demographic changes, but both populations had distinct sizes. Thereby, we cannot rule out that these changes may have occurred in mtDNA as well as what was observed in the species trees (Oliveira et al., 2021; Oswald et al., in press).

Some factors may be responsible for forming phylogeographic barriers, such as biological interactions, environmental heterogeneity, and climatic conditions (Lomolino et al., 2010). Environmental variables as temperature, humidity, and microhabitat distribution could be responsible for isolation by the environment, causing asynchronous genetic structure in a landscape (Wang & Bradburb, 2014). Serra do Espinhaço presents a wide latitudinal climatic variation, with moderate temperatures and low precipitation north of the central barrier and lower temperatures and higher precipitation south of this geographic break (Leite, 2012). We found a slight variation in the exact location of the central barrier for different species (Fig. 2), but this central region of Espinhaço Mineiro is associated with topographic and climatic discontinuities in Espinhaço Range (Leite, 2012). Although past climate changes were recovered as important factors influencing anuran diversification in Espinhaço Range (Magalhães et al., 2021; Oliveira et al., 2021; Oswald et al., in press), the latitudinal climate gradient may be important for the diversification as well. It would be interesting to investigate

this climate variation and discontinuities in the past since there are available reconstructions dating back to Pliocene (Brown et al., 2018), as well as the adaptations of each species to this climatic gradient.

The interspecific variation regarding location of the central barrier suggests that this break may have been displaced through time and that the particular biology of each species, environmental variation, or its interactions may have influenced the structure observed in each one of the species today (Wang & Bradburb, 2014). The phylogeographic break found for these species is in agreement with the division between endemism areas for plants (Echternacht et al., 2011; Chaves et al., 2015; Colli-Silva et al., 2019; Pacifico et al., 2021), reinforcing that it acted as a gene flow restrictor at different temporal scales in the Espinhaço Range. Furthermore, Oswald et al. (in press) demonstrated that *B. saxicola* is a complex of four evolutionarily independent lineages, treated as putative species, corroborating that the central barrier acted at different levels of genealogical depth in the endemic biota of Espinhaço. Our results reveal this highly concordant break as an important geographic element associated with species distributions, endemism, and genetic structuration in Espinhaço Range. Although we have not dug deep into the role of the barrier between the Cabral and the rest of Southern Espinhaço, we confirmed it as an important geographic break associated with lineage structuring for *B. saxicola* and *T. megatympanum*. Furthermore, it limits the distribution of *B. alvarengai, L. camaquara,* and *S. curicica.* Given the high degree of endemism of the Serra do Cabral biota (Echternacht et al. 2011; Leite, 2012; Fidanza et al., 2013; Assunção-Silva & Assis, 2021), we emphasize that it needs to be further investigated in a comparative framework as well since it is another important barrier in Espinhaço Range (e.g., Leite et al., 2011; Oliveira et al., 2011).

Espinhaço Range is classified as an OCBIL (Silveira et al., 2016). In this theory, diversification would be explained by long-term population isolation, the ancientness of landscapes, and historically stable climates, with no or little influence of Pleistocene climate changes in biota diversification (Hopper, 2009; Hopper et al., 2016). Consequently, the area would act as a museum of diversity, housing ancient and persistent lineages. In the last years, some studies have shown recent speciation in the biota of Espinhaço Range, and the high influence of climatic changes, challenging this stability to their biota (Magalhães et al., 2021; Oliveira et al., 2021; Oswald et al., in press). Our results suggest that Espinhaço Range can also act as a cradle of speciation, which is in accordance with results found for several other groups of organisms (Fiorini et al., 2019; Vasconcelos et al., 2020). The biogeographic history of the endemic anuran assemblage of Espinhaço Range suggests that the mountain fingerprint is more

complex than OCBIL's theory solely can explain. Co-distributed anurans are evolving idiosyncratically in Espinhaço Range, and it is difficult to define a mechanism responsible for local diversification (Rapini et al., 2020). The biology of each species, specific habitat tolerances, and adaptations may influence the geographical population's distributions, and studies on environmental-related traits may help us evaluate the effective influence of each environmental component in the diversification of species (Wang & Bradburb, 2014; Vasconcelos et al., 2020). These species-related traits should be better investigated, to help us understand the influences and factors that drove the diversification and, in some cases, like *Bokermannohyla saxicola*, speciation of the Espinhaço Range's biota (Papadopoulou & Knowles, 2016; Oswald et al., in press).

Tables

Table 1 – Species sampled, outgroup, mtDNA fragment, and the number of individuals sampled. COI = Citochrome oxidase, subunit I; Cyt-b = Citochrome B; 16S = Ribossomal gene encoding 16S rRNA.

Species	Outgroup	mtDNA fragment	Sample size
Bokermannohyla alvarengai	*Bokermannohyla oxente*	COI	56
Bokermannohyla saxicola	*Bokermannohyla nanuzae*	COI, Cyt-*b*	223
Leptodactylus camaquara	*Leptodactylus cunicularius*	16S	16
Pithecopus megacephalus	*Pithecopus ayeaye*	Cyt-*b*	76
Scinax curicica	*Scinax alter*	16S	21
Thoropa megatympanum	*Thoropa miliaris*	16S	107

Table 2 – Summary of the alternative models with ΔAIC ≤ 2 selection by PHRAPL. Values of Akaike Information Criterion (AIC); composite likelihood (lnL); the number of parameters of the model (params.K); the difference between AIC values of each model (ΔAIC); and Akaike Information Criterion weights (wAIC) of each taxon. Model numbers refer to the schematic models defined in Tale S2.

Species	Model	AIC	lnL	Params.k	ΔAIC	wAIC
Bokermannohyla alvarengai	1	39.28324	-18.6416	1	0	0.172789
	2	39.59904	-17.7995	2	0.316	0.147536
	3	39.59904	-17.7995	2	0.316	0.147536
	4	39.59904	-17.7995	2	0.316	0.147536
	6	39.59904	-17.7995	2	0.316	0.147536
Bokermannohyla saxicola	1	37.41687	-17.7084	1	0	0.326515
	2	39.41687	-17.7084	2	2	0.120118
	3	39.41687	-17.7084	2	2	0.120118
	4	39.41687	-17.7084	2	2	0.120118
	6	39.41687	-17.7084	2	2	0.120118
Leptodactylus camaquara	1	33.92453	-15.9623	1	0	0.326515
	2	35.92453	-15.9623	2	2	0.120118
	3	35.92453	-15.9623	2	2	0.120118
	4	35.92453	-15.9623	2	2	0.120118
	6	35.92453	-15.9623	2	2	0.120118
Scinax curicica	1	36.51198	-17.2560	1	0	0.326515
	2	38.51198	-17.2560	2	2	0.120118
	3	38.51198	-17.2560	2	2	0.120118
	4	38.51198	-17.2560	2	2	0.120118
	6	38.51198	-17.2560	2	2	0.120118
Thoropa megatympanum	1	37.13571	-17.5679	1	0	0.326515
	2	39.13571	-17.5679	2	2	0.120118
	3	39.13571	-17.5679	2	2	0.120118
	4	39.13571	-17.5679	2	2	0.120118
	6	39.13571	-17.5679	2	2	0.120118

Figures

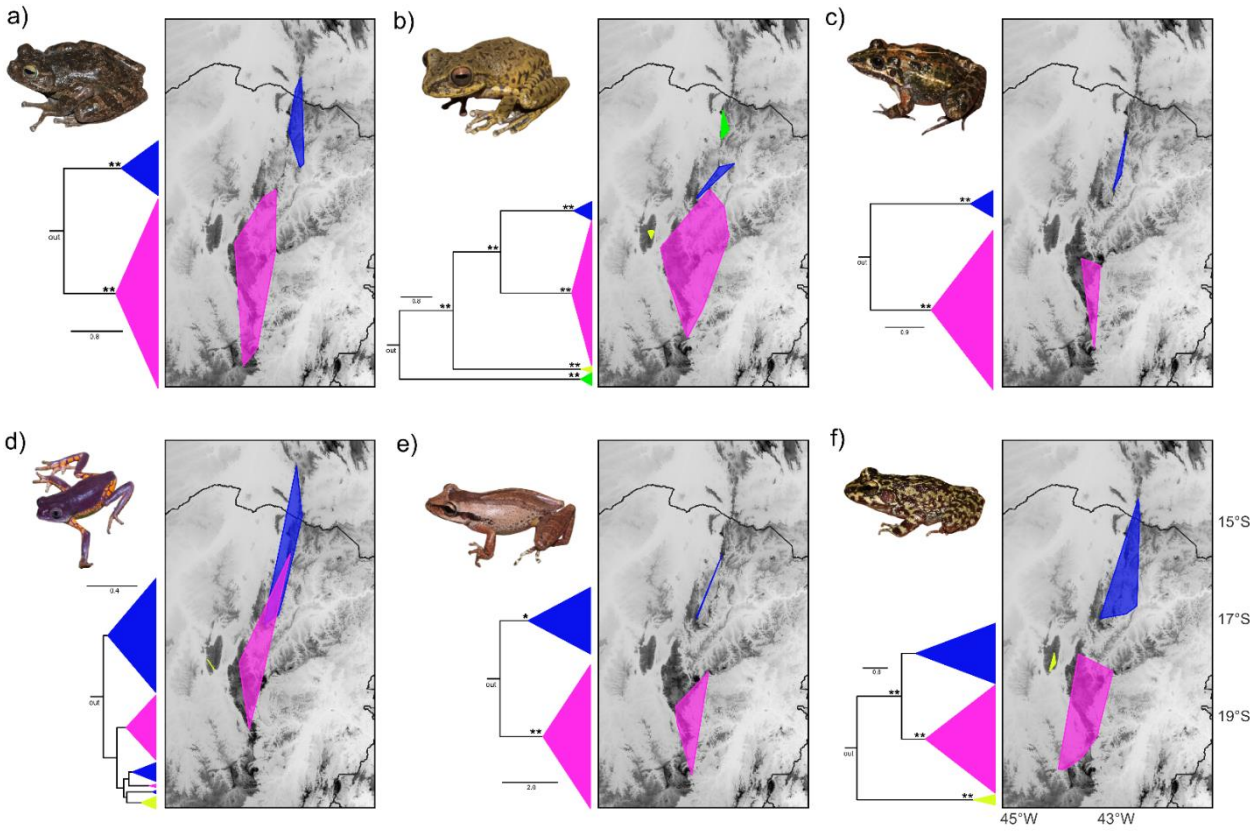

Fig 1 Mitochondrial trees, on the bottom left, sampled anurans photographs on the top left, and the minimum convex polygon of the distribution of each population, on the right, for a) *Bokermannohyla alvarengai*; b) *Bokermannohyla saxicola*; c) *Leptodactylus camaquara*; d) *Pithecopus megacephalus*; e) *Scinax curicica*; and f) *Thoropa megatympanum*. * on branches correspond to posterior probability higher than 0.90 and ** higher than 0.95. Blue represents the northern population and pink southern population in all species. Yellow represents the far north population of *Bokermannohyla saxicola*, and green represent Cabral populations in *B. saxicola*, and *P. megacephalus*, *T. megatympanum*. The terminals of the mtDNA tree were collapsed through the cartoon option in FigTree v. 1.4.4 (Rambaut, 2018) and the minimum convex polygon was drawn from sampling coordinates in QGis v. 3.20.3 (QGIS Development Team, 2021). Photographs: a, c-f: Tiago L. Pezzuti; b: André Yves

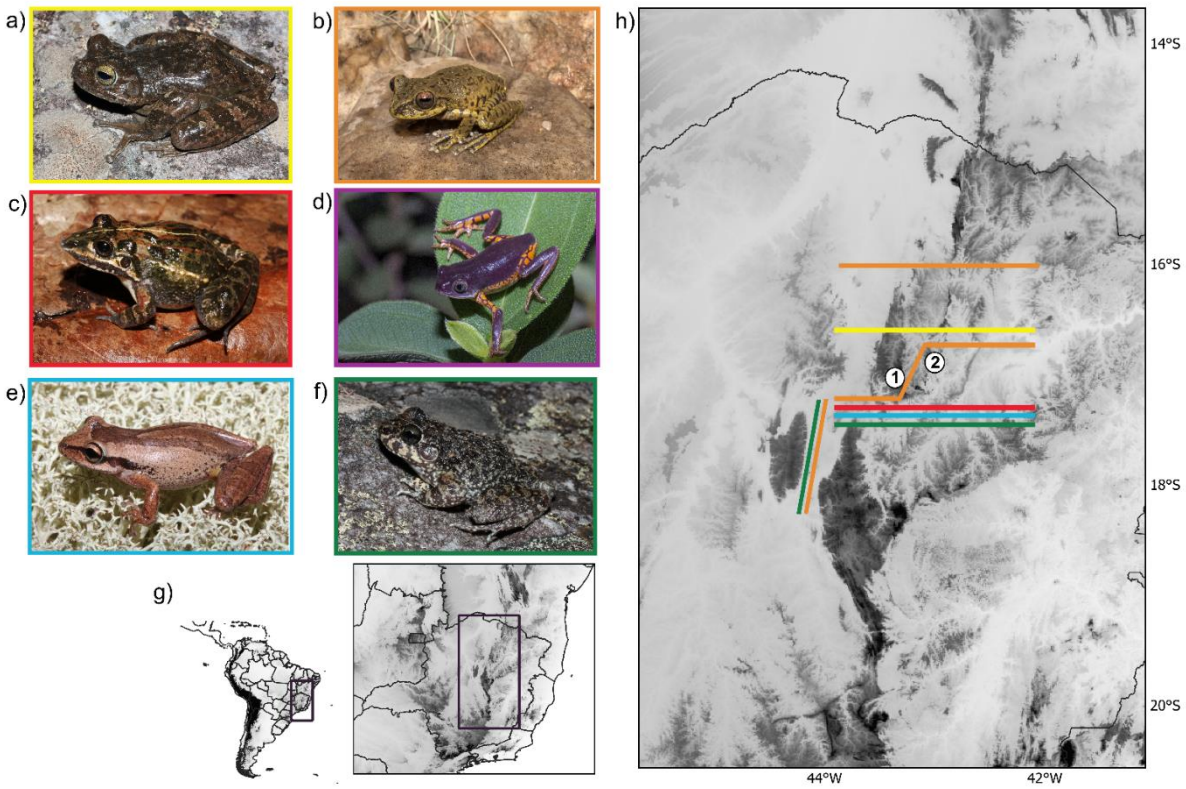

Fig 2 Illustrated dataset of endemic species sampled of Espinhaço Range; a) *Bokermannohyla alvarengai*; b) *Bokermannohyla saxicola*; c) *Leptodactylus camaquara*; d) *Pithecopus megacephalus*; e) *Scinax curicica*; and f) *Thoropa megatympanum*; g) Map of Brazilian Shield highlands and its location in South America (inset), with Espinhaço Mineiro and Quadrilátero Ferrífero highlighted and enlarged in (h); h) Phylogeographic barriers found in each species. Numbers correspond to locations, 1: Itacambira and 2: Botumirim. The colors surrounding the photographs match the barriers in the large map (h). Photographs: a, c-f: Tiago L. Pezzuti; b: André Yves

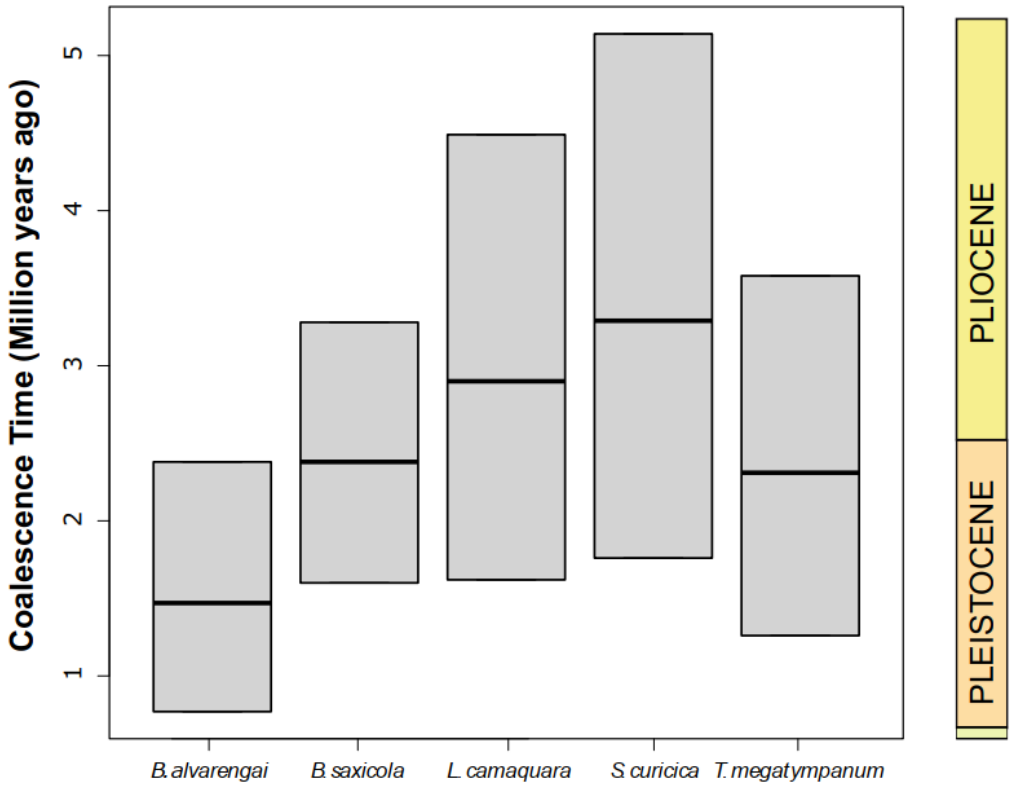

Fig 3 Mean and 95% HPD coalescence times (estimated in BEAST) between populations north and south of the central barrier. The geological time scale on the right corresponds to the y-axis time

References

Assunção-Silva, C. C., & Assis, L. C. de S. (2021). Areas of endemism of Lauraceae: new insights on the biogeographic regionalization of the Espinhaço Range, Brazil. *Cladistics*. https://doi.org/10.1111/cla.12481

Bonatelli, I. A. S., Perez, M. F., Peterson, A. T., Taylor, N. P., Zappi, D. C., Machado, M. C., Koch, I., Pires, A. H. C., & Moraes, E. M. (2014). Interglacial microrefugia and diversification of a cactus species complex: Phylogeography and palaeodistributional reconstructions for *Pilosocereus aurisetus* and allies. *Molecular Ecology*, *23*(12), 3044–3063. https://doi.org/10.1111/mec.12780

Bouckaert, R. R., & Drummond, A. J. (2017). bModelTest: Bayesian phylogenetic site model averaging and model comparison. *BMC Evolutionary Biology*, *17*(1), 1–11. https://doi.org/10.1186/s12862-017-0890-6

Bouckaert, R. R., Vaughan, T. G., Barido-Sottani, J., Duchêne, S., Fourment, M., Gavryushkina, A., Heled, J., Jones, G., Kühnert, D., de Maio, N., Matschiner, M., Mendes, F. K., Müller, N. F., Ogilvie, H. A., du Plessis, L., Popinga, A., Rambaut, A., Rasmussen, D., Siveroni, I., … Drummond, A. J. (2019). BEAST 2.5: An advanced software platform for Bayesian evolutionary analysis. *PLoS Computational Biology*, *15*(4), 1–28. https://doi.org/10.1371/journal.pcbi.1006650

Brandão, R. A., Leite, F. S. F., Françoso, R. D., & Faivovich, J. (2012). *Phyllomedusa megacephala* (Miranda-Ribeiro 1926) (Amphibia, Anura, Hylidae, Phyllomedusidae): Distribution extension, new state record and map. *Herpetology Notes*, *5*, 535–537.

Brown, J. L., Hill, D. J., Dolan, A. M., Carnaval, A. C., & Haywood, A. M. (2018). Paleoclim, high spatial resolution paleoclimate surfaces for global land areas. *Scientific Data*, *5*, 1–9. https://doi.org/10.1038/sdata.2018.254

Burnham, K. P., & Anderson, D. R. (2002). *Model Selection and Multimodel Inference: A Pratical Information-Theoretic Approach* (2nd ed.). Springer-Verlag.

Burnham, K. P., & Anderson, D. R. (2004). Multimodel inference: Understanding AIC and BIC in model selection. *Sociological Methods & Research*, *33*(2), 261–304. https://doi.org/10.1177/0049124104268644

Caramaschi, U. (2006). Redefinição Do Grupo de *Phyllomedusa hypochondrialis*, com redescrição de *P. megacephala* (Miranda-Ribeiro, 1926), revalidação de *P. azurea* Cope, 1862 e descrição de uma nova espécie (Amphibia, Anura, Hylidae). *Arquivos Do Museu Nacional, Rio de Janeiro*, *64*, 159–179. https://doi.org/10.5281/zenodo.2580067

Caramaschi, U., & Sazima, I. (1984). Uma nova espécie de *Thoropa* da Serra do Cipó, Minas Gerais, Brasil (Amphibia, Leptodactylidae). *Revista Brasileira de Zoologia*, *2*(3), 139–146.

Carvalho, T. R., Seger, K. R., Magalhães, F. M., Lourenço, L. B., & Haddad, C. F. B. (2021). Systematics and cryptic diversification of *Leptodactylus* frogs in the Brazilian campo rupestre. *Zoologica Scripta*, *50*, 300–317. https://doi.org/10.1111/zsc.12470

Chaves, A. V., Freitas, G. H. S., Vasconcelos, M. F., & Santos, F. R. (2015). Biogeographic patterns, origin and speciation of the endemic birds from eastern Brazilian mountaintops: a review. *Systematics and Biodiversity*, *13*(1), 1–16. https://doi.org/10.1080/14772000.2014.972477

Clark, K., Karsch-Mizrachi, I., Lipman, D. J., Ostell, J., & Sayers, E. W. (2016). GenBank. *Nucleic Acids Research*, *44*(D1), D67–D72. https://doi.org/10.1093/nar/gkv1276

Colli-Silva, M., Vasconcelos, T. N. C., & Pirani, J. R. (2019). Outstanding plant endemism levels strongly support the recognition of *campo rupestre* provinces in mountaintops of eastern South America. *Journal of Biogeography*, *46*(8), 1723–1733. https://doi.org/10.1111/jbi.13585

Echternacht, L., Trovó, M., Oliveira, C. T., & Pirani, J. R. (2011). Areas of endemism in the Espinhaço Range in Minas Gerais, Brazil. *Flora: Morphology, Distribution, Functional Ecology of Plants*, *206*(9), 782–791. https://doi.org/10.1016/j.flora.2011.04.003

Edgar, R. C. (2004). MUSCLE: Multiple sequence alignment with high accuracy and high throughput. *Nucleic Acids Research*, *32*(5), 1792–1797. https://doi.org/10.1093/nar/gkh340

Eterovick, P. C., & Brandão, R. A. (2001). A description of the tadpoles and advertisement calls of members of the *Hyla pseudopseudis* group. *Journal of Herpetology*, *35*(3), 442–450. https://doi.org/10.2307/1565962

Eterovick, P. C., Oliveira, F. F. R., & Tattersall, G. J. (2010). Threatened tadpoles of *Bokermannohyla alvarengai* (Anura: Hylidae) choose backgrounds that enhance crypsis potential. In *Biological Journal of the Linnean Society* (Vol. 101). https://academic.oup.com/biolinnean/article/101/2/437/2450584

Eterovick, P. C., Souza, A. M., & Sazima, I. (2020). Anfíbios da Serra do Cipó. In *Minas Gerais, Brasil* (1st ed., Vol. 1).

Felsenstein, J. (2006). Accuracy of coalescent likelihood estimates: Do we need more sites, more sequences, or more loci? *Molecular Biology and Evolution*, *23*(3), 691–700. https://doi.org/10.1093/molbev/msj079

Fernandes, G. W., Barbosa, N. P. U., Negreiros, D., & Paglia, A. P. (2014). Challenges for the conservation of vanishing megadiverse rupestrian grasslands. *Natureza & Conservação*, *2*(2), 162–165. https://doi.org/10.1016/j.ncon.2014.08.003

Fidanza, K., Martins, A. B., & Almeda, F. (2013). Four new species of *Trembleya* (Melastomataceae: Microlicieae) from Serra do Cabral, Minas Gerais, Brazil. *Brittonia*, *65*(3), 280–291. https://doi.org/10.1007/s12228-012-9281-x

Fiorini, C. F., Miranda, M. D., Silva-Pereira, V., Barbosa, A. R., Oliveira, U. de, Kamino, L. H. Y., Mota, N. F. D. O., Viana, P. L., & Borba, E. L. (2019). The phylogeography of Vellozia auriculata (Velloziaceae) supports low zygotic gene flow and local population persistence in the campo rupestre, a Neotropical OCBIL. *Botanical Journal of the Linnean Society*, *191*(3), 381–398. https://doi.org/10.1093/botlinnean/boz051

Flantua, S. G. A., & Hooghiemstra, H. (2018). Historical connectivity and mountain biodiversity. In C. Hoorn, Perrigo Allison, & A. Antonelli (Eds.), *Mountains, Climate and Biodiversity* (1st ed., Issue March 2019, pp. 171–185). John Wiley & Sons Ltda.

Fouquet, A., Noonan, B. P., Rodrigues, M. T., Pech, N., Gilles, A., & Gemmell, N. J. (2012). Multiple quaternary refugia in the eastern guiana shield revealed by comparative phylogeography of 12 frog species. *Systematic Biology*, *61*(3), 461–489. https://doi.org/10.1093/sysbio/syr130

García-Rodríguez, A., Velasco, J. A., Villalobos, F., & Parra-Olea, G. (2021). Effects of evolutionary time, speciation rates and local abiotic conditions on the origin and maintenance of amphibian montane diversity. *Global Ecology and Biogeography*, *30*(3), 674–684. https://doi.org/10.1111/geb.13249

Gernhard, T. (2008). The conditioned reconstructed process. *Journal of Theoretical Biology*, *253*(4), 769–778. https://doi.org/10.1016/j.jtbi.2008.04.005

Gill, M. S., Lemey, P., Faria, N. R., Rambaut, A., Shapiro, B., & Suchard, M. A. (2013). Improving bayesian population dynamics inference: A coalescent-based model for multiple loci. *Molecular Biology and Evolution*, *30*(3), 713–724. https://doi.org/10.1093/molbev/mss265

Haffer, J. (1969). Speciation in Amazonian Forest Birds. *Science*, *165*, 131–137.

Hickerson, M. J., Stahl, E., & Takebayashi, N. (2007). msBayes: Pipeline for testing comparative phylogeographic histories using hierarchical approximate Bayesian computation. *BMC Bioinformatics*, *8*, 1–7. https://doi.org/10.1186/1471-2105-8-268

Hopper, S. D. (2009). OCBIL theory: Towards an integrated understanding of the evolution, ecology and conservation of biodiversity on old, climatically buffered, infertile landscapes. *Plant and Soil*, *322*(1), 49–86. https://doi.org/10.1007/s11104-009-0068-0

Hopper, S. D. (2021). Out of the OCBILs: new hypotheses for the evolution, ecology and conservation of the eucalypts. *Biological Journal of the Linnean Society*, 1–31. https://doi.org/10.1093/biolinnean/blaa160

Hopper, S. D., Silveira, F. A. O., & Fiedler, P. L. (2016). Biodiversity hotspots and OCBIL theory. *Plant and Soil*, *403*(1–2), 167–216. https://doi.org/10.1007/s11104-015-2764-2

Huang, W., Takebayashi, N., Qi, Y., & Hickerson, M. J. (2011). MTML-msBayes: Approximate Bayesian comparative phylogeographic inference from multiple taxa and multiple loci with rate heterogeneity. *BMC Bioinformatics*, *12*(1), 1. https://doi.org/10.1186/1471-2105-12-1

Jackson, N. D., Morales, A. E., Carstens, B. C., & O'Meara, B. C. (2017). PHRAPL: Phylogeographic Inference Using Approximate Likelihoods. *Software for Systematics and Evolution*, *66*(6), 1045–1053. https://doi.org/10.1093/sysbio/syx001

Johns, G. C., & Avise, J. C. (1998). A comparative summary of genetic distances in the vertebrates from the mitochondrial cytochrome b gene. *Molecular Biology and Evolution*, *15*(11), 1481–1490. https://doi.org/10.1093/oxfordjournals.molbev.a025875

Larsson, A. (2014). AliView: A fast and lightweight alignment viewer and editor for large datasets. *Bioinformatics*, *30*(22), 3276–3278. https://doi.org/10.1093/bioinformatics/btu531

Leite, F. S. F. (2012). *Taxonomia, biogeografia e conservação dos anfíbios da Serra do Espinhaço* [Universidade Federal de Minas Gerais]. https://repositorio.ufmg.br/handle/1843/BUOS-96VGWR

Leite, F. S. F., Juncá, F. A., & Eterovick, P. C. (2008). Status do conhecimento, endemismo e conservação de anfíbios anuros da Cadeia do Espinhaço, Brasil. *Megadiversidade*, *4*(1–2), 158–176.

Leite, F. S. F., Pezzuti, T. L., & de Oliveira Drummond, L. (2011). A new species of bokermannohyla from the espinhao range, State of Minas Gerais, Southeastern Brazil. *Herpetologica*, *67*(4), 440–448. https://doi.org/10.1655/HERPETOLOGICA-D-11-00017.1

Lemmon, E. M., Lemmon, A. R., & Cannatella, D. C. (2007). Geological and climatic forces driving speciation in the continentally distributed trilling chorus frogs (Pseudacris). *Evolution*, *61*(9), 2086–2103. https://doi.org/10.1111/j.1558-5646.2007.00181.x

Lomolino, M. V., Riddle, B. R., Whittaker, R. J., & Brown, J. H. (2010). Distribution of species: Ecological Foundations. In *Biogeography* (4th ed., pp. 83–120). Sinauer Associates, Inc.

Magalhães, R. F., Lemes, P., Santos, M. T. T., Mol, R. M., Ramos, E. K. S., Oswald, C. B., Pezzuti, T. L., Santos, F. R., Brandão, R. A., & Garcia, P. C. A. (2021). Evidence of introgression in endemic frogs from the campo rupestre contradicts the reduced hybridization hypothesis. *Biological Journal of the Linnean Society*, *138*, 561–576. https://doi.org/10.1093/biolinnean/blaa142

Miola, D. T. B., Ramos, V. D. v, & Silveira, F. A. O. (2021). A brief history of research in campo rupestre: identifying research priorities and revisiting the geographical distribution

of an ancient, widespread Neotropical biome. *Biological Journal of the Linnean Society*, *133*(2), 464–480. https://doi.org/10.1093/biolinnean/blaa175

Myers, E. A., Xue, A. T., Gehara, M., Cox, C. L., Davis Rabosky, A. R., Lemos-Espinal, J., Martínez-Gómez, J. E., & Burbrink, F. T. (2019). Environmental heterogeneity and not vicariant biogeographic barriers generate community-wide population structure in desert-adapted snakes. *Molecular Ecology*, *28*(20), 4535–4548. https://doi.org/10.1111/mec.15182

Nali, R. C., Becker, C. G., Zamudio, K. R., & Prado, C. P. A. (2020). Topography, more than land cover, explains genetic diversity in a Neotropical savanna tree frog. *Diversity and Distributions*, *26*(12), 1798–1812. https://doi.org/10.1111/ddi.13154

Nascimento, A. C., Chaves, A. V., Leite, F. S. F., Eterovick, P. C., & Santos, F. R. (2018). Past vicariance promoting deep genetic divergence in an endemic frog species of the Espinhaço Range in Brazil: The historical biogeography of Bokermannohyla saxicola (Hylidae). *PLoS ONE*, *13*(11), 1–19. https://doi.org/10.1371/journal.pone.0206732

Oaks, J. R., L'Bahy, N., & Cobb, K. A. (2020). Insights from a general, full-likelihood Bayesian approach to inferring shared evolutionary events from genomic data: Inferring shared demographic events is challenging. *Evolution*, *74*(10), 2184–2206.

Oliveira, F. R. de, Gehara, M., Solé, M., Lyra, M., Haddad, C. F. B., Silva, D. P., Magalhães, R. F. de, Leite, F. S. F., & Burbrink, F. T. (2021). Quaternary climatic fluctuations influence the demographic history of two species of sky-island endemic amphibians in the Neotropics. *Molecular Phylogenetics and Evolution*, *160*. https://doi.org/10.1016/j.ympev.2021.107113

Oliveira, F. R. de, Nogueira, P. A. G., & Eterovick, P. C. (2012). Natural history of *Phyllomedusa megacephala* (Miranda-Ribeiro, 1926) (Anura: Hylidae) in southeastern Brazil, with descriptions of its breeding biology and male territorial behaviour. *Journal of Natural History*, *46*(1–2), 117–129. https://doi.org/10.1080/00222933.2011.626127

Oswald, C. B., Lemes, P., Thomé, M. T. C., Pezzuti, T. L., Santos, F. R., Garcia, P. C. A., Leite, F. S. F., & Magalhães, R. F. (in press). Colonization rather than fragmentation explains the geographic distribution and diversification of treefrogs endemic to Brazilian shield sky islands. *Journal of Biogeography*.

Pacifico, R., Almeda, F., & Fidanza, K. (2021). Modeling of Microlicieae (Melastomataceae) species composition provides insights into the evolution of *campo rupestre* vegetation on

eastern Brazilian mountaintops. *Flora: Morphology, Distribution, Functional Ecology of Plants*, *281*(June). https://doi.org/10.1016/j.flora.2021.151850

Papadopoulou, A., Knowles, L. L. (2016). Toward a paradigm shift in comparative phylogeography driven by trait-based hypotheses. *PNAS*, *113*, 8018-8024. https://doi.org/10.1073/pnas.1601069113

Paz, A., Ibáñez, R., Lips, K. R., & Crawford, A. J. (2015). Testing the role of ecology and life history in structuring genetic variation across a landscape: A trait-based phylogeographic approach. *Molecular Ecology*, *24*(14), 3723–3737. https://doi.org/10.1111/mec.13275

Perez, M. F., Bonatelli, I. A. S., Moraes, E. M., & Carstens, B. C. (2016). Model-based analysis supports interglacial refugia over long-dispersal events in the diversification of two South American cactus species. *Heredity*, *116*(6), 550–557. https://doi.org/10.1038/hdy.2016.17

Perez, M. F., Franco, F. F., Bombonato, J. R., Bonatelli, I. A. S., Khan, G., Romeiro-Brito, M., Fegies, A. C., Ribeiro, P. M., Silva, G. A. R., & Moraes, E. M. (2018). Assessing population structure in the face of isolation by distance: Are we neglecting the problem? *Diversity and Distributions*, *24*(12), 1883–1889. https://doi.org/10.1111/ddi.12816

Perrigo, A., Hoorn, C., & Antonelli, A. (2020). Why mountains matter for biodiversity. *Journal of Biogeography*, *47*(2), 315–325. https://doi.org/10.1111/jbi.13731

Pugliese, A., Pombal, J. P., & Sazima, I. (2004). A new species of *Scinax* (Anura: Hylidae) from rocky montane fields of the Serra do Cipó, Southeastern Brazil. *Zootaxa*, *688*(1), 1–15.

QGIS Development Team. (2020). *QGIS: A Free and Open Source Geographic Information System* (3.14.1 Pi). Open Source Geospatial Foundation Project.

Rambaut, A. (2018). *FigTree*. http://tree.bio.ed.ac.uk/software/figtree/

Rambaut, A., Drummond, A. J., Xie, D., Baele, G., & Suchard, M. A. (2018). Posterior summarization in Bayesian phylogenetics using Tracer 1.7. *Systematic Biology*, *67*(5), 901–904. https://doi.org/10.1093/sysbio/syy032

Ramos, E. K. S., de Magalhães, R. F., Sari, E. H. R., Rosa, A. H. B., Garcia, P. C. A., & Santos, F. R. (2018). Population genetics and distribution data reveal conservation concerns to the sky island endemic *Pithecopus megacephalus* (Anura, Phyllomedusidae). *Conservation Genetics*, *19*(1), 99–110. https://doi.org/10.1007/s10592-017-1013-z

Ramos, E. K. S., Magalhães, R. F. de, Marques, N. C. S., Baêta, D., Garcia, P. C. A., & Santos, F. R. (2019). Cryptic diversity in Brazilian endemic monkey frogs (Hylidae,

Phyllomedusinae, *Pithecopus*) revealed by multispecies coalescent and integrative approaches. *Molecular Phylogenetics and Evolution*, *132*, 105–116. https://doi.org/10.1016/j.ympev.2018.11.022

Rapini, A., Bitencourt, C., Luebert, F., & Cardoso, D. (2020). An escape-to-radiate model for explaining the high plant diversity and endemism in *campos rupestres*. *Biological Journal of the Linnean Society*, *133*, 481-498. https://doi.org/10.1093/biolinnean/blaa179

Rodríguez, A., Börner, M., Pabijan, M., Gehara, M., Haddad, C. F. B., & Vences, M. (2015). Genetic divergence in tropical anurans: deeper phylogeographic structure in forest specialists and in topographically complex regions. *Evolutionary Ecology*, *29*(5), 765–785. https://doi.org/10.1007/s10682-015-9774-7

Rull, V. (2011). Neotropical biodiversity: Timing and potential drivers. *Trends in Ecology and Evolution*, *26*(10), 508–513. https://doi.org/10.1016/j.tree.2011.05.011

Sabbag, A. F., Lyra, M. L., Zamudio, K. R., Haddad, C. F. B., Feio, R. N., Leite, F. S. F., Gasparini, J. L., & Brasileiro, C. A. (2018). Molecular phylogeny of Neotropical rock frogs reveals a long history of vicariant diversification in the Atlantic Forest. *Molecular Phylogenetics and Evolution*, *122*, 142–156. https://doi.org/10.1016/j.ympev.2018.01.017

Sambrook, J., & Russel, D. W. (2001). *Molecular Cloning: A Laboratory Manual*. CSH Laboratory Press.

Sánchez-Montes, G., Wang, J., Ariño, A. H., & Martínez-Solano, Í. (2018). Mountains as barriers to gene flow in amphibians: Quantifying the differential effect of a major mountain ridge on the genetic structure of four sympatric species with different life history traits. *Journal of Biogeography*, *45*(2), 318–331. https://doi.org/10.1111/jbi.13132

Santos, J. E., Santos, F. R., & Silveira, F. A. (2015). Hitting an unintended target: Phylogeography of *Bombus brasiliensis* Lepeletier, 1836 and the first new Brazilian bumblebee species in a century (Hymenoptera: Apidae). *PLoS ONE*, *10*(5), 1–21. https://doi.org/10.1371/journal.pone.0125847

Santos, M. T. T., de Magalhães, R. F., Lyra, M. L., Santos, F. R., Zaher, H., Giasson, L. O. M., Garcia, P. C. A., Carnaval, A. C., & Haddad, C. F. B. (2020). Multilocus phylogeny of Paratelmatobiinae (Anura: Leptodactylidae) reveals strong spatial structure and previously unknown diversity in the Atlantic Forest hotspot. *Molecular Phylogenetics and Evolution*, *148*(April), 106819. https://doi.org/10.1016/j.ympev.2020.106819

Sazima, I., & Bokermann, W. C. A. (1977). Anfíbios da Serra do Cipó, Minas Gerais, Brasil. 3: Observações sobre a biologia de *Hyla alvarengai* Bok. (Anura, Hylidae). *Revista Brasileira de Biologia*, *37*(2), 413–417. https://www.researchgate.net/publication/277776321

Sazima, I., & Bokermann, W. C. A. (1978). Cinco novas espécies de *Leptodactylus* do Centro e Sudeste brasileiro (Amphibia, Anura, Leptodactylidae). *Revista Brasileira de Biologia*, *38*(4), 899–912.

Silveira, F. A. O., Negreiros, D., Barbosa, N. P. U., Buisson, E., Carmo, F. F., Carstensen, D. W., Conceição, A. A., Cornelissen, T. G., Echternacht, L., Fernandes, G. W., Garcia, Q. S., Guerra, T. J., Jacobi, C. M., Lemos-Filho, J. P., le Stradic, S., Morellato, L. P. C., Neves, F. S., Oliveira, R. S., Schaefer, C. E., … Lambers, H. (2016). Ecology and evolution of plant diversity in the endangered *campo rupestre*: a neglected conservation priority. *Plant and Soil*, *403*(1–2), 129–152. https://doi.org/10.1007/s11104-015-2637-8

Steinbauer, M. J., Field, R., Grytnes, J. A., Trigas, P., Ah-Peng, C., Attorre, F., … Beierkuhnlein, C. (2016). Topography-driven isolation, speciation and a global increase of endemism with elevation. *Global Ecology and Biogeography*, *25*(9), 1097–1107. https://doi.org/10.1111/geb.12469

Stöck, M., Dufresnes, C., Litvinchuk, S. N., Lymberakis, P., Biollay, S., Berroneau, M., Borzée, A., Ghali, K., Ogielska, M., & Perrin, N. (2012). Cryptic diversity among Western Palearctic tree frogs: Postglacial range expansion, range limits, and secondary contacts of three European tree frog lineages (*Hyla arborea* group). *Molecular Phylogenetics and Evolution*, *65*, 1–9. https://doi.org/10.1016/j.ympev.2012.05.014

Thomé, M. T. C., Sequeira, F., Brusquetti, F., Carstens, B., Haddad, C. F. B., Rodrigues, M. T., & Alexandrino, J. (2016). Recurrent connections between Amazon and Atlantic forests shaped diversity in Caatinga four-eyed frogs. *Journal of Biogeography*, *43*(5), 1045–1056. https://doi.org/10.1111/jbi.12685

Vasconcelos, T. N. C., Alcantara, S., Andrino, C. O., Forest, F., Reginato, M., Simon, M. F., & Pirani, J. R. (2020). Fast diversification through a mosaic of evolutionary histories characterizes the endemic flora of ancient Neotropical mountains. *Proceedings of the Royal Society B: Biological Sciences*, *287*(1923). https://doi.org/10.1098/rspb.2019.2933

Wang, I. J., & Bradburd, G. S. (2014). Isolation by environment. *Molecular Ecology*, *23*, 5649–5662. https://doi.org/10.1111/mec.12938

Considerações finais

Entre as 44 espécies de anuros endêmicos da Serra do Espinhaço, poucas foram avaliadas quanto a sua estruturação espacial ao longo da Serra do Espinhaço. Esses estudos são necessários para planejamentos futuros de projetos de conservação, uma vez que a região sofre ameaças e tem grande importância econômica, social e ambiental (Fernandes et al., 2014; Silveira et al., 2016, UNESCO, 2005).

Apesar da região ser considerada um OCBIL ('paisagens antigas, climaticamente tamponadas e inférteis'), na qual a diversificação da biota seria explicada por isolamento antigo e estabilidade climática (Hopper, 2009; Silveira et al., 2016), a tese demonstra algumas quebras de premissas desta classificação. Ainda que a fragmentação seja um processo importante para a diversificação de algumas espécies de anuros, como *Rupirana* e *Crossodactylodes* (Santos et al., 2020), ela não é o único processo envolvido na diversificação dos anuros da Serra do Espinhaço. Diferentes processos como hibridização, colonização, são importantes para a evolução da biota da Serra do Espinhaço (Magalhães et al., 2021; Oswald et al., in press). A pequena influência das mudanças climáticas do Pleistoceno também está em desacordo com os resultados da tese. As estimativas de tempos de divergência das distintas abordagens (capítulo 2 e 3) são concordantes com os períodos Plioceno e Pleistoceno e como já demonstrado por outros estudos, a variação climática passada nestas épocas parece ter sido um importante fator para a diversificação do grupo (Oliveira et al., 2021; Magalhães et al., 2021). A história evolutiva da Serra do Espinhaço é complexa, e a teoria de OCBIL sozinha não pode não ser suficiente para explica-la. Precisamos considerar a multiplicidade de processos e fatores associados a diversificação de biota.

Novos estudos filogeográficos focados em espécies, principalmente em *Pithecopus megacephalus*, nos permitirão entender a falta de estruturação genética encontrada na espécie, que pode ser resultado de fluxo gênico recente ou não ou ser resultado de sorteamento incompleto de linhagens. Adicionalmente, a inclusão de dados nucleares, novas espécies endêmicas da Serra do Espinhaço e dados sobre a biologia das espécies bem como dados do ambiente, analisados sob a ótica da filogeografia comparativa, podem nos ajudar a entender melhor os diferentes pulsos de diversificação ocorrentes na Serra do Espinhaço ao longo do tempo.

Referências

Hopper, S. D. (2009). OCBIL theory: Towards an integrated understanding of the evolution, ecology and conservation of biodiversity on old, climatically buffered, infertile landscapes. *Plant and Soil 322*(1), 49–86. https://doi.org/10.1007/s11104-009-0068-0

Magalhães, R. F., Lemes, P., Santos, M. T. T., Mol, R. M., Ramos, E. K. S., Oswald, C. B., Pezzuti, T. L., Santos, F. R., Brandão, R. A., & Garcia, P. C. A. (2021). Evidence of introgression in endemic frogs from the campo rupestre contradicts the reduced hybridization hypothesis. *Biological Journal of the Linnean Society 138*, 561–576. https://doi.org/10.1093/biolinnean/blaa142

Santos, M. T. T., de Magalhães, R. F., Lyra, M. L., Santos, F. R., Zaher, H., Giasson, L. O. M., Garcia, P. C. A., Carnaval, A. C., & Haddad, C. F. B. (2020). Multilocus phylogeny of Paratelmatobiinae (Anura: Leptodactylidae) reveals strong spatial structure and previously unknown diversity in the Atlantic Forest hotspot. *Molecular Phylogenetics and Evolution 148*, 106819. https://doi.org/10.1016/j.ympev.2020.106819

Silveira, F. A. O., Negreiros, D., Barbosa, N. P. U., Buisson, E., Carmo, F. F., Carstensen, D. W., Conceição, A. A., Cornelissen, T. G., Echternacht, L., Fernandes, G. W., Garcia, Q. S., Guerra, T. J., Jacobi, C. M., Lemos-Filho, J. P., Le Stradic, S., Morellato, L. P. C., Neves, F. S., Oliveira, R. S., Schaefer, C. E., … Lambers, H. (2016). Ecology and evolution of plant diversity in the endangered *campo rupestre*: a neglected conservation priority. *Plant and Soil 403*(1–2), 129–152. https://doi.org/10.1007/s11104-015-2637-8

UNESCO – United Nations Educational, Scientific and Cultural Organization (2021) Biosphere reserves in Latin America and the Caribbean. (03 de maio de 2021). Acessível em: https://en.unesco.org/biosphere/lac

Apêndice

I) Material Suplementar – Capítulo 2

Colonization rather than fragmentation explains the geographic distribution and diversification of treefrogs endemic to Brazilian shield sky islands (Oswald et al., in press)

a) Supporting information

Additional details on methodology and results for sampling strategy, testing for multiple species, and testing for diversification scenarios

1 Material and Methods

1.1 Sampling strategy

1.1.1 Genetic data

The new genomic extraction was carried out following a standard phenol-chloroform extraction protocol (Sambrook & Russel, 2001).

The six fragments were obtained via polymerase chain reaction (PCR) using specific primers (Table S2). PCR was performed in a 15 μL reaction volume containing: 30 ng of genomic DNA, 1x Buffer, 1.25 μM each primer, 2.5 mM $MgCl_2$, 0.72 μg bovine serum albumin (BSA), 3 mM dNTPs, 0.625 U Platinum™ *Taq* DNA polymerase (Thermo Fisher Scientific). PCRs were performed under the following conditions for each marker:

Cyt-*b:* One initial denaturation step at 94°C for 5 minutes, followed by 35 cycles of denaturation at 94°C for 30 seconds, primer annealing at 58°C for 40 seconds, and extension at 72°C for one minute. For a complete extension of the amplified products, a final step of 72°C was added for 7 minutes.

COI: One initial denaturation step at 94°C for 5 minutes, followed by 35 cycles of denaturation at 94°C for 30 seconds, primer annealing at 58°C for 40 seconds, and extension at 72°C for one minute. For a complete extension of the amplified products, a final step of 72°C was added for 7 minutes.

β-cry: One initial denaturation step at 95°C for 5 minutes, followed by 35 cycles of denaturation at 95°C for 30 seconds, primer annealing at 54°C for 40 seconds and extension at 72°C for 25 seconds. For a complete extension of the amplified products, a final step of 72°C was added for 5 minutes.

β-fib: One initial denaturation step at 95°C for 5 minutes, followed by 35 cycles of denaturation at 95°C for 30 seconds, primer annealing at 59°C for one minute and extension at

72°C for 40 seconds. For a complete extension of the amplified products, a final step of 72°C was added for 7 minutes.

c-*myc:* One initial denaturation step at 94°C for 1 minute, followed by 35 cycles of denaturation at 94°C for 45 seconds, primer annealing at 54°C for one minute, and extension at 72°C for 35 seconds. For a complete extension of the amplified products, a final step of 72°C was added for 7 minutes.

DIA6: One initial denaturation step at 94°C for 5 minutes, followed by 40 cycles of denaturation at 94°C for 40 seconds, primer annealing at 60°C for one minute, and extension at 72°C for 30 seconds. For a complete extension of the amplified products, a final step of 72°C was added for 7 minutes.

POMC: One initial denaturation step at 94°C for 5 minutes, followed by 35 cycles of denaturation at 94°C for 30 seconds, primer annealing at 60°C for 50 seconds, and extension at 72°C for 35 seconds. For a complete extension of the amplified products, a final step of 72°C was added for 7 minutes.

SmarcB1: One initial denaturation step at 95°C for 5 minutes, followed by 40 cycles of denaturation at 95°C for 30 seconds, primer annealing at 60°C for one minute, and extension at 72°C for 30 seconds. For a complete extension of the amplified products, a final step of 72°C was added for 7 minutes.

DNA amplicons were purified using polyethylene glycol 20% to remove PCR residuals (Santos et al., 2015) and sequenced in both strands, using the same amplification primers from PCR (Table S2) plus BigDye Terminator v3.1 kit (Life Technologies™), in a Sanger automatized sequencer ABI 3130XL (Applied Biosystems™).

1.2 Testing for multiple species

1.2.1 Exploring genetic structure

To select *a priori* range of the number of populations, we ran an exploratory mtDNA delimitation using a Generalized Mixed Yule Coalescent (GMYC) model Pons et al., 2006). For this, the unique haplotypes of mtDNA were identified using the R package 'haplotypes' 1.1.2 (Aktas, 2020), and trees of these haplotypes were estimated in BEAST 2.6.2, assuming strict molecular clock and substitution rate fixed at one, Yule tree process, and root set in *Bokermannohyla nanuzae*. The evolutionary models were co-estimated with the tree through package 'bModelTest' (Bouckaert & Drummond, 2017). The analysis was conducted in three replicates, with 5×10^7 generations, 5×10^3 thinning, and 5% burn-in each. The results of all

runs were combined using LogCombiner 2.6.2 (Bouckaert et al., 2019), and the tree with maximum clade credibility (MCC) was annotated in TreeAnnotator 2.6.2 (Bouckaert et al., 2019). After removing the root, the MCC tree was submitted to a maximum likelihood implementation of GMYC with R package ‘splits’ 1.0-19 (Ezard et al., 2017), using the single-threshold algorithm.

1.2.2 Morphological species delimitation

Before ran morphometric analyses, we removed the allometric size effect from all adult morphometric data, following Lleonart, Salat, & Torres (2000). Initially, all variables were $\log_{10}$-transformed, and then we made a Principal Component Analysis (PCA) to find a proxy for body size (i.e. the variable with the highest loading value from the first principal component). The variance-covariance matrix eigenvectors were obtained using the *prcomp* function in R package ‘vegan’ v. 2.5-6 (Oksanen et al., 2019). The variable FLL was selected as a proxy for all adults. The residuals of the regression of the variables against proxies were used instead of the original variables for subsequent analyses using morphometric data (Lleonart et al., 2000). After the size correction, we calculated the variance inflation factors (VIF) among variables to estimate multicollinearity using the function *vif* in R package 'car’ v. 3.0-10 (Fox & Weisberg, 2019). All variables showed VIFs smaller than five, thus all of them were retained for analyses (Akinwande et al., 2015).

To test sexual dimorphism in adults' morphometric traits, we conducted a permutational analysis of variance (PERMANOVA) with Euclidian distance and 1×10^4 permutations in ‘vegan’ v. 2.5-6 R package (Oksanen et al., 2019). Additionally, we calculated the sexual size dimorphism index (SSDi; Smith, 1999). Males were sexed according to external characters, such as the presence of vocal slits under the tongue.

1.3 Testing for diversification scenarios

1.3.1 Demographic model selection

To estimate the relative population sizes (θ) between the lineages, we performed an exploratory analysis using the Bayesian algorithm of Migrate-n v. 3.7.2 (Beerli, 2006, 2007, 2009). The analysis was made in two parallel replicates, using one long and 14 short chains heated under the thermodynamic static strategy. The heating was made with the cold chain equal to 1, the hottest chain equal to 1×10^6, and the remaining chains growing at a cumulative exponential scale of 1.3, starting from 1.5. The run-length was set with 1×10^8 generations,

thinning of 100, and a burn-in period of 1×10^7. Convergence between replicates was accessed through the pairs strategy, and mixing was evaluated using ESSs plus the chains' update rates.

2 Results

2.1 Testing for multiple species

2.1.1 Exploring genetic structure

The GMYC analysis returned five mitochondrial entities, with a confidence interval from four to 11. The null hypothesis of only one putative species in mtDNA gene tree was rejected (likelihood ratio test = 63.71; $p < 0.01$). Two distinct mitochondrial lineages were recovered from southern (named here Southern 1 and Southern 2), one from center (named here Central), one from northern (named here Northern), and one from western (named here Cabral) of EM. The lineages Southern 1, Southern 2, and Central correspond, respectively, to the clades Diamantina plateau, Cipó, and Itacambira in (Nascimento et al., 2018), while Cabral and Northern received the exact identification. Both Southern lineages occurred in sympatry in Santana do Riacho and Congonhas do Norte municipalities (Figure S1; Figure 1). Southern 2 is still distributed in Augusto de Lima, Botumirim, Conceição do Mato Dentro, Diamantina, Itamarandiba, Rio Vermelho, Santana de Pirapama, São Gonçalo do Rio Preto, Serro, and Turmalina, while Southern 2 is also distributed in the municipalities of São Sebastião do Rio Preto and Barão de Cocais (Figure S1; Figure 1).

2.1.2 Morphological species delimitation

In total, 469 adults were measured, being 67 females and 402 males. Females and males diverge significantly in morphometric traits ($PP < 0.001$; Table S5), being females slightly larger than males (SSDi = 0.936). Therefore, only males' traits were used in the study's other analyses.

2.2 Testing for diversification scenarios

2.2.1 Demographic model selection

The θ value found for the southern lineage was at least four times higher than for the other lineages ($\theta_{center} = 8.710 \times 10^{-3}$; $\theta_{southern} = 3.837 \times 10^{-2}$; $\theta_{cabral} = 6.230 \times 10^{-3}$; $\theta_{northern} = 6.230 \times 10^{-3}$).

Reference

Akinwande, M. O., Dikko, H. G., & Samson, A. (2015). Variance Inflation Factor: As a Condition for the Inclusion of Suppressor Variable(s) in Regression Analysis. *Open Journal of Statistics*, *05*(07), 754–767. https://doi.org/10.4236/ojs.2015.57075

Aktas, C. (2020). *haplotypes: Manipulating DNA Sequences and Estimating Unambiguous Haplotype Network with Statistical Parsimony* (1.1.2). https://cran.r-project.org/package=haplotypes

Beerli, P. (2006). Comparison of Bayesian and maximum-likelihood inference of population genetic parameters. *Bioinformatics*, *22*(3), 341–345. https://doi.org/10.1093/bioinformatics/bti803

Beerli, P. (2007). Estimation of the population scaled mutation rate from microsatellite data. *Genetics*, *177*(3), 1967–1968. https://doi.org/10.1534/genetics.107.078931

Beerli, P. (2009). How to use MIGRATE or why are Markov chain Monte Carlo programs difficult to use? In G. Bertorelle, M. W. Bruford, H. C. Hauffe, A. Rizzoli, & C. Vernesi (Eds.), *Population Genetics for Animal Conservation* (pp. 42–79). Cambridge University Press. https://doi.org/10.1017/CBO9780511626920.004

Bouckaert, R. R., & Drummond, A. J. (2017). bModelTest: Bayesian phylogenetic site model averaging and model comparison. *BMC Evolutionary Biology*, *17*(1), 1–11. https://doi.org/10.1186/s12862-017-0890-6

Bouckaert, R. R., Vaughan, T. G., Barido-Sottani, J., Duchêne, S., Fourment, M., Gavryushkina, A., Heled, J., Jones, G., Kühnert, D., De Maio, N., Matschiner, M., Mendes, F. K., Müller, N. F., Ogilvie, H. A., Du Plessis, L., Popinga, A., Rambaut, A., Rasmussen, D., Siveroni, I., … Drummond, A. J. (2019). BEAST 2.5: An advanced software platform for Bayesian evolutionary analysis. *PLoS Computational Biology*, *15*(4), 1–28. https://doi.org/10.1371/journal.pcbi.1006650

Ezard, T., Fujisawa, T., & Barraclough, T. (2017). *splits: Species' Limits by Threshold Statistics* (1.0-19/r52). https://r-forge.r-project.org/projects/splits/

Fox, J., & Weisberg, S. (2019). *An {R} Companion to Applied Regression* (4th ed.). Sage Publications, Inc. https://socialsciences.mcmaster.ca/jfox/Books/Companion/

Lleonart, J., Salat, J., & Torres, G. J. (2000). Removing allometric effects of body size in morphological analysis. *Journal of Theoretical Biology*, *205*(1), 85–93. https://doi.org/10.1006/jtbi.2000.2043

Nascimento, A. C., Chaves, A. V., Leite, F. S. F., Eterovick, P. C., & Santos, F. R. (2018). Past

vicariance promoting deep genetic divergence in an endemic frog species of the Espinhaço Range in Brazil: The historical biogeography of *Bokermannohyla saxicola* (Hylidae). *PLoS ONE*, *13*(11), 1–19. https://doi.org/10.1371/journal.pone.0206732

Oksanen, J., Blanchet, F. G., Friendly, M., Kindt, R., Legendre, P., McGlinn, D., Minchin, P. R., O'Hara, R. B., Simpson, G. L., Solymos, P., Stevens, M. H. H., Szoecs, E., & Wagner, H. (2019). *vegan: Community Ecology Package* (2.5-6). https://cran.r-project.org/package=vegan

Pons, J., Barraclough, T. G., Gomez-Zurita, J., Cardoso, A., Duran, D. P., Hazell, S., Kamoun, S., Sumlin, W. D., & Vogler, A. P. (2006). Sequence-based species delimitation for the DNA taxonomy of undescribed insects. *Systematic Biology*, *55*(4), 595–609. https://doi.org/10.1080/10635150600852011

Sambrook, J., & Russel, D. W. (2001). *Molecular Cloning: A Laboratory Manual*. CSH Laboratory Press.

Santos, J. E., Santos, F. R., & Silveira, F. A. (2015). Hitting an unintended target: Phylogeography of Bombus brasiliensis lepeletier, 1836 and the first new Brazilian bumblebee species in a century (Hymenoptera: Apidae). *PLoS ONE*, *10*(5), 1–21. https://doi.org/10.1371/journal.pone.0125847

Smith, R. J. (1999). Statistics of sexual size dimorphism. *Journal of Human Evolution*, *36*(4), 423–458. https://doi.org/10.1006/jhev.1998.0281

b) Supplementary figures

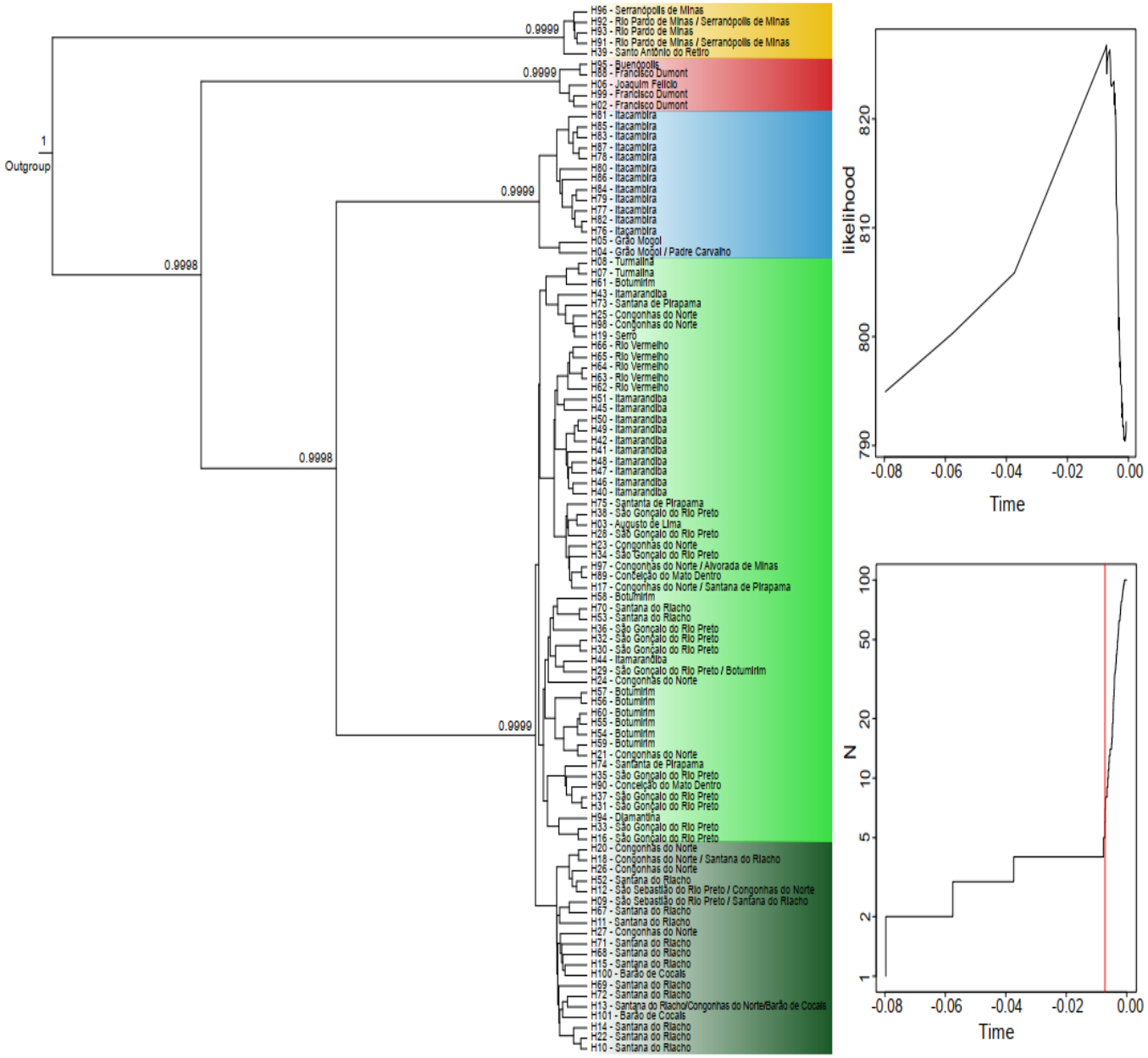

Figure S1 – Mitochondrial species delimitation generated by the ML-GMYC method. The numbers above nodes represent the posterior probabilities for each node in gene tree reconstruction. Colours represent distinct lineages of *Bokermannohyla saxicola* along the Espinhaço range: Northern (yellow), Cabral (red), Central (Blue), Southern 1 (green), Southern 2 (dark green)

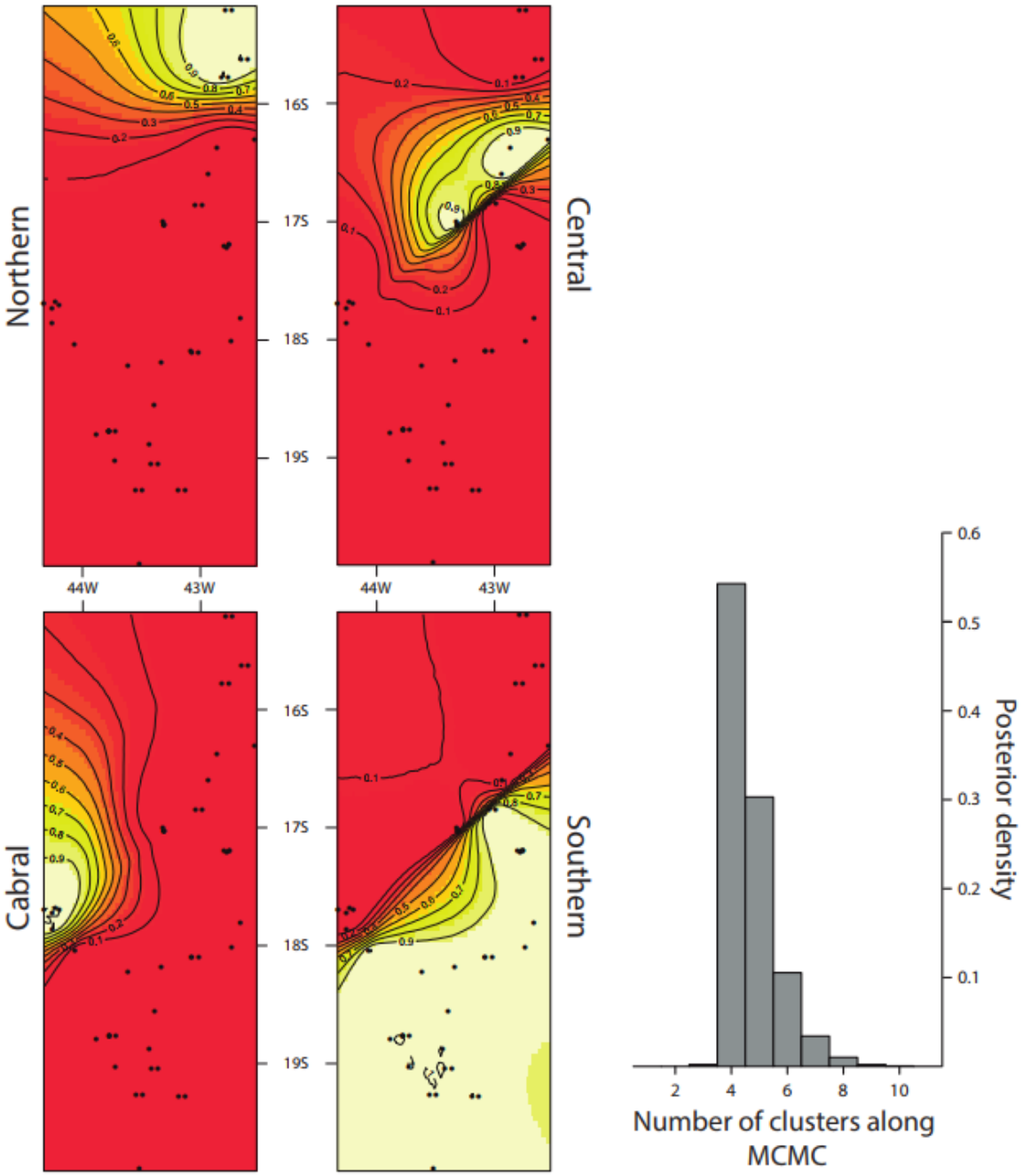

Figure S2 – Spatial probabilities of *Bokermannohyla saxicola* populations in the Espinhaço Range inferred through the Geneland method, including only genetic data records. Colours and isoclines indicate posterior probabilities of assignment to each lineage.

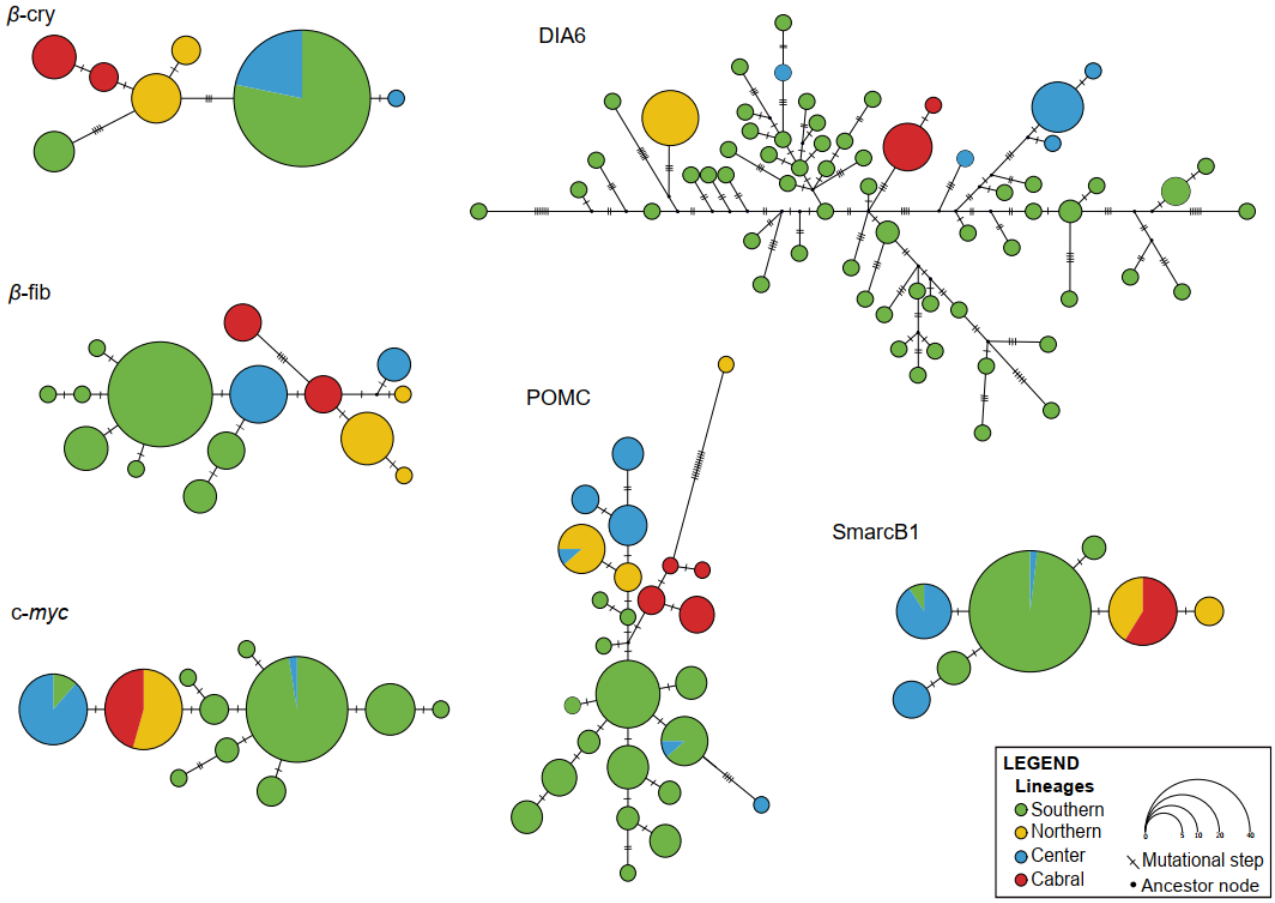

Figure S3 – Haplotype network for each nuclear loci sampled. Colours represent distinct lineages of *Bokermannohyla saxicola*.

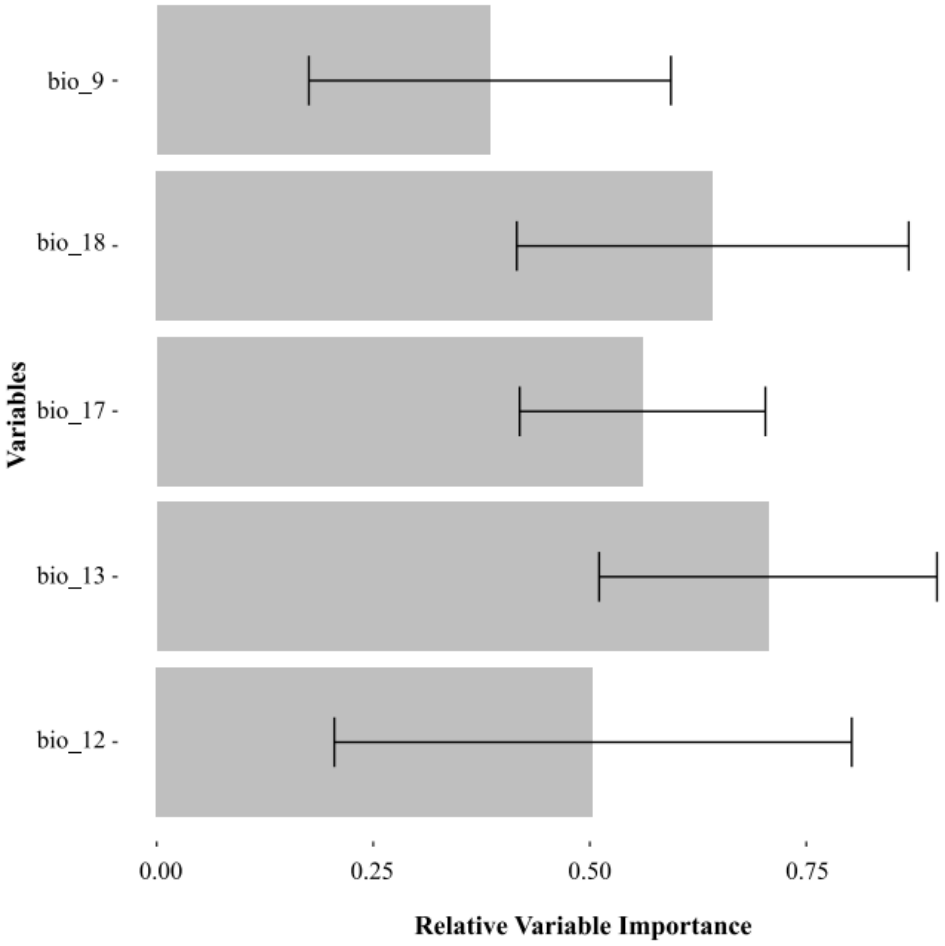

Figure S4 - Relative Variables Importance of distinct environmental dataset used for calibrating ecological niche modelling.

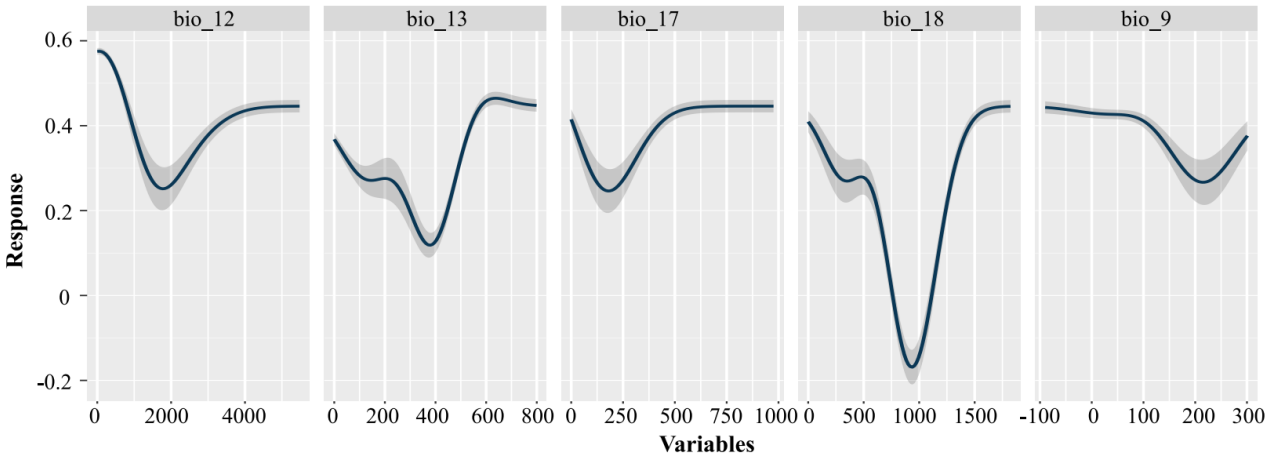

Figure S5 – Response curves of the distinct environmental dataset used in ecological niche modelling.

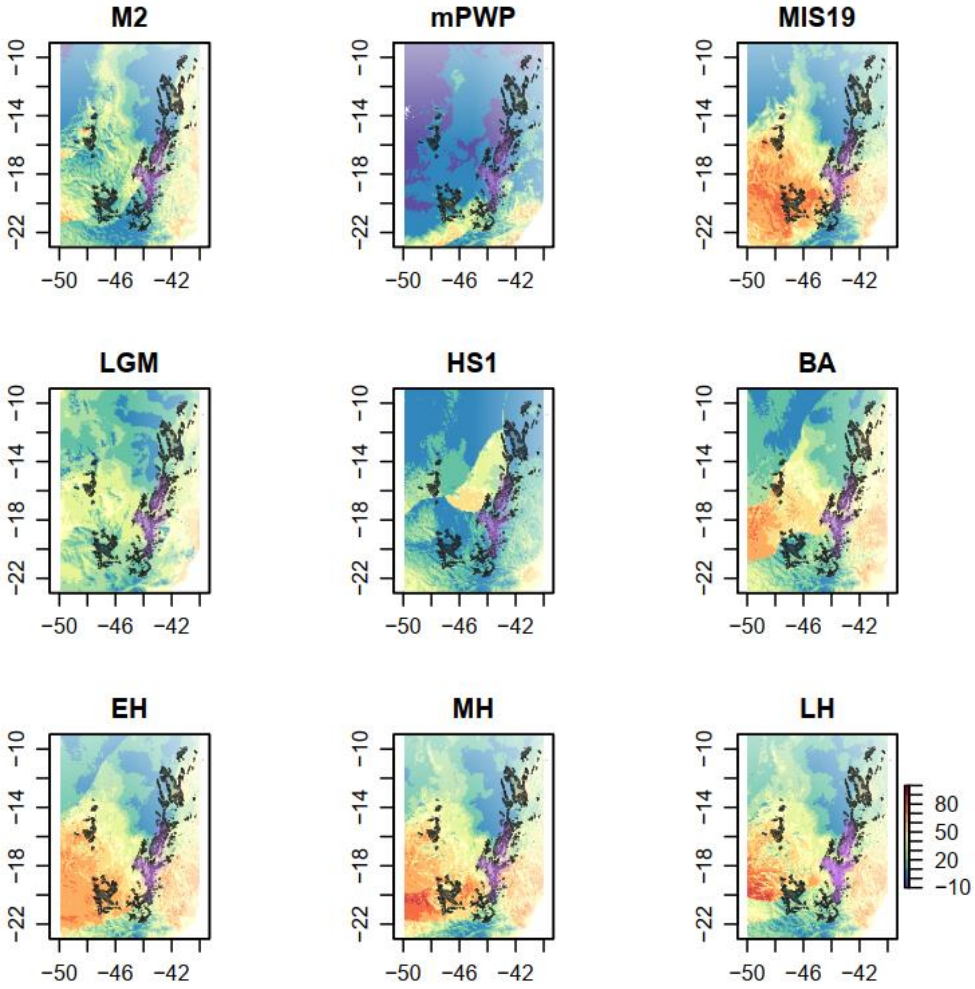

Figure S6 - Multivariate Environmental Similarity Surface (MESS) maps of past range generated using occurrence data. Positive MESS values correspond to sites in the projection of past range with similar climatic conditions in comparison to current areas, while negative MESS values (dark blue areas) indicate the degree of dissimilarity between past and current ranges. Purple dots on the MESS maps indicate the species occurrence from data training and black lines shape represents the limits of *campo rupestre*. The time slice abbreviations correspond to: M2 = Marine Isotope Stage in the late Pliocene, mPWP = mid-Pliocene Warm Period, MIS19 = Marine Isotope Stage in the Pleistocene, LIG = Last Interglacial past, LGM = Last Glacial Maximum, HS1 = Heinrich Event 1, BA = abrupt warming at the onset of the Bølling-Allerød, YD = rapid cooling at the onset of the Younger Dryas, EH = early-Holocene, MH = mid-Holocene, LH = late-Holocene.

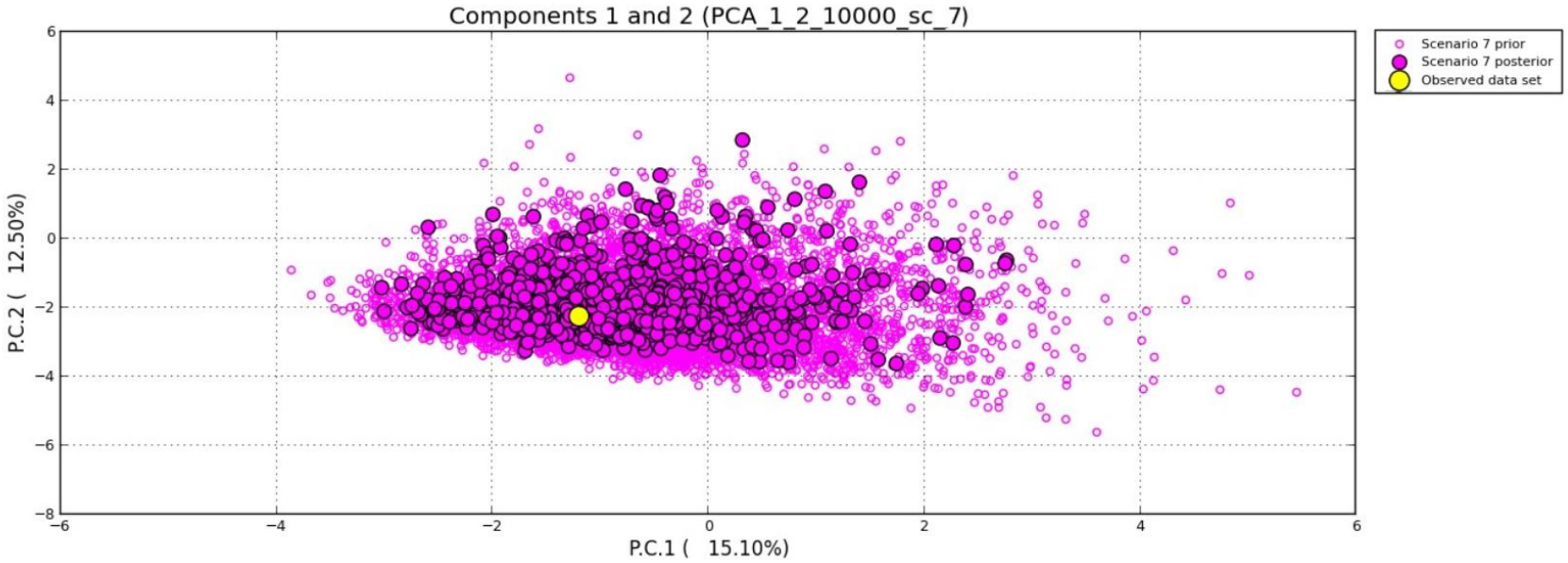

Figure S7 - PCA plot of model checking from DIYABC analysis. Each open pink circle represents a set of simulated data from the reference table (*prior*). The pink circles with a black border represent the data calculated *a posteriori*, and the yellow dot indicates the distribution of the observed data.

c) Supplementary tables

Table S1 Details for sampled individuals of *Bokermannohyla saxicola* used in the present study. For each sample is present lineage, voucher ID, haplotype in Figure S1 (GMYC), type of data, municipality in Minas Gerais Brazilian state, geographic coordinates, and Genbank accession numbers. UFMG = Centro de Coleções Taxonômicas da Universidade Federal de Minas Gerais; BS = code by Nascimento *et al.* 2018

Lineage		Voucher ID	mtDNA Haplotype (Hap: Figure S1)	Type of data			Municipally (Minas Gerais)
				Genetic			
This study	Nascimento et al. (2018) clade			mtDNA	nDNA	Morphometric	
Central	Itacambira	UFMG 15326	04	x	x	x	Grão Mogol
Central	Itacambira	UFMG 15299	04	x	x	x	Padre Carvalho
Central	Itacambira	UFMG 15398	05	x	x	x	Grão Mogol
Southern	Diamantina Plateau	UFMG 16343	03	x	x	x	Augusto de Lima
Southern	Diamantina Plateau	BS013	17	x	x		Congonhas do Norte
Southern	Diamantina Plateau	UFMG-G 547b	97	x	x		Alvorada de Minas
Southern	Diamantina Plateau	UFMG 12413	89	x	x		Conceição do Mato Dentro
Southern	Diamantina Plateau	UFMG 20438	41	x	x	x	Itamarandiba
Southern	Diamantina Plateau	UFMG 10888	63	x	x	x	Rio Vermelho
Southern	Diamantina Plateau	UFMG 11033	65	x	x	x	Rio Vermelho
Southern	Diamantina Plateau	UFMG 11037	62	x	x	x	Rio Vermelho
Southern	Diamantina Plateau	UFMG-T 419	94	x	x		Diamantina
Southern	Diamantina Plateau	BS012	16	x	x		São Gonçalo do Rio Preto
Southern	Diamantina Plateau	UFMG-T 105	90	x	x		Conceição do Mato Dentro
Southern	Cipó	BS014	18	x	x		Congonhas do Norte

Southern	Cipó	BS020	20	x	x		Congonhas do Norte
Southern	Cipó	UFMG-G 1646	69	x	x		Santana do Riacho
Southern	Cipó	BS016	12	x	x		Congonhas do Norte
Southern	Cipó	BS004	12	x	x		São Sebastião do Rio Preto
Southern	Cipó	UFMG 18965	100	x	x	x	Barão de Cocais
Southern	Cipó	BS007	11	x	x		Santana do Riacho
Southern	Cipó	BS001	09	x	x		São Sebastião do Rio Preto
Southern	Cipó	BS009	15	x	x		Santana do Riacho
Southern	Diamantina Plateau	UFMG 12342	60	x	x	x	Botumirim
Southern	Diamantina Plateau	UFMG 12345	57	x	x	x	Botumirim
Southern	Diamantina Plateau	BS023	21	x	x		Congonhas do Norte
Southern	Diamantina Plateau	UFMG 20439	42	x	x	x	Itamarandiba
Southern	Diamantina Plateau	BS015	19	x	x		Serro
Southern	Diamantina Plateau	UFMG 11111	73	x	x	x	Santana de Pirapama
Central	Itacambira	UFMG 11266	80	x	x		Itacambira
Central	Itacambira	UFMG 11276	83	x	x		Itacambira
Central	Itacambira	UFMG 11279	82	x	x		Itacambira
Central	Itacambira	UFMG 11274	77	x	x		Itacambira
Central	Itacambira	UFMG 11288	84	x	x		Itacambira
Cabral	Cabral	UFMG-G 1266a	1 specimen 5 specimens	99	x	x	x	Joaquim Felício
Cabral	Cabral	UFMG 16345	88	x	x	x	Francisco Dumont
Cabral	Cabral	UFMG-T 420	95	x	x		Buenópolis
Northern	Northern	UFMG 20490	39	x	x		Santo Antônio do Retiro
Northern	Northern	UFMG 20491	39	x	x		Santo Antônio do Retiro

Northern	Northern	UFMG-T 428	91	x	x		Serranópolis de Minas
Northern	Northern	UFMG-T 212	91	x	x		Rio Pardo de Minas
Northern	Northern	UFMG-T 215	92	x	x		Rio Pardo de Minas
Northern	Northern	UFMG-T 421	96	x	x		Serranópolis de Minas
Cabral	Cabral	UFMG 13953	06	x	x	x	Joaquim Felício
Cabral	Cabral	UFMG 13977	06	x	x	x	Joaquim Felício
Southern	Diamantina Plateau	UFMG 14333	07	x	x	x	Turmalina
Southern	Diamantina Plateau	UFMG 14337	08	x	x	x	Turmalina
Southern	Diamantina Plateau	UFMG 14367	07	x	x	x	Turmalina
Southern	Diamantina Plateau	UFMG 14386	08	x	x	x	Turmalina
Cabral	Cabral	UFMG 16342	02	x			Joaquim Felício
Southern	Cipó	BS002	10	x			Santana do Riacho
Southern	Cipó	BS003	11	x			Santana do Riacho
Southern	Cipó	BS005	13	x			Santana do Riacho
Southern	Cipó	BS006	13	x			Santana do Riacho
Southern	Cipó	BS008	14	x			Santana do Riacho
Southern	Diamantina Plateau	BS010	16	x			São Gonçalo do Rio Preto
Southern	Diamantina Plateau	BS011	16	x			São Gonçalo do Rio Preto
Southern	Cipó	BS019	18	x			Congonhas do Norte
Southern	Diamantina Plateau	BS021	17	x			Congonhas do Norte
Southern	Cipó	BS022	12	x			Congonhas do Norte
Southern	Cipó	BS024	12	x			Congonhas do Norte
Southern	Cipó	BS026	22	x			Santana do Riacho
Southern	Cipó	BS027	12	x			Santana do Riacho
Southern	Diamantina Plateau	BS031	23	x			Congonhas do Norte

Southern	Cipó	BS035	18	x		Congonhas do Norte
Southern	Cipó	BS039	18	x		Congonhas do Norte
Southern	Diamantina Plateau	BS041	24	x		Congonhas do Norte
Southern	Diamantina Plateau	BS044	25	x		Congonhas do Norte
Southern	Cipó	UFMG 20420	12	x	x	Congonhas do Norte
Southern	Cipó	UFMG 20422	26	x	x	Congonhas do Norte
Southern	Cipó	UFMG 20421	27	x	x	Congonhas do Norte
Southern	Cpó	UFMG 20417	18	x	x	Congonhas do Norte
Southern	Diamantina Plateau	UFMG 20418	17	x	x	Congonhas do Norte
Southern	Diamantina Plateau	BS070	28	x		São Gonçalo do Rio Preto
Southern	Diamantina Plateau	BS071	29	x		São Gonçalo do Rio Preto
Southern	Diamantina Plateau	BS073	29	x		São Gonçalo do Rio Preto
Southern	Diamantina Plateau	BS074	16	x		São Gonçalo do Rio Preto
Southern	Diamantina Plateau	BS075	29	x		São Gonçalo do Rio Preto
Southern	Diamantina Plateau	BS077	29	x		São Gonçalo do Rio Preto
Southern	Diamantina Plateau	BS078	30	x		São Gonçalo do Rio Preto
Southern	Diamantina Plateau	BS079	31	x		São Gonçalo do Rio Preto
Southern	Diamantina Plateau	BS080	32	x		São Gonçalo do Rio Preto
Southern	Diamantina Plateau	BS081	33	x		São Gonçalo do Rio Preto
Southern	Diamantina Plateau	BS083	29	x		São Gonçalo do Rio Preto
Southern	Diamantina Plateau	BS086	31	x		São Gonçalo do Rio Preto
Southern	Diamantina Plateau	UFMG 10404	29	x	x	São Gonçalo do Rio Preto
Southern	Diamantina Plateau	BS088	29	x		São Gonçalo do Rio Preto
Southern	Diamantina Plateau	BS091	29	x		São Gonçalo do Rio Preto
Southern	Diamantina Plateau	BS096	29	x		São Gonçalo do Rio Preto

Southern	Cipó	UFMG 20427	13	x	x	Congonhas do Norte
Southern	Cipó	BS104	22	x		Santana do Riacho
Southern	Diamantina Plateau	BS105	30	x		São Gonçalo do Rio Preto
Southern	Diamantina Plateau	BS106	30	x		São Gonçalo do Rio Preto
Southern	Diamantina Plateau	BS107	29	x		São Gonçalo do Rio Preto
Southern	Diamantina Plateau	BS108	29	x		São Gonçalo do Rio Preto
Southern	Diamantina Plateau	BS109	29	x		São Gonçalo do Rio Preto
Southern	Diamantina Plateau	BS110	34	x		São Gonçalo do Rio Preto
Southern	Diamantina Plateau	BS111	35	x		São Gonçalo do Rio Preto
Southern	Diamantina Plateau	BS112	29	x		São Gonçalo do Rio Preto
Southern	Diamantina Plateau	BS113	36	x		São Gonçalo do Rio Preto
Southern	Diamantina Plateau	BS114	32	x		São Gonçalo do Rio Preto
Southern	Diamantina Plateau	BS116	37	x		São Gonçalo do Rio Preto
Southern	Diamantina Plateau	BS117	29	x		São Gonçalo do Rio Preto
Southern	Diamantina Plateau	BS118	29	x		São Gonçalo do Rio Preto
Southern	Diamantina Plateau	BS119	38	x		São Gonçalo do Rio Preto
Northern	Northern	UFMG 20481	39	x		Santo Antônio do Retiro
Northern	Northern	UFMG 20483	39	x		Santo Antônio do Retiro
Northern	Northern	UFMG 20485	39	x		Santo Antônio do Retiro
Northern	Northern	UFMG 20488	39	x		Santo Antônio do Retiro
Northern	Northern	UFMG 20591	39	x		Santo Antônio do Retiro
Southern	Diamantina Plateau	UFMG 20431	40	x	x	Itamarandiba
Southern	Diamantina Plateau	UFMG 20432	40	x	x	Itamarandiba
Southern	Diamantina Plateau	UFMG 20435	40	x	x	Itamarandiba
Southern	Diamantina Plateau	UFMG 20436	40	x	x	Itamarandiba

Southern	Diamantina Plateau	UFMG 20437	40	x	x	Itamarandiba
Southern	Diamantina Plateau	UFMG 20440	43	x	x	Itamarandiba
Southern	Diamantina Plateau	UFMG 20442	44	x	x	Itamarandiba
Southern	Diamantina Plateau	UFMG 20445	45	x	x	Itamarandiba
Southern	Diamantina Plateau	UFMG 20446	46	x	x	Itamarandiba
Southern	Diamantina Plateau	UFMG 20447	40	x	x	Itamarandiba
Southern	Diamantina Plateau	UFMG 20448	40	x	x	Itamarandiba
Southern	Diamantina Plateau	UFMG 20449	40	x	x	Itamarandiba
Southern	Diamantina Plateau	UFMG 20450	47	x	x	Itamarandiba
Southern	Diamantina Plateau	UFMG 20451	40	x	x	Itamarandiba
Southern	Diamantina Plateau	UFMG 20452	48	x	x	Itamarandiba
Southern	Diamantina Plateau	UFMG 20454	49	x	x	Itamarandiba
Southern	Diamantina Plateau	UFMG 20455	50	x	x	Itamarandiba
Southern	Diamantina Plateau	UFMG 20456	40	x	x	Itamarandiba
Southern	Diamantina Plateau	UFMG 20457	40	x	x	Itamarandiba
Southern	Diamantina Plateau	UFMG 20458	48	x	x	Itamarandiba
Southern	Diamantina Plateau	UFMG 20459	51	x	x	Itamarandiba
Southern	Cipó	UFMG 11051	52	x	x	Santana do Riacho
Southern	Diamantina Plateau	UFMG 11052	53	x	x	Santana do Riacho
Southern	Cipó	UFMG 11053	13	x	x	Santana do Riacho
Southern	Diamantina Plateau	UFMG 12224	54	x	x	Botumirim
Southern	Diamantina Plateau	UFMG 12269	55	x	x	Botumirim
Southern	Diamantina Plateau	UFMG 12272	29	x	x	Botumirim
Southern	Diamantina Plateau	UFMG 12277	56	x		Botumirim
Southern	Diamantina Plateau	UFMG 12284	55	x	x	Botumirim

Southern	Diamantina Plateau	UFMG 12294	57	x	x	Botumirim
Southern	Diamantina Plateau	UFMG 12296	58	x	x	Botumirim
Southern	Diamantina Plateau	UFMG 12326	59	x	x	Botumirim
Southern	Diamantina Plateau	UFMG 12337	57	x	x	Botumirim
Southern	Diamantina Plateau	UFMG 12339	57	x	x	Botumirim
Southern	Diamantina Plateau	UFMG 12341	59	x	x	Botumirim
Southern	Diamantina Plateau	UFMG 12343	54	x	x	Botumirim
Southern	Diamantina Plateau	UFMG 12344	54	x	x	Botumirim
Southern	Diamantina Plateau	UFMG 12346	54	x	x	Botumirim
Southern	Diamantina Plateau	UFMG 12349	61	x	x	Botumirim
Southern	Diamantina Plateau	UFMG 12350	54	x	x	Botumirim
Southern	Diamantina Plateau	UFMG 12354	29	x	x	Botumirim
Southern	Diamantina Plateau	UFMG 10858	62	x	x	Rio Vermelho
Southern	Diamantina Plateau	UFMG 10876	63	x	x	Rio Vermelho
Southern	Diamantina Plateau	UFMG 10891	62	x	x	Rio Vermelho
Southern	Diamantina Plateau	UFMG 10905	63	x	x	Rio Vermelho
Southern	Diamantina Plateau	UFMG 10914	62	x		Rio Vermelho
Southern	Diamantina Plateau	UFMG 11002	63	x	x	Rio Vermelho
Southern	Diamantina Plateau	UFMG 11004	63	x	x	Rio Vermelho
Southern	Diamantina Plateau	UFMG 11006	63	x	x	Rio Vermelho
Southern	Diamantina Plateau	UFMG 11010	62	x	x	Rio Vermelho
Southern	Diamantina Plateau	UFMG 11013	64	x		Rio Vermelho
Southern	Diamantina Plateau	UFMG 11020	62	x	x	Rio Vermelho
Southern	Diamantina Plateau	UFMG 11022	63	x	x	Rio Vermelho
Southern	Diamantina Plateau	UFMG 11026	62	x	x	Rio Vermelho

Southern	Diamantina Plateau	UFMG 11029	63	x	x	Rio Vermelho
Southern	Diamantina Plateau	UFMG 11035	66	x	x	Rio Vermelho
Southern	Diamantina Plateau	UFMG 11039	63	x	x	Rio Vermelho
Southern	Diamantina Plateau	UFMG 11042	62	x	x	Rio Vermelho
Southern	Cipó	UFMG-G 1649	18	x		Santana do Riacho
Southern	Cipó	UFMG-G 1650	67	x		Santana do Riacho
Southern	Cipó	UFMG-G 1647	18	x		Santana do Riacho
Southern	Cipó	UFMG-G 1633	52	x		Santana do Riacho
Southern	Diamantina Plateau	UFMG-G 1635	53	x		Santana do Riacho
Southern	Cipó	UFMG-G 1634	10	x		Santana do Riacho
Southern	Cipó	UFMG-G 1643	18	x		Santana do Riacho
Southern	Cipó	UFMG-G 1645	68	x		Santana do Riacho
Southern	Diamantina Plateau	UFMG-G 1597	70	x		Santana do Riacho
Southern	Cipó	UFMG-G 1598 1 specimen 1 specimen	71	x	x	Santana do Riacho
Southern	Cipó	UFMG-G 1599	72	x		Santana do Riacho
Southern	Cipó	UFMG-G 1600	13	x		Santana do Riacho
Southern	Diamantina Plateau	UFMG 11110	17	x	x	Santana de Pirapama
Southern	Diamantina Plateau	UFMG 11112	74	x	x	Santana de Pirapama
Southern	Diamantina Plateau	UFMG 11113	75	x		Santana de Pirapama
Central	Itacambira	UFMG 11261	76	x		Itacambira
Central	Itacambira	UFMG 11262	77	x		Itacambira
Central	Itacambira	UFMG 11263	78	x		Itacambira
Central	Itacambira	UFMG 11265	79	x		Itacambira
Central	Itacambira	UFMG 11267	81	x		Itacambira

Central	Itacambira	UFMG 11271	77	x		Itacambira
Central	Itacambira	UFMG 11275	82	x		Itacambira
Central	Itacambira	UFMG 11277	82	x		Itacambira
Central	Itacambira	UFMG 11289	83	x		Itacambira
Central	Itacambira	UFMG 11291	82	x		Itacambira
Central	Itacambira	UFMG 11294	85	x		Itacambira
Central	Itacambira	UFMG 11296	86	x		Itacambira
Central	Itacambira	UFMG 11316	87	x		Itacambira
Central	Itacambira	UFMG 11320	77	x		Itacambira
Central	Itacambira	UFMG 11346	78	x		Itacambira
Southern	Diamantina Plateau	UFMG 16344	3	x		Augusto de Lima
Southern	Cipó	UFMG 10308	9	x		Santana do Riacho
Northern	Northern	UFMG-T 179	91	x		Rio Pardo de Minas
Northern	Northern	UFMG-T 213	92	x		Rio Pardo de Minas
Northern	Northern	UFMG-T 214	93	x		Rio Pardo de Minas
Northern	Northern	UFMG-T 216	91	x		Rio Pardo de Minas
Northern	Northern	UFMG-T 423	92	x		Serranópolis de Minas
Southern	Diamantina Plateau	UFMG-T 70	97	x		Congonhas do Norte
Southern	Cipó	UFMG 6672	26	x	x	Congonhas do Norte
Southern	Diamantina Plateau	UFMG 6673	98	x		Congonhas do Norte
Southern	Cipó	UFMG 6674	26	x	x	Congonhas do Norte
Southern	Diamantina Plateau	UFMG 6675	98	x	x	Congonhas do Norte
Southern	Cipó	UFMG 6677	12	x	x	Congonhas do Norte
Cabral	Cabral	UFMG-G 1266b	1 specimen 1 specimen	99	x	x	Joaquim Felício

Southern	Cipó	UFMG 18963	13	x	x	Barão de Cocais
Southern	Cipó	UFMG 18964	13	x	x	Barão de Cocais
Southern	Cipó	UFMG 18966	13	x	x	Barão de Cocais
Southern	Cipó	UFMG 18967	101	x	x	Barão de Cocais
Southern	Cipó	UFMG 18968	13	x	x	Barão de Cocais
Southern	Cipó	UFMG 18969	13	x	x	Barão de Cocais
Cabral	Cabral	UFMG 18962	2	x	x	Joaquim Felício
Southern	Cipó	UFMG-G 1136a	13	x		Barão de Cocais
Southern	Cipó	UFMG-G 1136b	100	x		Barão de Cocais
Southern	Cipó	UFMG-G 1136c	100	x		Barão de Cocais
Northern	NA	UFMG 17291			x	Rio Pardo de Minas
Northern	NA	UFMG 17305			x	Rio Pardo de Minas
Northern	NA	UFMG 17293			x	Rio Pardo de Minas
Northern	NA	UFMG 17301			x	Rio Pardo de Minas
Northern	NA	UFMG 17306			x	Rio Pardo de Minas
Northern	NA	UFMG 17303			x	Rio Pardo de Minas
Northern	NA	UFMG 17308			x	Rio Pardo de Minas
Northern	NA	UFMG 17294			x	Rio Pardo de Minas
Northern	NA	UFMG 17304			x	Rio Pardo de Minas
Northern	NA	UFMG 17283			x	Rio Pardo de Minas
Northern	NA	UFMG 17295			x	Rio Pardo de Minas
Northern	NA	UFMG 17307			x	Rio Pardo de Minas
Northern	NA	UFMG 17300			x	Rio Pardo de Minas
Northern	NA	UFMG 17299			x	Rio Pardo de Minas
Northern	NA	UFMG 17290			x	Rio Pardo de Minas

Northern	NA	UFMG 17287	x	Rio Pardo de Minas
Northern	NA	UFMG 17296	x	Rio Pardo de Minas
Northern	NA	UFMG 17302	x	Rio Pardo de Minas
Northern	NA	UFMG 17286	x	Rio Pardo de Minas
Northern	NA	UFMG 17289	x	Rio Pardo de Minas
Northern	NA	UFMG 17297	x	Rio Pardo de Minas
Northern	NA	UFMG 17292	x	Rio Pardo de Minas
Northern	NA	UFMG 17288	x	Rio Pardo de Minas
Northern	NA	UFMG 17284	x	Rio Pardo de Minas
Northern	NA	UFMG 17298	x	Rio Pardo de Minas
Northern	NA	UFMG 17285	x	Rio Pardo de Minas
Cabral	NA	UFMG 13974	x	Joaquim Felício
Cabral	NA	UFMG 7679	x	Joaquim Felício
Cabral	NA	UFMG 20644	x	Buenópolis
Cabral	NA	UFMG 13962	x	Buenópolis
Cabral	NA	UFMG 13965	x	Buenópolis
Cabral	NA	UFMG 13408	x	Augusto de Lima
Cabral	NA	UFMG 13979	x	Joaquim Felício
Cabral	NA	UFMG 13972	x	Joaquim Felício
Cabral	NA	UFMG 7682	x	Joaquim Felício
Cabral	NA	UFMG 18958	x	Joaquim Felício
Cabral	NA	UFMG 7678	x	Joaquim Felício
Cabral	NA	UFMG 7675	x	Joaquim Felício
Cabral	NA	UFMG 13964	x	Buenópolis
Cabral	NA	UFMG 13954	x	Joaquim Felício

Cabral	NA	UFMG 7676	x	Joaquim Felício
Cabral	NA	UFMG 13409	x	Augusto de Lima
Cabral	NA	UFMG 7680	x	Joaquim Felício
Cabral	NA	UFMG 13971	x	Joaquim Felício
Cabral	NA	UFMG 7683	x	Joaquim Felício
Cabral	NA	UFMG 7681	x	Joaquim Felício
Cabral	NA	UFMG 13963	x	Buenópolis
Cabral	NA	UFMG 7684	x	Joaquim Felício
Cabral	NA	UFMG 18959	x	Joaquim Felício
Cabral	NA	UFMG 13414	x	Joaquim Felício
Cabral	NA	UFMG 13976	x	Augusto de Lima
Cabral	NA	UFMG 13411	x	Joaquim Felício
Cabral	NA	UFMG 18961	x	Buenópolis
Cabral	NA	UFMG 13975	x	Buenópolis
Cabral	NA	UFMG 7673	x	Joaquim Felício
Cabral	NA	UFMG 13952	x	Joaquim Felício
Cabral	NA	UFMG 18960	x	Joaquim Felício
Cabral	NA	UFMG 13951	x	Joaquim Felício
Cabral	NA	UFMG 13970	x	Buenópolis
Cabral	NA	UFMG 13967	x	Buenópolis
Cabral	NA	UFMG 18957	x	Joaquim Felício
Cabral	NA	UFMG 13973	x	Joaquim Felício
Cabral	NA	UFMG 13980	x	Joaquim Felício
Cabral	NA	UFMG 7677	x	Joaquim Felício
Cabral	NA	UFMG 20643	x	Buenópolis

Cabral	NA	UFMG 13968	x	Buenópolis
Cabral	NA	UFMG 13966	x	Buenópolis
Cabral	NA	UFMG 13403	x	Augusto de Lima
Cabral	NA	UFMG 13978	x	Joaquim Felício
Cabral	NA	UFMG 13969	x	Buenópolis
Cabral	NA	UFMG 20902	x	Lassance
Cabral	NA	UFMG 21445	x	Augusto de Lima
Central	NA	UFMG 15319	x	Grão Mogol
Central	NA	UFMG 15370	x	Grão Mogol
Central	NA	UFMG 18754	x	Grão Mogol
Central	NA	UFMG 15330	x	Grão Mogol
Central	NA	UFMG 15316	x	Grão Mogol
Central	NA	UFMG 15329	x	Grão Mogol
Central	NA	UFMG 18755	x	Grão Mogol
Central	NA	UFMG 18752	x	Grão Mogol
Central	NA	UFMG 15318	x	Grão Mogol
Central	NA	UFMG 15327	x	Grão Mogol
Central	NA	UFMG 15275	x	Grão Mogol
Central	NA	UFMG 18753	x	Grão Mogol
Central	NA	UFMG 15282	x	Grão Mogol
Central	NA	UFMG 15399	x	Grão Mogol
Central	NA	UFMG 15298	x	Grão Mogol
Central	NA	UFMG 15281	x	Grão Mogol
Central	NA	UFMG 15284	x	Grão Mogol
Central	NA	UFMG 15328	x	Grão Mogol

Central	NA	UFMG 20531	x	Grão Mogol
Central	NA	UFMG 20517	x	Grão Mogol
Central	NA	UFMG 20511	x	Grão Mogol
Central	NA	UFMG 20523	x	Grão Mogol
Central	NA	UFMG 20518	x	Grão Mogol
Central	NA	UFMG 20613	x	Grão Mogol
Central	NA	UFMG 20519	x	Grão Mogol
Central	NA	UFMG 20522	x	Grão Mogol
Central	NA	UFMG 20525	x	Grão Mogol
Central	NA	UFMG 20524	x	Grão Mogol
Central	NA	UFMG 20527	x	Grão Mogol
Central	NA	UFMG 20512	x	Grão Mogol
Central	NA	UFMG 20514	x	Grão Mogol
Central	NA	UFMG 20520	x	Grão Mogol
Central	NA	UFMG 20528	x	Grão Mogol
Central	NA	UFMG 20515	x	Grão Mogol
Central	NA	UFMG 20530	x	Grão Mogol
Central	NA	UFMG 20513	x	Grão Mogol
Central	NA	UFMG 20521	x	Grão Mogol
Central	NA	UFMG 20529	x	Grão Mogol
Central	NA	UFMG 20526	x	Grão Mogol
Central	NA	UFMG 20516	x	Grão Mogol
Southern	NA	UFMG 8636	x	Morro do Pilar
Southern	NA	UFMG 14912	x	Morro do Pilar
Southern	NA	UFMG 817	x	Jaboticatubas

Southern	NA	UFMG 8861	x	Morro do Pilar
Southern	NA	UFMG 14388	x	Morro do Pilar
Southern	NA	UFMG 816	x	Jaboticatubas
Southern	NA	UFMG 9044	x	Jaboticatubas
Southern	NA	UFMG 813	x	Jaboticatubas
Southern	NA	UFMG 19837	x	Santana do Riacho
Southern	NA	UFMG 19560	x	Santa Barbara
Southern	NA	UFMG 19556	x	Santa Barbara
Southern	NA	UFMG 14911	x	Morro do Pilar
Southern	NA	UFMG 19558	x	Santa Barbara
Southern	NA	UFMG 19555	x	Santa Barbara
Southern	NA	UFMG 7011	x	Morro do Pilar
Southern	NA	UFMG 830	x	Santana do Riacho
Southern	NA	UFMG 8808	x	Morro do Pilar
Southern	NA	UFMG 14913	x	Morro do Pilar
Southern	NA	UFMG 814	x	Jaboticatubas
Southern	NA	UFMG 19559	x	Santa Barbara
Southern	NA	UFMG 19566	x	Itabirito
Southern	NA	UFMG 19561	x	Santa Barbara
Southern	NA	UFMG 19553	x	Santa Barbara
Southern	NA	UFMG 19564	x	Santa Barbara
Southern	NA	UFMG 19554	x	Santa Barbara
Southern	NA	UFMG 19563	x	Santa Barbara
Southern	NA	UFMG 19552	x	Santa Barbara
Southern	NA	UFMG 19565	x	Itabirito

Southern	NA	UFMG 19557	x	Santa Barbara
Southern	NA	UFMG 19562	x	Santa Barbara
Southern	NA	UFMG 10399	x	São Gonçalo do Rio Preto
Southern	NA	UFMG 10396	x	São Gonçalo do Rio Preto
Southern	NA	UFMG 10394	x	São Gonçalo do Rio Preto
Southern	NA	UFMG 10393	x	São Gonçalo do Rio Preto
Southern	NA	UFMG 10403	x	São Gonçalo do Rio Preto
Southern	NA	UFMG 10398	x	São Gonçalo do Rio Preto
Southern	NA	UFMG 10397	x	São Gonçalo do Rio Preto
Southern	NA	UFMG 10400	x	São Gonçalo do Rio Preto
Southern	NA	UFMG 10401	x	São Gonçalo do Rio Preto
Southern	NA	UFMG 10390	x	São Gonçalo do Rio Preto
Southern	NA	UFMG 10392	x	São Gonçalo do Rio Preto
Southern	NA	UFMG 10391	x	São Gonçalo do Rio Preto
Southern	NA	UFMG 10389	x	São Gonçalo do Rio Preto
Southern	NA	UFMG 10395	x	São Gonçalo do Rio Preto
Southern	NA	UFMG 10402	x	São Gonçalo do Rio Preto
Southern	NA	UFMG 828	x	Santana do Riacho
Southern	NA	UFMG 3471	x	Santana do Riacho
Southern	NA	UFMG 818	x	Santana do Riacho
Southern	NA	UFMG 5835	x	Santana do Riacho
Southern	NA	UFMG 831	x	Santana do Riacho
Southern	NA	UFMG 20359	x	Santana do Riacho
Southern	NA	UFMG 14296	x	Turmalina
Southern	NA	UFMG 14366	x	Turmalina

Southern	NA	UFMG 14301	x	Turmalina
Southern	NA	UFMG 14298	x	Turmalina
Southern	NA	UFMG 14365	x	Turmalina
Southern	NA	UFMG 14307	x	Turmalina
Southern	NA	UFMG 14295	x	Turmalina
Southern	NA	UFMG 14336	x	Turmalina
Southern	NA	UFMG 14368	x	Turmalina
Southern	NA	UFMG 14303	x	Turmalina
Southern	NA	UFMG 14369	x	Turmalina
Southern	NA	UFMG 14385	x	Turmalina
Southern	NA	UFMG 14302	x	Turmalina
Southern	NA	UFMG 14300	x	Turmalina
Southern	NA	UFMG 14338	x	Turmalina
Southern	NA	UFMG 14308	x	Turmalina
Southern	NA	UFMG 14370	x	Turmalina
Southern	NA	UFMG 14305	x	Turmalina
Southern	NA	UFMG 14299	x	Turmalina
Southern	NA	UFMG 14294	x	Turmalina
Southern	NA	UFMG 14304	x	Turmalina
Southern	NA	UFMG 14306	x	Turmalina
Southern	NA	UFMG 14297	x	Turmalina
Southern	NA	UFMG 20597	x	Barão de Cocais
Southern	NA	UFMG 20612	x	Barão de Cocais
Southern	NA	UFMG 14943	x	Barão de Cocais
Southern	NA	UFMG 14933	x	Barão de Cocais

Southern	NA	UFMG 14956	x	Barão de Cocais
Southern	NA	UFMG 14944	x	Barão de Cocais
Southern	NA	UFMG 20598	x	Barão de Cocais
Southern	NA	UFMG 20606	x	Barão de Cocais
Southern	NA	UFMG 20616	x	Barão de Cocais
Southern	NA	UFMG 19238	x	Barão de Cocais
Southern	NA	UFMG 20617	x	Barão de Cocais
Southern	NA	UFMG 20595	x	Barão de Cocais
Southern	NA	UFMG 20594	x	Barão de Cocais
Southern	NA	UFMG 20607	x	Barão de Cocais
Southern	NA	UFMG 20604	x	Barão de Cocais
Southern	NA	UFMG 20615	x	Barão de Cocais
Southern	NA	UFMG 20603	x	Barão de Cocais
Southern	NA	UFMG 20600	x	Barão de Cocais
Southern	NA	UFMG 20601	x	Barão de Cocais
Southern	NA	UFMG 20610	x	Barão de Cocais
Southern	NA	UFMG 20605	x	Barão de Cocais
Southern	NA	UFMG 20596	x	Barão de Cocais
Southern	NA	UFMG 6655	x	Barão de Cocais
Southern	NA	UFMG 20611	x	Barão de Cocais
Southern	NA	UFMG 20593	x	Barão de Cocais
Southern	NA	UFMG 14930	x	Barão de Cocais
Southern	NA	UFMG 20608	x	Barão de Cocais
Southern	NA	UFMG 20618	x	Barão de Cocais
Southern	NA	UFMG 20602	x	Barão de Cocais

Southern	NA	UFMG 20609	x	Barão de Cocais
Southern	NA	UFMG 14932	x	Barão de Cocais
Southern	NA	UFMG 14946	x	Barão de Cocais
Southern	NA	UFMG 14931	x	Barão de Cocais
Southern	NA	UFMG 20592	x	Barão de Cocais
Southern	NA	UFMG 14945	x	Barão de Cocais
Southern	NA	UFMG 20599	x	Barão de Cocais
Southern	NA	UFMG 20614	x	Barão de Cocais
Southern	NA	UFMG 14793	x	Santo Antônio do Itambé
Southern	NA	UFMG 14055	x	Serro
Southern	NA	UFMG 14837	x	Santo Antônio do Itambé
Southern	NA	UFMG 16049	x	Serra Azul de Minas
Southern	NA	UFMG 14284	x	Serra Azul de Minas
Southern	NA	UFMG 14285	x	Serra Azul de Minas
Southern	NA	UFMG 14783	x	Santo Antônio do Itambé
Southern	NA	UFMG 14835	x	Santo Antônio do Itambé
Southern	NA	UFMG 14826	x	Serro
Southern	NA	UFMG 14738	x	Santo Antônio do Itambé
Southern	NA	UFMG 14729	x	Santo Antônio do Itambé
Southern	NA	UFMG 14842	x	Santo Antônio do Itambé
Southern	NA	UFMG 16075	x	Santo Antônio do Itambé
Southern	NA	UFMG 14759	x	Santo Antônio do Itambé
Southern	NA	UFMG 14781	x	Santo Antônio do Itambé
Southern	NA	UFMG 14784	x	Santo Antônio do Itambé
Southern	NA	UFMG 14838	x	Santo Antônio do Itambé

Southern	NA	UFMG 16050	x	Santo Antônio do Itambé
Southern	NA	UFMG 14052	x	Serro
Southern	NA	UFMG 14081	x	Serro
Southern	NA	UFMG 14836	x	Santo Antônio do Itambé
Southern	NA	UFMG 16121	x	Santo Antônio do Itambé
Southern	NA	UFMG 14839	x	Santo Antônio do Itambé
Southern	NA	UFMG 14782	x	Santo Antônio do Itambé
Southern	NA	UFMG 14847	x	Santo Antônio do Itambé
Southern	NA	UFMG 14843	x	Santo Antônio do Itambé
Southern	NA	UFMG 14240	x	Serra Azul de Minas
Southern	NA	UFMG 14841	x	Santo Antônio do Itambé
Southern	NA	UFMG 14780	x	Santo Antônio do Itambé
Southern	NA	UFMG 14730	x	Santo Antônio do Itambé
Southern	NA	UFMG 14732	x	Santo Antônio do Itambé
Southern	NA	UFMG 14731	x	Santo Antônio do Itambé
Southern	NA	UFMG 14825	x	Serro
Southern	NA	UFMG 14733	x	Santo Antônio do Itambé
Southern	NA	UFMG 14792	x	Santo Antônio do Itambé
Southern	NA	UFMG 14840	x	Santo Antônio do Itambé
Southern	NA	UFMG 11038	x	Rio Vermelho
Southern	NA	UFMG 11030	x	Rio Vermelho
Southern	NA	UFMG 11009	x	Rio Vermelho
Southern	NA	UFMG 11024	x	Rio Vermelho
Southern	NA	UFMG 11025	x	Rio Vermelho
Southern	NA	UFMG 11018	x	Rio Vermelho

Southern	NA	UFMG 11021	x	Rio Vermelho
Southern	NA	UFMG 11040	x	Rio Vermelho
Southern	NA	UFMG 11041	x	Rio Vermelho
Southern	NA	UFMG 11034	x	Rio Vermelho
Southern	NA	UFMG 11036	x	Rio Vermelho
Southern	NA	UFMG 11023	x	Rio Vermelho
Southern	NA	UFMG 10890	x	Rio Vermelho
Southern	NA	UFMG 11031	x	Rio Vermelho
Southern	NA	UFMG 11019	x	Rio Vermelho
Southern	NA	UFMG 11028	x	Rio Vermelho
Southern	NA	UFMG 11027	x	Rio Vermelho
Southern	NA	UFMG 11001	x	Rio Vermelho
Southern	NA	UFMG 11043	x	Rio Vermelho
Southern	NA	UFMG 11032	x	Rio Vermelho
Southern	NA	UFMG 10889	x	Rio Vermelho
Southern	NA	UFMG 11007	x	Rio Vermelho
Southern	NA	UFMG 11005	x	Rio Vermelho
Southern	NA	UFMG 11003	x	Rio Vermelho
Southern	NA	UFMG 12287	x	Botumirim
Southern	NA	UFMG 12295	x	Botumirim
Southern	NA	UFMG 3801	x	Botumirim
Southern	NA	UFMG 12298	x	Botumirim
Southern	NA	UFMG 12286	x	Botumirim
Southern	NA	UFMG 12268	x	Botumirim
Southern	NA	UFMG 12265	x	Botumirim

Southern	NA	UFMG 3800	x	Botumirim
Southern	NA	UFMG 12270	x	Botumirim
Southern	NA	UFMG 12378	x	Botumirim
Southern	NA	UFMG 12283	x	Botumirim
Southern	NA	UFMG 12299	x	Botumirim
Southern	NA	UFMG 12377	x	Botumirim
Southern	NA	UFMG 12292	x	Botumirim
Southern	NA	UFMG 12340	x	Botumirim
Southern	NA	UFMG 12297	x	Botumirim
Southern	NA	UFMG 12285	x	Botumirim
Southern	NA	UFMG 12327	x	Botumirim
Southern	NA	UFMG 12328	x	Botumirim
Southern	NA	UFMG 12293	x	Botumirim
Southern	NA	UFMG 12329	x	Botumirim
Southern	NA	UFMG 12291	x	Botumirim
Southern	NA	UFMG 12271	x	Botumirim
Southern	NA	UFMG 3795	x	Botumirim
Southern	NA	UFMG 20462	x	Itamarandiba
Southern	NA	UFMG 20467	x	Itamarandiba
Southern	NA	UFMG 20465	x	Itamarandiba
Southern	NA	UFMG 20477	x	Itamarandiba
Southern	NA	UFMG 20416	x	Congonhas do Norte
Southern	NA	UFMG 20470	x	Itamarandiba
Southern	NA	UFMG 20475	x	Itamarandiba
Southern	NA	UFMG 20464	x	Itamarandiba

Southern	NA	UFMG 20469	x	Itamarandiba
Southern	NA	UFMG 20419	x	Congonhas do Norte
Southern	NA	UFMG 20441	x	Itamarandiba
Southern	NA	UFMG 20430	x	Itamarandiba
Southern	NA	UFMG 20472	x	Itamarandiba
Southern	NA	UFMG 20468	x	Itamarandiba
Southern	NA	UFMG 20428	x	Congonhas do Norte
Southern	NA	UFMG 20423	x	Congonhas do Norte
Southern	NA	UFMG 20463	x	Itamarandiba
Southern	NA	UFMG 20453	x	Itamarandiba
Southern	NA	UFMG 20461	x	Itamarandiba
Southern	NA	UFMG 6678	x	Congonhas do Norte
Southern	NA	UFMG 20443	x	Itamarandiba
Southern	NA	UFMG 20460	x	Itamarandiba
Southern	NA	UFMG 20471	x	Itamarandiba
Southern	NA	UFMG 20476	x	Itamarandiba
Southern	NA	UFMG 20415	x	Congonhas do Norte
Southern	NA	UFMG 20429	x	Congonhas do Norte
Southern	NA	UFMG 20425	x	Congonhas do Norte
Southern	NA	UFMG 20466	x	Itamarandiba
Southern	NA	UFMG 6676	x	Congonhas do Norte
Southern	NA	UFMG 20433	x	Itamarandiba
Southern	NA	UFMG 20474	x	Itamarandiba
Southern	NA	UFMG 20426	x	Congonhas do Norte
Southern	NA	UFMG 20444	x	Itamarandiba

Southern	NA	UFMG 20434	x	Itamarandiba
Southern	NA	UFMG 20473	x	Itamarandiba
Southern	NA	UFMG 20424	x	Congonhas do Norte
Southern	NA	UFMG 11444	x	Buenópolis
Southern	NA	UFMG 9435	x	Santana de Pirapama
Southern	NA	UFMG 20254	x	Santana do Riacho
Southern	NA	UFMG 19234	x	Serro
Southern	NA	UFMG 829	x	Serro
Southern	NA	UFMG 20235	x	Santana do Riacho
Southern	NA	UFMG 12537	x	Serro
Southern	NA	UFMG 6679	x	Congonhas do Norte
Southern	NA	UFMG 9434	x	Santana de Pirapama
Southern	NA	UFMG 17590	x	Diamantina
Southern	NA	UFMG 19195	x	Serro
Southern	NA	UFMG 12542	x	Diamantina
Southern	NA	UFMG 841	x	Diamantina
Southern	NA	UFMG 12533	x	Serro
Southern	NA	UFMG 10629	x	Barão de Cocais
Southern	NA	UFMG 20255	x	Santana do Riacho
Southern	NA	UFMG 16344	x	Augusto de Lima
Southern	NA	UFMG 9436	x	Santana de Pirapama
Southern	NA	UFMG 20242	x	Santana do Riacho
Southern	NA	UFMG 6670	x	Alvorada de Minas
Southern	NA	UFMG 19207	x	Serro
Southern	NA	UFMG 19838	x	Santana do Riacho

Southern	NA	UFMG 20236		x	Santana do Riacho
Southern	NA	UFMG 19211		x	Serro
Southern	NA	UFMG 19205		x	Serro
Southern	NA	UFMG 20256		x	Santana do Riacho
Southern	NA	UFMG 840		x	Presidente Kubitchek
Southern	NA	UFMG 9438		x	Santana de Pirapama
Southern	NA	UFMG 9437		x	Santana de Pirapama
Southern	NA	UFMG 17583		x	Diamantina
Southern	NA	UFMG 12559		x	Serro
Northern	NA	UFMG-G 415	1 specimen	x	Serranópolis de Minas
Northern	NA	UFMG-G 423	1 specimen	x	Serranópolis de Minas
Northern	NA	UFMG-G 530	1 specimen	x	Rio Pardo de Minas
Northern	NA	UFMG-G 530a	4 specimens	x	Rio Pardo de Minas
Northern	NA	UFMG-G 530b	1 specimen	x	Rio Pardo de Minas
Central	NA	UFMG-G 1585	1 specimen	x	Itacambira
Central	NA	UFMG-G 1589	2 specimens	x	Itacambira
Central	NA	UFMG-G 1590	3 specimens	x	Itacambira
Central	NA	UFMG-G 1592	2 specimens	x	Itacambira
Central	NA	UFMG-G 1593	2 specimens	x	Itacambira
Central	NA	UFMG-G 1595	3 specimens	x	Itacambira
Central	NA	UFMG-G 1644	1 specimen	x	Itacambira
Central	NA	UFMG-G 1648	4 specimens	x	Itacambira
Cabral	NA	UFMG-G 404a	3 specimens	x	Buenópolis
Cabral	NA	UFMG-G 404b	2 specimens	x	Buenópolis
Cabral	NA	UFMG-G 404c	3 specimens	x	Buenópolis

Cabral	NA	UFMG-G 1264	3 specimens	x	Joaquim Felício
Cabral	NA	UFMG-G 1515	5 specimens	x	Buenópolis
Cabral	NA	UFMG-G 1516	6 specimens	x	Buenópolis
Southern	NA	UFMG-G 44	5 specimens	x	Santana de Pirapama
Southern	NA	UFMG-G 256	4 specimens	x	São Gonçalo do Rio Preto
Southern	NA	UFMG-G 391	1 specimen	x	Diamantina
Southern	NA	UFMG-G 547	4 specimens	x	Alvorada de Minas
Southern	NA	UFMG-G 602a	3 specimens	x	Conceição do Mato Dentro
Southern	NA	UFMG-G 602b	6 specimens	x	Conceição do Mato Dentro
Southern	NA	UFMG-G 892	2 specimens	x	Barão de Cocais
Southern	NA	UFMG-G 901a	3 specimens	x	Barão de Cocais
Southern	NA	UFMG-G 901c	2 specimens	x	Barão de Cocais
Southern	NA	UFMG-G 946a	4 specimens	x	Barão de Cocais
Southern	NA	UFMG-G 946b	3 specimens	x	Barão de Cocais
Southern	NA	UFMG-G 946c	4 specimens	x	Barão de Cocais
Southern	NA	UFMG-G 954a	4 specimens	x	Barão de Cocais
Southern	NA	UFMG-G 954b	4 specimens	x	Barão de Cocais
Southern	NA	UFMG-G 986b	5 specimens	x	Barão de Cocais
Southern	NA	UFMG-G 989	1 specimen	x	Barão de Cocais
Southern	NA	UFMG-G 1012c	4 specimens	x	Santana do Riacho
Southern	NA	UFMG-G 1013b	4 specimens	x	Botumirim
Southern	NA	UFMG-G 1013c	3 specimens	x	Botumirim
Southern	NA	UFMG-G 1231	3 specimens	x	Santana do Riacho
Southern	NA	UFMG-G 1598	1 specimen	x	Jaboticatubas
Southern	NA	UFMG-G 2143	1 specimen	x	Santana do Riacho

Southern	NA	UFMG-G 2256	5 specimens				x	Barão de Cocais
Southern	NA	UFMG-G 2297	4 specimens				x	Grão Mogol
Bokermannohyla nanazae	NA	UFMG-T 4190	01	x	x			Santo Antônio do Itambé

Table S1 [CONT.] Details for sampled individuals of *Bokermannohyla saxicola* used in the present study. For each sample is present lineage voucher ID, haplotype in Figure S1 (GMYC), type of data, municipality in Minas Gerais Brazilian state, geographic coordinates, and Genbank accession numbers. UFMG = Centro de Coleções Taxonômicas da Universidade Federal de Minas Gerais; BS = code by Nascimento *et al.* 2018

Longitude (W)	**Latitude (S)**	**GenBank accession numbers**							
		COI	**cyt-*b***	***β*-cry**	***β*-fib**	**c-*myc***	**DIA6**	**POMC**	**smarcB1**
-42.92938	-16.587746	OL672838	OL653177	OL661345/OL661345	OL943995/OL943995	OL653183/OL653183	OL653236/OL653236	OL653195/OL653195	OL653222/OL653226
-42.53447	-16.29544	OL672838	OL653177	OL661345/OL661345	OL943995/OL943995	OL653183/OL653183	OL653236/OL653236	OL653195/OL653195	OL653223/OL653226
-42.856003	-16.370431	OL672839	OL653178	OL661345/OL661345	OL943995/OL943995	OL653183/OL653183	OL653236/OL653236	OL653199/OL653210	OL653222/OL653226
-44.061271	-18.032073	MF918882	MF918668	OL661345/OL661345	OL943994/OL943993	OL653187/OL653187	OL653251/OL653271	OL653208/OL653218	OL653223/OL653223
-43.770806	-18.759583	MF918895	MF918681	OL661345/OL661345	OL943994/OL943994	OL653187/OL653192	OL653266/OL653278	OL653214/OL653209	OL653223/OL653223
-43.430071	-18.870196	MF919052	MF918838	OL661345/OL661345	OL943994/OL943994	OL653187/OL653191	OL653268/OL653255	OL653216/OL653208	OL653223/OL653223
-43.412463	-19.042659	MF919033	MF918819	OL661345/OL661347	OL943994/OL943994	OL653187/OL653189	OL653248/OL653248	OL653216/OL653208	OL653223/OL653223
-42.731799	-18.002059	MF918954	MF918740	OL661345/OL661345	OL943994/OL943994	OL653192/OL653192	OL653239/OL653257	OL653217/OL653208	OL653224/OL653225
-43.07492	-18.08787	MF918996	MF918782	OL661345/OL661345	OL943994/OL943990	OL653186/OL653187	OL653238/OL653294	OL653210/OL653216	OL653223/OL653223
-43.06903	-18.09635	MF919009	MF918795	OL661345/OL661345	OL943996/OL943991	OL653187/OL653192	OL653253/OL653287	OL653216/OL653208	OL653223/OL653223
-43.06903	-18.09635	MF919011	MF918797	OL661345/OL661345	OL943994/OL943994	OL653187/OL653192	OL653245/OL653259	OL653210/OL653208	OL653223/OL653223
-43.609612	-18.215455	MF919035	MF918821	OL661345/OL661345	OL943994/OL943992	OL653185/OL653185	OL653254/OL653256	OL653208/OL653213	OL653223/OL653223
-43.328389	-18.178472	MF918894	MF918680	OL661345/OL661345	OL943994/OL943989	OL653187/OL653190	OL653258/OL653295	OL653210/OL653208	OL653223/OL653223

-43.412463	-19.042659	MF919034	MF918820	OL661345/OL661345	OL943994/OL943994	OL653191/OL653189	OL653233/OL653270	OL653208/OL653208	OL653223/OL653223
-43.770806	-18.759583	MF918896	MF918682	OL661345/OL661345	OL943996/OL943994	OL653187/OL653187	OL653276/OL653280	OL653210/OL653209	OL653223/OL653223
-43.770806	-18.759583	MF918900	MF918686	OL661345/OL661345	OL943994/OL943992	OL653187/OL653192	OL653241/OL653230	OL653219/OL653220	OL653223/OL653223
-43.720559	-19.01977	MF919022	MF918808	OL661345/OL661345	OL943992/OL943992	OL653187/OL653187	OL653262/OL653282	OL653213/OL653215	OL653223/OL653224
-43.181667	-19.266222	MF918898	MF918684	OL661345/OL661345	OL943996/OL943994	OL653187/OL653187	OL653242/OL653242	OL653208/OL653213	OL653223/OL653223
-43.181667	-19.266222	MF918886	MF918672	OL661345/OL661345	OL943994/OL943994	OL653187/OL653187	OL653283/OL653284	OL653210/OL653214	OL653223/OL653223
-43.512187	-19.887327	MF919044	MF918830	OL661345/OL661345	OL943994/OL943992	OL653187/OL653188	OL653289/OL653289	OL653208/OL653219	OL653223/OL653225
-43.543611	-19.257222	MF918889	MF918675	OL661345/OL661345	OL943994/OL943992	OL653187/OL653192	OL653275/OL653263	OL653219/OL653219	OL653223/OL653223
-43.181667	-19.266222	MF918883	MF918669	OL661345/OL661345	OL943994/OL943992	OL653187/OL653187	OL653281/OL653279	OL653208/OL653219	OL653223/OL653223
-43.543611	-19.257222	MF918891	MF918677	OL661345/OL661345	OL943994/OL943994	OL653187/OL653192	OL653252/OL653293	OL653208/OL653213	OL653223/OL653223
-43.03905	-16.844756	MF918986	MF918772	OL661345/OL661347	OL943997/OL943997	OL653187/OL653187	OL653240/OL653290	OL653208/OL653213	OL653223/OL653223
-43.03905	-16.844756	MF918989	MF918775	OL661345/OL661345	OL943997/OL943994	OL653187/OL653193	OL653242/OL653243	OL653202/OL653208	OL653222/OL653223
-43.770806	-18.759583	MF918903	MF918689	OL661345/OL661345	OL943996/OL943996	OL653192/OL653191	OL653267/OL653274	OL653208/OL653209	OL653223/OL653223
-42.655528	-17.806472	MF918955	MF918741	OL661345/OL661345	OL943994/OL943994	OL653187/OL653187	OL653247/OL653246	OL653210/OL653209	OL653223/OL653223
-43.384159	-18.546139	MF918897	MF918683	OL661345/OL661345	OL943994/OL943994	OL653187/OL653187	OL653286/OL653269	OL653210/OL653213	OL653223/OL653223
-43.87841	-18.7858	MF919028	MF918814	OL661345/OL661345	OL943994/OL943994	OL653185/OL653187	OL653260/OL653292	OL653210/OL653212	OL653223/OL653223
-43.31397	-16.98976	MF918850	MF918636	OL661345/OL661345	OL943995/OL944002	OL653183/OL653183	-	OL653196/OL653196	OL653222/OL653222
-43.30489	-17.01754	MF918855	MF918641	OL661345/OL661345	OL943995/OL944002	OL653183/OL653183	OL653236/OL653235	OL653197/OL653197	OL653222/OL653222
-43.30489	-17.01754	MF918857	MF918643	OL661345/OL661346	OL943995/OL944002	OL653183/OL653183	OL653236/OL653236	OL653196/OL653211	OL653222/OL653222
-43.30489	-17.01754	MF918853	MF918639	OL661345/OL661345	OL943995/OL944002	OL653183/OL653187	OL653232/OL653272	OL653196/OL653196	OL653222/OL653226
-43.30505	-17.01658	MF918858	MF918644	OL661345/OL661345	OL943995/OL943995	OL653183/OL653183	OL653236/OL653237	OL653196/OL653197	OL653222/OL653226
-44.22535	-17.671583	MF918843 -	MF918629 -	OL661350/OL661351 -	OL943998/OL944001 -	OL653184/OL653184 -	OL653264/OL653264 -	OL653206/OL653204 -	OL653227/OL653227 -
-44.322797	-17.685228	MF918841	MF918627	OL661350/OL661351	OL944001/OL944001	OL653184/OL653184	OL653264/OL653264	OL653204/OL653204	OL653227/OL653227
-44.249727	-17.851053	MF918842	MF918628	OL661351/OL661351	OL944001/OL944001	OL653184/OL653184	OL653264/OL653264	OL653203/OL653203	OL653227/OL653227
-42.781691	-15.19681	MF918870	MF918656	OL661348/OL661348	OL943999/OL943999	OL653184/OL653184	OL653291/OL653291	OL653199OL653199	OL653227/OL653227
-42.781691	-15.19681	MF918871	MF918657	OL661348/OL661348	OL943999/OL944000	OL653184/OL653184	OL653291/OL653291	OL653198/OL653199	OL653227/OL653228

-42.813397	-15.774997	MF918881	MF918667	OL661348/OL661349	OL943999/OL943999	OL653184/OL653184	OL653291/OL653291	OL653198/OL653199	OL653227/OL653228
-42.647589	-15.615717	MF918874	MF918660	OL661348/OL661349	OL943999/OL944003	OL653184/OL653184	OL653291/OL653291	OL653199/OL653207	-
-42.647589	-15.615717	MF918877	MF918663	OL661348/OL661349	OL943999/OL943999	OL653184/OL653184	OL653291/OL653291	OL653198/OL653199	OL653227/OL653228
-42.813397	-15.774997	MF918879	MF918665	OL661348/OL661348	OL943999/OL943999	OL653184/OL653184	OL653291/OL653291	OL653199/OL653199	OL653227/OL653227
-44.193178	-17.693408	OL672840	OL653179	OL661350/OL661351	OL943998/OL943998	OL653184/OL653184	OL653264/OL653265	OL653205/OL653204	OL653227/OL653227
-44.250565	-17.722982	OL672840	OL653179	OL661351/OL661351	OL943998/OL943998	OL653184/OL653184	OL653264/OL653264	OL653203/OL653204	OL653227/OL653227
-42.77316	-17.210003	OL672841	OL653180	OL661345/OL661347	OL943994/OL943994	OL653183/OL653187	OL653234/OL653288	OL653200/OL653218	OL653223/OL653223
-42.750619	-17.18678	OL672841	OL653181	OL661345/OL661347	OL943994/OL943994	OL653187/OL653187	OL653277/OL653285	OL653213/OL653220	OL653223/OL653225
-42.795961	-17.194273	OL672841	OL653180	OL661345/OL661347	OL943997/OL943994	OL653183/OL653187	OL653244/OL653261	OL653215/OL653201	OL653223/OL653223
-42.751164	-17.186037	OL672841	OL653181	OL661345/OL661347	OL943994/OL943994	OL653187/OL653187	OL653231/OL653273	OL653220/OL653220	OL653223/OL653225
-44.322797	-17.685228	MF918840	MF918626	-	-	-	-	-	-
-43.182	-19.266	MF918884	MF918670	-	-	-	-	-	-
-43.182	-19.266	MF918885	MF918671	-	-	-	-	-	-
-43.182	-19.266	MF918887	MF918673	-	-	-	-	-	-
-43.581	-19.268	MF918888	MF918674	-	-	-	-	-	-
-43.544	-19.257	MF918890	MF918676	-	-	-	-	-	-
-43.328	-18.178	MF918892	MF918678	-	-	-	-	-	-
-43.328	-18.178	MF918893	MF918679	-	-	-	-	-	-
-43.771	-18.76	MF918899	MF918685	-	-	-	-	-	-
-43.771	-18.76	MF918901	MF918687	-	-	-	-	-	-
-43.771	-18.76	MF918902	MF918688	-	-	-	-	-	-
-43.771	-18.76	MF918904	MF918690	-	-	-	-	-	-
-43.547	-19.267	MF918905	MF918691	-	-	-	-	-	-
-43.547	-19.267	MF918906	MF918692	-	-	-	-	-	-
-43.755	-18.811	MF918907	MF918693	-	-	-	-	-	-
-43.755	-18.811	MF918908	MF918694	-	-	-	-	-	-
-43.755	-18.811	MF918909	MF918695	-	-	-	-	-	-

-43.755	-18.811	MF918910	MF918696	-	-	-	-	-	-
-43.755	-18.811	MF918911	MF918697	-	-	-	-	-	-
-43.754623	-18.811414	MF918912	MF918698	-	-	-	-	-	-
-43.770797	-18.759635	MF918913	MF918699	-	-	-	-	-	-
-43.754623	-18.811414	MF918914	MF918700	-	-	-	-	-	-
-43.754623	-18.811414	MF918915	MF918701	-	-	-	-	-	-
-43.754623	-18.811414	MF918916	MF918702	-	-	-	-	-	-
-43.333	-18.218	MF918917	MF918703	-	-	-	-	-	-
-43.333	-18.218	MF918918	MF918704	-	-	-	-	-	-
-43.330	-18.225	MF918919	MF918705	-	-	-	-	-	-
-43.330	-18.225	MF918920	MF918706	-	-	-	-	-	-
-43.370	-18.129	MF918921	MF918707	-	-	-	-	-	-
-43.370	-18.129	MF918922	MF918708	-	-	-	-	-	-
-43.370	-18.129	MF918923	MF918709	-	-	-	-	-	-
-43.370	-18.129	MF918924	MF918710	-	-	-	-	-	-
-43.370	-18.129	MF918925	MF918711	-	-	-	-	-	-
-43.370	-18.129	MF918926	MF918712	-	-	-	-	-	-
-43.357	-18.125	MF918927	MF918713	-	-	-	-	-	-
-43.357	-18.125	MF918928	MF918714	-	-	-	-	-	-
-43.333	-18.218	MF918929	MF918715	-	-	-	-	-	-
-43.34	-18.199	MF918930	MF918716	-	-	-	-	-	-
-43.34	-18.199	MF918931	MF918717	-	-	-	-	-	-
-43.370	-18.129	MF918932	MF918718	-	-	-	-	-	-
-43.771	-18.76	MF918933	MF918719	-	-	-	-	-	-
-43.547	-19.267	MF918934	MF918720	-	-	-	-	-	-
-43.370	-18.129	MF918935	MF918721	-	-	-	-	-	-
-43.357	-18.125	MF918936	MF918722	-	-	-	-	-	-

-43.357	-18.125	MF918937	MF918723	-	-	-	-	-	-
-43.370	-18.129	MF918938	MF918724	-	-	-	-	-	-
-43.333	-18.218	MF918939	MF918725	-	-	-	-	-	-
-43.357	-18.125	MF918940	MF918726	-	-	-	-	-	-
-43.333	-18.218	MF918941	MF918727	-	-	-	-	-	-
-43.357	-18.125	MF918942	MF918728	-	-	-	-	-	-
-43.370	-18.129	MF918943	MF918729	-	-	-	-	-	-
-43.357	-18.125	MF918944	MF918730	-	-	-	-	-	-
-43.357	-18.126	MF918945	MF918731	-	-	-	-	-	-
-43.357	-18.126	MF918946	MF918732	-	-	-	-	-	-
-43.357	-18.126	MF918947	MF918733	-	-	-	-	-	-
-43.357	-18.125	MF918948	MF918734	-	-	-	-	-	-
-42.781691	-15.19681	MF918866	MF918652	-	-	-	-	-	-
-42.781691	-15.19681	MF918867	MF918653	-	-	-	-	-	-
-42.781691	-15.19681	MF918868	MF918654	-	-	-	-	-	-
-42.781691	-15.19681	MF918869	MF918655	-	-	-	-	-	-
-42.781691	-15.19681	MF918872	MF918658	-	-	-	-	-	-
-42.731799	-18.002059	MF918949	MF918735	-	-	-	-	-	-
-42.731799	-18.002059	MF918950	MF918736	-	-	-	-	-	-
-42.731799	-18.002059	MF918951	MF918737	-	-	-	-	-	-
-42.731799	-18.002059	MF918952	MF918738	-	-	-	-	-	-
-42.731799	-18.002059	MF918953	MF918739	-	-	-	-	-	-
-42.731799	-18.002059	MF918956	MF918742	-	-	-	-	-	-
-42.748094	-18.004977	MF918957	MF918743	-	-	-	-	-	-
-42.748094	-18.004977	MF918958	MF918744	-	-	-	-	-	-
-42.748094	-18.004977	MF918959	MF918745	-	-	-	-	-	-
-42.748094	-18.004977	MF918960	MF918746	-	-	-	-	-	-

-42.748094	-18.004977	MF918961	MF918747	-	-	-	-	-	-
-42.748094	-18.004977	MF918962	MF918748	-	-	-	-	-	-
-42.748094	-18.004977	MF918963	MF918749	-	-	-	-	-	-
-42.748094	-18.004977	MF918964	MF918750	-	-	-	-	-	-
-42.748094	-18.004977	MF918965	MF918751	-	-	-	-	-	-
-42.748094	-18.004977	MF918966	MF918752	-	-	-	-	-	-
-42.748094	-18.004977	MF918967	MF918753	-	-	-	-	-	-
-42.74986	-18.011618	MF918968	MF918754	-	-	-	-	-	-
-42.74986	-18.011618	MF918969	MF918755	-	-	-	-	-	-
-42.74986	-18.011618	MF918970	MF918756	-	-	-	-	-	-
-42.74986	-18.011618	MF918971	MF918757	-	-	-	-	-	-
-43.07013	-18.09548	MF918972	MF918758	-	-	-	-	-	-
-43.07013	-18.09548	MF918973	MF918759	-	-	-	-	-	-
-43.07013	-18.09548	MF918974	MF918760	-	-	-	-	-	-
-43.062558	-16.842739	MF918975	MF918761	-	-	-	-	-	-
-43.03905	-16.844756	MF918976	MF918762	-	-	-	-	-	-
-43.03905	-16.844756	MF918977	MF918763	-	-	-	-	-	-
-43.063	-16.843	MF918978	MF918764	-	-	-	-	-	-
-43.037972	-16.842694	MF918979	MF918765	-	-	-	-	-	-
-43.041489	-16.847922	MF918980	MF918766	-	-	-	-	-	-
-43.042217	-16.848186	MF918981	MF918767	-	-	-	-	-	-
-43.034522	-16.849244	MF918982	MF918768	-	-	-	-	-	-
-43.047692	-16.847889	MF918983	MF918769	-	-	-	-	-	-
-43.033528	-16.848469	MF918984	MF918770	-	-	-	-	-	-
-43.03905	-16.844756	MF918985	MF918771	-	-	-	-	-	-
-43.03905	-16.844756	MF918987	MF918773	-	-	-	-	-	-
-43.03905	-16.844756	MF918988	MF918774	-	-	-	-	-	-

-43.03905	-16.844756	MF918990	MF918776	-	-	-	-	-	-
-43.039508	-16.846083	MF918991	MF918777	-	-	-	-	-	-
-43.039508	-16.846083	MF918992	MF918778	-	-	-	-	-	-
-43.042217	-16.848186	MF918993	MF918779	-	-	-	-	-	-
-43.07151	-18.0893	MF918994	MF918780	-	-	-	-	-	-
-43.07492	-18.08787	MF918995	MF918781	-	-	-	-	-	-
-43.07492	-18.08787	MF918997	MF918783	-	-	-	-	-	-
-43.06224	-18.08207	MF918998	MF918784	-	-	-	-	-	-
-43.072	-18.089	MF918999	MF918785	-	-	-	-	-	-
-43.06224	-18.08207	MF919000	MF918786	-	-	-	-	-	-
-43.06224	-18.08207	MF919001	MF918787	-	-	-	-	-	-
-43.06903	-18.09635	MF919002	MF918788	-	-	-	-	-	-
-43.06903	-18.09635	MF919003	MF918789	-	-	-	-	-	-
-43.072	-18.089	MF919004	MF918790	-	-	-	-	-	-
-43.07013	-18.09548	MF919005	MF918791	-	-	-	-	-	-
-43.06903	-18.09635	MF919006	MF918792	-	-	-	-	-	-
-43.06903	-18.09635	MF919007	MF918793	-	-	-	-	-	-
-43.06903	-18.09635	MF919008	MF918794	-	-	-	-	-	-
-43.06903	-18.09635	MF919010	MF918796	-	-	-	-	-	-
-43.06903	-18.09635	MF919012	MF918798	-	-	-	-	-	-
-43.07013	-18.09548	MF919013	MF918799	-	-	-	-	-	-
-43.670	-19.110	MF919014	MF918800	-	-	-	-	-	-
-43.670	-19.110	MF919015	MF918801	-	-	-	-	-	-
-43.670	-19.110	MF919016	MF918802	-	-	-	-	-	-
-43.670	-19.110	MF919017	MF918803	-	-	-	-	-	-
-43.670	-19.110	MF919018	MF918804	-	-	-	-	-	-
-43.670	-19.110	MF919019	MF918805	-	-	-	-	-	-

-43.670	-19.110	MF919020	MF918806	-	-	-	-	-	-
-43.670	-19.110	MF919021	MF918807	-	-	-	-	-	-
-43.489	-19.210	MF919023	MF918809	-	-	-	-	-	-
-43.489	-19.210	MF919024 -	MF918810 -	- -	- -	- -	- -	- -	- -
-43.489	-19.210	MF919025	MF918811	-	-	-	-	-	-
-43.489	-19.210	MF919026	MF918812	-	-	-	-	-	-
-43.87841	-18.7858	MF919027	MF918813	-	-	-	-	-	-
-43.87891	-18.78681	MF919029	MF918815	-	-	-	-	-	-
-43.87891	-18.78681	MF919030	MF918816	-	-	-	-	-	-
-43.31653	-16.99057	MF918846	MF918632	-	-	-	-	-	-
-43.31653	-16.99057	MF918847	MF918633	-	-	-	-	-	-
-43.31397	-16.98976	MF918848	MF918634	-	-	-	-	-	-
-43.31397	-16.98976	MF918849	MF918635	-	-	-	-	-	-
-43.31397	-16.98976	MF918851	MF918637	-	-	-	-	-	-
-43.3148	-16.98987	MF918852	MF918638	-	-	-	-	-	-
-43.30489	-17.01754	MF918854	MF918640	-	-	-	-	-	-
-43.30489	-17.01754	MF918856	MF918642	-	-	-	-	-	-
-43.30505	-17.01658	MF918859	MF918645	-	-	-	-	-	-
-43.30505	-17.01658	MF918860	MF918646	-	-	-	-	-	-
-43.30553	-17.01559	MF918861	MF918647	-	-	-	-	-	-
-43.30561	-17.01414	MF918862	MF918648	-	-	-	-	-	-
-43.30951	-16.99585	MF918863	MF918649	-	-	-	-	-	-
-43.30319	-16.98374	MF918864	MF918650	-	-	-	-	-	-
-43.30319	-16.98374	MF918865	MF918651	-	-	-	-	-	-
-44.061271	-18.032073	MF919031	MF918817	-	-	-	-	-	-
-43.67	-19.11	MF919032	MF918818	-	-	-	-	-	-

-42.81	-15.61	MF918873	MF918659	-	-	-	-	-	-
-42.81	-15.61	MF918875	MF918661	-	-	-	-	-	-
-42.81	-15.61	MF918876	MF918662	-	-	-	-	-	-
-42.81	-15.61	MF918878	MF918664	-	-	-	-	-	-
-42.81	-15.79	MF918880	MF918666	-	-	-	-	-	-
-43.751991	-18.808053	MF919036	MF918822	-	-	-	-	-	-
-43.751991	-18.808053	MF919037	MF918823	-	-	-	-	-	-
-43.751991	-18.808053	MF919038	MF918824	-	-	-	-	-	-
-43.751991	-18.808053	MF919039	MF918825	-	-	-	-	-	-
-43.751991	-18.808053	MF919040	MF918826	-	-	-	-	-	-
-43.751991	-18.808053	MF919041	MF918827	-	-	-	-	-	-
-44.22535	-17.671583	MF918844 -	MF918630 -	-	-	-	-	-	-
-43.516195	-19.886619	MF919042	MF918828	-	-	-	-	-	-
-43.516195	-19.886619	MF919043	MF918829	-	-	-	-	-	-
-43.516195	-19.886619	MF919045	MF918831	-	-	-	-	-	-
-43.516195	-19.886619	MF919046	MF918832	-	-	-	-	-	-
-43.516195	-19.886619	MF919047	MF918833	-	-	-	-	-	-
-43.516195	-19.886619	MF919048	MF918834	-	-	-	-	-	-
-44.22535	-17.671583	MF918845	MF918631	-	-	-	-	-	-
-43.516195	-19.886619	MF919049	MF918835	-	-	-	-	-	-
-43.516195	-19.886619	MF919050	MF918836	-	-	-	-	-	-
-43.516195	-19.886619	MF919051	MF918837	-	-	-	-	-	-
-42.73958	-15.652947	-	-	-	-	-	-	-	-
-42.73958	-15.652947	-	-	-	-	-	-	-	-
-42.73958	-15.652947	-	-	-	-	-	-	-	-
-42.73958	-15.652947	-	-	-	-	-	-	-	-

-42.73958	-15.652947	-	-	-	-	-	-	-	-
-42.73958	-15.652947	-	-	-	-	-	-	-	-
-42.73958	-15.652947	-	-	-	-	-	-	-	-
-42.73958	-15.652947	-	-	-	-	-	-	-	-
-42.73958	-15.652947	-	-	-	-	-	-	-	-
-42.73958	-15.652947	-	-	-	-	-	-	-	-
-42.73958	-15.652947	-	-	-	-	-	-	-	-
-42.73958	-15.652947	-	-	-	-	-	-	-	-
-42.73958	-15.652947	-	-	-	-	-	-	-	-
-42.73958	-15.652947	-	-	-	-	-	-	-	-
-42.73958	-15.652947	-	-	-	-	-	-	-	-
-42.73958	-15.652947	-	-	-	-	-	-	-	-
-42.73958	-15.652947	-	-	-	-	-	-	-	-
-42.73958	-15.652947	-	-	-	-	-	-	-	-
-42.73958	-15.652947	-	-	-	-	-	-	-	-
-42.73958	-15.652947	-	-	-	-	-	-	-	-
-42.73958	-15.652947	-	-	-	-	-	-	-	-
-42.73958	-15.652947	-	-	-	-	-	-	-	-
-42.73958	-15.652947	-	-	-	-	-	-	-	-
-42.73958	-15.652947	-	-	-	-	-	-	-	-
-42.73958	-15.652947	-	-	-	-	-	-	-	-
-42.73958	-15.652947	-	-	-	-	-	-	-	-
-42.73958	-15.652947	-	-	-	-	-	-	-	-
-44.250565	-17.722982	-	-	-	-	-	-	-	-
-44.224181	-17.671551	-	-	-	-	-	-	-	-
-44.244004	-17.917024	-	-	-	-	-	-	-	-
-44.232849	-17.863159	-	-	-	-	-	-	-	-
-44.232849	-17.863159	-	-	-	-	-	-	-	-

-44.380153	-17.833585	-	-	-	-	-	-	-	-
-44.250565	-17.722982	-	-	-	-	-	-	-	-
-44.250565	-17.722982	-	-	-	-	-	-	-	-
-44.224181	-17.671551	-	-	-	-	-	-	-	-
-44.335462	-17.799797	-	-	-	-	-	-	-	-
-44.224181	-17.671551	-	-	-	-	-	-	-	-
-44.274333	-17.700081	-	-	-	-	-	-	-	-
-44.232849	-17.863159	-	-	-	-	-	-	-	-
-44.193178	-17.693408	-	-	-	-	-	-	-	-
-44.224181	-17.671551	-	-	-	-	-	-	-	-
-44.380153	-17.833585	-	-	-	-	-	-	-	-
-44.224181	-17.671551	-	-	-	-	-	-	-	-
-44.250565	-17.722982	-	-	-	-	-	-	-	-
-44.224181	-17.671551	-	-	-	-	-	-	-	-
-44.224181	-17.671551	-	-	-	-	-	-	-	-
-44.232849	-17.863159	-	-	-	-	-	-	-	-
-44.224181	-17.671551	-	-	-	-	-	-	-	-
-44.335462	-17.799797	-	-	-	-	-	-	-	-
-44.345461	-17.810768	-	-	-	-	-	-	-	-
-44.250565	-17.722982	-	-	-	-	-	-	-	-
-44.374731	-17.83778	-	-	-	-	-	-	-	-
-44.335462	-17.799797	-	-	-	-	-	-	-	-
-44.250565	-17.722982	-	-	-	-	-	-	-	-
-44.274333	-17.700081	-	-	-	-	-	-	-	-
-44.193178	-17.693408	-	-	-	-	-	-	-	-
-44.335462	-17.799797	-	-	-	-	-	-	-	-
-44.193178	-17.693408	-	-	-	-	-	-	-	-

-44.232849	-17.863159	-	-	-	-	-	-	-	-
-44.232849	-17.863159	-	-	-	-	-	-	-	-
-44.335462	-17.799797	-	-	-	-	-	-	-	-
-44.250565	-17.722982	-	-	-	-	-	-	-	-
-44.250565	-17.722982	-	-	-	-	-	-	-	-
-44.224181	-17.671551	-	-	-	-	-	-	-	-
-44.244004	-17.917024	-	-	-	-	-	-	-	-
-44.232849	-17.863159	-	-	-	-	-	-	-	-
-44.232849	-17.863159	-	-	-	-	-	-	-	-
-44.423796	-17.8401	-	-	-	-	-	-	-	-
-44.250565	-17.722982	-	-	-	-	-	-	-	-
-44.232849	-17.863159	-	-	-	-	-	-	-	-
-44.472626	-17.75627	-	-	-	-	-	-	-	-
-44.329233	-18.04465	-	-	-	-	-	-	-	-
-42.958568	-16.582053	-	-	-	-	-	-	-	-
-42.53447	-16.29544	-	-	-	-	-	-	-	-
-42.893695	-16.521367	-	-	-	-	-	-	-	-
-42.929380	-16.587746	-	-	-	-	-	-	-	-
-42.958568	-16.582053	-	-	-	-	-	-	-	-
-42.929380	-16.587746	-	-	-	-	-	-	-	-
-42.893695	-16.521367	-	-	-	-	-	-	-	-
-42.893695	-16.521367	-	-	-	-	-	-	-	-
-42.958568	-16.582053	-	-	-	-	-	-	-	-
-42.929380	-16.587746	-	-	-	-	-	-	-	-
-42.893695	-16.521367	-	-	-	-	-	-	-	-
-42.893695	-16.521367	-	-	-	-	-	-	-	-
-42.57289	-16.35789	-	-	-	-	-	-	-	-

-42.856003	-16.370431	-	-	-	-	-	-	-	-
-42.893695	-16.521367	-	-	-	-	-	-	-	-
-42.57289	-16.35789	-	-	-	-	-	-	-	-
-42.57289	-16.35789	-	-	-	-	-	-	-	-
-42.929380	-16.587746	-	-	-	-	-	-	-	-
-42.903438	-16.554894	-	-	-	-	-	-	-	-
-42.903438	-16.554894	-	-	-	-	-	-	-	-
-42.903438	-16.554894	-	-	-	-	-	-	-	-
-42.903438	-16.554894	-	-	-	-	-	-	-	-
-42.903438	-16.554894	-	-	-	-	-	-	-	-
-42.903438	-16.554894	-	-	-	-	-	-	-	-
-42.903438	-16.554894	-	-	-	-	-	-	-	-
-42.903438	-16.554894	-	-	-	-	-	-	-	-
-42.903438	-16.554894	-	-	-	-	-	-	-	-
-42.903438	-16.554894	-	-	-	-	-	-	-	-
-42.903438	-16.554894	-	-	-	-	-	-	-	-
-42.903438	-16.554894	-	-	-	-	-	-	-	-
-42.903438	-16.554894	-	-	-	-	-	-	-	-
-42.903438	-16.554894	-	-	-	-	-	-	-	-
-42.903438	-16.554894	-	-	-	-	-	-	-	-
-42.903438	-16.554894	-	-	-	-	-	-	-	-
-42.903438	-16.554894	-	-	-	-	-	-	-	-
-42.903438	-16.554894	-	-	-	-	-	-	-	-
-42.903438	-16.554894	-	-	-	-	-	-	-	-
-42.903438	-16.554894	-	-	-	-	-	-	-	-
-42.903438	-16.554894	-	-	-	-	-	-	-	-
-42.903438	-16.554894	-	-	-	-	-	-	-	-
-42.903438	-16.554894	-	-	-	-	-	-	-	-

-43.460686	-19.241314	-	-	-	-	-	-	-	-
-43.52696	-19.279545	-	-	-	-	-	-	-	-
-43.610287	-19.37784	-	-	-	-	-	-	-	-
-43.460686	-19.241314	-	-	-	-	-	-	-	-
-43.516542	-19.267823	-	-	-	-	-	-	-	-
-43.610287	-19.37784	-	-	-	-	-	-	-	-
-43.610287	-19.37784	-	-	-	-	-	-	-	-
-43.610287	-19.37784	-	-	-	-	-	-	-	-
-43.581447	-19.288556	-	-	-	-	-	-	-	-
-43.642541	-20.137329	-	-	-	-	-	-	-	-
-43.639618	-20.129085	-	-	-	-	-	-	-	-
-43.519365	-19.279763	-	-	-	-	-	-	-	-
-43.639618	-20.129085	-	-	-	-	-	-	-	-
-43.639618	-20.129085	-	-	-	-	-	-	-	-
-43.516542	-19.267823	-	-	-	-	-	-	-	-
-43.583333	-19.283333	-	-	-	-	-	-	-	-
-43.460686	-19.241314	-	-	-	-	-	-	-	-
-43.52696	-19.279545	-	-	-	-	-	-	-	-
-43.610287	-19.37784	-	-	-	-	-	-	-	-
-43.639618	-20.129085	-	-	-	-	-	-	-	-
-43.64997	-20.148797	-	-	-	-	-	-	-	-
-43.642541	-20.137329	-	-	-	-	-	-	-	-
-43.639618	-20.129085	-	-	-	-	-	-	-	-
-43.641993	-20.137614	-	-	-	-	-	-	-	-
-43.639618	-20.129085	-	-	-	-	-	-	-	-
-43.641993	-20.137614	-	-	-	-	-	-	-	-
-43.639618	-20.129085	-	-	-	-	-	-	-	-

-43.64997	-20.148797	-	-	-	-	-	-	-	-
-43.639618	-20.129085	-	-	-	-	-	-	-	-
-43.642541	-20.137329	-	-	-	-	-	-	-	-
-43.361917	-18.131778	-	-	-	-	-	-	-	-
-43.361917	-18.131778	-	-	-	-	-	-	-	-
-43.361917	-18.131778	-	-	-	-	-	-	-	-
-43.361917	-18.131778	-	-	-	-	-	-	-	-
-43.361917	-18.131778	-	-	-	-	-	-	-	-
-43.361917	-18.131778	-	-	-	-	-	-	-	-
-43.361917	-18.131778	-	-	-	-	-	-	-	-
-43.361917	-18.131778	-	-	-	-	-	-	-	-
-43.361917	-18.131778	-	-	-	-	-	-	-	-
-43.361917	-18.131778	-	-	-	-	-	-	-	-
-43.361917	-18.131778	-	-	-	-	-	-	-	-
-43.361917	-18.131778	-	-	-	-	-	-	-	-
-43.361917	-18.131778	-	-	-	-	-	-	-	-
-43.361917	-18.131778	-	-	-	-	-	-	-	-
-43.361917	-18.131778	-	-	-	-	-	-	-	-
-43.31	-19.21	-	-	-	-	-	-	-	-
-43.543611	-19.257222	-	-	-	-	-	-	-	-
-43.543611	-19.257222	-	-	-	-	-	-	-	-
-43.639728	-19.102956	-	-	-	-	-	-	-	-
-43.543611	-19.257222	-	-	-	-	-	-	-	-
-43.58116	-19.288221	-	-	-	-	-	-	-	-
-42.772413	-17.208821	-	-	-	-	-	-	-	-
-42.795961	-17.194273	-	-	-	-	-	-	-	-
-42.772413	-17.208821	-	-	-	-	-	-	-	-

-42.772413	-17.208821	-	-	-	-	-	-	-	-
-42.795961	-17.194273	-	-	-	-	-	-	-	-
-42.772413	-17.208821	-	-	-	-	-	-	-	-
-42.772413	-17.208821	-	-	-	-	-	-	-	-
-42.750619	-17.18678	-	-	-	-	-	-	-	-
-42.795961	-17.194273	-	-	-	-	-	-	-	-
-42.772413	-17.208821	-	-	-	-	-	-	-	-
-42.795961	-17.194273	-	-	-	-	-	-	-	-
-42.750619	-17.18678	-	-	-	-	-	-	-	-
-42.772413	-17.208821	-	-	-	-	-	-	-	-
-42.772413	-17.208821	-	-	-	-	-	-	-	-
-42.750619	-17.18678	-	-	-	-	-	-	-	-
-42.772413	-17.208821	-	-	-	-	-	-	-	-
-42.795961	-17.194273	-	-	-	-	-	-	-	-
-42.772413	-17.208821	-	-	-	-	-	-	-	-
-42.772413	-17.208821	-	-	-	-	-	-	-	-
-42.772413	-17.208821	-	-	-	-	-	-	-	-
-42.772413	-17.208821	-	-	-	-	-	-	-	-
-42.772413	-17.208821	-	-	-	-	-	-	-	-
-42.772413	-17.208821	-	-	-	-	-	-	-	-
-43.510709	-19.591989	-	-	-	-	-	-	-	-
-43.510709	-19.591989	-	-	-	-	-	-	-	-
-43.514661	-19.884222	-	-	-	-	-	-	-	-
-43.502282	-19.900741	-	-	-	-	-	-	-	-
-43.517869	-19.890464	-	-	-	-	-	-	-	-
-43.514661	-19.884222	-	-	-	-	-	-	-	-
-43.510709	-19.591989	-	-	-	-	-	-	-	-

-43.510109	-19.891989	-	-	-	-	-	-	-	-
-43.516195	-19.886619	-	-	-	-	-	-	-	-
-43.504567	-19.915658	-	-	-	-	-	-	-	-
-43.516195	-19.886619	-	-	-	-	-	-	-	-
-43.510109	-19.891989	-	-	-	-	-	-	-	-
-43.510109	-19.891989	-	-	-	-	-	-	-	-
-43.510109	-19.891989	-	-	-	-	-	-	-	-
-43.510109	-19.891989	-	-	-	-	-	-	-	-
-43.516195	-19.886619	-	-	-	-	-	-	-	-
-43.510109	-19.891989	-	-	-	-	-	-	-	-
-43.510109	-19.891989	-	-	-	-	-	-	-	-
-43.510109	-19.891989	-	-	-	-	-	-	-	-
-43.510109	-19.891989	-	-	-	-	-	-	-	-
-43.510109	-19.891989	-	-	-	-	-	-	-	-
-43.510109	-19.891989	-	-	-	-	-	-	-	-
-43.516195	-19.886619	-	-	-	-	-	-	-	-
-43.510109	-19.891989	-	-	-	-	-	-	-	-
-43.510109	-19.891989	-	-	-	-	-	-	-	-
-43.502252	-19.900741	-	-	-	-	-	-	-	-
-43.510109	-19.891989	-	-	-	-	-	-	-	-
-43.516195	-19.886619	-	-	-	-	-	-	-	-
-43.510109	-19.891989	-	-	-	-	-	-	-	-
-43.510109	-19.891989	-	-	-	-	-	-	-	-
-43.502252	-19.900741	-	-	-	-	-	-	-	-
-43.514661	-19.884222	-	-	-	-	-	-	-	-
-43.502252	-19.900741	-	-	-	-	-	-	-	-
-43.510109	-19.891989	-	-	-	-	-	-	-	-

-43.514661	-19.884222	-	-	-	-	-	-	-	-
-43.510109	-19.891989	-	-	-	-	-	-	-	-
-43.510109	-19.891989	-	-	-	-	-	-	-	-
-43.346164	-18.44551	-	-	-	-	-	-	-	-
-43.348759	-18.392822	-	-	-	-	-	-	-	-
-43.351439	-18.481978	-	-	-	-	-	-	-	-
-43.303952	-18.38744	-	-	-	-	-	-	-	-
-43.31364	-18.387789	-	-	-	-	-	-	-	-
-43.31364	-18.387789	-	-	-	-	-	-	-	-
-43.341969	-18.44364	-	-	-	-	-	-	-	-
-43.341969	-18.44364	-	-	-	-	-	-	-	-
-43.364224	-18.476884	-	-	-	-	-	-	-	-
-43.305873	-18.421276	-	-	-	-	-	-	-	-
-43.308059	-18.422334	-	-	-	-	-	-	-	-
-43.351439	-18.481978	-	-	-	-	-	-	-	-
-43.319076	-18.455555	-	-	-	-	-	-	-	-
-43.364224	-18.476884	-	-	-	-	-	-	-	-
-43.341969	-18.44364	-	-	-	-	-	-	-	-
-43.341969	-18.44364	-	-	-	-	-	-	-	-
-43.351439	-18.481978	-	-	-	-	-	-	-	-
-43.303952	-18.38744	-	-	-	-	-	-	-	-
-43.345911	-18.387855	-	-	-	-	-	-	-	-
-43.35909	-18.405254	-	-	-	-	-	-	-	-
-43.351439	-18.481978	-	-	-	-	-	-	-	-
-43.319815	-18.465175	-	-	-	-	-	-	-	-
-43.351439	-18.481978	-	-	-	-	-	-	-	-
-43.341969	-18.44364	-	-	-	-	-	-	-	-

-43.351439	-18.481978	-	-	-	-	-	-	-	-
-43.351439	-18.481978	-	-	-	-	-	-	-	-
-43.324932	-18.39733	-	-	-	-	-	-	-	-
-43.351439	-18.481978	-	-	-	-	-	-	-	-
-43.341969	-18.44364	-	-	-	-	-	-	-	-
-43.308059	-18.422334	-	-	-	-	-	-	-	-
-43.308059	-18.422334	-	-	-	-	-	-	-	-
-43.308059	-18.422334	-	-	-	-	-	-	-	-
-43.368	-18.490036	-	-	-	-	-	-	-	-
-43.308059	-18.422334	-	-	-	-	-	-	-	-
-43.346164	-18.44551	-	-	-	-	-	-	-	-
-43.351439	-18.481978	-	-	-	-	-	-	-	-
-43.06903	-18.09635	-	-	-	-	-	-	-	-
-43.06903	-18.09635	-	-	-	-	-	-	-	-
-43.06903	-18.09635	-	-	-	-	-	-	-	-
-43.06903	-18.09635	-	-	-	-	-	-	-	-
-43.06903	-18.09635	-	-	-	-	-	-	-	-
-43.07013	-18.09548	-	-	-	-	-	-	-	-
-43.06903	-18.09635	-	-	-	-	-	-	-	-
-43.06903	-18.09635	-	-	-	-	-	-	-	-
-43.06903	-18.09635	-	-	-	-	-	-	-	-
-43.06903	-18.09635	-	-	-	-	-	-	-	-
-43.06903	-18.09635	-	-	-	-	-	-	-	-
-43.06903	-18.09635	-	-	-	-	-	-	-	-
-43.06903	-18.09635	-	-	-	-	-	-	-	-
-43.07492	-18.08787	-	-	-	-	-	-	-	-
-43.06903	-18.09635	-	-	-	-	-	-	-	-
-43.07013	-18.09548	-	-	-	-	-	-	-	-

-43.06903	-18.09635	-	-	-	-	-	-	-	-
-43.06903	-18.09635	-	-	-	-	-	-	-	-
-43.06224	-18.08207	-	-	-	-	-	-	-	-
-43.07013	-18.09548	-	-	-	-	-	-	-	-
-43.06903	-18.09635	-	-	-	-	-	-	-	-
-43.07492	-18.08787	-	-	-	-	-	-	-	-
-43.06903	-18.09635	-	-	-	-	-	-	-	-
-43.06224	-18.08207	-	-	-	-	-	-	-	-
-43.06224	-18.08207	-	-	-	-	-	-	-	-
-43.040797	-16.847336	-	-	-	-	-	-	-	-
-43.041489	-16.847922	-	-	-	-	-	-	-	-
-43.041567	-17.114125	-	-	-	-	-	-	-	-
-43.042217	-16.848186	-	-	-	-	-	-	-	-
-43.039508	-16.846083	-	-	-	-	-	-	-	-
-43.03905	-16.844756	-	-	-	-	-	-	-	-
-43.062192	-16.843939	-	-	-	-	-	-	-	-
-43.041567	-17.114125	-	-	-	-	-	-	-	-
-43.03905	-16.844756	-	-	-	-	-	-	-	-
-43.047692	-16.847889	-	-	-	-	-	-	-	-
-43.037972	-16.842694	-	-	-	-	-	-	-	-
-43.042217	-16.848186	-	-	-	-	-	-	-	-
-43.047692	-16.847889	-	-	-	-	-	-	-	-
-43.041489	-16.847922	-	-	-	-	-	-	-	-
-43.03905	-16.844756	-	-	-	-	-	-	-	-
-43.042217	-16.848186	-	-	-	-	-	-	-	-
-43.039508	-16.846083	-	-	-	-	-	-	-	-
-43.034522	-16.849244	-	-	-	-	-	-	-	-

-43.034522	-16.849244	-	-	-	-	-	-	-	-
-43.041489	-16.847922	-	-	-	-	-	-	-	-
-43.033528	-16.848469	-	-	-	-	-	-	-	-
-43.041489	-16.847922	-	-	-	-	-	-	-	-
-43.03905	-16.844756	-	-	-	-	-	-	-	-
-43.041567	-17.114125	-	-	-	-	-	-	-	-
-42.74986	-18.011618	-	-	-	-	-	-	-	-
-42.74986	-18.011618	-	-	-	-	-	-	-	-
-42.74986	-18.011618	-	-	-	-	-	-	-	-
-42.74986	-18.011618	-	-	-	-	-	-	-	-
-43.712648	-19.879195	-	-	-	-	-	-	-	-
-42.74986	-18.011618	-	-	-	-	-	-	-	-
-42.748094	-18.004977	-	-	-	-	-	-	-	-
-42.74986	-18.011618	-	-	-	-	-	-	-	-
-42.74986	-18.011618	-	-	-	-	-	-	-	-
-43.712648	-19.879195	-	-	-	-	-	-	-	-
-42.748094	-18.004977	-	-	-	-	-	-	-	-
-42.731799	-18.002059	-	-	-	-	-	-	-	-
-42.748094	-18.004977	-	-	-	-	-	-	-	-
-42.74986	-18.011618	-	-	-	-	-	-	-	-
-43.750831	-18.812247	-	-	-	-	-	-	-	-
-43.770797	-18.759635	-	-	-	-	-	-	-	-
-42.74986	-18.011618	-	-	-	-	-	-	-	-
-42.748094	-18.004977	-	-	-	-	-	-	-	-
-42.74986	-18.011618	-	-	-	-	-	-	-	-
-43.751991	-18.808053	-	-	-	-	-	-	-	-
-42.748094	-18.004977	-	-	-	-	-	-	-	-

-42.74986	-18.011618	-	-	-	-	-	-	-	-
-42.74986	-18.011618	-	-	-	-	-	-	-	-
-42.748094	-18.004977	-	-	-	-	-	-	-	-
-43.712648	-19.879195	-	-	-	-	-	-	-	-
-43.750831	-18.812247	-	-	-	-	-	-	-	-
-43.770797	-18.759635	-	-	-	-	-	-	-	-
-42.74986	-18.011618	-	-	-	-	-	-	-	-
-43.751991	-18.808053	-	-	-	-	-	-	-	-
-42.731799	-18.002059	-	-	-	-	-	-	-	-
-42.748094	-18.004977	-	-	-	-	-	-	-	-
-43.770797	-18.759635	-	-	-	-	-	-	-	-
-42.748094	-18.004977	-	-	-	-	-	-	-	-
-42.731799	-18.002059	-	-	-	-	-	-	-	-
-42.748094	-18.004977	-	-	-	-	-	-	-	-
-43.770797	-18.759635	-	-	-	-	-	-	-	-
-43.9021	-17.92387	-	-	-	-	-	-	-	-
-43.87841	-18.7858	-	-	-	-	-	-	-	-
-43.581160	-19.288221	-	-	-	-	-	-	-	-
-43.515477	-18464610	-	-	-	-	-	-	-	-
-43.3844159	-18.546139	-	-	-	-	-	-	-	-
-43.581160	-19.288221	-	-	-	-	-	-	-	-
-43.487799	-18.484046	-	-	-	-	-	-	-	-
-43.751991	-18.808053	-	-	-	-	-	-	-	-
-43.87841	-18.7858	-	-	-	-	-	-	-	-
-43.609612	-18.215455	-	-	-	-	-	-	-	-
-43.515477	-18464610	-	-	-	-	-	-	-	-

-43.547631	-18.331546	-	-	-	-	-	-	-	-
-43.609612	-18.215455	-	-	-	-	-	-	-	-
-43.447631	-18.526875	-	-	-	-	-	-	-	-
-43.507639	-19.892628	-	-	-	-	-	-	-	-
-43.581160	-19.288221	-	-	-	-	-	-	-	-
-44.061271	-18.032073	-	-	-	-	-	-	-	-
-43.87841	-18.7858	-	-	-	-	-	-	-	-
-43.581160	-19.288221	-	-	-	-	-	-	-	-
-43.44838	-18.786386	-	-	-	-	-	-	-	-
-43.515477	-18464610	-	-	-	-	-	-	-	-
-43.581447	-19.288556	-	-	-	-	-	-	-	-
-43.581160	-19.288221	-	-	-	-	-	-	-	-
-43.515477	-18464610	-	-	-	-	-	-	-	-
-43.515477	-18464610	-	-	-	-	-	-	-	-
-43.581160	-19.288221	-	-	-	-	-	-	-	-
-43.57308	-18.62785	-	-	-	-	-	-	-	-
-43.87841	-18.7858	-	-	-	-	-	-	-	-
-43.87841	-18.7858	-	-	-	-	-	-	-	-
-43.609612	-18.215455	-	-	-	-	-	-	-	-
-43.422648	-18.547097	-	-	-	-	-	-	-	-
-42.779611	-15.797861	-	-	-	-	-	-	-	-
-42.779611	-15.797861	-	-	-	-	-	-	-	-
-42.756975	-15.655095	-	-	-	-	-	-	-	-
-42.756975	-15.655095	-	-	-	-	-	-	-	-
-42.756975	-15.655095	-	-	-	-	-	-	-	-
-43.316161	-16.990301	-	-	-	-	-	-	-	-
-43.316161	-16.990301	-	-	-	-	-	-	-	-

-43.308805	-17.011629	-	-	-	-	-	-	-	-
-43.308805	-17.011629	-	-	-	-	-	-	-	-
-43.308825	-17.011485	-	-	-	-	-	-	-	-
-43.308825	-17.011485	-	-	-	-	-	-	-	-
-43.308805	-17.011629	-	-	-	-	-	-	-	-
-43.308805	-17.011629	-	-	-	-	-	-	-	-
-44.242333	-17.921389	-	-	-	-	-	-	-	-
-44.242333	-17.921389	-	-	-	-	-	-	-	-
-44.242333	-17.921389	-	-	-	-	-	-	-	-
-44.250472	-17.722629	-	-	-	-	-	-	-	-
-44.232849	-17.863159	-	-	-	-	-	-	-	-
-44.232849	-17.863159	-	-	-	-	-	-	-	-
-43.87841	-18.7858	-	-	-	-	-	-	-	-
-43.500833	-18.195972	-	-	-	-	-	-	-	-
-43.991194	-18.287222	-	-	-	-	-	-	-	-
-43.430071	-18.870196	-	-	-	-	-	-	-	-
-43.430298	-18.870289	-	-	-	-	-	-	-	-
-43.430298	-18.870289	-	-	-	-	-	-	-	-
-43.516195	-19.886619	-	-	-	-	-	-	-	-
-43.516195	-19.886619	-	-	-	-	-	-	-	-
-43.516195	-19.886619	-	-	-	-	-	-	-	-
-43.516195	-19.886619	-	-	-	-	-	-	-	-
-43.516195	-19.886619	-	-	-	-	-	-	-	-
-43.516195	-19.886619	-	-	-	-	-	-	-	-
-43.516195	-19.886619	-	-	-	-	-	-	-	-
-43.516195	-19.886619	-	-	-	-	-	-	-	-
-43.516195	-19.886619	-	-	-	-	-	-	-	-

-43.516195	-19.886619	-	-	-	-	-	-	-	-
-43.580521	-19.29138	-	-	-	-	-	-	-	-
-43.041539	-17.114125	-	-	-	-	-	-	-	-
-43.041539	-17.114125	-	-	-	-	-	-	-	-
-43.580521	-19.29138	-	-	-	-	-	-	-	-
-43.610287	-19.37784	-	-	-	-	-	-	-	-
-43.583333	-19.283333	-	-	-	-	-	-	-	-
-43.516195	-19.886619	-	-	-	-	-	-	-	-
-42.893695	-16.521367	-	-	-	-	-	-	-	-
-43.351439	-18.481978	OL672842	OL653182	OL661352/OL661352	OL944004/OL944005	OL653194/OL653194	OL653249/OL653250	OL653221/OL653221	OL653229/OL653229

Table S2 Selected loci with their respective primers, sequences, anneling temperature and time, and original work

Locus	Primer	Sequence	Anneling temperature (°C)	Anneling time (s)	Reference
Citochrome oxidase, subunit I (COI)	Chmr4 Chmf4	ACYTCRGGRTGRCCRAARAATCA> TYTCWACWAAYCAYAAAGAYATCGG<	52	30	Che et al., 2012
Citochrome B (cyt-*b*)	MVZ15 ARH	GAACTAATGGCCCACACWWTACGNAA> TAWAAGGGTCTTCTACTGGTTG<	52	50	Moritz et al., 1992 Goebel et al., 1999
Beta-fibrinogen, Intron 7 (*β*-fib)	BFXF BFXR	CAGYACTTTYGAY1GAGACAAYGATGG > TTGTACCACCAKCCACCACCRTCTTC <	59	60	Sequeira et al., 2006
Beta-crystallin (*β*-cry)	CRYB1Ls CRYB2Ls	CGCCTGATGTCTTTCCGCC > CCAATGAAGTTCTCTTTCTCAA <	54	40	Dolman & Phillips, 2004
Proto-oncogene cellular myelotomatosis (c-*myc*)	cmyc1U cmyc-ex2dR	GAGGACATCTGGAARAARTT > TCATTCAATGGGTAAGGGAAGACC <	54	60	Crawford, 2003 Wiens et al., 2005
Disulphide Isomerase A6 Precursor, Intron 6 (DIA6)	MVZ37 MVZ38	AGAGGATTTCCCACAATTAAAATC > GCGACTATACAGAGCTGGTGTTC <	60	60	Bell et al., 2012
Proopiomelanocortin A (POMC)	POMC-1 POMC-2	GAATGTATYAAAGMMTGCAAGATGGWCCT> TAYTGRCCCTTYTTGTGGGCRTT<	60	50	Wiens et al., 2005
SWI/SNF related, matrix associated, actin dependent regulator of chromatin, subfamily b, member 1 (SmarcB1)	HexF HexR	ATTGCATGTCGCAGTGTGTT > AGCCTCGACACAGAGACGT <	60	60	Stöck et al., 2013

Table S3 Morphometric measurements of adults of *Bokermannohyla saxicola*. Bilateral measurements were performed on the left side in dorsal view, except for some individuals with poor preservation or malformation, for which the right side was measured. F corresponds to female and M to males. The definition and reference of each measure are available in the metadata table

Voucher (UFMG)	SEX	SVL	PL	FAW	TD	ED	IOD	AMD	EN	IND	NS	UAL	FLL	HAL	THL	TL	TSL	FL	HL	HW	CW	UED
8636	F	47.92	3.93	3.47	2.86	5.25	5.68	8.7	4.17	3.31	2.99	10.13	9.35	15.08	25.26	24.93	13.73	21.67	17.51	17.48	14.42	14.2
817	F	40.49	3.12	3.11	2.47	4.85	4.35	7.14	4.24	3.25	2.71	8.35	7.36	12.13	21.25	21.45	11.92	17.34	14.85	14.96	12.55	11.43
9044	F	43.4	2.86	2.42	2.38	4.91	5.39	8.19	4.04	3.41	2.29	7.52	8.42	11.91	23.08	23.04	12.66	17.87	14.19	15.08	9.75	11.23
19556	F	50.85	3.83	3.29	2.62	4.9	5.36	8.63	4.73	3.74	2.34	8.02	8.71	14.67	25.09	24.73	13.52	20.57	16.19	17.02	16.29	13.94
19555	F	49.19	4.02	3.08	2.78	5.85	5.87	8.23	3.98	3.72	2.64	7.98	9.45	14.99	24.14	23.98	13.23	21.04	17.34	17.7	17.25	14.15
19557	F	50.16	3.86	2.96	2.73	5.58	5.69	8.97	4.29	4.05	2.92	8.89	8.85	16.26	25.76	25.17	14.22	21.57	17.28	17.98	17.29	14.59
10397	F	48.22	3.65	3.41	2.63	5.91	4.9	8.13	4.47	3.46	2.85	8.1	8.1	13.82	25.53	25.2	13.94	19.99	16.48	16.84	15.6	13.93
818	F	50.65	3.91	3.4	2.51	5.54	5.78	9.04	4.14	4.34	3.2	7.25	9.86	15.47	25.52	26.19	16.26	20.84	17.63	18.1	16.68	15.83
5835	F	47.9	3.81	3.17	2.56	5.82	5.66	8.67	4.22	4.3	2.49	9.18	9.22	15.46	24.93	25.75	13.96	21.64	15.82	16.94	16.82	15.04
14367	F	59.83	4.07	3.43	2.68	6.48	6.58	10.03	5.16	4.72	2.54	8.24	10.95	18.87	28.97	27.16	13.87	24.47	20.07	20.43	18.67	15.77
14296	F	54.74	4.14	3.13	2.69	5.65	6.21	9.27	4.57	3.98	2.68	8.27	10.56	16.62	26.56	25.77	13.69	23.29	18.79	19.2	19.22	14.63
14301	F	56.84	4.33	3.44	2.99	6.62	6.26	9.88	4.63	4.53	2.86	9.99	10.92	18.23	28.69	28.05	14.43	23.43	18.44	19.18	18.66	15.63
14298	F	47.97	4.04	2.91	2.08	4.7	4.85	8.71	4.36	3.84	2.77	8.85	9.09	15.06	25.68	25.58	13.14	20.55	15.78	16.74	15.51	14.17
14368	F	54.02	3.91	3.02	2.56	4.95	5.48	9.01	4.46	3.95	2.71	8.86	9.7	17.02	27.57	26.46	14.09	22.57	18.88	18.81	17.66	13.1
14302	F	59.79	4.68	3.65	2.42	6.07	6.78	9.87	4.57	4.43	3.24	9.63	10.39	17.36	27.86	26.59	14.47	22.84	20.11	19.24	18.53	15.86
14300	F	49.66	4.23	2.94	2.38	4.88	5.78	8.58	3.98	3.7	2.92	8.39	9.05	16.72	26.9	25.89	13.98	21.98	17.1	17.36	16.19	14.7
14338	F	52.88	3.91	3.08	2.57	5.39	5.15	9.28	4.04	4.21	2.78	9.34	10.24	16.1	28.12	27.07	13.83	23.72	16.95	17.11	17.78	14.11
14308	F	49.1	3.67	2.69	2.3	4.57	5.35	8.1	4.05	3.48	2.15	8.21	9.78	16.03	25.18	25.01	14.26	21.28	16.08	15.94	15.75	12.68
14370	F	52.59	3.66	3.05	2.37	5.18	5.93	8.79	4.6	3.96	2.74	9.27	10.03	17.42	27.49	26.22	13.62	22.74	17.84	17.85	16.47	14.49
14299	F	49.73	4.27	2.59	2.33	4.48	5.57	8.73	3.87	3.76	2.21	8.45	9.94	15.76	26.44	25.93	13.53	21.61	16.4	17.01	14.67	13.48
14304	F	47.27	3.93	2.46	2.37	4.63	5.41	8.46	4.27	3.93	2.49	9.06	9.81	16.24	26.92	26.58	14.08	21.53	15.68	16.03	14.61	13.62
20616	F	51.53	3.82	3.01	2.35	5.09	6.33	9.01	4.21	3.53	2.24	9.04	9.92	16.11	26.31	27.24	14.79	22.06	17.84	18.22	18.43	15.39
19238	F	43.66	4.02	2.45	2.52	4.74	6.05	7.85	3.76	3.27	2.33	8.65	8.65	14.89	25.61	25.19	13.02	20.71	15.93	15.4	14.7	13.59
14930	F	47.37	3.96	2.6	2.78	5.14	5.87	8.39	3.95	3.73	2.36	7.13	8.51	15.17	25.4	24.25	14.25	21.56	16.27	16.02	14.97	13.24
14946	F	47.34	3.76	3.07	2.78	4.35	4.69	7.86	4.16	3.24	2.3	8.57	8.93	15.01	25.34	24.01	13.35	20.47	16.74	17.41	14.18	13.01

14931	F	54.04	4.46	3.03	3.07	5.24	5.75	9.07	4.09	3.87	2.19	8.7	9.72	17.06	29.69	28.6	15.02	23.74	17.78	19.01	18.72	15.01
14783	F	54.62	4.19	3.05	2.62	5.94	5.72	8.88	4.01	3.77	2.84	8.79	9.42	17.3	26.72	25.9	13.4	23.02	18.99	19.12	18.33	16.27
14738	F	45.9	3.81	2.89	2.43	5.52	4.88	8.11	3.96	3.46	2.44	9.68	8.4	15.42	25.97	25.7	14.22	20.47	16.09	15.98	15.34	13.36
14784	F	52.34	4.44	2.93	2.88	4.81	5.19	8.85	4.02	4.08	2.76	9.35	11.03	16.06	28.28	27.61	14.98	24.01	18.88	17.91	18.13	15.06
16050	F	52.16	4.1	2.64	3.24	5.14	6.59	9.15	4.34	4.09	2.51	9.86	9.59	16.76	28	27.7	14.56	23.82	18.43	18.1	17.85	14.66
14730	F	51.2	3.74	2.58	2.4	4.82	6.58	9.31	3.98	3.9	2.56	9.39	8.84	16.77	27.14	26.34	13.5	22.82	18.13	18.41	18.09	15.26
14732	F	46.87	3.65	2.24	2.74	5.08	5.94	8.64	3.88	3.33	2.26	9.18	8.89	13.98	24.89	23.56	12.54	19.86	16.35	16.92	14.76	12.98
14731	F	51.49	3.58	2.49	2.74	4.71	5.87	8.51	4.16	3.63	2.41	8.9	9.64	16.07	27.09	26.3	13.89	22.33	17.37	17.85	17.22	14.63
11025	F	44.96	2.86	2.09	2.38	4.69	5.36	7.44	3.59	3.18	2.35	7.65	8.2	13.58	23.85	23.5	12.49	18.57	15.39	14.95	14.38	13.21
11035	F	45.49	3.51	2.02	2.25	4.11	4.95	8.05	3.75	3.23	2.54	7.82	7.43	13.85	24.13	23.47	12.64	19.86	15.02	15.42	15.58	12.28
11005	F	45.15	3.25	2.29	2.45	3.32	5.18	7.92	4.39	3.44	2.28	6.69	8.57	13.61	23.29	23.04	13.14	19.51	15.86	15.18	16.46	11.9
3801	F	47.37	3.7	2.51	2.52	4.21	5.17	8.69	4.19	3.74	2.08	7.58	8.3	14.21	23.9	23.37	12.37	20.12	16.61	16.62	15.52	13.41
12296	F	53.13	3.93	2.89	3.15	4.84	4.93	8.47	3.57	3.91	2.55	9.96	9.45	16.02	27.39	24.46	13.48	22.98	17.84	18.18	17.12	15.19
12329	F	53.16	4.36	2.88	3.3	4.99	6.75	9.22	4.23	4.1	2.93	9.96	10.7	17.66	27.59	25.79	13.54	21.87	18.58	18.46	19.56	15.31
3795	F	42.81	3.78	2.34	2.86	4.5	5.17	7.66	3.14	3.24	1.6	8.42	8.1	14.57	24.66	23.18	11.76	19.74	14.84	14.53	14.01	12.97
20456	F	55.88	4.59	2.92	2.89	4.78	5.95	8.84	4.67	3.79	2.69	9.37	10.29	17.57	28.67	27.45	14.15	24.09	17.94	18.17	19.02	15.14
20477	F	57.41	4.12	2.68	2.57	4.63	5.74	9.69	4.85	3.37	2.74	9.53	10.36	18.05	28.93	27.96	14.35	24.36	19.52	19.07	20.64	16.36
20437	F	54.51	3.81	2.77	2.75	5.04	5.81	9.06	4.28	3.67	2.41	8.95	9.48	16.67	27.29	26.13	12.85	21.59	19.07	18.35	16.74	14.85
20460	F	55.29	4.33	2.56	2.82	4.83	5.35	8.97	4.69	3.64	2.85	11.48	10.39	16.79	28.17	26.43	13.87	23.14	18.76	18.69	15.84	14.78
19234	F	49.24	3.6	2.78	2.89	5.98	6.44	9.17	4.73	4.21	2.88	8.54	9.53	16.61	23.8	25.01	13.36	23.1	18.64	17.65	17.27	15.89
12542	F	49.02	3.94	2.52	2.22	4.87	6.01	8.52	4.14	3.71	2.26	8.33	8.52	15.78	26.66	25.18	12.58	21.5	15.46	16.49	15.34	13.56
6672	F	44.41	3.02	2.34	2.09	4.6	5.07	7.94	3.63	3.47	2.41	6.67	7.39	12.58	21.41	22.03	11.22	18.03	14.49	14.94	15.61	12.32
12559	F	40.09	2.82	2.21	2.22	4.64	5.43	7.54	3.54	3.28	2.29	7.72	7.51	13.17	22.17	22.78	11.45	19.18	14.77	14.43	14.08	12.61
17304	F	43.5	2.92	2.35	2.47	4.73	4.57	8.01	3.95	3.65	2.77	6.3	7.76	14.44	22.57	22.38	12.23	19.42	14.32	14.89	15.9	12.47
17296	F	40.6	3.39	2.47	2.11	4.61	5.31	7.81	3.2	3.89	2.14	6.87	6.91	13.49	21.18	20.49	11.48	17.29	13.66	14.09	13.21	11.42
17297	F	46.27	3.34	2.65	2.65	5.25	5.35	8.83	4.07	4.05	2.82	7.18	7.7	13.62	22.99	22.12	11.94	18.43	15.78	16.13	14.4	13.13
17292	F	45.52	3.63	2.54	2.43	4.99	4.95	8.68	4.58	3.92	2.36	7.72	7.52	13.75	22.3	21.12	11.5	18.47	14.71	15.34	14.88	12.41
17298	F	43.72	3.6	2.51	2.46	4.71	4.83	7.85	3.82	4.03	2.52	6.88	7.71	13.74	22.56	21.75	11.89	17.9	14.5	14.73	15.33	12.38
13962	F	47.31	3.95	2.51	2.67	5.71	6.16	8.89	4.42	4.47	2.61	8.79	9.57	15.17	23.56	21.98	12.26	21.07	17.53	17.76	16.58	14.02
18958	F	45.86	3.74	2.72	2.67	5.6	5.54	8.29	4.17	4.15	2.5	7.49	8.29	14.39	23.58	22.4	12.13	19.45	17.03	16.67	16.51	14.71
13954	F	47.42	3.86	2.86	2.54	4.99	6.45	8.53	4.29	3.49	2.53	7.95	9.35	15.32	23.93	22.34	12.07	19.88	17.31	18.01	16.37	13.56
13963	F	45.87	3.69	2.28	2.67	5.51	5.44	8.57	3.85	3.76	2.56	8.61	7.99	14.23	24.02	22.54	11.47	20.07	14.53	14.96	16.23	13.04

18959	F	44.32	3.75	2.98	2.46	5.03	5.1	8.35	3.19	4.09	2.38	8.18	9.12	14.55	24.11	23.2	12.34	20.22	14.69	16.04	15.6	13.48
18961	F	42.81	3.04	2.27	2.34	4.85	5.53	7.92	3.84	3.49	2.58	8.81	7.82	13.68	22.5	21.38	11.29	19.23	14.95	15.69	14.52	13.38
18960	F	45.09	3.87	2.34	2.46	4.83	5.74	8.36	4.02	3.51	3.07	8.67	8.91	14.53	24.18	22.01	11.4	19.52	16.07	15.93	15.58	13.98
18957	F	40.96	3.64	2.82	2.46	4.87	4.89	7.93	4.1	3.51	2.17	6.83	8.22	12.61	21.61	21.22	10.97	17.79	14.92	15.66	16.19	12.56
15316	F	45	3.65	2.48	2.98	5.69	5.29	8.72	3.99	3.95	3.1	7.13	8.66	14.11	23.87	22.89	12.36	20.09	15.73	16.16	14.84	12.64
18753	F	38.19	3.6	2.72	2.28	4.76	5.44	7.55	3.95	3.22	2.49	5.72	7.31	13.66	20.24	19.79	10.73	17.57	13.06	14.23	14.04	12.2
20531	F	48.78	3.74	3.26	2.69	6.11	4.44	8.28	4.12	4.53	2.65	6.89	8.93	14.96	24.05	22.8	12.05	20.04	16.55	17.61	16.43	15.27
20525	F	52.21	4.21	3.07	3.1	5.81	6.18	9.09	4.7	4.49	2.86	6.72	8.79	16.46	26.63	25.05	13.37	21.75	17.98	18.11	16.63	13.91
20514	F	46.74	4.17	3.04	2.76	5.18	5.37	8.26	3.75	4.1	2.53	8.11	9.68	14.06	25.21	22.94	12.62	19.78	15.54	17.29	15.97	13.43
20520	F	47.2	4.17	2.96	2.72	5.48	5.47	7.99	3.66	4.29	2.46	6.78	8.35	14.81	25.7	23.97	12.72	20.61	16.19	16.82	15.75	12.36
14912	M	46.34	4.08	3.66	2.06	5.48	6.25	8.72	4.88	3.83	3.35	8.47	8.75	15.54	23.36	24.12	13.31	20.17	16.9	16.55	15.63	13.38
8861	M	45.74	3.69	3.19	2.68	4.97	5.65	7.94	4.71	3.53	2.94	8.27	7.68	14.37	24.04	24.4	13.76	20.62	16.93	16.28	14.42	13.51
14388	M	45.26	4	3.42	2.46	4.96	5.89	8.75	3.97	3.88	2.91	8.68	9.01	14.73	24.91	24.06	13.38	20.52	17.07	16.06	13.92	12.42
816	M	47.62	3.76	3.68	1.82	5.53	5.32	8.51	4.76	4.07	2.67	8.24	10.7	14.23	25.65	24.17	13.85	20.95	17.97	17.46	15.64	14.93
813	M	46.34	3.19	2.53	2.48	4.8	5.28	7.49	3.84	3.18	2.24	8.35	8.87	12.5	23.4	24.13	13.61	19.17	16.4	16.96	15.68	12.77
19837	M	44.52	3.34	3.22	2.12	5.16	4.51	8.19	3.45	3.37	2.44	6.51	7.42	13.27	21.79	22.43	12.39	18.64	14.93	14.91	16.03	13.75
19560	M	49.62	3.94	3.64	2.85	5.52	5.36	8.3	4.72	3.7	3.3	6.89	8.46	15.46	23.65	23.81	13.28	21.53	17.09	17.87	18.78	13.63
14911	M	47.38	3.96	3.87	2.22	5.23	6.12	8.92	4.39	4.06	3.38	10.11	9.25	15.35	26.05	25.67	14.37	21.91	17.18	17.71	15.3	12.87
19558	M	50.33	4.28	3.73	3.16	6.1	7.22	8.53	5.06	4.11	2.63	7.49	9.14	15.33	26.02	25.18	14.39	21.07	16.65	16.85	17.42	14.67
7011	M	49.13	4.23	3.78	2.24	4.85	5.79	8.59	4.97	3.44	2.57	8.08	9.22	14.7	24.36	24.82	14.49	20.37	17.93	17.31	16.27	15.29
830	M	44.79	3.96	3.46	2.66	5.19	5.53	7.85	3.6	3.39	3.01	7.23	8.11	14.6	23.86	22.81	12.89	20.22	15.73	16.46	15.24	13.78
8808	M	44.91	4.16	3.79	2.58	5.68	5.67	7.71	3.35	3.68	2.37	8.19	9	15.46	26.12	25.08	13.64	21.63	15.57	15.97	16.38	13.04
14913	M	45.91	4.31	3.62	2.9	4.93	5.36	8.74	4.26	3.29	2.49	9.04	9.53	15.75	25.86	26.03	15.38	21.7	16.47	16.91	15.98	13.15
814	M	47.05	3.98	3.57	2.36	4.79	5.58	7.82	3.66	3.19	2.58	6.39	8.81	14.16	24.33	23.59	12.66	18.63	17.04	17.33	14.03	13.66
19559	M	53.1	4.19	4.32	2.69	5.32	5.93	9.85	4.08	4.33	3.03	8.2	9.28	17.45	26.62	27.13	14.49	23.23	18.19	18.49	15.62	15.98
19566	M	45.99	3.62	3.73	2.62	6.22	5.36	8.45	3.78	3.47	2.41	7.13	8.59	15.38	24.07	23.4	13.45	20.64	18	17.02	16.27	14.6
19561	M	48.55	3.81	3.48	2.38	5.36	5.9	8.63	3.88	3.42	3.01	8.58	8.87	15.56	23.94	23.26	12.73	20.48	16.31	17.8	16.33	14.11
19553	M	49.51	3.99	2.84	2.88	5.72	5.8	8.87	3.78	3.94	3.07	7.64	9.86	16.2	26.1	25.69	13.76	22.43	17.67	17.78	17.87	14.55
19564	M	47.04	3.92	3.42	2.15	5.74	4.89	8.81	3.88	4.2	2.42	7.59	8.75	15.38	24.27	24.61	13.58	20.45	16.53	17.32	15.97	14.02
19554	M	48.23	3.96	3.08	2.55	5.5	5.19	8.53	3.82	3.57	3.04	7.73	8.7	14.69	25.19	25.01	13.51	22.03	16.76	17.34	17.52	14.47
19563	M	48.35	4.06	3.4	2.69	5.22	5.71	8.81	3.91	3.8	2.01	7.4	8.69	15.28	24.83	24.17	12.89	21.61	16.5	17.58	17.91	13.84
19552	M	44.42	3.4	3.36	2.25	4.98	5.57	8.41	3.57	3.83	2.53	6.48	7.69	14.48	19.94	21.83	11.99	19.01	15.18	16.16	14.78	13.94

19565	M	46.35	3.53	3.34	2.25	5.56	5.79	8.35	4.02	3.48	2.23	7.84	7.92	15.37	22.04	23.26	13.19	20.47	16.55	16.79	16.15	13.45
19562	M	49.38	4.1	3.52	2.86	5.19	5.98	8.87	4.29	3.72	2.29	7.57	8.69	16.02	24.36	24.74	14.25	21.38	16.45	17.77	16.62	14.06
10399	M	48.72	4.22	3.6	2.65	5.57	5.87	8.54	3.99	4.16	2.68	7.9	8.19	14.9	23.35	24.65	14.46	20.36	16.49	17.84	15.67	14.93
10396	M	49.71	4.33	3.89	2.42	5.92	5.26	8.46	4.28	3.63	2.96	5.84	8.54	15.09	21.45	24.05	12.47	20.65	15.59	18.04	16.43	15.5
10394	M	48.96	4.06	3.31	2.41	5.52	5.33	8.71	4.11	3.96	3.38	7.23	8.74	15.51	25.86	25.03	14.78	20.96	16.7	18.08	15.23	15
10393	M	43.24	3.41	3.13	2.43	4.95	5.42	8.72	3.9	3.86	2.7	6.43	7.49	13.66	18.73	21.9	11.49	17.84	14.96	16	15.36	13.17
10403	M	45.45	3.67	3.33	2.9	5.33	5.5	8.2	4.37	3.62	2.82	7.75	8.77	14.17	23.73	22.94	12.27	19.22	13.51	16.26	17.26	13.37
10398	M	49.34	4.27	3.76	2.79	6.74	5.83	8.6	3.56	3.77	2.82	7.82	8.81	15.23	23.87	24.92	13.16	20.47	17.33	18.09	15.67	13.69
10400	M	47.61	3.96	4.16	2.71	6.39	4.92	8.4	4.07	4.13	2.68	6.1	7.68	14.79	21.08	23.58	13.84	19.41	13.79	16.51	15.58	14.95
10401	M	46.12	3.89	4.11	2.64	5.35	5.49	8.74	3.82	3.72	2.25	7.23	8.98	14.76	25.06	23.65	13.6	20.38	15.17	16.97	15.2	13.72
10390	M	49.38	3.92	3.53	2.98	5.23	5.14	9.04	4.32	4.11	2.69	8.01	10.1	15.47	25.33	25.38	13.85	21.13	14.77	18.4	18.02	13.89
10392	M	44.7	3.2	3.28	2.4	5.51	5.1	7.83	3.8	3.59	3.16	6.9	8.43	12.91	20.07	22.12	12.67	18.47	15.29	16.58	15.62	14
10391	M	40.9	3.76	3.15	1.87	4.87	5.25	7.8	3.46	3.92	2.89	6.59	7.84	13.32	17.14	21.52	11.99	18.05	14.08	15.41	14.51	13.8
10389	M	41.54	3.39	3.35	2.04	5.36	5.31	8.27	3.49	2.97	2.46	5.31	7.31	12.65	18.19	21.22	11.42	16.71	15.57	16.35	13.74	13.36
10395	M	44.2	3.53	3.51	2.41	5.03	4.94	8.05	3.59	3.52	2.42	7.36	7.61	13.94	19.66	21.91	12.92	18.29	12.83	16.49	14.34	13.69
10402	M	40.88	3.88	3.63	2.05	4.75	5.07	8.25	3.54	4.1	2.18	5.6	8.05	14.53	22	21.27	12.44	18.56	14.58	16.45	13.61	12.88
10404	M	44.15	3.61	3.28	2.35	4.94	5.4	8.07	3.85	4.24	2.41	7.87	7.46	15.02	22.82	22.06	11.86	18.71	15.1	16.79	12.74	13.94
828	M	47.95	3.69	2.99	2.36	5.1	5.37	9.05	4.14	3.92	2.34	7.7	9.01	14.35	24.96	24.08	12.29	20.16	15.98	16.51	15.87	12.77
3471	M	51.24	4.36	3.72	2.46	5.27	5.47	8.69	4.27	4.03	2.5	8.13	9.24	16.65	26.17	24.99	12.77	22.46	17.48	17.68	18.14	14.66
11052	M	46.72	4.08	3.24	2.34	5.55	5.25	8.11	3.63	3.91	2.73	7.03	8.89	14.14	24.68	23.23	13.15	20.08	16.17	16.98	16.66	12.38
11051	M	48.13	4.38	3.51	2.63	5.28	5.65	8.83	3.99	3.98	2.76	8.38	9.33	15.93	25.91	24.73	13.72	21.15	17.16	17.15	16.46	13.71
831	M	46.81	3.17	3.01	2.14	4.86	5.7	7.92	3.68	4.36	2.55	5.49	8.48	13.65	25.2	24.58	13.29	20.35	15.64	16.03	13.78	12.26
11053	M	47.95	3.92	3.18	2.35	4.81	5.88	8.91	4.74	4.35	2.74	8.99	9.47	16.18	26.39	25.86	13.55	22.61	17.47	17.85	15.96	13.01
20359	M	41.47	4.02	3.05	2.29	5.37	4.95	8.17	3.95	3.84	2.62	8.47	8.83	13.38	23.28	22.41	12.25	19.26	15.86	15.66	14.48	12.89
14386	M	50.79	4.29	3.42	2.51	5.81	5.83	8.56	4.24	4.01	2.35	8.41	9.53	15.81	26.93	26.19	14.37	22.59	18.16	17.62	15.98	14.85
14366	M	47.53	3.93	3.07	2.77	5.7	5.29	8.57	4.43	4.22	2.84	8.33	8.94	15.61	24.97	24.41	13	20.75	16.86	17.84	14.6	13.18
14365	M	46.24	4.14	3.48	2.41	5.09	5.72	8.9	3.75	4.02	3.13	8.26	9.43	16.19	25.23	24.36	12.61	20.42	16.13	16.86	15.89	13.33
14307	M	46.22	4.11	3.17	2.46	4.45	5.87	8.48	4.26	3.41	2.58	8.03	9.29	14.88	24.56	23.81	12.79	21.23	15.99	16.19	14.53	13.69
14295	M	47.92	4.11	3.36	2.38	5	5.7	8.11	4.26	3.28	2.64	7.92	9.28	16.02	25.43	25.28	13.46	21.05	16.42	17.51	17.53	13.6
14336	M	48.66	3.84	3.78	2.6	5.06	6.02	8.8	4.14	3.98	3.01	7.72	9.24	15.81	25.95	24.78	13.28	21.04	15.64	16.28	17.26	14.4
14303	M	53.48	4.57	3.76	2.96	5.56	6.7	9.41	4.22	3.87	2.56	9.44	9.14	16.78	27.95	25.92	13.98	22.45	18.41	18.15	18.16	15.53
14369	M	46.79	3.94	3.39	2.57	4.53	5.69	8.12	4.21	3.77	2.71	8.93	9.72	15.35	24.95	23.96	12.94	20.63	16.64	15.99	14.95	13.13

14333	M	45.24	4.67	3.63	2.78	5.22	6.01	8.79	4.25	4.04	2.54	8.83	10.05	15.68	25.16	23.98	12.94	20.82	15.66	17.1	16.25	14.4
14385	M	46.12	4.16	3.31	2.12	4.93	6.89	8.64	4.1	3.88	2.29	8.69	9.15	15.53	25.57	23.99	13.39	21.25	15.93	16.88	16.34	13.29
14305	M	48.19	4.07	3.33	2.24	5.99	5.87	8.82	3.9	3.85	2.58	8.67	9.3	16.09	26.53	25.08	13.57	20.76	17.1	17.31	14.59	13.58
14337	M	49.02	4.65	3.88	3.01	5.12	5.67	8.12	4.74	4.28	2.72	8.07	9.48	15.89	25.41	24.61	13.36	19.83	16.96	17.37	16.72	15.45
14294	M	47.04	3.97	3.36	2.47	4.51	5.21	8.59	3.65	3.79	2.48	7.52	8.96	15.1	24.71	23.1	12.49	21	16.15	16.11	15.81	13.28
14306	M	48.22	4.1	3.23	2.78	4.67	5.28	8.33	4.26	3.69	2.54	7.77	8.86	15.58	25.37	25.41	13.11	21.07	16.5	17.35	15.86	13.94
14297	M	48.87	4.19	3.51	2.71	4.37	6.06	8.61	4.5	3.99	2.69	8.74	10.02	15.67	26.27	24.51	13.32	20.51	16.72	17.8	14.85	13.93
20597	M	48.71	4.41	3.34	2.72	5.17	5.63	9.06	4.17	3.67	2.69	8.21	8.83	15.12	25.09	25.22	13.49	21.39	17.69	17.72	16.66	14.99
18964	M	48.78	3.86	3.14	2.68	5.92	5.82	9.17	3.86	3.78	2.91	8.67	8.33	15.95	26.92	25.94	13.71	21.55	16.79	17.85	15.62	14.89
20612	M	46.11	3.65	3.06	2.63	4.85	5.55	8.24	4.01	3.73	2.27	6.74	8.63	14.59	23.7	24.76	12.43	19.35	16.08	15.89	16.49	13.99
14943	M	44.97	4.17	3.56	2.47	5.31	5.67	8.37	4.18	3.56	2.58	6.83	8.63	14.91	23.85	22.79	12.24	19.75	16.44	17.75	16.04	12.76
14933	M	46.56	4.18	3.11	2.59	4.74	5.84	8.68	3.99	3.24	2.39	8.07	8.95	14.64	25.32	24.78	13.37	20.74	16.83	16.52	16.91	13.79
14956	M	48.27	3.93	3.09	2.92	5.08	5.33	8.55	4.13	3.47	2.48	7.28	9.11	15.05	25.53	24.77	13.13	21.63	15.94	16.73	17.83	13.97
14944	M	46.27	4.18	3.25	2.36	5.74	5.78	8.81	3.97	3.41	2.61	7.14	8.73	14.81	24.55	23.2	13.04	19.74	16.5	16.63	17.05	13.77
20598	M	50.65	4.14	3.29	2.58	4.96	6.1	8.44	3.93	3.68	2.38	8.62	9.82	16.51	27.28	26.74	13.52	22.56	17.15	16.49	17.34	14.44
20606	M	47.81	3.84	2.85	2.52	5.26	5.74	8.16	3.66	3.48	2.31	8.03	8.44	15.39	26.96	24.71	13.41	21.17	16.24	17.4	16.72	14.34
20617	M	46.66	4.1	3.03	2.42	4.86	6.05	8.16	4.07	3.51	2.09	8.37	8.64	15.32	26.8	25.25	13.48	20.71	15.58	16.45	15.23	14.87
20595	M	46.82	4.13	2.83	2.08	5.44	5.69	8.72	3.82	3.82	2.21	9.57	8.41	15.14	25.94	24.41	13.03	19.3	15.54	16.32	16.33	12.99
18966	M	48.56	4.1	3.19	2.92	5.43	6.66	8.81	4.08	3.58	2.49	8.95	9.62	15.27	26.16	26.14	13.12	22.08	17.14	17.16	16.65	14.76
20594	M	51.11	3.96	3.44	2.7	5.31	6.17	9.8	4.34	4.1	3.06	8.97	9.23	16.06	26.69	26.35	14.39	22.31	18.4	18.57	18.27	16.53
20607	M	45.21	3.83	2.97	2.33	4.76	5.09	8.73	3.71	3.33	2.44	7.86	8.52	15.07	24.37	24.39	12.42	21.36	15.95	16.52	15.26	14.24
20604	M	46.76	3.82	2.93	2.49	4.98	5.49	8.77	3.85	3.66	2.46	7.68	8.38	13.56	23.82	17.68	11.48	19.52	15.76	17.13	17.12	14.26
20615	M	46.3	4.27	2.79	2.34	5.58	5.37	8.43	3.99	3.5	2.27	7.09	8.24	14.82	24.96	24.41	12.99	20.52	16.35	16.63	16.28	14.09
20603	M	48.47	3.51	2.89	2.46	5.29	5.83	8.72	4.32	3.78	2.08	8.85	8.58	15.39	26.38	25.91	13.48	22.31	15.21	16.32	18.49	14.66
20600	M	50.23	3.89	3.17	2.66	4.99	5.96	8.51	3.8	3.86	2.02	8.31	9.64	14.85	27.37	25.59	13.44	21.13	16.47	17.18	18.92	13.9
20601	M	50.9	4.4	3.09	2.65	5.96	6.07	8.96	4.39	3.79	2.94	9.57	9.17	16.08	27.27	25.64	13.53	22.17	17.82	17.84	18.69	15.56
20610	M	43.46	3.82	3.32	2.66	4.67	5.94	8.61	4.13	4.14	1.92	6.87	9.09	15.21	24.64	24.59	13.07	20.22	16.39	16.14	17.75	14.47
20605	M	49.28	3.88	3.18	2.71	6.15	5.44	9.15	3.77	3.83	2.62	7.85	8.45	15.61	26.47	26.26	13.58	21.83	17.14	17.49	17.37	15.16
20596	M	47.19	4.04	2.81	2.27	5.25	6.15	8.14	4.14	4.06	2.29	8.03	9.33	14.49	25.77	25.29	13.21	21.87	16.47	16.64	17.81	13.36
6655	M	43.17	3.95	2.53	2.31	4.32	5.55	8.11	3.66	3.48	2.25	6.88	7.42	15.02	22.39	21.12	11.36	19.12	15.4	16.08	15.59	13.73
18968	M	49.08	4.34	3.08	2.78	6.23	6.1	8.95	3.72	4.27	3.04	9.3	8.93	16.72	27.12	26.15	13.55	23.17	17.23	17.68	18.6	14.1
18967	M	46.88	3.96	3.01	2.59	5.48	5.86	8.32	3.71	3.82	2.04	8.46	8.19	15.03	25.09	24.98	12.99	21.05	16	17.41	15.92	14.38

20611	M	45.29	3.61	2.86	2.68	5.39	4.98	8.6	3.92	3.88	1.78	7.72	8.44	14.75	25.44	25.04	13.42	20.85	16.48	16.79	17.27	14.82
20593	M	48.64	3.79	2.9	2.81	5.42	6.16	9.36	4.23	3.62	2.46	8	10.33	15.29	26.4	25.28	13.88	21.17	17.05	17.7	17.04	14.18
20608	M	48.23	3.93	3.16	2.88	5.23	5.5	8.28	4.02	3.99	2.23	6.85	9.43	16.03	25.92	24.9	13.87	21.25	16.6	17.15	15.99	14.78
20618	M	46.56	3.83	3.1	2.34	6.25	5.84	9.11	4.17	3.84	2.61	8.12	9.2	14.75	25.42	24.65	13.07	21.91	16.8	17.16	17.47	15.51
20602	M	46.71	3.51	3.09	2.46	4.98	5.35	8.26	3.86	3.93	2.34	7.86	8.83	14.68	24.94	24.53	12.91	20.45	16.46	16.14	16.19	14.08
20609	M	49.93	4.31	3.17	2.61	5.14	5.46	8.72	4.42	3.82	2.49	8.61	9.84	16.61	26.9	28.12	14.36	23.58	18.32	18.42	18.73	15.03
14932	M	46.06	3.76	3.02	2.53	4.51	5.53	8.64	3.64	3.32	2.69	8.18	8.77	14.73	25.09	24.75	12.84	20.88	16.18	16.84	16.1	14.27
18965	M	47.92	3.78	2.84	3.25	6.09	5.28	8.66	4.11	3.69	2.52	8.9	8.82	17.7	25.65	25.56	13.57	21.44	17.39	16.83	17.44	14.43
18963	M	48.37	3.89	3	3.31	5.36	5.88	8.85	4.13	4.21	2.64	8.5	8.74	16.09	26.48	25.42	13.86	22.37	15.33	18.78	17.64	14.87
18969	M	49.85	3.79	3.21	2.77	5.18	5.53	8.85	4.41	3.69	2.55	8.05	8.62	16.34	27.19	26.68	13.26	22.78	16.4	17.32	18.53	15.5
20592	M	49.65	4.11	3.08	2.8	5.24	5.93	9.06	4.42	3.7	2.84	7.74	8.95	16.09	27.15	27.39	15.04	21.87	18.46	17.64	18.24	15.08
14945	M	46.12	4.34	3.05	2.49	5.6	6.11	8.44	3.34	3.65	2.25	7.98	8.26	14.27	23.42	22.62	12.13	19.76	14.61	16.12	17.29	13.63
20599	M	46.59	3.83	2.76	2.52	4.66	5.41	8.32	3.94	3.09	2.18	7.36	8.4	15.29	25.27	24.25	12.36	20.43	15.79	15.61	16.44	13.97
20614	M	44.26	3.53	2.86	2.18	5.13	5.53	7.51	3.34	3.58	2.46	8.08	7.58	14.15	23.45	22.66	12.6	19.44	14.59	16.04	16.57	14.62
14793	M	46.4	3.82	3.12	2.54	4.39	5.74	8.61	3.76	3.36	2.82	8.18	8.65	14.94	25.08	23.94	12.99	20.44	15.55	16.83	16.57	14.36
14055	M	48.88	4.75	3.25	2.78	5.16	5.9	9.08	3.91	3.57	2.88	8.34	9.57	16.68	26.37	26.28	14.04	21.61	16.64	16.95	18.69	14.9
14837	M	49.74	4.34	3.2	2.15	6.13	5.28	8.46	3.64	3.5	2.41	9.19	10.67	16.51	26.95	25.79	13.36	23.11	16.91	18.49	18.12	15.14
16049	M	46.44	3.97	3.08	2.26	5.29	5.86	8.63	3.77	3.88	2.44	7.77	9.23	14.65	25.36	24.43	12.53	19.54	15.71	16.71	15.93	14.7
14284	M	51.71	4.36	3.39	2.51	5.2	5.59	9.26	3.91	3.73	3.16	9.16	9.52	16.43	26.37	25.23	13.21	22.31	17.71	19.18	19.1	16.28
14285	M	49.53	3.86	2.99	2.18	4.69	5.11	8.75	3.68	3.51	2.85	9.06	9.75	16.51	26.33	25.71	13.31	21.44	17.95	17.78	19.26	14.25
14835	M	47.27	4.45	3.37	2.58	4.94	5.17	7.64	3.47	3.47	2.41	8.95	10.04	15.74	25.94	25.22	13.69	21.53	16.85	16.63	17.23	13.78
14826	M	50.8	4.66	3.03	2.42	4.9	5.91	8.65	4.11	4.07	2.69	9.67	9.68	16.18	26.93	26.06	13.38	23.01	16.39	17.78	16.99	14.96
14729	M	46.42	3.59	2.41	2.28	4.71	5.58	8.85	4.42	3.74	2.57	9.04	8.68	15.99	26.01	24.76	12.87	22.27	16.41	17.12	17.02	14.5
14842	M	48.62	4.69	3.72	2.7	5.63	5.01	8.42	3.95	3.63	2.64	9.35	9.84	15.78	26.93	25.71	13.61	22.58	17.37	17.67	17.61	14.21
16075	M	50.01	4.17	2.91	2.54	5.06	5.38	9.19	4.77	3.72	2.58	9.95	10.73	16.26	27.32	26.01	13.66	22.31	17.72	17.92	15.81	14.33
14759	M	54.67	4.98	3.92	2.75	6.04	6.59	9.61	4.75	4.49	2.73	7.66	10.19	17.93	30.06	28.11	14.8	25.46	18.9	18.4	19.36	16.36
14781	M	51.7	4.29	3.06	2.43	5.52	5.35	9.12	4.29	4.11	2.68	9.4	9.65	17.25	28.01	26.74	14.59	23.15	17.69	17.78	17.04	15.1
14838	M	48.48	4.61	3.45	2.79	5.02	5.99	8.87	4.17	3.94	2.79	7.91	9.11	16.11	26.89	25.84	13.77	21.81	17.27	17.45	17.24	14.24
14052	M	49.2	4.61	3.13	2.36	4.99	5.89	8.82	3.95	3.65	2.79	8.94	9.16	16.13	26.47	25.15	13.23	21.59	16.13	17.4	16.87	14.18
14081	M	49.24	4.18	3.31	2.48	4.81	5.08	8.28	3.83	3.67	2.9	9.65	9.11	16.49	27.1	26.13	13.56	21.55	17.04	17.7	17.84	15.11
14836	M	47.63	4.06	3.35	2.62	4.14	5.17	8.39	3.78	3.73	2.43	8.82	9.49	16.28	25.9	25.26	13.06	21.22	17.48	17.33	18.05	14.62
16121	M	45.44	4.05	3.08	2.5	5.39	5.24	8.11	3.74	4.06	2.67	8.87	8.89	15.75	25.41	24.57	12.72	20.8	17.02	16.62	17.84	14.15

14839	M	52.67	4.47	3.86	2.62	5.53	5.59	9.14	4.15	4.26	2.92	9.26	10.25	17.05	28.84	27.38	14.79	24.24	19.13	18.38	17.68	16.28
14782	M	48	4.32	3.23	2.22	4.31	5.17	8.78	3.88	4.01	2.61	9.53	9.03	15.89	25.47	24.73	13.19	21.95	16.69	18.18	16.98	14.26
14847	M	46.99	4.39	3.16	2.26	4.59	5.82	8.73	3.72	3.72	2.53	9.53	8.89	16.19	25.32	25.03	12.91	22.14	18.26	18.13	16.03	14.12
14843	M	48.96	4.07	3.02	2.57	5.29	5.32	8.45	4.31	4.13	2.78	9.8	9.76	16.47	26.32	24.95	13.16	22.28	15.94	17.64	17.13	14.4
14240	M	51.04	4.56	3.4	2.39	4.96	5.68	9.48	3.81	3.94	2.92	9.96	9.47	18.04	27.97	26.59	13.57	23.33	17.63	18.95	18.39	15.55
14841	M	48.68	4.74	3.47	2.67	5.54	5.94	8.92	4.13	4.03	2.32	8.89	9.24	17.04	26.71	25.9	14.05	23.3	16.21	17.72	18.06	15.37
14780	M	46.09	4.25	2.97	2.62	4.66	5.57	8.29	3.72	3.45	2.69	8.99	8.59	15.8	25.97	24.28	11.39	20.98	15.42	17.05	16.81	14.11
14825	M	49.4	4.23	3.21	2.57	5.07	5.86	8.81	3.74	3.87	2.81	10.7	9.39	16.43	27.72	26.44	14.2	23.4	16.59	18.68	17.98	14.44
14733	M	46.92	4.41	3.18	2.16	4.23	5.52	8.13	4.04	3.73	2.42	9.19	9.13	15.09	26.04	24.95	13.41	21.85	16.81	17.92	18.31	13.12
14792	M	48.98	3.88	3.47	2.53	5.68	6.09	8.73	3.58	4.06	2.73	9.13	9.23	16.03	26.22	25.24	12.83	21.03	17.53	17.19	18.27	15.26
14840	M	49.39	4.39	3.31	2.68	4.93	5.79	8.25	3.97	3.53	2.39	9.59	9.9	16.97	26.41	25.77	13.37	22.36	16.97	18.05	18.19	13.32
10905	M	49.93	4.21	3.22	2.53	5.02	5.83	8.65	3.55	3.86	2.4	7.9	8.89	15.7	26.49	25.21	13.4	20.92	16.98	17.05	15.36	15.47
11038	M	44.42	3.6	2.83	1.96	4.51	5.58	7.8	3.41	3.28	2.56	7.68	8.19	14.7	23.82	22.5	11.74	18.99	15.85	15.39	14.94	14.91
11030	M	42.44	3.75	2.53	2.45	4.15	4.71	8.07	3.16	3.14	1.72	7.19	8.81	13.66	23.27	21.77	11.48	19.06	14.27	14.87	14.46	13.06
11009	M	43.31	3.99	2.74	2.21	3.95	5.3	7.58	3.3	3.09	1.8	7.23	8.51	13.88	22.75	22.1	11.54	19.35	14.86	14.55	15.04	12.72
11024	M	43.37	3.84	2.95	2.84	4.05	5.16	8.28	3.37	3.27	2.12	7.15	7.78	14.32	23.07	22.62	11.18	19.91	14.99	15.2	15.03	13.37
11018	M	41.51	3.55	2.82	2.27	3.87	5.25	7.65	3.06	3.15	2.24	6.61	7.86	13.27	22.49	21.18	11.48	18.43	15.2	14.54	14.31	12.96
11021	M	42.56	3.98	2.69	2.26	4.23	5.03	8.29	3.68	3.82	2.48	7.29	7.96	14.36	22.58	21.51	10.88	18.93	15.78	15.38	15.16	13.13
11010	M	46.05	4.04	3.18	2.33	4.86	5.53	7.94	3.87	3.87	2.41	7.63	7.93	15.23	24.73	23.81	12.45	20.14	16.86	16.67	16.15	13.92
11040	M	45.98	3.7	2.79	2.51	5.42	5.64	8.25	3.69	3.94	2.26	8.23	8.67	14.43	23.19	23.06	12.04	19.45	15.38	16.35	14.51	13.53
11041	M	44.12	3.92	2.87	2.31	4.41	5.32	7.94	3.66	3.49	2.55	7.86	8.32	14.57	22.63	22.58	11.95	19.77	16.29	15.14	14.95	13.71
11034	M	43.44	3.52	3.07	2.08	3.97	4.81	7.66	3.35	3.33	2.21	8.07	7.86	14.29	23.44	22.09	11.89	18.59	14.06	14.87	14.96	12.39
10876	M	51.11	4.24	3.05	2.31	4.84	5.87	8.66	3.87	3.52	2.55	8.21	9.53	14.82	24.66	23.53	12.7	21.04	16.81	17.2	16.55	14.66
11022	M	42.22	3.53	3.02	2.46	4.23	5.71	8.29	3.42	3.41	1.87	7.64	8.11	14.43	22.79	21.67	11.43	18.96	14.9	15.58	15.46	13.68
11036	M	45.17	3.61	3.08	2.44	3.76	5.23	8.18	3.66	3.23	2.08	7.77	8.18	14.35	23.09	22.38	11.53	19.22	14.98	15.41	16.04	12.7
11004	M	42.58	3.67	2.9	2.37	3.97	4.96	7.99	3.71	3.46	2.33	6.61	7.88	13.9	23	22.03	11.44	17.94	14.28	14.78	14.43	12.56
11033	M	45.13	3.76	3.01	2.12	4.48	5.17	8.51	3.63	4.68	3.48	7.31	7.99	14.49	24.66	23.27	11.95	20.04	15.75	15.87	15.6	13.56
11023	M	42.06	3.73	2.85	1.96	3.77	4.94	8.23	3.26	3.1	1.92	6.46	7.41	14.15	22.42	22.12	11.64	19.53	14.24	15.45	16.64	13.11
11037	M	44.52	3.75	2.8	2.03	4.2	4.69	7.95	4.02	3.64	2.56	6.46	8.22	14.18	22.54	21.58	11.32	19.21	15.3	15.73	15.48	13.2
11026	M	41.81	3.88	2.95	2.17	3.89	4.87	7.64	4.15	3.46	2.25	6.55	8.09	14.31	22.96	22.59	11.83	18.87	15.16	14.97	15.02	12.94
11042	M	44.79	3.57	2.85	1.91	4.28	5.26	7.89	3.48	3.31	2.06	8.08	7.54	14.43	22.5	22.38	12.04	18.59	15.26	16.08	14.83	13.85
10891	M	43.26	3.84	3.08	2.18	4.46	4.68	8.13	3.53	3.51	2.4	6.42	8.17	14.25	22.91	22.09	11.67	18.08	15.26	16.29	15.32	13.55

10890	M	46.53	3.94	3.07	2.64	4.39	5.21	8.24	3.71	3.62	2.32	7.97	7.64	14.51	24.07	22.77	11.61	19.61	15.46	14.76	16.98	14.52
11039	M	42.17	3.86	2.74	2.34	3.9	5.3	7.75	3.42	3.51	2.37	8.24	8.1	13.55	22.03	21.47	11.46	17.47	15.48	14.99	16.13	14.01
11006	M	42.58	3.95	2.84	1.93	4.96	5.26	7.77	3.55	3.3	2.44	7.36	8.28	13.66	23.14	22.44	10.61	18.89	16.46	16.12	15.02	13.3
11020	M	46.8	3.88	3.29	2.39	4.16	5.44	9.08	3.75	3.68	2.69	8.7	8.77	14.9	25.03	23.93	12.86	20.92	16.46	16.72	16.68	13.75
11031	M	42.6	3.97	3.17	2.63	4.23	5.67	7.75	4.34	3.47	2.62	7.59	8.18	13.57	23.08	22.09	11.24	18.78	15.43	16.01	15.36	12.12
11019	M	42.98	3.56	3.17	2.68	3.76	5.48	8.31	3.65	3.92	1.87	7.99	7.97	13.28	22.18	21.57	11.32	17.64	15.35	15.45	14.99	13.06
11028	M	42.89	3.27	2.95	2.04	4.03	5.69	7.83	3.55	3.7	2.49	7.16	7.94	12.89	21.97	21.4	11.52	17.93	15.5	15.07	15.02	13.23
11027	M	45.45	3.8	3.27	2.04	4.26	5.25	8.28	3.12	3.41	2.39	7.04	7.76	14.14	23.86	22.98	12.21	19.57	15.26	15.68	16.16	14.23
11001	M	43.82	4.07	3.12	2.4	4.42	5.65	7.78	3.99	3.58	2.58	6.49	8.33	15.12	21.43	23.05	11.56	20.28	16.33	16.07	16.9	13.64
11029	M	41.23	4.02	2.94	2.84	4.4	5.02	7.54	3.63	3.46	2.26	7.19	8.53	14.22	22.14	23.33	11.64	19.81	15.22	15.79	17.17	12.44
11043	M	44.95	3.91	3.29	2.65	4.97	5.78	7.35	3.53	3.37	2.24	7.32	8.24	13.97	24.11	23.38	12.2	18.99	16.14	16.11	13.91	13.61
11032	M	42.91	3.81	2.97	2.34	3.93	4.76	7.99	3.78	3.14	2.05	6.87	7.77	14.6	22.59	22.26	10.45	19.25	14.97	15.34	14.14	13.26
10889	M	40.94	3.59	3.13	2.38	4.24	5.23	7.76	3.18	3.54	2.24	7.22	7.91	14.01	23.04	22.25	11.79	19.01	14.33	14.63	15.3	12.46
10888	M	45.55	3.81	3.32	2.47	4.63	4.89	8.06	3.99	3.34	2.34	7.7	8.94	14.73	25.1	24.76	12.11	20.1	17.04	16.38	15.4	14.41
11002	M	48.76	4.02	3.39	2.75	4.84	5.83	8.47	3.77	3.32	2.54	7.51	8.76	15.34	25.52	24.41	12.97	21.53	16.77	17.09	16.13	14.43
11007	M	42.2	3.72	2.88	2.24	4.38	5.27	7.79	3.55	3.46	2.01	6.25	8.05	13.67	22.46	21.75	11.21	18.55	15.74	14.83	15.46	13.31
10858	M	43.2	3.91	3	2.49	3.79	4.77	7.25	3.29	3.55	2.23	7.3	8.18	14.67	23.42	22.72	12.75	19.91	15.64	15.66	15.99	12.72
11003	M	40.76	3.51	3.02	2.49	4.51	4.69	7.46	3.23	3.32	2.38	6.94	7.39	13.46	21.93	21.13	11.1	18.87	14.91	14.91	13.72	12.18
12339	M	45.89	3.79	2.97	2.44	4.66	5.27	8.22	3.72	3.82	2.26	8.48	7.66	14.81	23.51	22.41	11.63	19.7	13.53	16.02	17.36	13.87
12287	M	43.08	3.95	3.12	2.28	3.96	5.35	8.13	3.36	3.4	2.38	8.27	8.28	13.61	23.73	23.55	12.53	18.63	14.22	15.95	16.15	13.72
12343	M	47.49	4.2	3.22	2.23	5.04	5.65	8.48	4.35	3.33	2.69	9.72	9.13	15.41	24.68	24.07	12.63	21.15	16.52	16.92	16.93	14.65
12295	M	44.94	3.39	2.66	2.74	4.46	5.62	7.87	3.76	3.58	2.4	8.31	8.39	14.3	23.46	22.75	11.82	18.55	15.21	15.58	15.6	12.66
12298	M	45.84	3.65	2.98	2.7	3.87	5.33	8.34	4.67	3.88	2.19	7.34	8.78	14.86	24.48	23.32	11.97	19.77	15.52	15.5	15.74	13.31
12286	M	48.76	4.46	3.18	2.41	4.51	5.09	8.02	4.38	3.74	2.28	7.83	8.76	15.55	25.62	24.33	12.86	20.87	17.38	16.39	14.6	14.46
12268	M	46.32	4.06	3.01	2.47	5.17	4.89	8.16	3.91	3.58	2.32	7.82	9.17	15.01	24.31	23.32	12.33	20.28	16.33	16.5	15.32	13.9
12265	M	47.74	4.01	3.22	2.3	5.54	5.73	8.37	3.93	4.18	2.74	9.08	9.1	15.56	25.12	24.6	12.76	20.54	17.39	17.63	16.19	14.56
3800	M	42.37	3.89	2.46	2.17	4.67	4.58	7.98	3.58	3.51	2.04	7.64	8.61	13.78	22.49	21.8	11.13	18.59	15.24	15.3	13.18	12.59
12270	M	46.97	4.34	3.65	2.25	5.09	5.37	7.94	3.81	3.41	2.52	8.54	9.31	15.32	25.93	24.39	12.89	20.46	17.45	17.73	16.61	14.86
12272	M	44.14	3.15	2.91	2.58	5.23	4.63	8.06	4.12	3.57	2.05	7.11	7.67	14.21	23.61	22.23	12.32	18.63	16.24	15.54	15.48	13.24
12378	M	42.73	4.05	3.15	2.23	3.73	4.78	7.68	3.51	3.34	2.06	6.88	8.61	12.28	22.21	22.43	11.39	18.26	15.38	15.93	15.85	13.61
12341	M	49.63	4.47	3.26	2.65	5.66	6.21	8.58	4.1	3.76	2.49	8.68	8.88	15.68	25.34	24.77	13.56	20.52	16.95	17.47	18.08	15.51
12354	M	45.68	3.89	3.24	2.33	4.73	5.52	8.28	3.81	3.77	2.69	9.31	8.27	15.64	24.34	23.43	12.74	20.25	16.78	16.04	15.65	13.66

12283	M	49.9	3.99	3.09	2.55	5.79	5.25	8.75	3.74	3.65	2.28	10.27	9.42	16.64	26.39	25.22	13.85	22.1	17.49	18.48	16.67	13.86
12299	M	41.85	3.34	2.93	2.21	4.04	4.21	7.6	3.61	3.55	2.26	7.49	7.98	13.37	23.42	22.96	11.38	18.38	15.04	14.89	14.42	13.54
12377	M	41.91	3.99	3.04	2.14	3.64	5.01	7.97	3.24	3.86	2.34	7.07	8.53	13.25	22.56	22.52	12.21	18.18	15.23	15.75	16.67	12.95
12346	M	44.25	3.97	3.21	2.38	4.46	5.74	8.12	3.46	3.31	2.09	9.83	8.46	14.18	24.25	23.62	12.94	18.81	15.35	15.93	16.03	14.87
12292	M	47.77	3.74	3.21	2.48	4.58	5.86	8.51	3.8	3.76	2.27	7.94	9.09	15.36	25.02	24.11	13.21	20.97	16.98	17.16	17.98	15.06
12342	M	42.51	3.85	3.25	2.17	4.87	5.42	8.19	3.44	3.71	2.18	8.03	8.22	14.12	22.87	22.26	12.17	18.63	14.76	15.2	14.6	13.4
12344	M	42.18	3.87	3.06	2.09	5.55	4.82	7.62	3.66	3.65	2.28	8.1	8.13	13.64	23.52	22.58	11.95	19.07	15.49	14.69	16.19	12.69
12340	M	46.05	4.09	3.17	2.38	4.99	5.77	8.44	4.09	3.86	2.13	8.67	8.92	15.07	25.14	23.4	12.09	20.27	16.69	17	17.32	14.09
12297	M	49.88	4.25	3.34	3.08	5.22	5.67	9.49	4.08	3.96	2.35	9.63	9.25	16.03	26.57	25.31	13.34	20.89	17.66	17.94	15.9	14.87
12285	M	45.65	4.05	2.86	2.11	4.14	4.94	7.49	3.24	3.6	1.92	8.11	8.36	14.39	24.01	21.86	12.48	19.37	15.91	16.41	13.94	14.2
12327	M	40.52	3.88	2.64	2.23	4.53	5.26	7.35	3.67	3.35	2.4	7.3	8.24	13.94	23.5	22.84	12.19	17.76	14.53	14.45	14.32	12.8
12328	M	50.51	4.53	3.31	2.6	4.82	5.92	9.16	4.47	4.1	2.83	8.81	9.5	16.24	26.64	25.96	13.54	21.63	18.24	17.56	18.68	15.76
12337	M	49.56	4.41	3.28	2.67	4.92	5.37	8.09	4.03	4.06	2.86	8.43	9.18	16.02	26.62	25.16	13.11	21.33	16.8	17.28	17.25	13.98
12293	M	47.67	3.42	3.36	2.23	5.42	5.51	7.83	3.86	3.99	2.64	7.03	7.67	14.13	22.48	22.56	11.67	20.22	16.27	16.47	16.07	13.5
12326	M	48.33	4.05	3.26	2.18	5.04	5.62	7.82	3.93	3.58	2.41	8.63	8.72	14.69	24.64	24.26	12.57	19.93	16.41	17.06	17.59	15.24
12269	M	45.17	3.95	3.14	2.22	5.54	5.52	8.31	3.81	3.96	2.35	8.73	8.72	14.16	23.82	23.03	12.15	19.35	16.09	17.43	16.14	13.97
12284	M	47.13	4.03	3.09	2.57	4.78	5.23	8.16	4	3.88	2.42	9.15	8.81	15.45	25.22	24.22	12.27	21.17	16.59	17.39	16.4	14.77
12345	M	43.84	3.86	3.03	2.17	4.21	4.38	7.35	4.01	3.42	2.25	5.85	7.7	14.16	21.22	23.99	12.23	19.31	16.11	14.89	15.68	12.62
12294	M	45.92	3.83	3.06	2.35	4.23	4.75	7.91	3.96	4.02	2.86	8.58	8.27	13.41	24.2	23.29	12.29	19.64	15.78	15.15	16.06	13.86
12224	M	48.22	4.1	3.09	2.63	5.03	6.08	8.46	3.88	3.95	2.29	8.7	9.05	16.42	27.2	25.99	13.2	22.54	17.49	17.43	17.25	14.08
12350	M	42.41	3.86	3.06	2.52	4.64	5.54	8.04	3.55	3.22	2.35	8.71	7.95	14.94	24.06	22.55	11.73	19.23	15.51	15.32	15.57	12.55
12291	M	47.57	3.87	3.24	2.51	4.3	5.14	8.14	3.49	3.55	2.47	8.02	8.19	15.71	24.32	23.37	11.89	19.44	15.67	16.01	15.86	13.76
12271	M	46.7	4.05	3.24	2.44	5.13	5.57	8.43	5.37	3.67	2.22	7.93	8.86	14.92	25.21	23.75	12.33	20.18	17.23	17.84	16.92	15.42
12349	M	42.4	3.87	3.11	2.25	4.32	5.39	8.57	3.35	3.29	2.39	7.29	7.93	14.71	23.66	22.92	12.04	19.07	14.68	14.92	15.21	13.73
20462	M	50.17	4.33	3.19	2.74	4.81	6.52	8.89	4.11	3.84	2.97	7.86	9.72	16.75	24.31	25.81	13.14	23.12	17.95	18.22	21.21	14.96
20458	M	50.87	3.94	3.11	2.59	5.13	5.86	9.16	4.28	3.85	2.67	7.84	8.72	16.32	25.27	24.26	12.54	21.08	17.21	17.59	16.87	14.5
20450	M	49.65	4.16	3.14	2.83	5.08	5.38	9.17	4.03	4.04	2.58	8.44	9.47	16.09	25.79	25.38	13.1	22.62	18.61	18.22	17.75	16.11
20467	M	51.99	4.6	3.36	2.25	4.94	6.17	8.82	3.85	4.05	2.57	8.11	9.68	16.3	27.1	26.31	13.65	22.28	17.41	18.02	19.42	14.12
20439	M	51.47	4.83	3.26	2.49	5.13	5.33	8.53	3.65	3.76	3.95	8.55	9.37	16.75	27.47	26.09	13.64	23.47	18.02	17.82	18.14	15.18
20465	M	53.7	4.5	3.48	2.81	5.43	6.07	9.68	4.2	4.01	2.3	7.97	9.35	17.43	26.76	26.58	13.22	23.22	19.2	19.63	20.13	15.01
20436	M	49.46	4.55	3.19	2.77	5.15	5.66	8.93	3.84	3.92	3.05	9.19	9.25	16.56	26.57	25.8	13.42	23.4	18.23	18.02	18.27	14.61
20448	M	49.32	4.09	3.14	2.55	4.18	5.76	8.92	4.17	3.6	2.46	8.48	9.16	15.43	27.46	25.72	13.06	22.19	17.28	17.16	16.99	14.51

20420	M	43.58	3.69	2.98	2.14	3.91	4.41	7.67	3.95	3.18	2.41	6.89	7.67	13.51	21.57	22.38	11.72	18.69	15.25	15.86	14.73	14.34
20416	M	48.24	4.35	3.43	2.15	4.54	5.75	8.71	4.13	3.24	2.54	7.76	9.68	14.58	25.93	25.81	13.02	20.69	17.85	17.27	16.75	16.24
20442	M	47.55	4.27	3.2	2.09	4.43	6.21	8.51	4.09	4.07	2.4	6.76	8.72	16.19	26.13	25.02	12.85	22.18	17.44	17.47	16.56	13.81
20470	M	51.95	5.01	3.46	2.6	4.74	5.47	9.15	4.22	4.06	2.55	8.41	10.19	16.51	28.1	26.53	14.15	23.97	18.83	18.08	20.28	15.95
20440	M	48.46	3.89	3.22	2.69	4.49	5.42	8.51	3.83	3.87	2.16	7.96	8.94	16.73	26.17	24.97	12.59	22.32	16.21	17.12	18.51	14.22
20475	M	50.76	4.28	3.08	2.71	4.36	5.53	8.8	4.27	3.84	3.04	7.94	9.07	16.64	27.44	25.77	13.37	21.6	18.39	18.88	19.85	15.34
20421	M	47.68	4.19	2.96	2.74	4.41	4.77	8.03	4.05	3.39	2.81	7.39	7.89	14.66	23.37	24.27	12.54	20.27	15.85	16.19	17.33	13.73
20464	M	52.67	3.96	3.52	2.67	5.36	6.63	9.14	4.47	4.07	2.86	9.61	9.54	15.92	26.27	26.18	12.83	22.08	18.97	19.22	19.73	14.87
20469	M	50.56	4.28	3.29	2.55	4.41	6.32	8.68	4.09	3.81	2.53	8.31	9.55	16.38	26.71	25.73	13.09	22.87	17.77	17.92	18.47	14.93
20419	M	44.18	4.22	3.08	2.36	4.52	4.83	8.42	4.02	3.59	2.17	7.64	8.28	14.41	23.69	23.71	12.15	19.7	16.43	16.24	15.77	14.44
20417	M	42.33	3.57	2.72	1.87	4.26	4.69	7.46	3.98	3.19	2.39	7.86	7.89	13.62	22.97	23.07	12.13	18.87	15.64	15.49	15.78	12.07
20441	M	52.04	4.53	3.16	2.32	5.17	5.52	9.54	4.37	4.04	2.76	8.89	9.73	17.09	27.34	26.53	13.36	23.55	19.1	18.26	20.63	15.29
20431	M	49.65	4.11	3.44	2.37	4.33	5.26	8.71	4.26	3.66	2.67	8.38	9.01	16.44	26.79	25.2	14.05	22.53	17.33	17.36	19.55	15.31
20430	M	51.87	4.08	3.29	2.45	5.36	6.04	9.18	4.35	3.95	2.27	10.45	9.79	17.58	27.9	26.39	13.59	23.14	18.04	18.85	18.66	16.16
20472	M	50.74	4.73	3.39	2.79	4.83	5.74	8.71	4.02	3.93	2.48	8.9	9.74	17.11	26.66	25.87	13.02	22.92	17.61	17.5	17.59	14.45
20468	M	50.13	4.37	3.31	2.1	4.92	6.55	9.31	4.12	3.48	2.31	9.11	9.42	17.26	27.48	26.35	13.87	23.1	18.56	18.43	18.54	15.37
20457	M	52.31	4.18	3.33	2.92	4.75	5.66	8.89	4.12	4.01	2.72	8.65	9.59	17.28	28.51	26.61	14.28	23.38	17.8	18.52	18.12	14.49
20428	M	44.38	4.5	3.3	2.87	4.89	5.87	8.35	3.99	3.15	2.69	6.76	8.32	14.35	24.81	23.76	12.25	19.87	15.03	16.28	13.55	14.62
20452	M	48.8	4.03	3.38	2.49	4.82	5.8	8.62	4.16	3.87	2.29	9.19	9.45	16.83	26.04	25.95	12.98	23.01	18.05	18.05	18.24	15.51
20423	M	42.33	3.61	3.12	2.03	4.1	4.87	7.67	3.46	3.22	2.41	7.4	7.93	13.41	21.61	22.3	12.02	19.37	15.37	15.34	16.16	13.27
20455	M	47.67	4.46	3.15	2.25	4.79	5.37	8.21	3.87	4.08	2.21	8.97	8.49	15.86	25.72	24.38	12.13	21.78	15.94	16.08	16.13	14.06
20451	M	48.04	3.52	3.15	2.19	4.47	5.44	8.53	3.98	3.79	2.63	9.73	8.93	16.48	25.89	25.08	12.82	20.79	17.15	18.03	16.57	15.24
20432	M	53.08	4.27	3.26	2.51	4.52	5.91	8.96	4.02	3.78	2.57	9.98	9.35	16.31	26.86	25.58	13.27	22.69	18.15	17.93	18.26	15.23
20418	M	47.78	3.95	2.94	2.21	4.51	4.93	8.26	3.89	3.06	2.22	8.91	9.19	14.28	23.43	24.69	12.49	20.74	16.07	15.97	15.32	14.13
20463	M	49.88	4.31	3.46	2.62	4.75	5.36	8.98	4.37	3.86	2.88	7.84	9.55	17.04	27.4	27.12	13.89	23.87	17.84	18.14	18.64	14.94
20453	M	52.06	4.21	3.28	2.73	4.49	5.43	8.97	4.12	3.98	2.37	9.17	9.15	17.15	27.42	26.64	13.46	22.87	17.56	18.5	19.31	15.21
20446	M	50.06	4.24	3.26	2.46	4.03	5.83	8.57	3.87	3.82	2.42	7.06	9.22	15.65	26.79	26.72	13.26	23.66	17.33	17.1	17.25	14.47
20461	M	52.13	4.79	3.62	2.89	5.05	6.37	8.91	4.08	3.96	2.8	9.36	8.83	17.87	28.2	26.7	13.79	23.68	18.49	18.95	19.82	15.14
20454	M	49.15	4.33	3.13	2.58	4.49	5.05	8.36	4.01	3.63	2.64	10.05	9.19	15.7	25.37	25.34	13.26	22.36	16.83	18.45	16.64	14.77
20447	M	51.52	4.28	3.63	2.99	5.32	5.95	9.04	4.75	3.69	2.91	9.54	10.34	17.18	23.87	25.87	13.49	23.77	18.21	18.29	18.04	14.67
6678	M	48.39	3.58	3.09	2.43	4.53	5.84	8.41	4.03	3.44	2.69	7.23	7.16	14.24	23.69	23.26	11.55	20.09	16.74	17.64	17.41	13.82
20459	M	51.45	4.22	3.25	2.32	4.62	6.24	8.75	4.03	3.88	3.76	8.78	8.74	17.32	26.28	25.28	13.52	22.41	17.56	18.58	18.32	14.92

20422	M	42.92	3.88	3.11	2.46	3.97	5.27	7.73	4.04	3.26	2.34	7.26	7.33	14.55	22.8	22.33	12.03	20.58	15.58	15.27	16.24	13.77
20443	M	51.81	4.18	3.23	2.24	4.06	5.86	9.02	3.71	3.84	2.76	9.71	9.34	16.79	26.04	25.19	12.39	22.3	17.45	17.91	18.26	14.88
20435	M	48.81	4.74	3.35	2.42	4.53	5.92	8.41	4.02	3.99	2.69	8.44	9.67	16.02	27.33	25.49	13.21	21.55	17.2	17.29	18.03	14.32
20471	M	52.63	4.82	3.36	2.45	5.04	6.31	8.9	4.28	4.01	2.62	8.96	9.46	17.51	28.57	27.05	13.98	23.41	18.09	18.71	19.45	13.95
20476	M	52.19	4.16	3.67	2.67	5.46	5.81	9.32	3.93	3.92	3.12	8.25	9.36	17.27	27.44	26.44	13.93	22.65	19.33	18.55	18.79	16.17
20449	M	49.18	4.02	3.08	2.68	4.45	5.51	8.79	4.13	3.72	2.9	9.95	9.61	16.16	26.11	25.25	13.78	21.38	17.85	17.93	18.44	15.41
20415	M	43.22	3.4	2.91	2.31	3.49	4.64	7.52	3.49	3.29	3.95	7.51	6.99	13.94	22.27	22.26	11.17	18.84	15.07	15.07	15.71	13.24
20429	M	42.72	3.83	2.67	2.31	3.96	4.83	7.2	3.57	3.63	2.6	7.48	7.33	14.33	22.96	21.89	10.85	18.76	14.66	15.62	14.05	12.5
20425	M	43.74	3.75	3.03	2.31	4.48	5.54	8.06	3.48	3.32	2.65	6.47	7.49	14.43	22.21	22.54	11.93	20.79	15.7	16.29	16	13.79
20438	M	50.68	4.09	3.04	2.24	4.81	5.42	8.63	3.87	3.56	2.49	10.84	9.44	16.97	27.98	25.31	13.56	23.1	18.14	17.49	17.15	14.37
20466	M	52.49	4.24	4.11	2.69	4.95	6.02	8.87	4.32	3.96	2.69	7.64	8.56	16.31	26.08	26.35	13.59	22.12	18.43	19.21	20.68	15.5
6676	M	49.91	4.4	3.1	2.23	5.19	4.88	8.53	4.02	3.24	2.23	8.19	8.88	15.36	26.22	24.69	12.49	21.01	16.42	16.09	17.86	14.11
20433	M	50.77	4.61	3.06	2.86	4.78	6.39	8.99	4.19	3.94	2.75	9.4	9.84	16.91	27.08	26.07	13.46	23.51	18.26	18.65	18.78	14.54
20474	M	52.26	4.81	3.42	2.71	5.06	6.03	8.87	4.64	4.23	4.67	9.51	9.73	17.24	28.12	27.71	14.11	24.11	18.63	18.79	18.41	15.56
20426	M	43.21	3.28	3.01	2.29	4.08	5.46	8.14	3.61	3.57	2.29	7.2	7.69	13.09	22.94	22.22	11.21	18.94	15.24	16.05	14.91	13.85
20445	M	41.19	4.27	2.47	2.11	4.14	4.84	7.63	3.44	3.27	2.12	7.85	7.58	13.56	22.28	21.6	11.61	18.46	14.13	14.89	14.52	12.46
20444	M	51.58	4.07	3.02	2.82	5.16	5.77	8.77	3.99	4.57	2.75	7.64	9.29	16.3	25.48	25.16	13.41	21.94	17.96	18.13	17.05	15.18
20427	M	41.36	3.82	2.63	2.26	3.86	4.82	7.78	3.69	3.41	2.38	7.2	7.62	14.03	21.36	21.82	11.68	19.86	14.92	16.14	14.45	13.24
20434	M	47.5	4.18	3.38	2.28	4.05	5.38	8.84	3.94	3.99	2.61	8.87	9.48	15.48	27.08	25.5	13.43	21.11	18.14	17.56	17.37	14.17
21445	M	48.62	3.61	3.26	2.38	4.65	5.25	8.84	4.09	3.93	2.8	6.53	9.17	16.22	24.66	24.89	12.92	21.69	16.79	17.13	16.57	14.51
20473	M	49.12	3.72	3.35	2.81	4.88	5.54	8.54	4	3.46	2.75	8.42	10.27	17.16	27.48	25.81	13.83	22.38	17.47	17.85	17.71	13.97
20424	M	44.07	3.76	3.06	3.01	3.94	5.61	8.14	3.64	3.39	2.85	8.37	7.47	14.42	21.72	23.08	12.19	20.27	13.77	16.46	16.77	13.86
11444	M	44.15	3.61	2.79	2.54	5.35	4.95	8.24	3.99	3.72	2.68	7.25	8.6	14.48	24.15	22.89	12.14	18.77	15.29	15.04	15.2	12.78
9435	M	47.66	4.06	3.74	2.88	5.07	5.46	8.65	4.03	3.9	2.67	7.81	8.65	15.74	24.91	24.27	12.42	21.19	17.54	16.89	17.43	14.23
20254	M	44.27	3.93	3.31	2.27	5.03	5.63	8.57	3.58	3.75	3.11	8.95	8.78	13.74	25.11	23.56	12.59	19.49	17.16	17.05	14.04	13.25
829	M	45.7	3.93	2.93	2.17	5.04	5.85	8.24	3.98	4.06	2.25	6.85	8.29	14.12	23.38	23.63	12.49	18.74	15.51	16.23	13.55	13.99
20235	M	46.73	3.79	3.13	2.35	5.07	5.84	8.48	3.66	4.1	2.41	8.16	8.69	14.67	24.76	24.51	12.63	20.31	16.43	17.01	16.84	13.87
12537	M	44.07	3.64	3.09	2.12	4.35	4.86	8.31	4.33	3.89	2.23	8.56	7.64	14.34	23.35	21.85	11.67	18.34	16.09	15.53	15.44	12.63
6679	M	42.77	3.64	2.56	2.29	4.97	5.37	8.08	3.71	3.87	2.36	6.64	7.27	13.59	22.36	21.6	11.25	17.77	15.82	15.77	16.22	13.4
9434	M	47.05	3.41	3.16	2.59	5.34	6.27	8.08	3.85	3.73	2.23	7.62	8.62	13.77	24.77	23.62	12.11	20.62	16.94	16.84	16.68	13.88
17590	M	42.25	3.57	2.65	2.24	4.86	5.81	8.41	3.76	3.96	2.34	8.91	8.36	14.83	24.23	23.22	12.86	20.32	15.88	16.19	15.12	13.45
6677	M	43.85	3.34	3.03	1.99	4.88	5.52	7.98	3.82	3.72	2.22	6.64	7.75	13	22.19	22.56	11.28	18.19	15.06	15.47	16.58	12.01

11110	M	46.67	3.63	3.37	2.39	4.83	6.17	8.61	3.75	3.67	2.71	8.03	8.28	15.07	24.96	23.16	12.53	19.86	16.4	16.81	17.85	13.67
19195	M	42.42	4.33	3.03	2.16	4.87	6.18	8.2	4.32	3.67	2.06	8.03	8.22	15.61	23.52	24.64	12.27	20.24	16.6	16.82	15.1	13.29
841	M	43.92	3.53	2.95	2.15	5.11	5.34	7.87	3.51	3.53	3.86	9.83	9.01	14.62	23.98	23.55	11.85	19.56	15.86	15.88	13.41	12.95
12533	M	45.12	3.66	3.04	2.34	4.43	5.83	8.56	4.03	3.87	2.47	8.13	8.71	14.91	23.82	23.59	12.07	21.01	16.17	16.08	15.08	13.03
10629	M	48.31	3.49	3.01	2.29	5.07	5.88	8.08	4.14	3.93	2.43	7.81	8.5	14.87	24.34	24.22	12.26	20.28	15.39	17.16	17.98	13.93
6675	M	49.21	3.56	3.35	2.55	5.37	5.84	9.08	4.27	3.91	2.49	8.68	9.15	15.25	24.56	24.49	13.29	20.67	17.39	17.51	18.48	12.91
20255	M	45.32	4.08	3.12	2.32	5.11	5.25	8.21	3.89	4.02	2.34	7.87	8.27	15.07	24.42	23.91	13.06	19.77	16.37	16.04	15.74	13.6
16344	M	43.43	4.21	2.96	2.15	3.92	5.31	8.31	4.01	3.26	1.85	6.59	7.95	14.61	23.93	23.26	11.53	19.79	14.64	14.82	13.57	12.49
9436	M	46.49	3.91	3.07	2.56	4.79	4.96	8.27	3.85	3.73	2.32	7.32	8.89	15.18	24.46	23.44	11.76	20.44	16.86	16.53	16.57	13.87
11111	M	50.09	4.25	3.23	2.25	5.27	5.64	8.38	4.05	3.89	2.63	8.36	8.96	15.61	26.86	24.29	12.4	21.62	17.62	16.73	16.03	13.33
20242	M	44.3	3.89	3.62	2.76	4.94	5.88	7.84	3.31	3.51	2.56	7.66	8.07	14.42	24.47	23.54	12.09	20.09	15.45	15.74	16.8	12.48
6670	M	45.64	3.27	2.71	2.57	4.38	4.72	8.06	3.51	3.36	2.47	7.86	8.57	14.6	23.86	23.31	13.36	19.57	15.43	15.65	14.37	13.74
16343	M	43.95	4.14	3.12	2.36	4.08	4.73	8.26	3.98	3.3	3.63	7.86	8.14	14.24	23.67	22.78	11.44	19.25	15.61	15.44	13.84	13.15
19207	M	39.39	3.24	2.95	2.08	4.14	4.81	7.51	3.79	3	2.25	7.72	7.49	15.22	21.32	21.76	10.85	18.44	14.96	14.18	13.55	12.49
19838	M	42.53	3.57	2.66	2.03	4.13	5.57	7.93	3.54	3.52	2.14	7.16	7.96	13.15	21.45	21.7	11.33	17.34	15.92	15.51	15.42	12.76
20236	M	44.74	3.96	3.28	2.43	5.93	5.84	8.46	3.99	4.02	2.38	8.24	8.18	14.67	23.54	22.92	11.81	20.25	16.96	15.92	15.37	12.73
19211	M	42.09	3.49	2.98	2.25	4.45	4.73	7.85	3.39	3.48	2.23	7.4	8.31	13.98	21.2	22.28	11.56	19.67	14.14	14.96	13.38	12.32
19205	M	44.72	3.45	2.91	2.59	4.89	5.13	8.39	4.37	3.93	2.34	8.56	8.39	15.31	23.11	23.12	11.58	19.89	16.84	16.39	13.43	13.42
11112	M	48.59	4.19	3.62	2.69	5.16	5.76	8.43	4.71	3.79	2.43	6.62	8.96	15.54	26.01	24.98	12.56	21.45	16.95	17.1	16.92	14.74
20256	M	42.17	3.8	3.02	2.28	4.6	5.07	8.18	3.82	3.82	1.95	7.71	8.06	14.12	24.8	23.68	12.95	19.6	16.34	16.34	16.42	12.68
840	M	41.49	3.69	3.09	2.4	5.39	5.19	8.19	4.01	4.09	2.51	6.58	8.25	14.31	24.42	23.71	11.97	19.55	16.74	16.32	15.09	14.05
9438	M	47.09	3.71	3.18	2.49	5.18	5.13	8.24	4.13	3.96	2.65	9.14	8.44	14.96	25.28	23.37	11.97	20.62	16.46	17.08	17.43	14.12
6674	M	50.36	4.45	3.28	3.01	5.83	5.26	8.86	4.05	3.49	2.45	7.92	8.65	15.01	24.89	25.16	13.22	20.83	17.05	17.34	18.42	13.98
9437	M	48.85	4.07	3.33	1.97	5.04	5.27	8.09	3.98	3.75	2.65	7.36	8.19	14.84	24.86	23.43	12.22	20.33	16.35	16.88	17.65	14.58
17583	M	40.42	3.03	2.62	2.18	4.74	5.02	7.43	3.41	3.5	2.15	6.69	7.07	12.65	22.08	21.22	11.79	18.25	14.42	14.66	14.27	12.47
17291	M	40.8	3.42	2.93	1.92	4.45	4.73	7.74	3.54	3.35	2.54	6.81	7.67	12.96	21.65	20.75	11.06	17.66	14.07	15.03	14.84	11.07
17305	M	41.07	3.34	3.01	1.97	5.49	5.04	7.86	3.38	3.68	2.08	7.6	7.71	12.78	21.48	20.74	11.35	17.96	14.83	14.87	13.1	12.16
17293	M	42.98	3.59	3.02	2.62	5.3	5.69	7.83	3.69	3.34	2.39	7.73	8.27	13.58	22.44	21.63	12.24	18.04	15.55	16.12	14.49	12.35
17301	M	39.49	3.32	2.89	2.22	4.84	5.68	8.41	3.91	4	1.85	6.93	7.46	13.32	22.18	20.68	11.68	17.73	14.16	14.25	14.93	12.2
17306	M	36.69	3.13	2.82	2.43	4.73	5.26	7.84	3.59	3.58	2.28	6.09	6.86	12.27	20.86	19.74	11	16.77	12.57	13.81	12.49	10.85
17303	M	39.19	3.36	2.91	2.15	4.51	5.73	7.96	3.39	3.62	2.45	7.17	7.05	13.81	21.68	20.29	10.91	16.89	13.89	15.32	13.81	11.88
17308	M	44.18	3.73	3.16	2.31	4.95	5.59	8	3.7	4.13	2.66	6.97	8.21	15.37	23.63	22.09	11.65	19.58	15.55	15.6	14.87	12.68

17294	M	43.98	3.55	3.33	2.41	5.53	4.99	8.08	5.18	4.01	2.37	7.56	8.29	14.44	22.95	22.06	12.32	19.21	14.62	15.53	14.73	13.06
17283	M	43.58	3.86	2.84	2.74	4.83	5.28	8.45	4.07	4.29	2.64	7.08	8.04	14.35	22.57	20.83	11.33	18.57	15.13	15.66	15.28	12.24
17295	M	37.54	3.34	2.85	1.92	4.37	4.92	7.75	3.74	3.63	2.24	7.15	6.69	13.27	21.7	20.21	11.09	17.16	12.64	13.57	13.23	11.3
17307	M	38.61	3.39	3.03	2.19	4.45	5.69	8.01	3.75	4	2.26	7.03	6.84	13.14	21.57	20.18	10.5	17.79	13.59	15.07	14.38	11.82
17300	M	40.39	2.95	3.11	2.05	4.55	5.07	7.73	3.77	3.37	2.43	7.49	7.11	13.48	21.96	21.04	11.25	17.13	14.08	14.97	13.81	11.64
17299	M	43.78	3.46	3.22	2.47	5.34	5.2	8.19	4.29	3.62	2.76	8.59	7.68	14.4	22.65	21.43	11.58	18.67	14.3	15.26	14.25	11.68
17290	M	39.85	3.53	2.76	1.92	4.71	5.81	7.88	4.13	3.65	2.59	6.93	8.08	13.14	20.92	20.31	11.1	17.64	14.8	14.77	12.62	11.26
17287	M	43.01	3.88	3.02	2.77	5.36	4.68	8.43	3.76	3.69	2.18	7.31	8.35	13.39	22	20.95	11.31	18.25	14.81	14.63	13.83	12.56
17302	M	42.93	3.38	2.83	2.27	5.52	5.06	8.36	3.78	3.96	2.97	7.91	8.06	13.92	22.25	21.2	11.16	18.54	14.92	16.22	13.12	12.85
17286	M	42.88	3.47	3	2.46	5.29	4.92	8.32	3.85	3.96	2.46	7.47	7.86	14.51	22.73	22.04	11.58	18.89	15.03	16.27	15.03	12.53
17289	M	39.12	3.12	3.02	2.01	4.41	4.85	7.72	3.67	3.49	2.36	7.01	7.6	12.64	21.31	20.05	10.7	16.94	13.44	14.67	13.4	11.51
17288	M	40.34	3.22	2.81	2.23	4.63	5.54	7.48	4.26	3.95	2.86	7.68	7.12	13.48	21.74	20.38	11.24	17.56	14.27	14.92	12.64	12.15
17284	M	36.55	3.11	2.67	1.83	4.18	5.26	7.09	3.78	3.49	1.97	6.55	6.73	11.81	19.95	19.34	10.48	15.89	11.61	14.2	13.08	10.72
17285	M	38.54	3.52	2.61	2.25	4.59	4.93	7.85	3.77	3.9	1.93	7.17	8.01	13.5	22.22	21.23	11.39	18.34	13.58	15.81	13.91	11.6
13974	M	42.66	3.82	2.99	2.24	4.24	5.5	8.48	4.13	4.59	3.03	7.47	7.96	14.15	22.09	20.92	11.51	18.92	14.69	15.85	16.34	11.58
7679	M	41.64	3.34	2.86	2.08	5.11	5.26	8.09	3.44	3.49	2.28	7.22	8.39	14.86	21.73	20.27	11.35	17.67	15.36	16.13	18.1	12.34
20644	M	40.11	3.64	2.71	2.14	4.75	4.9	7.9	4.19	3.32	2.17	6.18	7.49	13.35	21.39	20.03	11.02	17.82	14.12	14.84	15.31	12.17
13965	M	43.11	3.63	3.14	2.91	5.55	5.16	8.07	3.91	3.75	3.49	8.31	8.36	14.17	23.39	21.97	11.75	18.95	15.66	16.03	14.98	13
13408	M	40.02	3.66	2.66	2.13	4.63	5.15	7.75	3.86	3.52	2.07	6.54	8.1	12.47	20.55	19.78	10.37	17.57	15.05	14.49	15.5	12.32
13979	M	42.18	3.9	3.02	2.11	4.49	5.71	7.7	3.98	3.43	2.66	8.47	8.48	14.16	22.54	21.44	11.26	18.99	15.14	15.51	16.02	11.97
13972	M	39.75	3.54	2.78	2.26	4.83	5.53	7.74	3.72	3.72	2.65	6.73	8.01	14.08	21.2	20.49	11.05	18.8	15.23	15.38	14.78	11.63
7682	M	38.51	3.21	2.84	2.25	4.55	5.44	7.6	3.82	3.85	2.14	6.62	7.71	12.8	18.72	19.19	11.62	17.07	13.94	15.41	15.44	10.96
7678	M	42.2	3.19	3.06	1.78	4.41	4.85	7.53	3.72	3.73	2.22	7.42	7.92	13.96	21.7	21.28	11.5	19.17	14.08	14.53	16.75	11.01
7675	M	44.71	3.58	3.03	2.4	4.84	5.77	8.53	3.51	3.65	2.62	6.89	8.59	14.26	23.8	22.29	12.4	19.46	16.06	17.22	17.69	12.55
13964	M	44.8	4.13	3.1	2.63	5.18	5.61	8.96	4.13	3.93	2.48	7.8	7.99	15.17	22.29	21.05	10.92	19.12	14.51	17.26	15.98	14.23
7676	M	41.41	3.49	2.91	2.12	4.39	5.29	8.34	3.66	3.71	2.43	6.46	8.65	13.81	22.25	22	12.32	18.38	14.81	16.04	16.43	12.03
13409	M	40.12	3.45	3.01	2.2	4.4	4.93	8.1	3.91	3.29	2.41	6.83	8.13	12.58	21.09	19.85	10.98	17.28	14.76	14.74	15.51	12.53
13953	M	40.58	3.68	3.05	2.03	4.04	5.17	8.13	3.73	3.88	2.74	7.08	8.25	13.44	21.73	20.41	10.31	17.8	14.65	15.77	14.16	12.48
7680	M	42.61	3.39	3.06	2.68	4.48	5.78	7.71	3.35	3.42	2.77	6.44	7.72	14.2	21.94	21.83	11.84	19.12	15.32	15.61	17.08	11.77
13971	M	39.71	3.33	2.65	2.15	4.49	5.16	7.86	3.73	3.4	2.25	7.69	7.49	13.59	21.51	20.48	11.49	18.59	13.58	14.77	13.89	10.56
7683	M	39.72	3.6	2.57	2.42	4.71	5.09	7.3	3.66	3.74	2.54	6.75	7.53	13.27	21.04	20.25	10.83	17.42	14.62	15.72	16.2	11.58
16345	M	40.48	3.38	3.08	2.24	4.15	4.79	8.21	3.51	4.07	2.58	7.28	7.99	12.93	22.13	21.2	11.7	18.95	13.51	15.43	14.15	12.64

7681	M	39.16	3.17	3.03	2.26	4.5	5.6	8.48	3.72	3.76	2.44	7.33	8.66	12.99	22.37	22.05	11.97	17.82	14.78	16.73	15.63	11.75
13977	M	40.94	3.68	2.49	2.14	4.46	5.37	7.67	3.7	3.82	2.32	7.12	7.76	13.46	20.94	19.96	10.97	17.39	14.05	15.27	14.95	11.61
7684	M	42.09	3.42	3.17	2.53	4.64	5.61	8.01	3.42	3.53	2.54	7.22	7.75	14.85	22.45	22.09	11.63	19.29	15.62	15.73	17.35	13.21
13414	M	41.3	3.51	2.83	2.57	4.97	5.44	7.45	3.85	3.55	2.71	6.37	8.01	14.58	22.38	20.85	11.58	18.59	15.26	15.11	15.2	12.68
18962	M	43.86	3.92	3.05	2.39	5.45	5.68	7.79	3.86	3.84	2.49	8.74	8.45	14.57	24.33	23.29	12.41	20.03	14.39	16.05	15.04	13.03
13976	M	43.5	3.64	3.04	2.57	5.34	5.07	8.09	3.88	4.26	2.51	8.78	8.38	14.41	23.03	21.8	11.36	19.32	15.81	16.16	14.32	13.12
13411	M	41.23	3.37	3.02	2.58	5.29	5.52	7.88	3.87	4.29	2.69	6.85	8.19	13.96	21.68	20.11	11.08	18.52	15.24	15.51	15.54	13.21
13975	M	44.3	4.2	2.92	2.69	5.26	5.69	8	3.69	3.85	2.82	7.88	8.17	14.52	23.13	21.88	11.98	19.91	15.84	16.5	15.92	13.15
7673	M	41.13	3.21	2.57	2.3	4.41	5.18	7.43	3.61	3.56	2.19	7.21	7.99	13.82	21.42	20.5	10.94	17.79	13.38	14.58	16.43	10.74
13952	M	41.34	3.61	3.35	2.22	4.9	6.55	8.16	3.92	3.56	2.41	7.44	7.98	13.66	22.46	21.53	11.02	19.07	14.88	15.45	16.09	13.48
13951	M	41.03	3.3	2.57	2.36	4.66	4.94	8.22	3.78	3.33	2.64	7.49	7.89	12.93	21.61	19.96	10.29	18.36	13.18	16.12	14.29	12.92
13970	M	43.53	3.74	3.01	2.25	4.68	6.23	8.14	3.89	3.86	2.21	7.85	8.39	13.59	22.77	21.76	12.23	19.7	15.09	15.61	17.15	12.86
13967	M	42.06	3.61	2.97	2.22	4.2	4.68	8.37	3.74	3.65	2.55	7.57	8.44	14.11	22.59	21.36	11.47	18.48	14.55	15.14	16.63	11
13973	M	43.24	3.91	3.01	2.53	3.74	5.67	8.39	4.37	4.07	2.34	7.22	8.73	14.28	22.75	17.84	11.49	19.09	15.41	16.17	15.37	12.64
13980	M	40.35	4.02	2.64	2.13	4.23	5.42	8.08	3.58	3.72	2.45	7.22	7.52	13.24	21.76	19.86	10.66	17.24	13.89	14.67	14.32	12.21
7677	M	40.16	3.46	2.45	2.14	4.26	4.76	7.62	3.26	3.37	2.25	6.44	8.11	13.56	22.07	20.54	11.25	17.94	14.16	14.93	15.96	10.71
20643	M	38.34	3.61	2.49	2.2	4.75	4.64	6.94	3.54	3.07	2	7.06	7.82	12.41	21.98	20.14	10.6	17.81	14.49	14.6	13.1	11.59
13968	M	41.04	3.81	3.19	2.28	4.18	4.79	8.08	3.96	3.42	2.73	7.94	8.61	14.55	21.77	20.44	11.24	17.83	13.56	15.52	16.84	10.83
13966	M	41.32	3.57	2.93	2.47	4.97	5.53	7.81	4.16	3.21	2.65	8.86	7.97	14.36	21.4	17.39	11.16	19.32	14.98	15.76	14.96	12.23
13403	M	38.54	3.06	3.09	2.22	5.01	4.98	7.99	3.3	3.63	2.07	7.53	7.27	13.36	21.49	19.88	10.79	17.48	13.82	14.34	15.81	12.08
13978	M	42.26	3.7	2.89	2.34	5.5	4.84	7.66	3.96	4.17	2.77	7.13	8.83	13.89	22.78	21.34	10.98	18.84	14.86	15.47	16.79	12.39
13969	M	40.65	3.55	2.41	2.18	3.98	5.36	7.72	3.53	3.52	2.66	6.86	8.55	13.28	21.8	20.84	11.96	19.05	13.73	15.11	15.89	10.24
20902	M	41.61	3.57	2.42	2.7	4.1	4.1	7.67	3.52	3.52	2.21	6.81	7.48	13.24	21.44	19.94	10.79	17.44	12.85	16.09	15.84	12.73
15319	M	40.73	3.16	3.04	2.28	4.6	4.89	7.78	3.96	3.22	2.21	8.86	7.3	13.21	22.01	21.24	11.05	18.71	12.94	15.05	14.2	11.65
15398	M	45.74	3.56	3	2.1	5.73	5.55	8.72	4.5	3.75	2.54	6.78	7.82	14.76	23.51	23.21	12.39	19.85	14.6	16.21	16.81	12.85
15370	M	45.63	3.58	3.01	2.15	5.69	5.97	8.58	4.66	3.88	2.69	7.78	8.27	14.44	22.82	21.79	11.5	18.58	15.85	15.84	16.96	12.72
18754	M	44.73	3.71	2.92	2.22	5.44	5.78	8.38	3.81	3.84	2.79	8.55	9.05	14.95	24.15	22.14	12.13	19.84	15.24	16.67	13.27	13.3
15330	M	42.26	3.6	2.52	2.45	4.89	5.15	8.03	3.68	3.84	2.97	7.99	7.91	14.56	22.58	21.39	12.08	18.88	15.71	15.54	14.76	12.04
15329	M	43.55	3.78	2.92	2.26	4.95	5.68	8.16	3.74	3.61	2.63	7.85	8.88	14	23.27	21.78	12.7	18.65	14.57	17.19	14.47	12.32
15326	M	41.2	3.16	2.76	2.3	4.88	5.43	8.26	3.96	4.12	2.61	7.1	7.33	13.48	21.56	21.08	11.46	18.11	12.83	15.06	13.95	11.83
18755	M	42.66	3.48	2.67	2.57	5.52	5.07	8.31	3.83	4.05	2.82	7.81	10.67	13.69	22.61	20.87	11.64	19.06	14.93	16.22	13.23	13.37
18752	M	42.23	3.13	2.72	2.5	5.58	4.74	8.18	3.89	3.86	3.17	7.69	7.4	14.32	23.33	21.02	12.16	18.98	15.02	15.65	13.38	12.87

15318	M	43.93	3.61	2.94	2.34	5.57	5.71	7.86	3.92	3.87	2.53	8.4	8.77	14.64	24.2	23.4	12.46	19.21	15.56	16.74	15.65	13.2
15327	M	40.72	3.22	2.82	2.23	5.19	5.53	7.96	3.99	3.32	2.52	7.94	7.56	12.5	22.08	21.21	11.47	17.71	13.98	13.5	12.89	12.4
15275	M	38.22	3.15	2.71	2.19	4.52	5.76	7.57	3.26	2.84	2.37	7.07	7.06	13.07	21.52	20.26	11.96	17.24	13.56	13.96	11.15	10.63
15282	M	39.63	3.54	2.26	2.4	5.18	4.18	7.79	3.62	3.99	1.85	6.42	7.14	13.78	22.82	21.74	11.47	17.85	14.37	14.69	13.89	11.3
15399	M	42.51	4.01	2.71	2.12	5.13	5.54	8.37	4.03	3.84	2.11	6.13	8.32	14.06	22.69	22.27	12.28	19.05	14.57	15.13	14.08	11.41
15299	M	41.31	3.33	2.65	2.76	4.97	5.37	7.86	3.73	3.54	2.65	6.72	7.3	14.36	21.96	20.91	12.16	18.98	14.78	15.18	15.36	11.19
15298	M	39.11	3.41	2.69	1.9	4.71	4.6	7.74	3.99	3.42	2.08	7.76	6.88	13.33	21.41	20.34	11.42	17.52	14.06	14.69	13.29	11.37
15281	M	42.14	3.38	2.35	2.23	5.54	5.08	7.99	4.51	3.82	2.39	7.24	7.37	13.91	23.21	22.23	12.52	19.22	14.71	14.33	12.16	12
15284	M	40.31	3.28	2.24	2.24	5.34	5.57	8.1	3.71	3.75	2.42	7.55	7.33	13.91	22.74	21.35	11.96	18.25	14.76	14.97	12.88	12.2
15328	M	40.16	3.4	2.28	2.1	4.72	5.09	7.66	3.49	3.81	2.17	7.67	7.36	13.06	22.51	22.28	12.02	17.88	13.8	13.09	12.01	12.17
20517	M	41.37	3.56	3.48	2.29	5.01	5.62	8.14	3.64	3.88	2.83	6.73	7.63	13.4	23.17	22.11	12.03	17.83	13.89	16.24	14.99	13.86
20511	M	41.44	3.51	3.17	2.55	4.48	5.18	7.73	3.82	3.56	2.63	5.68	7.89	13.5	23.32	21.93	11.56	17.77	14.12	15.18	14.04	12.84
20523	M	46.08	4.17	3.41	2.91	5.02	4.74	8.28	4.06	4.46	2.62	6.3	7.95	15.06	22.54	20.08	12.16	20.19	16.46	16.27	15.96	14.08
20518	M	46.79	3.73	3.52	2.44	5.28	5.74	8.41	4.19	3.85	2.64	6.78	8.61	15.94	25.85	24.02	12.48	20.29	16.06	17.33	15.42	14.23
20613	M	41.63	3.77	3.34	2.07	5.16	5.07	8.22	3.9	4.28	2.71	6.61	8.21	14.32	21.96	22.44	12.15	19.17	14.84	16.43	15.56	13.28
20519	M	45.22	3.52	3.19	2.57	4.42	5.74	8.02	3.89	4.16	2.36	6.57	8.49	13.53	23.91	22.4	11.57	18.26	14.92	16.72	14.31	12.57
20522	M	48.47	4.12	3.03	2.46	5.57	5.97	8.67	4.12	4.42	2.33	8.28	8.59	15.97	26.42	25.59	13.36	21.17	16.95	17.49	17.78	13.27
20524	M	45.67	3.91	3.28	2.35	5.83	5.11	8.54	4.68	3.75	2.77	6.67	8.44	14.45	24.8	23.33	12.63	19.87	15.74	16.58	14.96	12.62
20527	M	46.23	3.61	3.42	2.62	4.44	6.12	9.25	4.1	4.28	2.89	7.5	8.51	14.06	23.74	23.01	12.62	18.54	16.16	16.97	15.86	15.34
20512	M	45.89	4.12	3.43	2.83	5.05	6.15	8.76	4.65	3.93	2.16	7.26	9.05	14.56	24.76	23.25	12.52	20.9	14.54	16.14	15.09	12.69
20528	M	48.45	4.29	3.53	2.93	5.03	5.76	8.65	3.93	4.13	2.73	7.07	9.57	14.79	24.44	23.9	12.88	20.31	17.02	17.57	15.14	14.06
20515	M	47.79	3.93	3.43	2.77	4.91	5.8	8.81	3.97	4.38	2.91	6.61	8.72	14.82	25.6	23.71	12.56	20.11	16.64	17.44	15.59	14.74
20530	M	45.33	4	3.13	2.14	4.59	5.61	8.52	3.64	4.06	2.31	7.35	8.39	14.63	24.68	22.04	11.72	19.88	16.41	16.76	15.65	13.38
20513	M	44.36	4.23	3.16	2.51	5.16	5.97	8.58	3.88	4.64	2.89	6.91	8.6	14.24	22.98	21.36	11.61	19.78	15.43	16.31	13.57	13.74
20521	M	43.69	3.78	3.04	2.57	4.91	6.14	8.57	3.86	3.66	2.81	6.82	8.37	13.78	23.67	22.64	12.73	19.53	15.14	15.97	14.29	13.25
20529	M	44.21	3.67	3.47	2.35	5.21	5.79	8.38	4.08	4.03	2.99	6.84	8.58	13.84	23.35	22.72	12.26	19.09	15.84	17.42	14.2	13.52
20526	M	43.7	3.28	3.12	2.42	5.05	5.67	8.14	3.45	3.82	2.45	7.67	7.52	13.45	21.87	21.48	12.33	18.28	14.52	15.59	14.54	13.27
20516	M	42.61	3.48	2.67	2.04	4.73	4.7	6.97	3.19	3.73	2.35	6.76	7.8	12.61	21.49	20.34	10.61	17.32	13.39	14.48	13.47	10.29

Table S4 Morphometric measurements of tadpole of *Bokermannohyla saxicola*. The definition and reference of each measure are available in the metadata table

Voucher (UFMG)	Stage (Gosner, 1960)	BW	BWE	IOD	IND	BWN	ESD	NSD	END	ND	TMW	ODW	BL	TAL	TL	BH	SVD	SSD	ED	SL	TMH	MTH	VFH	DFH	DFiA
415_1	25	7.54	6.50	3.76	2.83	4.98	4.80	2.04	0.99	0.42	2.78	3.12	10.96	NA	NA	6.09	3.53	8.16	1.19	0.91	2.69	7.70	2.18	3.00	34.11
423_1	25	11.81	10.91	5.77	4.20	8.58	7.63	3.08	1.85	0.69	5.13	4.34	17.90	26.59	44.34	9.71	3.69	12.09	2.58	0.69	4.96	12.54	3.12	4.83	35.49
530_1	25	14.99	11.81	6.60	4.64	8.81	7.88	3.13	2.00	0.55	5.62	5.83	19.89	36.13	55.91	11.49	5.64	13.18	2.57	0.63	5.30	13.67	3.74	5.10	30.92
530a_1	36	16.23	13.74	9.08	6.16	7.55	7.76	1.82	3.12	0.91	7.59	7.13	26.82	63.28	89.36	16.84	11.20	15.85	4.63	1.08	9.67	16.64	4.89	6.66	25.38
530a_2	28	19.29	16.00	8.37	5.86	10.86	10.44	3.67	3.02	0.61	7.42	6.99	26.45	50.42	76.76	12.16	8.68	17.53	3.19	1.42	9.06	16.34	4.20	5.44	31.40
530a_3	29	18.48	14.97	8.10	5.98	9.18	9.92	3.99	2.62	0.51	8.13	6.99	16.65	47.74	64.08	11.80	2.96	8.53	2.55	0.94	7.07	13.69	3.73	5.06	37.68
530a_4	25	12.70	10.09	6.40	4.62	5.97	6.32	2.25	1.87	0.41	5.07	5.47	18.18	35.90	52.89	8.75	3.31	13.20	2.87	0.86	5.35	11.36	2.80	4.15	34.18
530b_1	31	16.86	14.65	8.51	5.94	10.32	10.00	4.11	3.10	0.66	7.07	5.34	26.32	46.06	72.09	11.48	5.32	17.55	3.77	1.75	7.60	16.75	4.50	6.77	23.01
1585_1	25	17.21	13.30	7.74	5.20	8.94	8.67	2.89	2.76	0.51	7.69	7.07	25.95	45.75	71.35	15.48	7.59	14.97	3.57	1.54	8.57	17.61	4.11	6.00	28.51
1589_1	25	14.51	12.56	7.05	4.80	8.12	8.08	3.12	2.29	0.51	5.38	6.27	22.98	40.77	63.30	11.78	6.38	13.45	3.11	1.56	6.38	14.01	4.08	5.00	33.44
1589_2	25	13.98	12.47	6.95	5.01	7.94	8.25	3.08	2.64	0.60	5.23	5.42	19.58	35.22	54.57	9.68	4.17	13.25	2.54	1.66	5.17	12.14	3.64	4.84	35.99
1590_1	25	17.66	14.97	8.17	5.80	10.60	9.76	3.58	2.92	0.75	7.30	7.38	23.33	47.02	70.16	12.03	6.78	14.30	2.82	1.49	6.47	14.48	4.27	5.49	25.03
1590_2	39-40	24.08	18.12	10.88	6.34	12.26	11.88	4.43	3.24	1.14	9.89	7.79	30.94	54.93	85.37	16.50	8.80	17.80	4.46	1.19	9.31	19.70	5.14	7.16	31.33
1590_3	36	19.98	17.19	10.39	6.80	11.74	11.51	4.37	3.22	0.91	8.89	7.75	26.61	53.80	80.03	13.20	5.41	15.05	3.69	1.26	8.17	17.53	4.79	6.39	32.87
1592_1	25	9.73	8.94	4.85	3.55	6.54	6.20	2.15	1.34	0.53	3.20	3.80	14.38	29.02	42.96	6.42	3.42	9.75	1.45	1.10	3.31	9.04	2.79	3.54	32.52
1592_2	25	8.99	8.71	4.21	3.23	6.66	5.78	2.47	1.45	0.56	3.15	3.77	14.40	29.77	43.92	6.59	3.50	10.04	1.88	1.20	3.32	9.23	2.76	3.91	39.34
1593_1	25	12.46	9.60	6.07	3.96	5.59	6.23	2.33	2.12	0.45	4.59	4.70	18.93	38.74	57.29	9.47	4.85	11.55	2.50	1.24	5.63	11.93	3.56	4.54	34.82
1593_2	25	14.04	12.63	7.28	5.19	8.42	8.86	3.24	2.39	0.63	5.65	5.46	21.90	41.96	63.18	10.68	5.02	13.61	3.06	1.29	6.16	12.57	3.77	4.79	26.77
1595_1	39-40	20.96	15.70	9.54	5.80	11.47	10.72	4.11	2.70	0.84	9.22	6.63	28.61	53.82	82.10	13.89	4.55	15.50	4.17	2.34	9.74	18.66	4.99	7.06	29.66
1595_2	39	20.94	16.58	8.94	6.24	10.68	11.29	4.54	2.92	0.91	8.91	5.99	27.34	49.75	76.71	13.94	5.84	15.57	4.05	1.08	9.14	17.37	5.21	6.22	32.70
1595_3	37	19.32	15.88	9.63	6.10	10.82	10.68	4.29	2.82	0.70	8.22	7.68	26.54	44.52	70.77	14.16	5.94	15.97	3.43	1.54	9.10	18.66	4.71	6.83	31.43
1644_1	25	11.09	9.67	4.92	3.83	7.34	6.78	2.58	1.53	0.60	4.36	4.25	15.51	34.29	49.62	8.79	3.68	8.81	2.00	0.99	4.36	10.19	3.36	4.27	20.14
1648_1	25	11.18	10.23	5.55	3.95	8.05	7.39	3.10	1.81	0.61	4.89	4.71	15.74	31.51	47.16	8.62	3.98	9.06	2.03	0.93	4.96	10.73	2.86	3.69	35.54
1648_2	25	10.21	8.62	4.97	3.52	6.45	5.97	2.43	1.52	0.45	4.06	4.19	15.75	34.39	49.86	8.72	3.90	9.42	2.24	0.96	4.72	11.17	3.07	4.09	33.69
1648_3	34	18.05	13.98	7.70	5.59	9.79	9.54	3.93	2.61	0.62	7.58	7.07	25.84	46.82	72.74	14.37	8.65	15.69	3.05	1.57	8.66	17.08	5.43	6.35	43.05
1648_4	39-40	22.21	16.93	10.31	5.65	12.22	11.48	4.14	3.02	0.91	9.85	7.73	23.90	40.27	64.24	12.13	6.77	13.41	3.23	1.36	7.79	15.00	3.83	5.84	37.34

404a_1	25	14.87	12.52	8.12	5.09	8.49	8.19	3.05	2.45	0.65	7.88	5.07	20.24	40.13	59.93	11.60	5.72	12.18	3.23	0.81	8.75	15.06	3.67	5.12	30.06
404a_2	25	15.08	12.87	8.19	5.11	8.99	8.69	3.28	2.63	0.56	8.21	5.35	25.46	51.10	76.07	13.57	6.16	15.20	3.46	1.22	11.63	17.78	4.22	5.99	35.09
404a_3	25	20.16	16.68	10.80	7.03	12.11	11.64	4.67	3.44	0.64	11.11	6.44	28.21	61.84	90.12	16.04	6.30	15.68	3.96	1.67	12.62	18.65	5.49	7.16	NA
404b_1	25	17.74	15.00	9.78	6.31	10.69	10.38	4.41	2.83	0.73	9.48	6.53	26.42	NA	NA	14.07	5.31	13.93	3.72	1.71	10.17	16.27	4.39	6.49	NA
404b_2	25	16.75	13.65	8.86	6.00	10.11	9.67	4.08	2.66	0.60	9.60	6.52	23.00	46.50	68.82	11.63	5.02	14.82	3.13	1.68	10.08	13.94	3.73	4.57	23.43
404c_1	25	19.40	14.74	9.52	6.31	10.40	10.25	3.86	2.91	0.77	10.46	5.70	26.63	54.52	80.68	15.05	7.89	15.82	3.62	2.22	11.29	18.11	4.02	6.47	32.62
404c_2	25	15.76	13.20	8.48	5.89	10.02	9.44	3.91	7.47	0.74	9.26	7.32	25.09	49.72	74.68	14.21	6.16	13.63	3.53	1.48	11.64	15.34	4.21	6.35	NA
404c_3	25	16.42	14.08	8.93	5.80	9.64	8.54	3.50	2.85	0.64	9.07	6.70	24.69	46.38	70.97	13.31	6.16	15.33	3.54	1.22	10.44	16.88	4.43	6.06	28.95
1264_1	25	12.72	10.29	5.76	4.37	7.66	7.49	3.26	2.03	0.35	4.93	5.31	17.99	28.50	46.33	9.76	4.75	11.57	2.54	0.78	5.11	11.03	3.31	4.48	22.91
1264_2	25	13.09	10.07	6.17	4.41	7.40	7.02	3.00	1.85	0.48	4.41	4.68	16.92	24.46	43.90	9.76	5.16	10.33	2.41	1.64	4.98	11.25	3.26	4.26	23.40
1264_3	25	12.34	10.61	6.28	4.17	8.09	7.48	3.11	2.08	0.39	5.69	5.63	17.57	37.45	54.67	10.28	5.77	10.59	2.54	1.10	6.26	10.91	3.00	4.02	28.65
1266a_1	25	7.58	7.01	3.71	3.23	5.57	5.06	2.27	1.15	0.39	3.59	3.56	11.14	23.42	34.60	6.00	3.11	6.86	1.71	0.53	3.66	8.04	2.08	3.12	25.35
1266a_2	25	18.05	14.83	8.33	5.68	11.40	10.40	4.26	2.74	0.79	8.38	7.67	24.73	41.52	66.43	14.16	6.58	16.18	3.59	2.40	10.10	17.16	4.33	6.25	29.09
1266a_3	25	18.69	14.98	8.59	5.96	11.63	10.34	4.26	2.80	0.72	8.51	7.54	25.02	45.24	70.10	14.05	6.68	14.43	3.71	1.32	10.25	18.53	4.50	5.83	40.66
1266a_4	25	15.07	11.73	6.77	4.95	8.85	8.15	3.60	2.09	0.58	5.97	5.64	21.69	44.83	66.38	12.33	6.26	11.25	2.97	0.96	8.35	15.26	4.23	5.47	46.86
1266a_5	25	14.52	12.48	7.79	5.05	9.82	9.25	3.78	2.34	0.52	6.77	5.48	19.54	40.24	59.55	10.86	5.27	11.63	2.35	1.20	6.77	13.91	3.69	4.86	32.20
1266b_1	25	21.44	17.04	10.47	7.26	11.97	12.31	4.97	3.68	0.75	10.36	7.16	30.06	57.84	88.32	17.21	6.74	20.11	4.01	3.22	12.17	18.71	5.29	6.00	27.52
1515_1	25	17.42	14.26	8.65	5.93	10.17	9.67	3.90	2.60	0.66	8.25	7.09	23.63	47.66	71.05	13.06	6.37	13.08	3.36	1.47	9.03	16.49	4.51	6.15	36.38
1515_2	25	17.48	16.22	8.81	6.21	11.73	11.12	4.18	3.14	0.77	9.08	7.02	25.80	50.12	75.66	13.76	5.90	15.03	3.68	1.82	10.01	16.88	4.61	5.41	23.58
1515_3	25	16.00	13.01	7.80	5.54	9.63	9.16	3.76	2.34	0.80	7.89	6.72	20.98	40.33	60.81	11.22	3.91	11.64	2.96	0.95	7.60	14.66	3.57	5.28	27.17
1515_4	25	12.54	10.97	6.39	4.62	8.22	7.95	3.36	2.01	0.65	5.82	6.01	16.27	33.38	49.56	9.27	4.06	8.96	2.37	1.16	6.02	12.63	3.33	4.44	28.21
1515_5	25	8.93	7.89	4.11	3.30	6.23	5.86	2.59	1.21	0.54	3.14	4.20	13.92	24.05	37.73	7.20	3.25	8.37	1.87	0.87	3.51	8.50	2.32	3.43	NA
1516_1	25	19.87	16.90	9.43	6.51	12.56	11.70	4.74	3.11	0.77	10.63	7.58	28.90	47.57	76.54	16.00	5.84	17.43	3.12	2.14	12.96	20.81	5.02	6.85	21.96
1516_2	25	16.12	13.61	8.04	5.42	10.13	9.29	3.94	2.43	0.70	7.56	7.21	22.80	41.97	64.51	12.83	6.29	13.12	3.22	1.11	9.07	17.06	4.48	7.03	35.69
1516_3	25	14.81	11.90	7.03	4.97	8.99	8.69	3.53	2.18	0.62	7.14	6.69	20.29	35.60	55.55	11.41	4.83	12.46	3.20	1.24	7.72	14.27	4.02	4.79	29.98
1516_4	25	14.23	12.19	6.81	4.71	9.00	8.39	3.59	2.16	0.72	7.06	6.35	21.45	35.71	56.68	11.02	4.96	13.27	3.16	1.12	7.52	14.35	4.04	4.83	27.25
1516_5	25	14.22	11.58	6.73	4.74	8.71	8.13	3.63	2.01	0.60	7.05	5.43	18.57	30.35	48.94	10.81	4.88	12.00	2.77	1.12	6.98	13.08	3.51	5.12	29.46
1516_6	25	12.99	11.24	6.76	4.76	8.26	7.89	3.37	1.92	0.53	6.49	5.45	19.26	31.23	50.24	10.39	4.96	12.40	2.96	1.13	7.08	14.05	3.92	4.81	49.83
44_1	38	13.09	11.07	6.37	3.68	7.86	7.57	2.95	1.86	0.61	5.50	4.72	18.98	39.23	58.07	8.75	2.57	10.72	2.47	2.12	4.71	9.61	2.93	3.77	38.80
44_2	38	11.97	9.67	5.51	3.44	7.84	7.54	3.15	1.90	0.44	4.81	5.26	18.90	34.82	53.33	8.54	2.53	10.52	2.98	1.30	4.81	10.44	2.94	4.11	33.84
44_3	36	11.70	9.85	5.33	3.70	7.80	7.63	3.36	1.90	0.61	4.92	5.21	16.79	33.40	49.71	7.53	3.39	8.72	2.37	0.85	4.60	6.80	2.63	2.15	NA
44_4	31-32	11.65	8.84	4.91	3.52	5.77	5.66	1.73	1.81	0.45	3.52	5.11	15.70	30.88	46.73	7.68	2.80	9.57	2.84	1.33	4.17	10.05	3.13	4.26	21.83

44_5	28	10.30	8.63	4.45	3.68	6.36	6.27	2.91	1.99	0.48	3.99	4.94	16.20	29.50	44.96	7.97	3.44	9.91	2.24	1.29	3.71	7.26	2.55	2.93	NA
256_1	25	19.99	16.72	9.90	6.59	12.93	12.07	4.59	3.05	0.75	10.45	7.38	28.18	5.71	81.58	15.95	7.11	17.05	3.97	2.27	12.19	16.97	5.14	6.10	23.13
256_2	25	15.93	14.13	7.66	5.29	11.21	9.51	3.82	2.46	0.66	7.60	6.34	19.31	33.95	53.32	10.38	5.43	10.88	2.94	1.33	7.31	12.73	3.75	4.53	30.14
256_3	25	14.52	12.84	7.09	5.37	10.76	9.32	4.10	2.52	0.68	7.30	6.75	16.70	36.11	52.66	8.86	3.79	10.14	2.21	1.45	7.16	11.03	2.86	4.07	38.19
256_4	25	14.72	13.80	7.37	5.71	10.96	9.68	4.00	2.48	0.74	7.53	5.98	19.72	46.81	66.59	10.08	5.11	11.75	2.40	1.14	7.51	13.10	3.57	4.68	22.17
391_1	25	5.60	5.18	2.92	2.56	4.02	3.87	1.85	0.95	0.33	2.22	2.48	9.37	16.67	25.98	3.70	1.86	7.02	1.43	0.72	2.55	6.35	1.73	2.21	28.61
547_1	25	20.38	16.54	9.22	6.14	11.42	10.99	4.05	3.41	0.75	7.36	7.32	23.53	45.71	68.97	13.24	6.49	13.62	3.16	2.20	7.36	16.02	4.56	4.16	41.99
547_2	25	10.78	9.02	4.78	3.90	7.39	5.93	2.37	1.31	0.29	3.68	4.36	15.18	28.81	43.79	7.73	3.57	10.02	2.03	0.96	3.96	9.55	2.67	3.40	37.88
547_3	25	12.02	9.61	4.52	3.98	7.54	6.45	2.56	1.63	0.41	3.80	5.43	13.57	25.18	38.56	7.53	3.37	7.82	1.82	1.28	3.68	9.12	2.41	3.10	45.00
547_4	25	9.67	8.36	4.22	3.43	6.50	5.79	2.47	1.39	0.46	3.99	4.69	15.51	30.17	45.73	8.53	4.22	10.77	2.21	1.10	5.10	10.73	2.72	3.63	38.25
602a_1	39-40	21.17	16.03	10.81	5.22	10.14	9.73	2.24	3.19	1.20	11.05	7.96	27.63	63.18	89.11	13.66	6.60	16.26	3.75	1.29	10.86	17.87	5.11	5.79	43.91
602a_2	25	19.69	16.33	9.37	6.29	11.17	10.78	3.88	3.05	0.77	8.67	7.34	27.22	51.96	79.09	14.79	8.13	15.69	3.76	2.05	10.10	20.19	4.33	7.29	31.07
602a_3	25	19.26	15.61	8.66	6.11	10.79	9.86	3.62	2.39	0.84	7.63	6.95	25.40	NA	NA	13.69	6.31	15.59	3.99	1.76	8.35	19.92	6.13	7.66	43.16
602b_1	25	17.27	13.86	7.08	5.46	10.03	9.09	3.32	2.69	0.72	6.98	6.04	20.57	41.08	61.44	11.80	5.43	12.10	2.53	1.51	6.82	14.44	4.20	4.70	24.76
602b_2	25	17.97	14.31	8.91	5.30	10.44	9.56	3.65	2.24	0.51	7.36	7.18	21.67	46.05	67.68	12.36	4.92	12.21	2.88	1.68	7.25	16.53	4.79	5.81	33.41
602b_3	25	10.12	8.98	5.11	3.52	6.31	5.98	2.28	1.74	0.37	3.88	3.69	13.77	27.99	41.75	7.45	3.96	8.58	1.95	1.14	3.90	9.69	2.48	3.18	43.81
602b_4	25	9.45	8.14	4.60	3.14	6.20	5.59	2.25	1.36	0.40	3.40	3.61	11.33	25.30	36.64	6.91	3.04	6.39	1.79	0.73	3.64	8.04	2.30	3.13	36.38
602b_5	25	9.87	8.31	3.94	3.36	6.56	5.53	2.45	1.45	0.36	3.61	3.81	12.55	24.98	37.44	7.37	4.18	7.68	2.02	1.12	3.59	7.86	2.56	3.14	28.79
602b_6	25	7.39	6.64	3.02	2.78	5.34	4.24	1.97	1.01	0.21	2.79	3.23	9.02	15.17	24.18	5.66	2.58	6.74	1.56	0.71	2.67	4.62	1.48	1.60	28.18
892_1	39-40	17.65	13.87	9.06	3.49	7.02	8.12	1.96	2.60	0.83	8.68	5.96	23.40	53.52	76.60	12.20	5.01	13.79	3.36	1.12	9.22	17.84	4.51	6.00	25.88
892_2	34	18.25	16.67	9.30	6.17	12.26	11.37	4.74	3.05	0.89	7.43	7.41	21.69	43.22	64.74	12.57	4.53	13.89	3.06	2.51	7.74	16.44	4.30	5.18	50.36
901a_1	39-40	18.14	14.79	9.82	4.00	8.59	9.36	2.11	2.71	1.19	9.91	7.84	23.70	57.66	81.58	12.67	3.57	15.16	3.53	1.93	9.43	16.82	4.90	5.80	48.57
901a_2	37	22.05	17.52	10.92	6.57	11.95	10.97	3.78	3.11	0.93	9.64	7.60	25.16	50.88	76.11	15.39	6.81	13.71	3.78	2.00	9.39	20.30	5.56	6.43	52.39
901a_3	37	20.43	16.78	10.03	6.35	12.09	10.73	4.09	3.02	0.85	9.44	6.94	25.44	50.32	75.88	14.36	6.68	15.71	3.83	1.80	11.48	20.96	5.13	7.22	37.92
901c_1	27	20.46	16.22	9.81	6.59	11.27	10.65	4.02	3.02	0.85	9.95	NA	26.50	NA	NA	15.24	7.22	17.69	3.57	1.72	10.30	21.33	5.15	7.89	22.61
901c_2	37	20.11	16.95	9.77	6.36	12.66	10.79	3.98	2.77	0.90	9.04	7.80	28.51	57.49	85.66	16.19	5.54	18.13	4.51	1.99	10.65	20.72	5.58	8.10	42.22
946a_1	25	16.76	15.27	8.73	5.98	10.73	9.93	3.62	2.94	0.64	6.48	7.62	25.97	49.11	74.91	14.22	6.93	15.49	3.41	2.32	7.37	17.73	5.30	6.06	38.89
946a_2	25	14.41	13.35	7.19	5.36	9.70	8.88	3.65	2.52	0.83	5.65	6.57	21.73	42.23	63.57	11.89	5.33	13.29	3.12	1.40	6.08	14.36	4.09	4.70	24.61
946a_3	25	14.07	13.05	7.95	5.74	9.38	8.29	3.39	2.37	0.83	3.89	5.07	20.15	34.51	54.40	10.93	4.91	11.51	3.03	1.98	4.63	15.53	4.36	5.09	47.15
946a_4	25	13.12	11.25	6.69	4.60	8.46	8.00	3.54	2.15	0.48	4.75	6.11	16.16	32.71	48.74	9.50	3.75	9.60	2.29	1.20	5.03	11.67	3.48	3.67	39.21
946b_1	31	19.82	17.71	10.27	6.83	12.75	11.55	4.54	3.15	0.79	7.83	7.22	27.20	51.90	79.17	15.29	5.53	16.20	3.51	2.14	7.70	18.90	5.48	6.53	39.81
946b_2	25	17.30	14.41	8.81	5.93	10.59	9.44	3.77	2.68	0.62	6.70	7.03	24.08	47.50	71.66	14.14	7.11	15.35	3.31	2.47	7.77	16.19	5.00	5.36	29.72

946b_3	25	14.26	13.45	7.75	5.12	9.22	8.52	3.12	2.57	0.47	5.39	6.18	23.36	44.66	68.11	11.86	5.31	14.68	2.98	1.22	6.02	15.56	4.24	5.25	24.17
946c_1	28	21.53	18.33	10.71	7.49	12.74	11.97	4.70	3.55	0.91	8.80	8.17	26.60	52.17	78.60	15.24	6.70	15.29	3.41	1.89	9.15	19.25	5.28	6.57	41.07
946c_2	25	17.24	14.42	8.24	5.78	10.45	9.31	3.55	2.89	0.75	6.70	6.88	25.52	47.41	72.96	14.12	5.79	15.59	3.28	2.91	7.76	18.34	4.87	5.81	23.38
946c_3	26	13.27	13.09	7.73	5.19	8.46	8.31	2.97	2.64	0.61	3.82	6.10	22.10	37.87	59.43	11.69	4.19	12.16	3.36	2.19	5.24	16.18	4.10	5.14	28.81
946c_4	25	16.61	15.53	8.58	6.05	11.64	10.72	4.46	2.90	0.64	6.87	7.67	23.99	45.08	69.31	12.37	5.64	15.95	3.29	1.64	7.48	16.05	3.96	5.56	35.53
954a_1	25	15.28	12.54	7.58	5.45	8.99	8.60	3.32	2.42	0.67	6.26	6.50	19.47	39.98	59.31	11.77	4.66	12.96	2.65	1.33	7.36	14.24	3.92	4.62	20.94
954a_3	25	9.82	8.77	5.24	3.91	6.11	5.61	2.07	1.34	0.65	4.07	4.44	14.51	28.96	43.62	7.83	2.95	9.44	2.10	1.06	4.93	9.50	2.80	2.60	25.64
954a_4	25	9.31	8.08	4.91	3.49	5.32	5.03	1.92	1.23	0.56	3.51	4.38	12.36	24.85	37.16	7.40	3.66	7.47	1.82	0.98	4.38	8.33	2.51	3.21	15.73
954b_1	26	14.72	14.51	7.16	5.67	10.44	9.92	3.90	2.57	0.49	7.79	6.19	21.51	48.20	69.61	11.29	5.27	14.26	3.20	1.77	8.24	16.92	4.29	5.65	35.75
954b_2	26	11.87	13.42	6.92	5.71	10.69	10.47	4.50	2.60	0.88	7.28	7.42	22.58	50.70	73.14	9.29	2.61	13.58	3.16	1.39	7.71	14.36	3.82	4.50	25.99
954b_3	26	10.66	11.60	6.59	4.86	8.61	7.75	2.66	2.24	0.67	4.56	5.48	16.76	31.63	48.04	8.39	3.78	12.22	2.71	1.09	4.26	12.30	3.41	4.35	35.54
954b_4	25	11.64	10.00	5.97	4.07	7.51	6.94	3.24	1.70	0.60	4.94	4.96	14.55	30.12	44.27	8.44	4.74	8.78	2.12	0.98	5.03	10.47	2.56	2.96	43.61
986b_1	25	17.36	16.02	9.50	6.36	12.18	11.33	4.58	3.01	0.86	9.12	7.72	27.65	54.57	82.39	12.98	4.78	16.05	3.69	1.65	8.48	20.21	4.69	5.30	21.07
986b_2	25	18.57	16.33	9.55	6.27	12.41	11.03	4.52	3.10	0.77	9.05	7.81	28.51	57.34	85.45	13.53	5.33	16.27	3.18	1.43	8.77	21.22	5.06	6.12	27.07
986b_3	25	16.30	15.66	9.60	5.98	11.29	10.58	4.13	3.11	0.78	7.68	7.54	26.29	NA	NA	12.44	4.59	17.10	3.48	1.62	8.12	17.04	5.32	6.35	22.31
986b_4	26	11.83	11.59	7.02	4.76	8.23	8.17	3.13	2.30	0.56	5.67	4.62	19.73	42.07	61.15	9.03	3.63	10.81	2.88	1.02	5.97	14.28	3.45	4.95	22.58
986b_5	25	9.43	9.24	5.13	4.16	6.94	6.64	2.89	1.56	0.50	3.80	3.72	15.96	21.39	37.25	7.28	3.34	9.85	2.40	0.70	4.12	10.33	2.89	3.77	31.37
989_1	25	12.90	11.83	7.85	4.33	8.35	8.33	2.62	2.47	1.12	6.96	5.03	23.87	47.34	70.89	12.27	6.53	18.89	3.10	1.74	7.63	13.40	3.34	4.07	22.75
1012c_1	25	12.15	13.34	7.47	5.54	11.06	9.98	4.15	2.63	0.77	7.11	8.09	22.10	46.07	67.95	9.06	3.73	13.65	2.77	1.35	6.37	15.02	3.76	4.92	24.01
1012c_2	25	10.92	12.44	6.87	4.92	9.76	9.20	4.00	2.32	0.68	6.77	6.90	20.99	48.25	69.41	8.90	3.44	13.89	3.13	1.64	6.85	14.64	3.92	4.38	26.58
1012c_3	25	10.64	11.99	6.03	5.00	9.68	9.14	4.19	2.27	0.69	5.87	6.73	20.72	43.78	64.33	8.99	3.48	13.77	2.80	1.29	6.46	13.54	3.59	4.47	23.81
1012c_4	25	10.35	11.10	5.39	4.42	8.83	8.06	3.59	1.98	0.63	5.38	6.74	19.16	NA	NA	8.64	4.34	13.07	2.74	1.67	5.50	12.82	3.47	4.50	33.23
1013b_1	36	24.19	18.73	11.04	7.20	13.69	12.63	5.15	3.55	0.79	12.40	8.14	31.25	60.22	91.39	15.68	8.29	17.57	5.12	2.38	12.26	22.07	5.77	7.17	22.69
1013b_2	25	15.89	12.53	6.82	4.83	9.40	8.11	3.43	2.32	0.49	6.66	5.66	24.09	47.70	71.59	11.60	4.69	13.24	3.15	1.91	7.29	13.23	3.83	4.94	14.57
1013b_3	25	11.43	10.71	5.91	4.46	8.69	7.73	3.10	1.94	0.42	5.15	5.75	17.96	35.31	52.98	8.09	3.36	11.81	2.67	1.32	5.05	11.16	3.12	4.04	34.05
1013b_4	25	10.48	9.43	4.83	3.47	7.18	6.58	2.71	1.55	0.57	4.08	3.84	15.92	30.70	46.58	8.28	4.43	10.24	2.52	0.95	4.22	10.36	3.01	3.61	21.26
1013c_1	25	28.12	20.35	11.70	7.28	14.88	13.26	5.71	3.81	0.82	11.84	8.14	33.56	57.84	91.50	20.62	10.66	19.94	4.29	2.19	13.49	21.34	6.11	7.33	32.89
1013c_2	25	11.03	9.58	5.26	3.82	7.57	6.90	2.92	1.60	0.55	4.49	4.31	15.11	30.78	45.89	8.21	4.22	9.06	2.44	0.89	4.77	10.77	3.05	3.91	24.57
1013c_3	25	9.97	8.86	4.74	3.52	7.21	6.47	2.72	1.63	0.47	4.10	4.38	14.27	32.59	46.84	7.28	4.13	7.78	1.81	1.79	3.67	8.81	2.52	3.25	31.99
1231_1	27	15.13	14.52	8.69	5.95	10.68	10.42	4.08	2.86	0.87	7.64	6.81	25.39	NA	NA	12.71	5.54	17.20	3.46	1.89	8.76	17.32	3.75	5.97	24.16
1231_2	25	15.60	13.17	7.56	5.40	10.16	8.93	4.19	2.27	0.82	6.45	6.34	19.61	36.20	55.95	10.69	5.70	12.90	2.85	1.85	6.36	13.42	3.63	4.74	26.31
1231_3	25	15.05	13.12	7.64	5.43	9.69	8.45	3.06	2.44	0.79	7.17	6.83	21.83	45.96	67.83	11.97	5.46	13.81	3.28	0.97	7.86	17.41	4.63	6.13	42.88

1598_1	25	14.44	15.33	7.74	5.72	12.48	11.46	5.24	2.50	0.66	8.40	8.06	24.08	NA	NA	11.17	5.57	16.78	3.39	2.47	8.19	15.21	2.81	4.69	29.35
2143_1	28	10.35	9.37	5.01	3.48	6.58	6.58	2.48	1.78	0.44	3.94	4.19	12.84	27.71	40.24	6.89	2.96	6.70	2.12	1.02	3.60	10.20	3.14	3.68	18.48
2256_1	25	18.74	15.51	9.51	6.40	11.63	10.60	4.60	2.85	0.65	9.57	9.18	25.55	58.65	84.26	14.26	5.22	15.76	3.45	2.05	10.00	21.16	5.86	7.28	33.57
2256_2	26	14.95	13.71	7.50	5.40	9.63	9.17	3.46	2.53	0.76	6.32	7.49	23.24	46.64	69.59	11.43	5.81	13.37	3.53	2.17	7.19	17.53	4.05	5.62	33.02
2256_3	26	14.28	13.36	7.62	5.42	10.17	9.15	3.85	2.47	0.83	6.62	7.89	20.85	39.15	59.99	10.33	5.53	13.72	2.91	1.52	6.42	13.94	3.98	4.76	27.99
2256_4	25	12.88	10.30	5.87	4.22	7.62	6.79	2.81	1.47	0.56	4.66	5.81	16.09	35.72	51.66	10.26	4.34	8.98	2.36	1.22	4.85	11.97	3.50	4.39	30.10
2256_5	25	10.74	9.28	4.87	3.74	7.17	6.65	3.04	1.76	0.45	4.49	5.80	15.90	31.14	47.05	8.42	4.69	10.37	2.21	0.87	4.73	10.48	3.04	3.68	35.81
2297_1	39	22.07	17.45	9.59	6.30	12.33	12.02	4.18	3.41	0.67	8.78	8.41	28.03	47.87	75.89	13.55	5.25	14.89	3.84	1.49	8.90	18.35	4.93	6.88	25.34
2297_2	25	17.48	15.74	9.21	6.09	11.32	10.33	4.11	2.92	0.88	8.78	7.62	29.22	44.65	73.62	14.04	5.67	18.76	3.73	2.17	10.15	20.50	5.80	7.45	30.80
2297_3	25	17.58	14.20	7.97	5.40	10.83	9.94	4.43	2.63	0.56	7.54	7.89	24.73	43.26	68.04	13.81	5.87	15.45	3.06	1.90	7.62	15.91	4.39	5.52	30.70
2297_4	25	15.91	13.85	7.88	5.64	10.44	9.45	3.99	2.67	0.53	6.51	6.84	22.73	45.69	68.47	12.72	6.43	13.78	3.08	1.84	7.13	16.35	4.55	5.79	25.82

Table S5 Results of Permutational of variance (PERMANOVA) between male and female of *Bokermannohyla saxicola*

	Df	**Sum sqs**	**Mean sqs**	**F model**	**R2**	**Pr (>F)**
Sex	1	1.705	1.70462	14.416	0.02995	9.999 e-05
Residuals	467	55.220	0.11824		0.97005	
Total	468	56.924			1	

Table S6 Summary statistics and estimated substitution rate from DNA data. To this analysis we did not considered outgroup. Substitution rate were only estimated for non-recombinant genes. *p>0.05

Gene	Size	Number of haplotypes	*Hd*	π	Segregating sites	Tajima's D	Φ test's (p-value)	Substitution rate (Mean ± stdev)
COI	495	34	0.983	0.056	102	0.770*	0.352	1.174x10-2 ± 2.297x10-3
Cyt-*b*	506	37	0.986	0.06	107	0.974*	0.626	1.388x10-2 ± 1.618x10-3
***β*-cry**	223	7	0.49	0.009	11	-0.039*	1	2.023x10-3 ± 6.838x10-4
***β*-fib**	499	17	0.814	0.005	17	-0.973*	0.036	-
c-*myc*	378	11	0.766	0.003	9	-0.661*	0.013	-
DIA6	479	64	0.967	0.018	70	-1.299*	0.945	6.186x10-3 ± 2.340x10-3
POMC	621	26	0.937	0.006	31	-1.324*	0.824	3.307x10-3 ± 9.085x10-4
SmarcB1	479	7	0.64	0.002	5	-0.188*	0.89	5.940x10-4 ± 4.681x10-4

Table S7 Posterior probabilities for each node in distinct trees for each gamma prior combinations for theta (Θ) and tau (τ) in iBPP analysis. First and second lines refers to each two-independent analysis

Priors	Adults (males) Trees with node probabilities	PP	Tadpoles Trees with node probabilities	PP
Θ~g (2,100), τ~g (2, 200)	(((CE, S)'#1', CA)'#1', N)'#1'	1.000	(((CE, S)'#1', CA)'#1', N)'#1'	1.000
	(((CE, S)'#1', N)'#1', CA)'#1'	1.000	(((CE, S)'#1', N)'#1', CA)'#1'	1.000
Θ~g (2,100), τ~g (2, 2000)	(((CE, S)'#1', CA)'#1', N)'#1'	1.000	(((CE, S)'#1', CA)'#1', N)'#1'	1.000
	(((CE, S)'#1', N)'#1', CA)'#1'	1.000	(((CE, S)'#1', N)'#1', CA)'#1'	1.000
Θ~g (2,1000), τ~g (2, 2000)	(((CE, S)'#1', CA)'#1', N)'#1'	1.000	(((CE, S)'#1', CA)'#1', N)'#1'	1.000
	(((CE, S)'#1', N)'#1', CA)'#1'	1.000	(((CE, S)'#1', N)'#1', CA)'#1'	1.000
Θ~g (2,1000), τ~g (2, 200)	(((CE, S)'#1', CA)'#1', N)'#1'	1.000	(((CE, S)'#0.99897', CA)'#1', N)'#1'	0.999
	(((CE, S)'#1', N)'#1', CA)'#1'	1.000	(((CE, S)'#1', N)'#1', CA)'#1'	1.000

Table S8 Posterior probabilities for seven diversification scenarios simulated for *Bokermannohyla saxicola*

Scenarios	**Demographic pattern**	**Posterior Probability**	
		Direct	**Logistic**
Scenario 1	Vicariance with no demographic change	0.024	0.003
Scenario 2	Vicariance with southern expansion and other stable	0.019	0.119
Scenario 3	Vicariance with southern stable and other retraction	0.007	0
Scenario 4	Diffusion with no demographic change	0.011	0.001
Scenario 5	Diffusion with southern expansion and other stable	0.02	0.134
Scenario 6	Diffusion with southern stable and other retraction	0.013	0
Scenario 7	Jump Dispersal	0.906	0. 743

Metadata – Tables S3/ S4

Adults (Table S3)	Legend	Reference
SVL	Snout-vent length	Watters et al., 2016
PL	Prepolex length	Total length of prepolex
FAW	Forearm width	Watters et al., 2016
TD	Tympanum diameter	Watters et al., 2016
ED	Eye diameter	Watters et al., 2016
IOD	Interorbital distance	Watters et al., 2016
AMD	Distance between the anterior margins of eyes	Garcia et al., 2003
EN	Eye-nostril distance	Watters et al., 2016
IND	Internarial distance	Watters et al., 2016
NS	Snout-nostril length	Watters et al., 2016
UAL	Upper arm length	Watters et al., 2016
FLL	Forearm length	Watters et al., 2016
HAL	Hand length	Watters et al., 2016
THL	Thigh length	Watters et al., 2016
TL	Tibia length	Watters et al., 2016
TSL	Tarsus length	Watters et al., 2016
FL	Foot length	Watters et al., 2016
HL	Head length	Watters et al., 2016
HW	Head width	Watters et al., 2016
CW	Chest width	Ventral distance between both axillae
UED	Upper eyelids distance	Greatest distance between the outer margins of the upper eyelids

Tadpoles (Table S4)	Legend	Reference
BW	Body width	Lavilla & Scrocchi, 1986
BWE	Body width at eye level	Lavilla & Scrocchi, 1986
IOD	Interorbital distance	Altig & McDiarmid, 1999
IND	Internarial distance	Altig & McDiarmid, 1999
BWN	Body width at nostril level	Lavilla & Scrocchi, 1986
ESD	Eye-snout distance	Lavilla & Scrocchi, 1986
NSD	Nostril-snout distance	Lavilla & Scrocchi, 1986
END	Eye-nostril distance	Lavilla & Scrocchi, 1986
ND	Nostril diameter	Lavilla & Scrocchi, 1986
TMW	Tail muscle width	Altig & McDiarmid, 1999
ODW	Oral disc width	Lavilla & Scrocchi, 1986
BL	Body length	Altig & McDiarmid, 1999
TAL	Tail length	Altig & McDiarmid, 1999
TL	Total length	Altig & McDiarmid, 1999
BH	Body height	Lavilla & Scrocchi, 1986
SVD	Spiracular-venter distance	Lins et al., 2018
SSD	Snout-spiracular distance	Lavilla & Scrocchi, 1986

ED	Eye diameter	Lavilla & Scrocchi, 1986
SL	Spiracle length	Lins et al., 2018
TMH	Tail muscle height	Altig & McDiarmid, 1999
MTH	Maximum tail height	Altig & McDiarmid, 1999
VFH	Ventral fin height	Grosjean, 2005
DFH	Dorsal fin height	Grosjean, 2005
DFiA	Dorsal-fin insertion angle	Pinheiro et al., 2012

References

Altig, R., & McDiarmid, R. W. (1999). Body plan: development and morphology. In R. W. Mcdiarmid & R. Altig (Eds.), *Tadpoles: The Biology of Anuran Larvae* (pp. 24–51). The University of Chicago Press.

Garcia, P. C. A., Vinciprova, G., & Haddad, C. F. B. (2003). The Taxonomic Status of *Hyla pulchella joaquini* (Anura: Hylidae) With Description of Its Tadpole and Vocalization. *Herpetologica, 59*(3), 350–363.222

Gosner, K. L. (1960). A Simplified Table for Staging Anuran Embryos and Larvae with Notes on Identification. *Herpetologica, 16*(3), 183–190.

Grosjean, S. (2005). The choice of external morphological characters and developmental stages for tadpole-based anuran taxonomy: A case study in *Rana* (*Sylvirana*) *nigrovittata* (Blyth, 1855) (Amphibia, Anura, Ranidae). *Contributions to Zoology, 74*(1–2), 61–76. https://doi.org/10.1163/18759866-0740102005

Lavilla, E. O., & Scrocchi, G. J. (1986). Morfometria larval de los generos de Telamatobinae (Anura: Leptodactylidae) de Argentina Y Chile. *Physis, 44*, 39–43.

Lins, A. C. R., Magalhães, R. F., Costa, R. N., Brandão, R. A., Py-Daniel, T. R., Miranda, N. E. de O., Maciel, N. M., Nomura, F., & Pezzuti, T. L. (2018). The larvae of two species of *Bokermannohyla* (anura, hylidae, cophomantini) endemic to the highlands of central Brazil. *Zootaxa, 4527*(4), 501–520. https://doi.org/10.11646/zootaxa.4527.4.3

Pinheiro, P. D. P., Pezzuti, T. L., & Garcia, P. C. de A. (2012). The Tadpole and Vocalizations of *Hypsiboas polytaenius* (Cope, 1870) (Anura, Hylidae, Hylinae). South American *Journal of Herpetology, 7*(2), 123–133. https://doi.org/10.2994/057.007.0202

Watters, J. L., Cummings, S. T., Flanagan, R. L., & Siler, C. D. (2016). Review of morphometric measurements used in anuran species descriptions and recommendations for a standardized approach. *Zootaxa, 4072*(4), 477–495. https://doi.org/10.11646/zootaxa.4072.4.6

II) Material Suplementar – Capítulo 3

Comparative Phylogeography of anurans endemic to Espinhaço Mountain Range, the largest extra-Andean mountain chain in South America (Oswald et al. in prep)

a) Supplementary figures

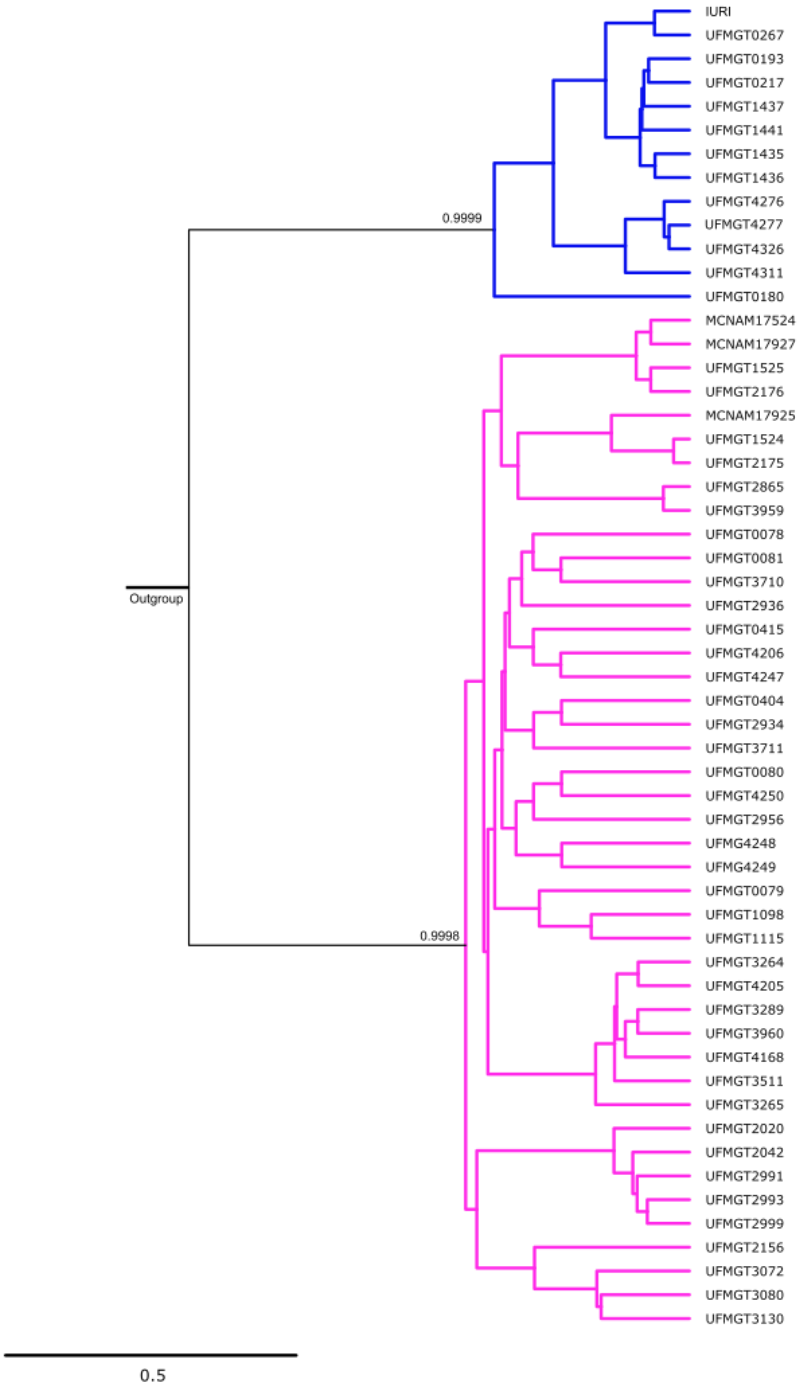

Fig S1 Mitochondrial gene tree of *Bokermannohyla alvarengai*. Blue corresponds to the northern population and pink to the southern population of the central barrier

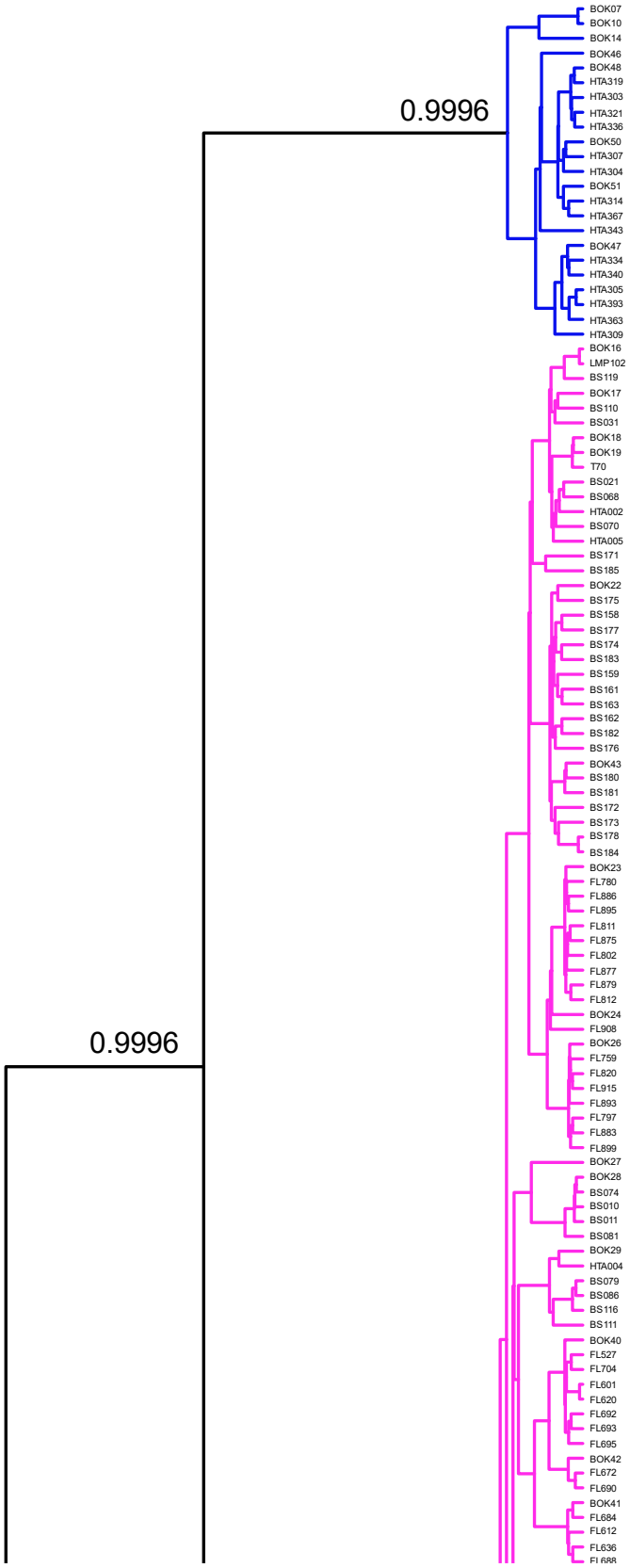
0.9996
0.9996
BOK07
BOK10
BOK14
BOK46
BOK48
HTA319
HTA303
HTA321
HTA336
BOK50
HTA307
HTA304
BOK51
HTA314
HTA367
HTA343
BOK47
HTA334
HTA340
HTA305
HTA393
HTA363
HTA309
BOK16
LMP102
BS119
BOK17
BS110
BS031
BOK18
BOK19
T70
BS021
BS068
HTA002
BS070
HTA005
BS171
BS185
BOK22
BS175
BS158
BS177
BS174
BS183
BS159
BS161
BS163
BS162
BS182
BS176
BOK43
BS180
BS181
BS172
BS173
BS178
BS184
BOK23
FL780
FL886
FL895
FL811
FL875
FL802
FL877
FL879
FL812
BOK24
FL908
BOK26
FL759
FL820
FL915
FL893
FL797
FL883
FL899
BOK27
BOK28
BS074
BS010
BS011
BS081
BOK29
HTA004
BS079
BS086
BS116
BS111
BOK40
FL527
FL704
FL601
FL620
FL692
FL693
FL695
BOK42
FL672
FL690
BOK41
FL684
FL612
FL636
FL688

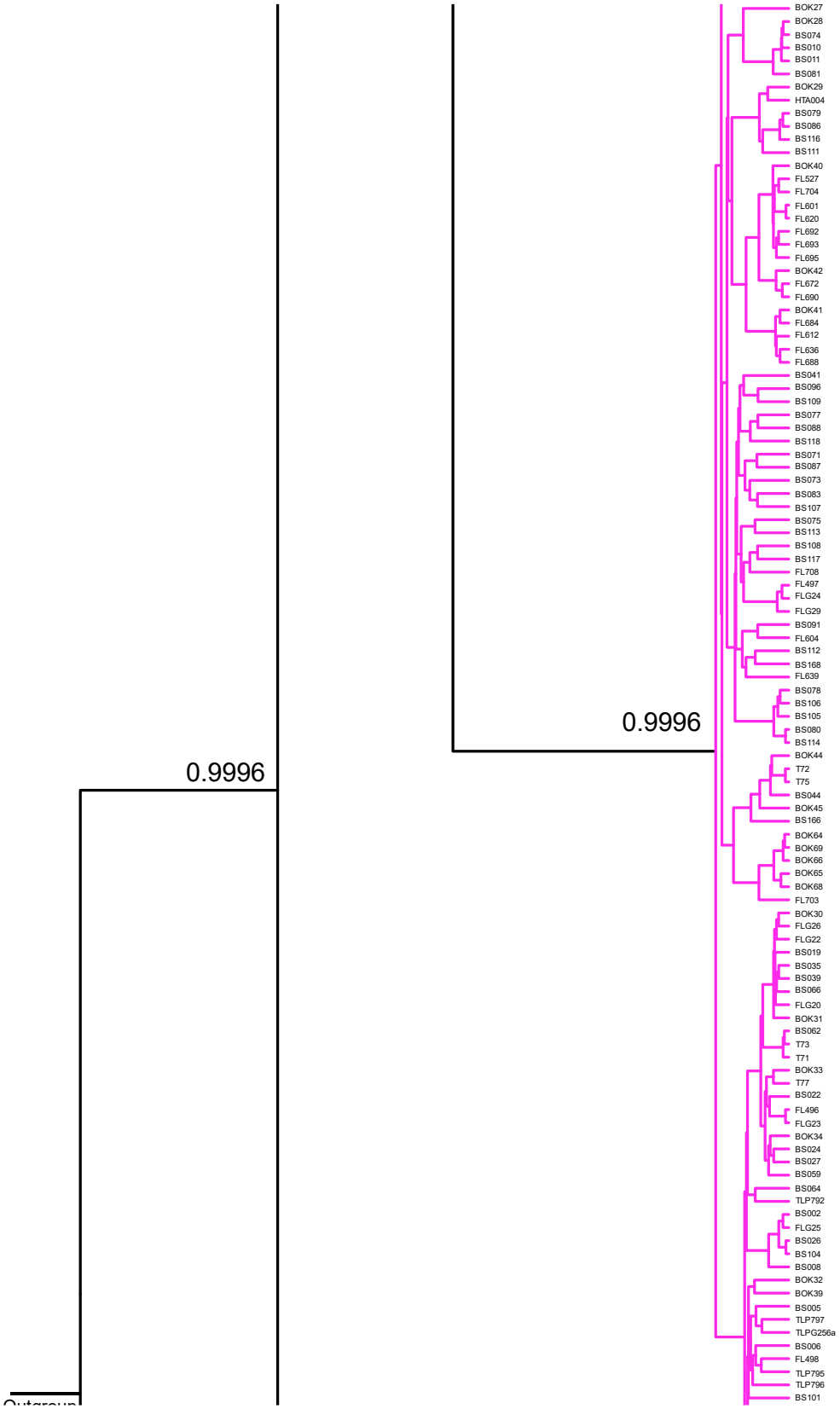
0.9996
0.9996
Outgroup
BOK27
BOK28
BS074
BS010
BS011
BS081
BOK29
HTA004
BS079
BS086
BS116
BS111
BOK40
FL527
FL704
FL601
FL620
FL692
FL693
FL695
BOK42
FL672
FL690
BOK41
FL684
FL612
FL636
FL688
BS041
BS096
BS109
BS077
BS088
BS118
BS071
BS087
BS073
BS083
BS107
BS075
BS113
BS108
BS117
FL708
FL497
FLG24
FLG29
BS091
FL604
BS112
BS168
FL639
BS078
BS106
BS105
BS080
BS114
BOK44
T72
T75
BS044
BOK45
BS166
BOK64
BOK69
BOK66
BOK65
BOK68
FL703
BOK30
FLG26
FLG22
BS019
BS035
BS039
BS066
FLG20
BOK31
BS062
T73
T71
BOK33
T77
BS022
FL496
FLG23
BOK34
BS024
BS027
BS059
BS064
TLP792
BS002
FLG25
BS026
BS104
BS008
BOK32
BOK39
BS005
TLP797
TLPG256a
BS006
FL498
TLP795
TLP796
BS101

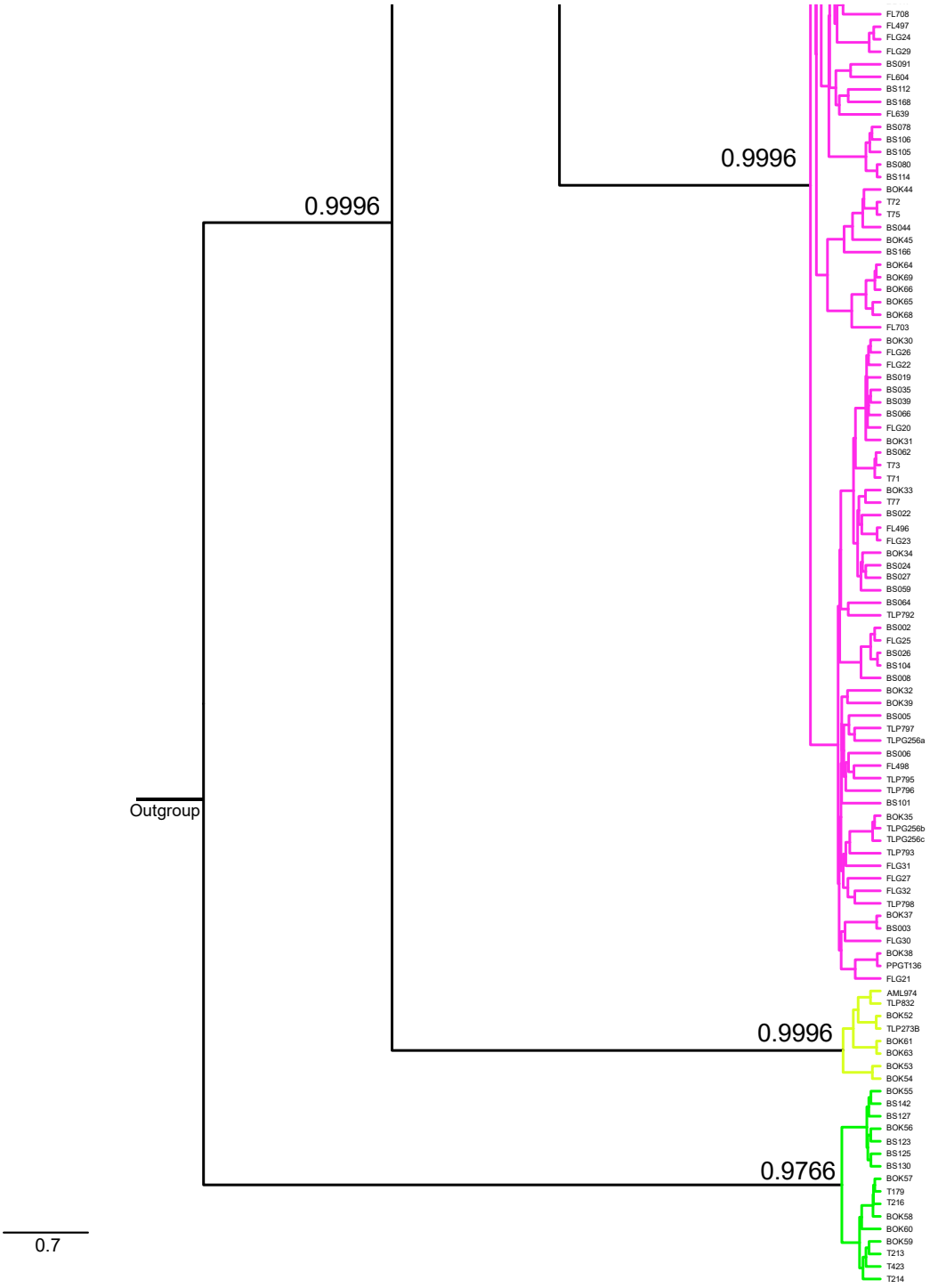

Fig S2 Mitochondrial gene tree of *Bokermannohyla saxicola*. Blue corresponded Northern population and pink of Southern population of central barrier, yellow to the population of Cabral and green the far north population (i.e., Northern population in Oswald et al., in press)

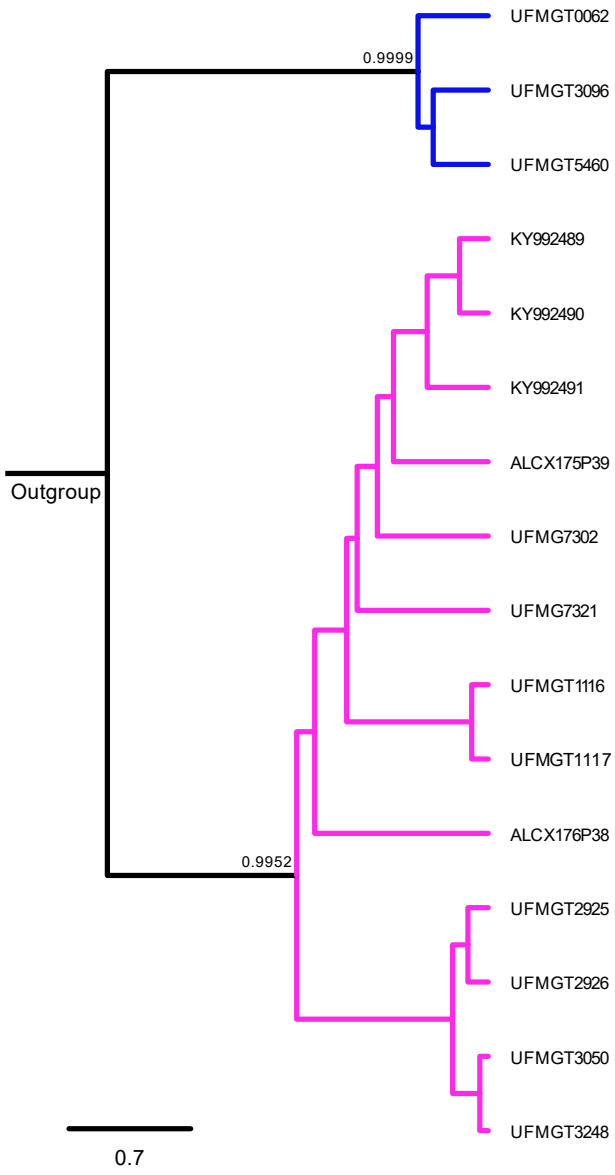

Fig S3 Mitochondrial gene tree of *Leptodactylus camaquara*. Blue corresponds to the northern population and pink to the southern population of the central barrier

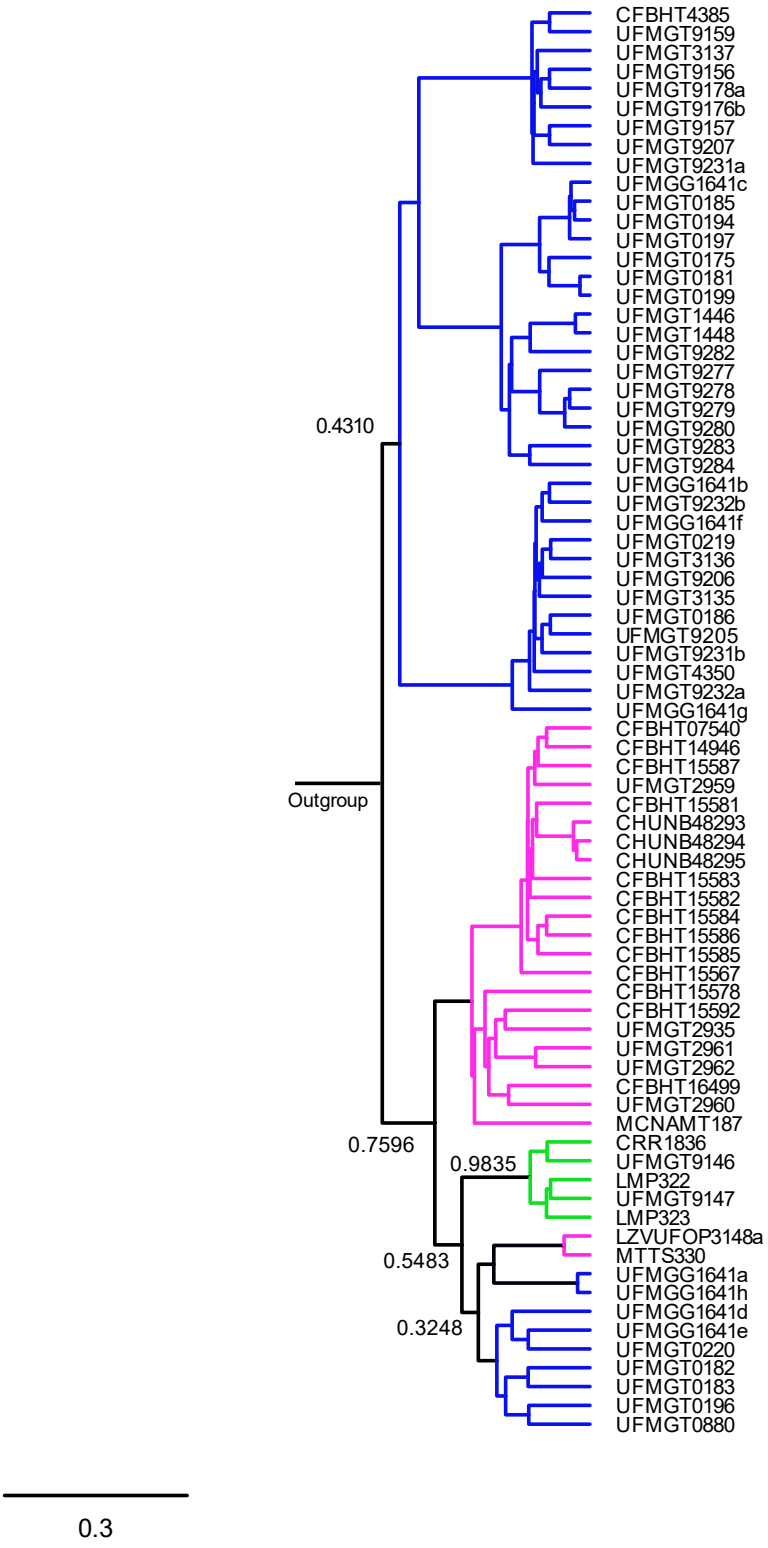

Fig S4 Mitochondrial gene tree of *Pithecopus megacephalus*. Blue corresponds to the northern population and pink to the southern population of the central barrier, and yellow to the population of Cabral

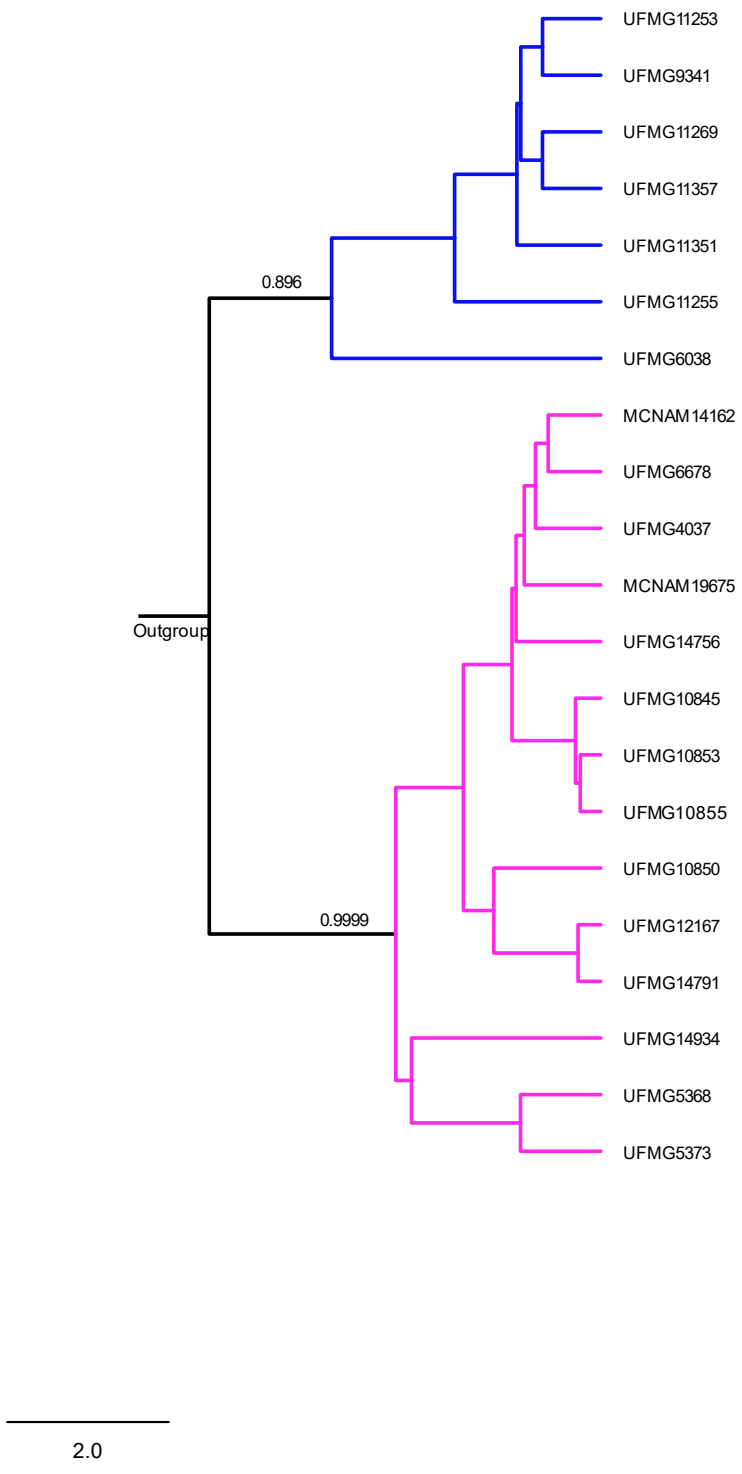

Fig S5 Mitochondrial gene tree of *Scinax curicica*. Blue corresponds to the northern population and pink to the southern population of the central barrier

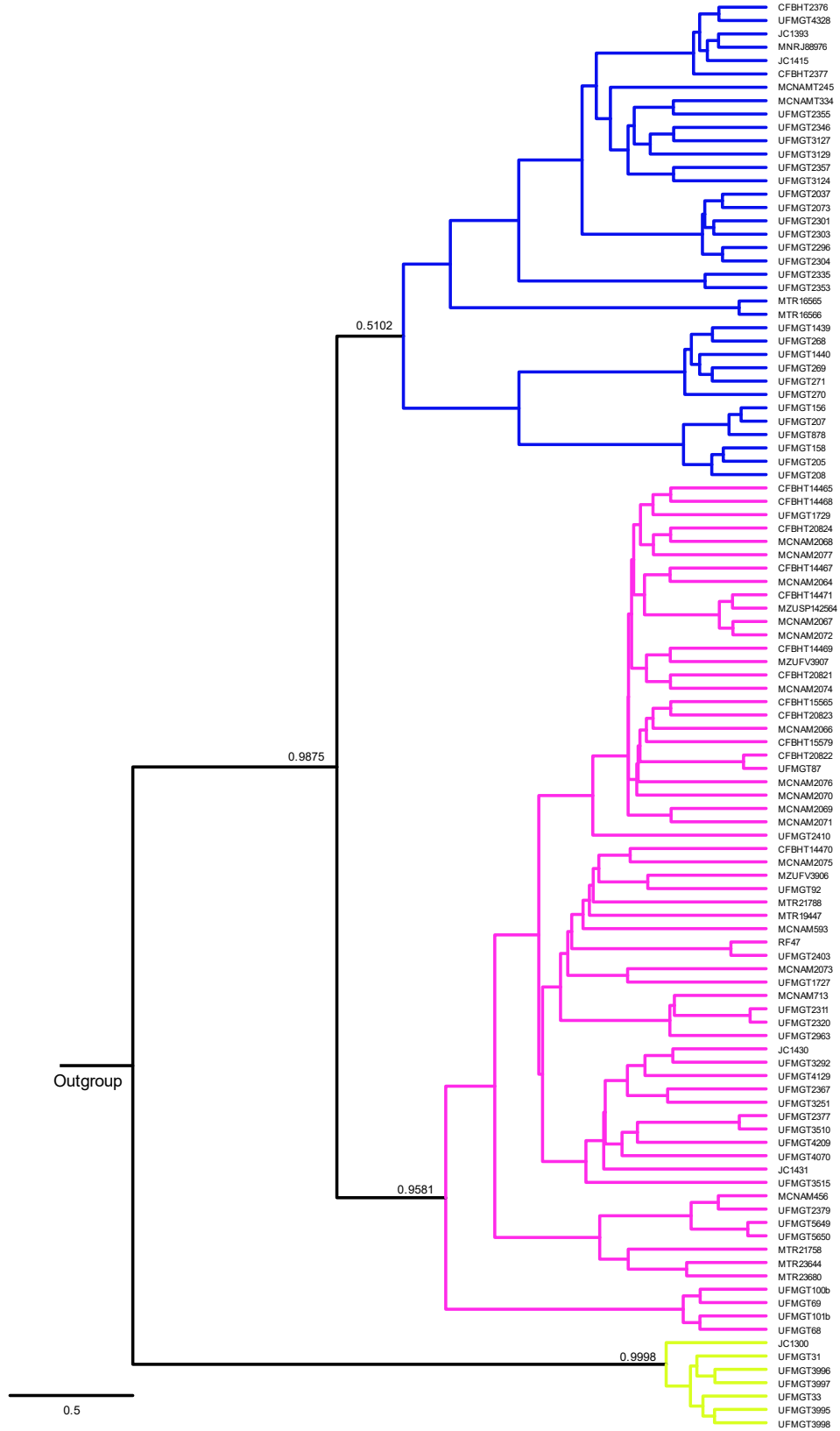

Fig S6 Mitochondrial gene tree of *Thoropa megatympanum*. Blue corresponds to the northern population and pink to the southern population of the central barrier, and yellow to the population of Cabral

b) Supplementary tables

Table S1 Details for sampled individuals used in the present study. For each sample is present voucher ID, municipality, state, geographic coordinates, and Genbank acession numbers. Herpetological collections: CHUNB = Universidade de Brasília; CFBH = Célio Fernando Baptista Haddad; LZVUFOP = Laboratório de Zoologia de Vertebrados da Universidade Federal de Ouro Preto; MCNAM = Museu de Ciências Naturais da Pontifícia Universidade Católica de Minas Gerais; MTR = Miguel Tefault Rodrigues; UFMG = Centro de Coleções Taxonômicas da Universidade Federal de Minas Gerais. *Sequences will be deposited and available at Genbank upon manuscript acceptance

Species	Voucher ID	Municipally	Brazilian State	Longitude (W)	Latitude (S)	Genbank acession numbers		
						COI	Cyt-*b*	16S
Bokermannohyla alvarengai	ID 115	Urandi	Bahia	-42.655	-14.771	MW193612	-	-
	MCNAM 17524	Santana do Riacho	Minas Gerais	-43.59	-19.288	MW193613	-	-
	MCNAM 17927	Santana do Riacho	Minas Gerais	-43.59	-19.288	MW193614	-	-
	MCNAM 17925	Santana do Riacho	Minas Gerais	-43.59	-19.288	MW193615	-	-
	UFMG 4020	Congonhas do Norte	Minas Gerais	-43.752	-18.808	MW193616	-	-
	UFMG 4021	Congonhas do Norte	Minas Gerais	-43.752	-18.808	MW193617	-	-
	UFMG 4022	Congonhas do Norte	Minas Gerais	-43.752	-18.808	MW193618	-	-
	UFMG 4023	Congonhas do Norte	Minas Gerais	-43.752	-18.808	MW193619	-	-
	UFMG 5579	Rio Pardo de Minas	Minas Gerais	-42.795	-15.642	MW193620	-	-
	UFMG 5582	Rio Pardo de Minas	Minas Gerais	-42.795	-15.642	MW193621	-	-
	UFMG 5583	Rio Pardo de Minas	Minas Gerais	-42.795	-15.642	MW193622	-	-
	UFMG 5853	Caetité	Bahia	-42.535	-14.519	MW193623	-	-
	UFMG 5143	Ouro Branco	Minas Gerais	-43.73	-20.469	MW193624	-	-
	UFMG 7401	Diamantina	Minas Gerais	-43.902	-17.924	MW193625	-	-
	UFMG 3722	Santana do Riacho	Minas Gerais	-43.512186	-19.293971	MW193626	-	-
	UFMG 5568	Catas Altas	Minas Gerais	-43.447944	-20.111806	MW193627	-	-
	UFMG 4761	Jacaraci	Bahia	-42.516851	-14.89655	MW193628	-	-
	UFMG 4762	Jacaraci	Bahia	-42.516851	-14.89655	MW193629	-	-

UFMG 4763	Jacaraci	Bahia	-42.516851	-14.89655	MW193630	-	-
UFMG 4767	Jacaraci	Bahia	-42.517699	-14.895584	MW193631	-	-
UFMG 5383	Morro do Pilar	Minas Gerais	-43.513714	-19.162183	MW193632	-	-
UFMG 5384	Morro do Pilar	Minas Gerais	-43.513714	-19.162183	MW193633	-	-
UFMG 11272	Itacambira	Minas Gerais	-43.31653	-16.99057	MW193634	-	-
UFMG 11313	Itacambira	Minas Gerais	-43.31267	-16.99079	MW193635	-	-
UFMG 11174	Santana do Riacho	Minas Gerais	-43.582	-19.291	MW193636	-	-
UFMG-T 2175	Santana do Riacho	Minas Gerais	-43.582	-19.291	MW193637	-	-
UFMG-T 2176	Santana do Riacho	Minas Gerais	-43.582	-19.291	MW193638	-	-
UFMG 10904	RioVermelho	Minas Gerais	-43.06224	-18.08207	MW193639	-	-
UFMG 10790	Diamantina	Minas Gerais	-43.745367	-18.265694	MW193640	-	-
UFMG 10792	Diamantina	Minas Gerais	-43.717181	-18.250936	MW193641	-	-
UFMG 10771	Diamantina	Minas Gerais	-43.738664	-18.246897	MW193642	-	-
UFMG 9319	Itacambira	Minas Gerais	-43.315556	-16.989722	MW193643	-	-
UFMG 9321	Itacambira	Minas Gerais	-43.315556	-16.989722	MW193644	-	-
UFMG 9327	Itacambira	Minas Gerais	-43.312222	-16.990278	MW193645	-	-
UFMG 12213	Botumirim	Minas Gerais	-43.062089	-16.844053	MW193646	-	-
UFMG 12379	Botumirim	Minas Gerais	-43.054592	-16.854492	MW193647	-	-
UFMG 12309	Botumirim	Minas Gerais	-43.059067	-16.834819	MW193648	-	-
UFMG 14262	Santo Antônio do Itambé	Minas Gerais	-43.368	-18.49	MW193649	-	-
UFMG 14263	Santo Antônio do Itambé	Minas Gerais	-43.368	-18.49	MW193650	-	-
UFMG 14287	Santo Antônio do Itambé	Minas Gerais	-43.368	-18.49	MW193651	-	-
UFMG 10871	Rio Vermelho	Minas Gerais	-43.07492	-18.08787	MW193652	-	-
UFMG 12125	Diamantina	Minas Gerais	-43.78367	-17.95758	MW193653	-	-
UFMG 12126	Diamantina	Minas Gerais	-43.76809	-17.74504	MW193654	-	-
UFMG 11044	Rio Vermelho	Minas Gerais	-43.07013	-18.09548	MW193655	-	-
UFMG 11045	Rio Vermelho	Minas Gerais	-43.07013	-18.09548	MW193656	-	-

	UFMG 14824	Santo Antônio do Itambé	Minas Gerais	-43.368	-18.490036	MW193657	-	-
	UFMF 14853	Santo Antônio do Itambé	Minas Gerais	-43.369785	-18.460542	MW193658	-	-
	UFMF 14854	Santo Antônio do Itambé	Minas Gerais	-43.369785	-18.460542	MW193659	-	-
	UFMG 14950	Barão de Cocais	Minas Gerais	-43.520381	-19.893566	MW193660	-	-
	UFMG 14951	Barão de Cocais	Minas Gerais	-43.520381	-19.893566	MW193661	-	-
	UFMG 14952	Barão de Cocais	Minas Gerais	-43.520381	-19.893566	MW193662	-	-
	UFMG 14953	Barão de Cocais	Minas Gerais	-43.520381	-19.893566	MW193663	-	-
	UFMG 14953	Grão Mogol	Minas Gerais	-42.48030	-16.30747	MW193664	-	-
	UFMG 15286	Grão Mogol	Minas Gerais	-42.48030	-16.30747	MW193665	-	-
	UFMG 15314	Grão Mogol	Minas Gerais	-42.55247	-16.37075	MW193666	-	-
	UFMG 15315	Padre Carvalho	Minas Gerais	-42.57514	-16.34923	MW193667	-	-
Bokermannohyla oxente	UFMG 4225	Macugê	Bahia	-41.471654	-12.772692	MW193700.1	-	-
Bokermannohyla saxicola	UFMG 15326	Grão Mogol	Minas Gerais	-42.92938	-16.587746	OL672838	OL653177	-
	UFMG 15299	Padre Carvalho	Minas Gerais	-42.53447	-16.29544	OL672838	OL653177	-
	UFMG 15398	Grão Mogol	Minas Gerais	-42.856003	-16.370431	OL672839	OL653178	-
	UFMG 16343	Augusto de Lima	Minas Gerais	-44.061271	-18.032073	MF918882	MF918668	-
	BS013	Congonhas do Norte	Minas Gerais	-43.770806	-18.759583	MF918882	MF918668	-
	UFMG-G 547b	Alvorada de Minas	Minas Gerais	-43.430071	-18.870196	MF918895	MF918681	-
	UFMG 12413	Conceição do Mato Dentro	Minas Gerais	-43.412463	-19.042659	MF919052	MF918838	-
	UFMG 20438	Itamarandiba	Minas Gerais	-42.731799	-18.002059	MF919033	MF918819	-
	UFMG 10888	Rio Vermelho	Minas Gerais	-43.07492	-18.08787	MF918954	MF918740	-
	UFMG 11033	Rio Vermelho	Minas Gerais	-43.06903	-18.09635	MF918996	MF918782	-
	UFMG 11037	Rio Vermelho	Minas Gerais	-43.06903	-18.09635	MF919009	MF918795	-
	UFMG-T 419	Diamantina	Minas Gerais	-43.609612	-18.215455	MF919011	MF918797	-
	BS012	São Gonçalo do Rio Preto	Minas Gerais	-43.328389	-18.178472	MF919035	MF918821	-
	UFMG-T 105	Conceição do Mato Dentro	Minas Gerais	-43.412463	-19.042659	MF918894	MF918680	-

BS014	Congonhas do Norte	Minas Gerais	-43.770806	-18.759583	MF919034	MF918820	-
BS020	Congonhas do Norte	Minas Gerais	-43.770806	-18.759583	MF918896	MF918682	-
UFMG-G 1646	Santana do Riacho	Minas Gerais	-43.720559	-19.01977	MF918900	MF918686	-
BS016	Congonhas do Norte	Minas Gerais	-43.181667	-19.266222	MF919022	MF918808	-
BS004	São Sebastião do Rio Preto	Minas Gerais	-43.181667	-19.266222	MF918898	MF918684	-
UFMG 18965	Barão de Cocais	Minas Gerais	-43.512187	-19.887327	MF918886	MF918672	-
BS007	Santana do Riacho	Minas Gerais	-43.543611	-19.257222	MF919044	MF918830	-
BS001	São Sebastião do Rio Preto	Minas Gerais	-43.181667	-19.266222	MF918889	MF918675	-
BS009	Santana do Riacho	Minas Gerais	-43.543611	-19.257222	MF918883	MF918669	-
UFMG 12342	Botumirim	Minas Gerais	-43.03905	-16.844756	MF918891	MF918677	-
UFMG 12345	Botumirim	Minas Gerais	-43.03905	-16.844756	MF918986	MF918772	-
BS023	Congonhas do Norte	Minas Gerais	-43.770806	-18.759583	MF918989	MF918775	-
UFMG 20439	Itamarandiba	Minas Gerais	-42.655528	-17.806472	MF918903	MF918689	-
BS015	Serro	Minas Gerais	-43.384159	-18.546139	MF918955	MF918741	-
UFMG 11111	Santana de Pirapama	Minas Gerais	-43.87841	-18.7858	MF918897	MF918683	-
UFMG 11266	Itacambira	Minas Gerais	-43.31397	-16.98976	MF919028	MF918814	-
UFMG 11276	Itacambira	Minas Gerais	-43.30489	-17.01754	MF918850	MF918636	-
UFMG 11279	Itacambira	Minas Gerais	-43.30489	-17.01754	MF918855	MF918641	-
UFMG 11274	Itacambira	Minas Gerais	-43.30489	-17.01754	MF918857	MF918643	-
UFMG 11288	Itacambira	Minas Gerais	-43.30505	-17.01658	MF918853	MF918639	-
UFMG-G 1266a	Joaquim Felício	Minas Gerais	-44.22535	-17.671583	MF918858	MF918644	-
UFMG 16345	Francisco Dumont	Minas Gerais	-44.322797	-17.685228	MF918843	MF918629	-
UFMG-T 420	Buenópolis	Minas Gerais	-44.249727	-17.851053	MF918841	MF918627	-
UFMG 20490	Santo Antônio do Retiro	Minas Gerais	-42.781691	-15.19681	MF918842	MF918628	-
UFMG 20491	Santo Antônio do Retiro	Minas Gerais	-42.781691	-15.19681	MF918870	MF918656	-
UFMG-T 428	Serranópolis de Minas	Minas Gerais	-42.813397	-15.774997	MF918871	MF918657	-

UFMG-T 212	Rio Pardo de Minas	Minas Gerais	-42.647589	-15.615717	MF918881	MF918667	-
UFMG-T 215	Rio Pardo de Minas	Minas Gerais	-42.647589	-15.615717	MF918874	MF918660	-
UFMG-T 421	Serranópolis de Minas	Minas Gerais	-42.813397	-15.774997	MF918877	MF918663	-
UFMG 13953	Joaquim Felício	Minas Gerais	-44.193178	-17.693408	MF918879	MF918665	-
UFMG 13977	Joaquim Felício	Minas Gerais	-44.250565	-17.722982	OL672840	OL653179	-
UFMG 14333	Turmalina	Minas Gerais	-42.77316	-17.210003	OL672841	OL653180	-
UFMG 14337	Turmalina	Minas Gerais	-42.750619	-17.18678	OL672841	OL653181	-
UFMG 14367	Turmalina	Minas Gerais	-42.795961	-17.194273	OL672841	OL653180	-
UFMG 14386	Turmalina	Minas Gerais	-42.751164	-17.186037	OL672841	OL653181	-
UFMG 16342	Joaquim Felício	Minas Gerais	-44.322797	-17.685228	MF918840	MF918626	-
BS002	Santana do Riacho	Minas Gerais	-43.182	-19.266	MF918884	MF918670	-
BS003	Santana do Riacho	Minas Gerais	-43.182	-19.266	MF918885	MF918671	-
BS005	Santana do Riacho	Minas Gerais	-43.182	-19.266	MF918887	MF918673	-
BS006	Santana do Riacho	Minas Gerais	-43.581	-19.268	MF918888	MF918674	-
BS008	Santana do Riacho	Minas Gerais	-43.544	-19.257	MF918890	MF918676	-
BS010	São Gonçalo do Rio Preto	Minas Gerais	-43.328	-18.178	MF918892	MF918678	-
BS011	São Gonçalo do Rio Preto	Minas Gerais	-43.328	-18.178	MF918893	MF918679	-
BS019	Congonhas do Norte	Minas Gerais	-43.771	-18.76	MF918899	MF918685	-
BS021	Congonhas do Norte	Minas Gerais	-43.771	-18.76	MF918901	MF918687	-
BS022	Congonhas do Norte	Minas Gerais	-43.771	-18.76	MF918902	MF918688	-
BS024	Congonhas do Norte	Minas Gerais	-43.771	-18.76	MF918904	MF918690	-
BS026	Santana do Riacho	Minas Gerais	-43.547	-19.267	MF918905	MF918691	-
BS027	Santana do Riacho	Minas Gerais	-43.547	-19.267	MF918906	MF918692	-
BS031	Congonhas do Norte	Minas Gerais	-43.755	-18.811	MF918907	MF918693	-
BS035	Congonhas do Norte	Minas Gerais	-43.755	-18.811	MF918908	MF918694	-
BS039	Congonhas do Norte	Minas Gerais	-43.755	-18.811	MF918909	MF918695	-
BS041	Congonhas do Norte	Minas Gerais	-43.755	-18.811	MF918910	MF918696	-
BS044	Congonhas do Norte	Minas Gerais	-43.755	-18.811	MF918911	MF918697	-

UFMG 20420	Congonhas do Norte	Minas Gerais	-43.754623	-18.811414	MF918912	MF918698	-
UFMG 20422	Congonhas do Norte	Minas Gerais	-43.770797	-18.759635	MF918913	MF918699	-
UFMG 20421	Congonhas do Norte	Minas Gerais	-43.754623	-18.811414	MF918914	MF918700	-
UFMG 20417	Congonhas do Norte	Minas Gerais	-43.754623	-18.811414	MF918915	MF918701	-
UFMG 20418	Congonhas do Norte	Minas Gerais	-43.754623	-18.811414	MF918916	MF918702	-
BS070	São Gonçalo do Rio Preto	Minas Gerais	-43.333	-18.218	MF918917	MF918703	-
BS071	São Gonçalo do Rio Preto	Minas Gerais	-43.333	-18.218	MF918918	MF918704	-
BS073	São Gonçalo do Rio Preto	Minas Gerais	-43.330	-18.225	MF918919	MF918705	-
BS074	São Gonçalo do Rio Preto	Minas Gerais	-43.330	-18.225	MF918920	MF918706	-
BS075	São Gonçalo do Rio Preto	Minas Gerais	-43.370	-18.129	MF918921	MF918707	-
BS077	São Gonçalo do Rio Preto	Minas Gerais	-43.370	-18.129	MF918922	MF918708	-
BS078	São Gonçalo do Rio Preto	Minas Gerais	-43.370	-18.129	MF918923	MF918709	-
BS079	São Gonçalo do Rio Preto	Minas Gerais	-43.370	-18.129	MF918924	MF918710	-
BS080	São Gonçalo do Rio Preto	Minas Gerais	-43.370	-18.129	MF918925	MF918711	-
BS081	São Gonçalo do Rio Preto	Minas Gerais	-43.370	-18.129	MF918926	MF918712	-
BS083	São Gonçalo do Rio Preto	Minas Gerais	-43.357	-18.125	MF918927	MF918713	-
BS086	São Gonçalo do Rio Preto	Minas Gerais	-43.357	-18.125	MF918928	MF918714	-
UFMG 10404	São Gonçalo do Rio Preto	Minas Gerais	-43.333	-18.218	MF918929	MF918715	-
BS088	São Gonçalo do Rio Preto	Minas Gerais	-43.34	-18.199	MF918930	MF918716	-
BS091	São Gonçalo do Rio Preto	Minas Gerais	-43.34	-18.199	MF918931	MF918717	-

BS096	São Gonçalo do Rio Preto	Minas Gerais	-43.370	-18.129	MF918932	MF918718	-
UFMG 20427	Congonhas do Norte	Minas Gerais	-43.771	-18.76	MF918933	MF918719	-
BS104	Santana do Riacho	Minas Gerais	-43.547	-19.267	MF918934	MF918720	-
BS105	São Gonçalo do Rio Preto	Minas Gerais	-43.370	-18.129	MF918935	MF918721	-
BS106	São Gonçalo do Rio Preto	Minas Gerais	-43.357	-18.125	MF918936	MF918722	-
BS107	São Gonçalo do Rio Preto	Minas Gerais	-43.357	-18.125	MF918937	MF918723	-
BS108	São Gonçalo do Rio Preto	Minas Gerais	-43.370	-18.129	MF918938	MF918724	-
BS109	São Gonçalo do Rio Preto	Minas Gerais	-43.333	-18.218	MF918939	MF918725	-
BS110	São Gonçalo do Rio Preto	Minas Gerais	-43.357	-18.125	MF918940	MF918726	-
BS111	São Gonçalo do Rio Preto	Minas Gerais	-43.333	-18.218	MF918941	MF918727	-
BS112	São Gonçalo do Rio Preto	Minas Gerais	-43.357	-18.125	MF918942	MF918728	-
BS113	São Gonçalo do Rio Preto	Minas Gerais	-43.370	-18.129	MF918943	MF918729	-
BS114	São Gonçalo do Rio Preto	Minas Gerais	-43.357	-18.125	MF918944	MF918730	-
BS116	São Gonçalo do Rio Preto	Minas Gerais	-43.357	-18.126	MF918945	MF918731	-
BS117	São Gonçalo do Rio Preto	Minas Gerais	-43.357	-18.126	MF918946	MF918732	-
BS118	São Gonçalo do Rio Preto	Minas Gerais	-43.357	-18.126	MF918947	MF918733	-
BS119	São Gonçalo do Rio Preto	Minas Gerais	-43.357	-18.125	MF918948	MF918734	-
UFMG 20481	Santo Antônio do Retiro	Minas Gerais	-42.781691	-15.19681	MF918866	MF918652	-
UFMG 20483	Santo Antônio do Retiro	Minas Gerais	-42.781691	-15.19681	MF918867	MF918653	-

UFMG 20485	Santo Antônio do Retiro	Minas Gerais	-42.781691	-15.19681	MF918868	MF918654	-
UFMG 20488	Santo Antônio do Retiro	Minas Gerais	-42.781691	-15.19681	MF918869	MF918655	-
UFMG 20591	Santo Antônio do Retiro	Minas Gerais	-42.781691	-15.19681	MF918872	MF918658	-
UFMG 20431	Itamarandiba	Minas Gerais	-42.731799	-18.002059	MF918949	MF918735	-
UFMG 20432	Itamarandiba	Minas Gerais	-42.731799	-18.002059	MF918950	MF918736	-
UFMG 20435	Itamarandiba	Minas Gerais	-42.731799	-18.002059	MF918951	MF918737	-
UFMG 20436	Itamarandiba	Minas Gerais	-42.731799	-18.002059	MF918952	MF918738	-
UFMG 20437	Itamarandiba	Minas Gerais	-42.731799	-18.002059	MF918953	MF918739	-
UFMG 20440	Itamarandiba	Minas Gerais	-42.731799	-18.002059	MF918956	MF918742	-
UFMG 20442	Itamarandiba	Minas Gerais	-42.748094	-18.004977	MF918957	MF918743	-
UFMG 20445	Itamarandiba	Minas Gerais	-42.748094	-18.004977	MF918958	MF918744	-
UFMG 20446	Itamarandiba	Minas Gerais	-42.748094	-18.004977	MF918959	MF918745	-
UFMG 20447	Itamarandiba	Minas Gerais	-42.748094	-18.004977	MF918960	MF918746	-
UFMG 20448	Itamarandiba	Minas Gerais	-42.748094	-18.004977	MF918961	MF918747	-
UFMG 20449	Itamarandiba	Minas Gerais	-42.748094	-18.004977	MF918962	MF918748	-
UFMG 20450	Itamarandiba	Minas Gerais	-42.748094	-18.004977	MF918963	MF918749	-
UFMG 20451	Itamarandiba	Minas Gerais	-42.748094	-18.004977	MF918964	MF918750	-
UFMG 20452	Itamarandiba	Minas Gerais	-42.748094	-18.004977	MF918965	MF918751	-
UFMG 20454	Itamarandiba	Minas Gerais	-42.748094	-18.004977	MF918966	MF918752	-
UFMG 20455	Itamarandiba	Minas Gerais	-42.748094	-18.004977	MF918967	MF918753	-
UFMG 20456	Itamarandiba	Minas Gerais	-42.74986	-18.011618	MF918968	MF918754	-
UFMG 20457	Itamarandiba	Minas Gerais	-42.74986	-18.011618	MF918969	MF918755	-
UFMG 20458	Itamarandiba	Minas Gerais	-42.74986	-18.011618	MF918970	MF918756	-
UFMG 20459	Itamarandiba	Minas Gerais	-42.74986	-18.011618	MF918971	MF918757	-
UFMG 11051	Santana do Riacho	Minas Gerais	-43.07013	-18.09548	MF918972	MF918758	-
UFMG 11052	Santana do Riacho	Minas Gerais	-43.07013	-18.09548	MF918973	MF918759	-
UFMG 11053	Santana do Riacho	Minas Gerais	-43.07013	-18.09548	MF918974	MF918760	-
UFMG 12224	Botumirim	Minas Gerais	-43.062558	-16.842739	MF918975	MF918761	-

UFMG 12269	Botumirim	Minas Gerais	-43.03905	-16.844756	MF918976	MF918762	-
UFMG 12272	Botumirim	Minas Gerais	-43.03905	-16.844756	MF918977	MF918763	-
UFMG 12277	Botumirim	Minas Gerais	-43.063	-16.843	MF918978	MF918764	-
UFMG 12284	Botumirim	Minas Gerais	-43.037972	-16.842694	MF918979	MF918765	-
UFMG 12294	Botumirim	Minas Gerais	-43.041489	-16.847922	MF918980	MF918766	-
UFMG 12296	Botumirim	Minas Gerais	-43.042217	-16.848186	MF918981	MF918767	-
UFMG 12326	Botumirim	Minas Gerais	-43.034522	-16.849244	MF918982	MF918768	-
UFMG 12337	Botumirim	Minas Gerais	-43.047692	-16.847889	MF918983	MF918769	-
UFMG 12339	Botumirim	Minas Gerais	-43.033528	-16.848469	MF918984	MF918770	-
UFMG 12341	Botumirim	Minas Gerais	-43.03905	-16.844756	MF918985	MF918771	-
UFMG 12343	Botumirim	Minas Gerais	-43.03905	-16.844756	MF918987	MF918773	-
UFMG 12344	Botumirim	Minas Gerais	-43.03905	-16.844756	MF918988	MF918774	-
UFMG 12346	Botumirim	Minas Gerais	-43.03905	-16.844756	MF918990	MF918776	-
UFMG 12349	Botumirim	Minas Gerais	-43.039508	-16.846083	MF918991	MF918777	-
UFMG 12350	Botumirim	Minas Gerais	-43.039508	-16.846083	MF918992	MF918778	-
UFMG 12354	Botumirim	Minas Gerais	-43.042217	-16.848186	MF918993	MF918779	-
UFMG 10858	Rio Vermelho	Minas Gerais	-43.07151	-18.0893	MF918994	MF918780	-
UFMG 10876	Rio Vermelho	Minas Gerais	-43.07492	-18.08787	MF918995	MF918781	-
UFMG 10891	Rio Vermelho	Minas Gerais	-43.07492	-18.08787	MF918997	MF918783	-
UFMG 10905	Rio Vermelho	Minas Gerais	-43.06224	-18.08207	MF918998	MF918784	-
UFMG 10914	Rio Vermelho	Minas Gerais	-43.072	-18.089	MF918999	MF918785	-
UFMG 11002	Rio Vermelho	Minas Gerais	-43.06224	-18.08207	MF919000	MF918786	-
UFMG 11004	Rio Vermelho	Minas Gerais	-43.06224	-18.08207	MF919001	MF918787	-
UFMG 11006	Rio Vermelho	Minas Gerais	-43.06903	-18.09635	MF919002	MF918788	-
UFMG 11010	Rio Vermelho	Minas Gerais	-43.06903	-18.09635	MF919003	MF918789	-
UFMG 11013	Rio Vermelho	Minas Gerais	-43.072	-18.089	MF919004	MF918790	-
UFMG 11020	Rio Vermelho	Minas Gerais	-43.07013	-18.09548	MF919005	MF918791	-
UFMG 11022	Rio Vermelho	Minas Gerais	-43.06903	-18.09635	MF919006	MF918792	-
UFMG 11026	Rio Vermelho	Minas Gerais	-43.06903	-18.09635	MF919007	MF918793	-
UFMG 11029	Rio Vermelho	Minas Gerais	-43.06903	-18.09635	MF919008	MF918794	-

UFMG 11035	Rio Vermelho	Minas Gerais	-43.06903	-18.09635	MF919010	MF918796	-
UFMG 11039	Rio Vermelho	Minas Gerais	-43.06903	-18.09635	MF919012	MF918798	-
UFMG 11042	Rio Vermelho	Minas Gerais	-43.07013	-18.09548	MF919013	MF918799	-
UFMG-G 1649	Santana do Riacho	Minas Gerais	-43.670	-19.110	MF919014	MF918800	-
UFMG-G 1650	Santana do Riacho	Minas Gerais	-43.670	-19.110	MF919015	MF918801	-
UFMG-G 1647	Santana do Riacho	Minas Gerais	-43.670	-19.110	MF919016	MF918802	-
UFMG-G 1633	Santana do Riacho	Minas Gerais	-43.670	-19.110	MF919017	MF918803	-
UFMG-G 1635	Santana do Riacho	Minas Gerais	-43.670	-19.110	MF919018	MF918804	-
UFMG-G 1634	Santana do Riacho	Minas Gerais	-43.670	-19.110	MF919019	MF918805	-
UFMG-G 1643	Santana do Riacho	Minas Gerais	-43.670	-19.110	MF919020	MF918806	-
UFMG-G 1645	Santana do Riacho	Minas Gerais	-43.670	-19.110	MF919021	MF918807	-
UFMG-G 1597	Santana do Riacho	Minas Gerais	-43.489	-19.210	MF919023	MF918809	-
UFMG-G 1598	Santana do Riacho	Minas Gerais	-43.489	-19.210	MF919024	MF918810	-
UFMG-G 1599	Santana do Riacho	Minas Gerais	-43.489	-19.210	MF919025	MF918811	-
UFMG-G 1600	Santana do Riacho	Minas Gerais	-43.489	-19.210	MF919026	MF918812	-
UFMG 11110	Santana de Pirapama	Minas Gerais	-43.87841	-18.7858	MF919027	MF918813	-
UFMG 11112	Santana de Pirapama	Minas Gerais	-43.87891	-18.78681	MF919029	MF918815	-
UFMG 11113	Santana de Pirapama	Minas Gerais	-43.87891	-18.78681	MF919030	MF918816	-
UFMG 11261	Itacambira	Minas Gerais	-43.31653	-16.99057	MF918846	MF918632	-
UFMG 11262	Itacambira	Minas Gerais	-43.31653	-16.99057	MF918847	MF918633	-
UFMG 11263	Itacambira	Minas Gerais	-43.31397	-16.98976	MF918848	MF918634	-
UFMG 11265	Itacambira	Minas Gerais	-43.31397	-16.98976	MF918849	MF918635	-
UFMG 11267	Itacambira	Minas Gerais	-43.31397	-16.98976	MF918851	MF918637	-
UFMG 11271	Itacambira	Minas Gerais	-43.3148	-16.98987	MF918852	MF918638	-
UFMG 11275	Itacambira	Minas Gerais	-43.30489	-17.01754	MF918854	MF918640	-
UFMG 11277	Itacambira	Minas Gerais	-43.30489	-17.01754	MF918856	MF918642	-
UFMG 11289	Itacambira	Minas Gerais	-43.30505	-17.01658	MF918859	MF918645	-
UFMG 11291	Itacambira	Minas Gerais	-43.30505	-17.01658	MF918860	MF918646	-

UFMG 11294	Itacambira	Minas Gerais	-43.30553	-17.01559	MF918861	MF918647	-
UFMG 11296	Itacambira	Minas Gerais	-43.30561	-17.01414	MF918862	MF918648	-
UFMG 11316	Itacambira	Minas Gerais	-43.30951	-16.99585	MF918863	MF918649	-
UFMG 11320	Itacambira	Minas Gerais	-43.30319	-16.98374	MF918864	MF918650	-
UFMG 11346	Itacambira	Minas Gerais	-43.30319	-16.98374	MF918865	MF918651	-
UFMG 16344	Augusto de Lima	Minas Gerais	-44.061271	-18.032073	MF919031	MF918817	-
UFMG 10308	Santana do Riacho	Minas Gerais	-43.67	-19.11	MF919032	MF918818	-
UFMG-T 179	Rio Pardo de Minas	Minas Gerais	-42.81	-15.61	MF918873	MF918659	-
UFMG-T 213	Rio Pardo de Minas	Minas Gerais	-42.81	-15.61	MF918875	MF918661	-
UFMG-T 214	Rio Pardo de Minas	Minas Gerais	-42.81	-15.61	MF918876	MF918662	-
UFMG-T 216	Rio Pardo de Minas	Minas Gerais	-42.81	-15.61	MF918878	MF918664	-
UFMG-T 423	Serranópolis de Minas	Minas Gerais	-42.81	-15.79	MF918880	MF918666	-
UFMG-T 70	Congonhas do Norte	Minas Gerais	-43.751991	-18.808053	MF919036	MF918822	-
UFMG 6672	Congonhas do Norte	Minas Gerais	-43.751991	-18.808053	MF919037	MF918823	-
UFMG 6673	Congonhas do Norte	Minas Gerais	-43.751991	-18.808053	MF919038	MF918824	-
UFMG 6674	Congonhas do Norte	Minas Gerais	-43.751991	-18.808053	MF919039	MF918825	-
UFMG 6675	Congonhas do Norte	Minas Gerais	-43.751991	-18.808053	MF919040	MF918826	-
UFMG 6677	Congonhas do Norte	Minas Gerais	-43.751991	-18.808053	MF919041	MF918827	-
UFMG-G 1266b	Joaquim Felício	Minas Gerais	-44.22535	-17.671583	MF918844	MF918630	-
UFMG 18963	Barão de Cocais	Minas Gerais	-43.516195	-19.886619	MF919042	MF918828	-
UFMG 18964	Barão de Cocais	Minas Gerais	-43.516195	-19.886619	MF919043	MF918829	-
UFMG 18966	Barão de Cocais	Minas Gerais	-43.516195	-19.886619	MF919045	MF918831	-
UFMG 18967	Barão de Cocais	Minas Gerais	-43.516195	-19.886619	MF919046	MF918832	-
UFMG 18968	Barão de Cocais	Minas Gerais	-43.516195	-19.886619	MF919047	MF918833	-
UFMG 18969	Barão de Cocais	Minas Gerais	-43.516195	-19.886619	MF919048	MF918834	-
UFMG 18962	Joaquim Felício	Minas Gerais	-44.22535	-17.671583	MF918845	MF918631	-
UFMG-G 1136a	Barão de Cocais	Minas Gerais	-43.516195	-19.886619	MF919049	MF918835	-
UFMG-G 1136b	Barão de Cocais	Minas Gerais	-43.516195	-19.886619	MF919050	MF918836	-
UFMG-G 1136c	Barão de Cocais	Minas Gerais	-43.516195	-19.886619	MF919051	MF918837	-

Bokermannohyla nanuzae	UFMG 4190	Santo Antônio do Itambé	Minas Gerais	-43.351439	-18.481978	OL672842	OL653182	
Leptodactylus camaquara	ALCX175P39	Santana do Riacho	Minas Gerais	-43.5187	-19.2355	-	-	*
	ALCX176P38	Santana do Riacho	Minas Gerais	-43.5187	-19.2355	-	-	*
	MTR 19591	Santana do Riacho	Minas Gerais	-43.5187	-19.2355	-	-	KY992489
	MTR 19592	Santana do Riacho	Minas Gerais	-43.5187	-19.2355	-	-	KY992490
	MTR 19593	Santana do Riacho	Minas Gerais	-43.5187	-19.2355	-	-	KY992491
	UFMG 6043	Porteirinnha	Minas Gerais	-42.785422	-15.66048	-	-	*
	UFMG 5569	Catas Altas	Minas Gerais	-43.447944	-20.111806	-	-	*
	UFMG 5570	Catas Altas	Minas Gerais	-43.447944	-20.111806	-	-	*
	UFMG 10797	Diamantina	Minas Gerais	-43.715736	-18.254278	-	-	*
	UFMG 10798	Diamantina	Minas Gerais	-43.715736	-18.254278	-	-	*
	UFMG 10712	Diamantina	Minas Gerais	-43.719389	-18.249556	-	-	*
	UFMG 12230	Botumirim	Minas Gerais	-43.061833	-16.845231	-	-	*
	UFMG 14246	Serra Azul de Minas	Minas Gerais	-43.324932	-18.39733	-	-	*
	UFMG 15591	Cristália	Minas Gerais	-42.893695	-16.521367	-	-	*
	UFMG 20263	Santana do Riacho	Minas Gerais	-43.5811	-19.2882	-	-	MW316302
	UFMG 20339	Santana do Riacho	Minas Gerais	-43.5143	-19.1625	-	-	MW316303
Leptodactylus cunicularius	UFU 1919	Chapada Gaúcha	Minas Gerais	-45.86559	-14.8731	-	-	KY992452.1
Pithecopus megacephalus	CFBH-T 07540	Santana do Riacho	Minas Gerais	-43.609222	-19.280417	-	*	-
	CFBH-T 14946	Santana do Riacho	Minas Gerais	-43.609222	-19.280417	-	*	-
	CFBH-T 15567	Santana do Riacho	Minas Gerais	-43.609222	-19.280417	-	MF171778	-
	CFBH-T 15578	Santana do Riacho	Minas Gerais	-43.609222	-19.280417	-	MF171779.1	-
	CFBH-T 15581	Santana do Riacho	Minas Gerais	-43.609222	-19.280417	-	*	-
	CFBH-T 15582	Santana do Riacho	Minas Gerais	-43.609222	-19.280417	-	MF171780.1	-
	CFBH-T 15583	Santana do Riacho	Minas Gerais	-43.609222	-19.280417	-	*	-
	CFBH-T 15584	Santana do Riacho	Minas Gerais	-43.609222	-19.280417	-	*	-
	CFBH-T 15585	Santana do Riacho	Minas Gerais	-43.609222	-19.280417	-	*	-
	CFBH-T 15586	Santana do Riacho	Minas Gerais	-43.609222	-19.280417	-	*	-

CFBH-T 15587	Santana do Riacho	Minas Gerais	-43.609222	-19.280417	-	*	-
CFBH-T 15592	Santana do Riacho	Minas Gerais	-43.609222	-19.280417	-	MF171781	-
CFBH-T 16499	Santana do Riacho	Minas Gerais	-43.609222	-19.280417	-	*	-
CFBH-T 4385	Grão Mogol	Minas Gerais	-42.861389	-16.388611	-	*	-
CHUNB 48293	Santana do Riacho	Minas Gerais	-43.609222	-19.280417	-	MF171775.1	-
CHUNB 48294	Santana do Riacho	Minas Gerais	-43.609222	-19.280417	-	*	-
CHUNB 48295	Santana do Riacho	Minas Gerais	-43.609222	-19.280417	-	*	-
LMP 322	Augusto de Lima	Minas Gerais	-44.329722	-18.045280	-	MF171782.1	-
LMP 323	Augusto de Lima	Minas Gerais	-44.329722	-18.045280	-	MF171783.1	-
MCNAM-T 187	Buenópolis	Minas Gerais	-43.814500	-17.908900	-	MF171787.1	-
MTTS 330	São Gonçalo do Rio Preto	Minas Gerais	-43.336667	-18.199722	-	MF171784.1	-
CRR 1836	Lassence	Minas Gerais	-44.467500	-17.837780	-	MF171785.1	-
LZV-UFOP 3148a	São Gonçalo do Rio Preto	Minas Gerais	-43.336944	-18.169444	-	MF171786.1	-
UFMG-G 1641a	Rio Pardo de Minas	Minas Gerais	-42.758300	-15.656000	-	MF171788.1	-
UFMG-G 1641b	Rio Pardo de Minas	Minas Gerais	-42.758300	-15.656000	-	*	-
UFMG-G 1641c	Rio Pardo de Minas	Minas Gerais	-42.758300	-15.656000	-	*	-
UFMG-G 1641d	Rio Pardo de Minas	Minas Gerais	-42.758300	-15.656000	-	*	-
UFMG-G 1641e	Rio Pardo de Minas	Minas Gerais	-42.758300	-15.656000	-	*	-
UFMG-G 1641f	Rio Pardo de Minas	Minas Gerais	-42.758300	-15.656000	-	*	-
UFMG-G 1641g	Rio Pardo de Minas	Minas Gerais	-42.758300	-15.656000	-	MF171789.1	-
UFMG-G 1641h	Rio Pardo de Minas	Minas Gerais	-42.758300	-15.656000	-	*	-
UFMG-T 0175	Rio Pardo de Minas	Minas Gerais	-42.758300	-15.656000	-	MF171773	-
UFMG-T 0181	Rio Pardo de Minas	Minas Gerais	-42.758300	-15.656000	-	MF171774.1	-
UFMG-T 0182	Rio Pardo de Minas	Minas Gerais	-42.758300	-15.656000	-	*	-
UFMG-T 0183	Rio Pardo de Minas	Minas Gerais	-42.758300	-15.656000	-	*	-
UFMG-T 0185	Rio Pardo de Minas	Minas Gerais	-42.758300	-15.656000	-	*	-
UFMG-T 0186	Rio Pardo de Minas	Minas Gerais	-42.758300	-15.656000	-	*	-
UFMG-T 0194	Rio Pardo de Minas	Minas Gerais	-42.758300	-15.656000	-	MF171772.1	-

UFMG-T 0196	Rio Pardo de Minas	Minas Gerais	-42.758300	-15.656000	-	*	-
UFMG-T 0197	Rio Pardo de Minas	Minas Gerais	-42.758300	-15.656000	-	*	-
UFMG-T 0199	Rio Pardo de Minas	Minas Gerais	-42.758300	-15.656000	-	*	-
UFMG-T 0219	Rio Pardo de Minas	Minas Gerais	-42.758300	-15.656000	-	MF171771.1	-
UFMG-T 0220	Rio Pardo de Minas	Minas Gerais	-42.758300	-15.656000	-	*	-
UFMG-T 0880	Rio Pardo de Minas	Minas Gerais	-42.758251	-15.656048	-	MF171767.1	-
UFMG-T 1446	Jacaraci	Bahia	-42.516900	-14.893400	-	MF171765.1	-
UFMG-T 1448	Jacaraci	Bahia	-42.517200	-14.880700	-	*	-
UFMG-T 2935	Diamantina	Minas Gerais	-43.716667	-18.249722	-	MF171768.1	-
UFMG-T 2959	Diamantina	Minas Gerais	-43.731389	-18.248611	-	MF171769.1	-
UFMG-T 2960	Diamantina	Minas Gerais	-43.731389	-18.248611	-	MF171770.1	-
UFMG-T 2961	Diamantina	Minas Gerais	-43.731389	-18.248611	-	MF171766.1	-
UFMG-T 2962	Diamantina	Minas Gerais	-43.731389	-18.248611	-	*	-
UFMG-T 3135	Diamantina	Minas Gerais	-43.061100	-16.837903	-	*	-
UFMG-T 3136	Diamantina	Minas Gerais	-43.061100	-16.837903	-	*	-
UFMG-T 3137	Diamantina	Minas Gerais	-43.061100	-16.837903	-	*	-
UFMG-T 4350	Grão Mogol	Minas Gerais	-42.861389	-16.388611	-	*	-
UFMG-T 9146	Augusto de Lima	Minas Gerais	-44.329230	-18.044650	-	*	-
UFMG-T 9147	Augusto de Lima	Minas Gerais	-44.329230	-18.044650	-	*	-
UFMG-T 9156	Itacambira	Minas Gerais	-43.302966	-17.104150	-	*	-
UFMG-T 9157	Itacambira	Minas Gerais	-43.302966	-17.104150	-	*	-
UFMG-T 9159	Itacambira	Minas Gerais	-43.300083	-17.114733	-	*	-
UFMG-T 9176b	Itacambira	Minas Gerais	-43.300083	-17.114733	-	*	-
UFMG-T 9178a	Itacambira	Minas Gerais	-43.304133	-17.123033	-	*	-
UFMG-T 9205	Botumirim	Minas Gerais	-42.999500	-16.909778	-	*	-
UFMG-T 9206	Botumirim	Minas Gerais	-42.999500	-16.909778	-	*	-
UFMG-T 9207	Botumirim	Minas Gerais	-42.999500	-16.909778	-	*	-
UFMG-T 9231a	Botumirim	Minas Gerais	-42.999500	-16.909778	-	*	-
UFMG-T 9231b	Botumirim	Minas Gerais	-42.999500	-16.909778	-	*	-
UFMG-T 9232a	Botumirim	Minas Gerais	-42.999750	-16.909806	-	*	-

	UFMG-T 9232b	Botumirim	Minas Gerais	-42.999750	-16.909806	-	*	-
	UFMG-T 9277	Jacaraci	Bahia	-42.516722	-14.880972	-	*	-
	UFMG-T 9278	Jacaraci	Bahia	-42.516722	-14.880972	-	*	-
	UFMG-T 9279	Jacaraci	Bahia	-42.516722	-14.880972	-	*	-
	UFMG-T 9280	Igaporã	Bahia	-42.632306	-13.847806	-	*	-
	UFMG-T 9282	Igaporã	Bahia	-42.632306	-13.847806	-	*	-
	UFMG-T 9283	Igaporã	Bahia	-42.632306	-13.847806	-	*	-
	UFMG-T 9284	Igaporã	Bahia	-42.632306	-13.847806	-	*	-
Pithecopus ayeaye	UFMG-T 3858	Ouro Preto	Minas Gerais	-43.51005	-20.39974	-	MF158429.1	-
Scinax curicica	MCNAM 19675	Santana do Riacho	Minas Gerais	-43.71480	-19.16940	-	-	*
	MCNAM 14162	Santana do Riacho	Minas Gerais	-43.71480	-19.16940	-	-	*
	UFMG 10845	Rio Vermelho	Minas Gerais	-43.07069	-18.08921	-	-	*
	UFMG 10850	Rio Vermelho	Minas Gerais	-43.07069	-18.08921	-	-	*
	UFMG 10853	Rio Vermelho	Minas Gerais	-43.07069	-18.08921	-	-	*
	UFMG 10855	Rio Vermelho	Minas Gerais	-43.07069	-18.08921	-	-	*
	UFMG 11253	Itacambira	Minas Gerais	-43.33620	-17.00071	-	-	*
	UFMG 11255	Itacambira	Minas Gerais	-43.33620	-17.00071	-	-	*
	UFMG 11269	Itacambira	Minas Gerais	-43.31397	-16.98976	-	-	*
	UFMG 11351	Itacambira	Minas Gerais	-43.33620	-17.00071	-	-	*
	UFMG 11357	Itacambira	Minas Gerais	-43.33620	-17.00071	-	-	*
	UFMG 12167	Diamantina	Minas Gerais	-43 .82272	-17.90982	-	-	*
	UFMG 14756	Santo Antônio do Itambé	Minas Gerais	-43.36422	-18.47688	-	-	*
	UFMG 14791	Santo Antônio do Itambé	Minas Gerais	-43.34412	-18.44452	-	-	*
	UFMG 14934	Barão de Cocais	Minas Gerais	-43.50225	-19.90074	-	-	*
	UFMG-T 99	Congonhas do Norte	Minas Gerais	-43.67853	-18.81078	-	-	*
	UFMG 5368	Mariana	Minas Gerais	-43.41874	-20.22832	-	-	*
	UFMG 5373	Mariana	Minas Gerais	-43.41874	-20.22832	-	-	*
	UFMG 6038	Rio Pardo de Minas	Minas Gerais	-42.78542	-15.66048	-	-	*

	UFMG-T 96	Congonhas do Norte	Minas Gerais	-43.75199	-18.80805	-	-	*
	UFMG 9341	Itacambira	Minas Gerais	-43.31111	-16.98806	-	-	*
Scinax alter	MNRJ 38384	Santa Teresa	Espírito Santo	-40.5999	-19.93176	-	-	MK266759.1
Thoropa megatympanum	CFBHT 2376	Grão Mogol	Minas Gerais	-42.89814	-16.5790724	-	-	*
	CFBHT 2377	Grão Mogol	Minas Gerais	-42.89814	-16.5790724	-	-	*
	RF47	Augusto de Lima	Minas Gerais	-44.19808	-18.1092668	-	-	*
	MCNAM2064	Jaboticatubas	Minas Gerais	-43.60412	-19.301725	-	-	*
	MCNAM2066	Jaboticatubas	Minas Gerais	-43.60412	-19.301725	-	-	*
	MCNAM2067	Jaboticatubas	Minas Gerais	-43.60412	-19.301725	-	-	*
	MCNAM2068	Jaboticatubas	Minas Gerais	-43.60412	-19.301725	-	-	*
	MCNAM2069	Jaboticatubas	Minas Gerais	-43.60412	-19.301725	-	-	*
	MCNAM2070	Jaboticatubas	Minas Gerais	-43.60412	-19.301725	-	-	*
	MCNAM2071	Jaboticatubas	Minas Gerais	-43.60412	-19.301725	-	-	*
	MCNAM2072	Jaboticatubas	Minas Gerais	-43.60412	-19.301725	-	-	MG799575
	MCNAM2073	Jaboticatubas	Minas Gerais	-43.60412	-19.301725	-	-	*
	MCNAM2074	Jaboticatubas	Minas Gerais	-43.60412	-19.301725	-	-	*
	MCNAM2075	Jaboticatubas	Minas Gerais	-43.60412	-19.301725	-	-	*
	MCNAM2076	Jaboticatubas	Minas Gerais	-43.60412	-19.301725	-	-	*
	MCNAM2077	Jaboticatubas	Minas Gerais	-43.60412	-19.301725	-	-	*
	CFBHT 14465	Santana do Riacho	Minas Gerais	-43.58247	-19.2868333	-	-	*
	CFBHT 14467	Santana do Riacho	Minas Gerais	-43.58213	-19.2870667	-	-	*
	CFBHT 14468	Santana do Riacho	Minas Gerais	-43.58282	-19.2868667	-	-	*
	CFBHT 14469	Santana do Riacho	Minas Gerais	-43.58302	-19.2868167	-	-	*
	CFBHT 14470	Santana do Riacho	Minas Gerais	-43.58375	-19.2873667	-	-	*
	CFBHT 14471	Santana do Riacho	Minas Gerais	-43.58247	-19.2868333	-	-	*
	MZUFV3906	Jaboticatubas	Minas Gerais	-43.55846	-19.248077	-	-	*
	MZUFV3907	Jaboticatubas	Minas Gerais	-43.55846	-19.248077	-	-	*
	UFMG-T 100b	Conceição do Mato Dentro	Minas Gerais	-43.43007	-18.8701965	-	-	*

UFMG-T 101b	Conceição do Mato Dentro	Minas Gerais	-43.43007	-18.8701965	-	-	*
CFBH-T 15565	Santana do Riacho	Minas Gerais	-43.64333	-19.3413889	-	-	*
CFBH-T 15579	Santana do Riacho	Minas Gerais	-43.60922	-19.2804167	-	-	*
UFMG-T 1727	Santana do Pirapama	Minas Gerais	-43.87902	-18.78663	-	-	*
UFMG-T 1729	Santana do Pirapama	Minas Gerais	-43.87565	-18.786483	-	-	MG799590
UFMG-T 2303	Itacambira	Minas Gerais	-43.32222	-16.9884167	-	-	*
UFMG-T 2304	Itacambira	Minas Gerais	-43.32222	-16.9884167	-	-	*
UFMG-T 2311	Diamantina	Minas Gerais	-43.71718	-18.2517389	-	-	*
UFMG-T 2320	Diamantina	Minas Gerais	-43.73866	-18.2468972	-	-	*
UFMG-T 2353	Botumirim	Minas Gerais	-43.04222	-16.8481861	-	-	MG799588
UFMG-T 2357	Botumirim	Minas Gerais	-43.04222	-16.8481861	-	-	*
UFMG-T 2367	Rio Vermelho	Minas Gerais	-43.07531	-18.08765	-	-	*
UFMG-T 2377	Rio Vermelho	Minas Gerais	-43.06903	-18.09635	-	-	*
UFMG-T 2379	Brumadinho	Minas Gerais	-44.19109	-20.0994722	-	-	MG799591
UFMG-T 2403	Diamantina	Minas Gerais	-43.76809	-17.74504	-	-	*
UFMG-T 2410	Diamantina	Minas Gerais	-43.77730	-17.72929	-	-	MG799592
UFMG-T 2037	Itacambira	Minas Gerais	-43.31267	-16.99079	-	-	*
UFMG-T 2073	Itacambira	Minas Gerais	-43.33620	-17.00071	-	-	*
UFMG-T 031	Joaquim Felício	Minas Gerais	-44.27433	-17.7008056	-	-	*
UFMG-T 033	Buenópolis	Minas Gerais	-44.24586	-17.9187222	-	-	*
UFMG-T 068	Alvorada de Minas	Minas Gerais	-43.46495	-18.802705	-	-	*
UFMG-T 069	Alvorada de Minas	Minas Gerais	-43.464948	-18.802705	-	-	*
UFMG-T 087	Congonhas do Norte	Minas Gerais	-43.695862	-18.8485229	-	-	*
UFMG-T 092	Congonhas do Norte	Minas Gerais	-43.751991	-18.808053	-	-	*
UFMG-T 207	Rio Pardo de Minas	Minas Gerais	-42.756975	-15.6550949	-	-	*
UFMG-T 208	Rio Pardo de Minas	Minas Gerais	-42.756975	-15.6550949	-	-	*
UFMG-T 878	Rio Pardo de Minas	Minas Gerais	-42.756975	-15.65509	-	-	*
UFMG-T 268	Licinio de Almeida	Bahia	-42.54000	-14.524367	-	-	*

UFMG-T 269	Licinio de Almeida	Bahia	-42.539996	-14.524367	-	-	*
UFMG-T 270	Licinio de Almeida	Bahia	-42.539996	-14.524367	-	-	MG799589
UFMG-T 271	Licinio de Almeida	Bahia	-42.539996	-14.524367	-	-	*
UFMG-T 1439	Jacaraci	Bahia	-42.5168515	-14.8965505	-	-	*
UFMG-T 1440	Jacaraci	Bahia	-42.5169251	-14.8933713	-	-	*
CFBHT 20821	Santana do Riacho	Minas Gerais	-43.59832	-19.20534	-	-	*
CFBHT 20822	Santana do Riacho	Minas Gerais	-43.59832	-19.20534	-	-	*
CFBHT 20823	Santana do Riacho	Minas Gerais	-43.59832	-19.20534	-	-	*
CFBHT 20824	Santana do Riacho	Minas Gerais	-43.59832	-19.20534	-	-	*
MNRJ 88976	Grão Mogol	Minas Gerais	-42.85021	-16.55810	-	-	*
MZUSP 142564	Mariana	Minas Gerais	-43.52750	-19.32500	-	-	*
MTR JC1300	Augusto de Lima	Minas Gerais	-44.37360	-18.084446	-	-	*
MTR JC1393	Grão Mogol	Minas Gerais	-42.99375	-16.4640791	-	-	*
MTR JC1415	Grão Mogol	Minas Gerais	-42.99375	-16.4640791	-	-	*
MTR JC1430	Serro	Minas Gerais	-43.45613	-18.513686	-	-	*
MTR JC1431	Serro	Minas Gerais	-43.45613	-18.513686	-	-	*
MTR 16565	Grão Mogol	Minas Gerais	-42.86297	-16.2317778	-	-	*
MTR 16566	Grão Mogol	Minas Gerais	-42.86297	-16.2317778	-	-	*
MTR 19447	Santana do Riacho	Minas Gerais	-43.558459	-19.248077	-	-	*
MTR 21758	Itabira	Minas Gerais	-43.48254	-19.4903802	-	-	*
MTR 21788	Itabira	Minas Gerais	-43.48908	-19.488066	-	-	*
MTR 23644	Itambé do Mato Dentro	Minas Gerais	-43.40103	-19.42835	-	-	*
MTR 23680	Itambé do Mato Dentro	Minas Gerais	-43.39507	-19.4212167	-	-	*
UFMG-T 156	Rio Pardo de Minas	Minas Gerais	-42.78663	-15.657321	-	-	*
UFMG-T 158	Rio Pardo de Minas	Minas Gerais	-42.78663	-15.657321	-	-	*
UFMG-T 205	Rio Pardo de Minas	Minas Gerais	-42.75697	-15.6550949	-	-	*
UFMG-T 2296	Itacambira	Minas Gerais	-43.31083	-16.9883333	-	-	*
UFMG-T 2301	Itacambira	Minas Gerais	-43.31083	-16.9883333	-	-	*

	UFMG-T 2335	Botumirim	Minas Gerais	-43.05459	-16.8544917	-	-	*
	UFMG-T 2346	Botumirim	Minas Gerais	-43.05398	-16.8528639	-	-	*
	UFMG-T 2355	Botumirim	Minas Gerais	-43.04222	-16.8481861	-	-	*
	UFMG-T 2963	Diamantina	Minas Gerais	-43.74369	-18.2642278	-	-	*
	UFMG-T 3124	Botumirim	Minas Gerais	-43.05929	-16.8300778	-	-	*
	UFMG-T 3127	Botumirim	Minas Gerais	-43.05853	-16.8317528	-	-	*
	UFMG-T 3129	Botumirim	Minas Gerais	-43.06198	-16.8393222	-	-	*
	UFMG-T 3251	Santo Antônio do Itambé	Minas Gerais	-43.32493	-18.3973301	-	-	*
	UFMG-T 3292	Santo Antônio do Itambé	Minas Gerais	-43.34099	-18.3984377	-	-	*
	UFMG-T 3510	Rio Vermelho	Minas Gerais	-43.07531	-18.08765	-	-	*
	UFMG-T 3515	Rio Vermelho	Minas Gerais	-43.06224	-18.08207	-	-	*
	UFMG-T 3995	Buenópolis	Minas Gerais	-44.24609	-17.9126219	-	-	*
	UFMG-T 3996	Buenópolis	Minas Gerais	-44.24609	-17.9126219	-	-	*
	UFMG-T 3997	Buenópolis	Minas Gerais	-44.24609	-17.9126219	-	-	*
	UFMG-T 3998	Buenópolis	Minas Gerais	-44.24609	-17.9126219	-	-	*
	UFMG-T 4070	Serro	Minas Gerais	-43.35144	-18.4819778	-	-	*
	UFMG-T 4129	Santo Antônio do Itambé	Minas Gerais	-43.34197	-18.4436403	-	-	*
	UFMG-T 4209	Serro	Minas Gerais	-43.36978	-18.4605424	-	-	*
	UFMG-T 4328	Grão Mogol	Minas Gerais	-42.95857	-16.582053	-	-	*
	UFMG-T 5649	Brumadinho	Minas Gerais	-44.02243	-20.0919667	-	-	*
	UFMG-T 5650	Brumadinho	Minas Gerais	-44.02243	-20.0919667	-	-	*
	MCNAM-T 245	Grão Mogol	Minas Gerais	-42.57500	-16.7375	-	-	*
	MCNAM-T 334	Berilo	Minas Gerais	-42.78759	-16.900036	-	-	*
	MCNAM-T 456	Caeté	Minas Gerais	-43.67432	-19.824536	-	-	*
	MCNAM-T 593	Bocaiúva	Minas Gerais	-43.79297	-17.904378	-	-	*
	MCNAM-T 713	Bocaiúva	Minas Gerais	-43.79297	-17.904378	-	-	*
Thoropa miliaris	MNRJ 70701	Macaé	Rio de Janeiro	-41.99391	-22.31410	-	-	MG799612.1

Table S2 Scenarios design by PHRAPL, following Isolation only, one coalescent event

Scenario	Population	Collapse Matrix	Complete	Multiplier Map	Growth Map	Migration Array	Class
1	[1,]	1	True	1	0	Na 0	Migration Individual
	[2,]	1		1	0	0 Na	
2	[1,]	1	True	1	1	Na 0	Migration Individual
	[2,]	1		1	0	0 Na	
3	[1,]	1	True	1	0	Na 0	Migration Individual
	[2,]	1		1	1	0 Na	
4	[1,]	1	true	1	1	Na 0	Migration Individual
	[2,]	1		1	1	0 Na	
5	[1,]	1	True	1	1	Na 0	Migration Individual
	[2,]	1		1	2	0 Na	
6	[1,]	1	True	1	0	Na 0	Migration Individual
	[2,]	1		2	0	0 Na	
7	[1,]	1	True	1	1	Na 0	Migration Individual
	[2,]	1		2	0	0 Na	
8	[1,]	1	True	1	0	Na 0	Migration Individual
	[2,]	1		2	1	0 Na	
9	[1,]	1	True	1	1	Na 0	Migration Individual
	[2,]	1		2	1	0 Na	
10	[1,]	1	True	1	1	Na 0	Migration Individual
	[2,]	1		2	2	0 Na	

Table S3 Summary of the alternative models with ΔAIC ≤ 2 selection by PHRAPL. Values of Akaike Information Criterion (AIC); composite likelihood (lnL); number of parameters of the model (params.K); the difference between AIC values of each model (ΔAIC); and Akaike Information Criterion weights (wAIC) of each taxon. Model numbers refer to the schematic models defined in Tale S2

Species	**Model**	**AIC**	**lnL**	**Params.k**	**ΔAIC**	**wAIC**
Bokermannohyla alvarengai	1	39.28324	-18.6416	1	0	0.172789
	2	39.59904	-17.7995	2	0.316	0.147536
	3	39.59904	-17.7995	2	0.316	0.147536
	4	39.59904	-17.7995	2	0.316	0.147536
	6	39.59904	-17.7995	2	0.316	0.147536
	5	41.5990431	-17.799522	3	2.316	0.054275361
	7	41.5990431	-17.799522	3	2.316	0.054275361
	8	41.5990431	-17.799522	3	2.316	0.054275361
	9	41.5990431	-17.799522	3	2.316	0.054275361

	10	43.5990431	-17.799522	4	4.316	0.019966789
Bokermannohyla saxicola	1	37.41687	-17.7084	1	0	0.326515
	2	39.41687	-17.7084	2	2	0.120118
	3	39.41687	-17.7084	2	2	0.120118
	4	39.41687	-17.7084	2	2	0.120118
	6	39.41687	-17.7084	2	2	0.120118
	5	41.4168725	-17.708436	3	4	0.044189007
	7	41.4168725	-17.708436	3	4	0.044189007
	8	41.4168725	-17.708436	3	4	0.044189007
	9	41.4168725	-17.708436	3	4	0.044189007
	10	43.4168725	-17.708436	4	6	0.016256227
Leptodactylus camaquara	1	33.92453	-15.9623	1	0	0.326515
	2	35.92453	-15.9623	2	2	0.120118
	3	35.92453	-15.9623	2	2	0.120118
	4	35.92453	-15.9623	2	2	0.120118
	6	35.92453	-15.9623	2	2	0.120118
	5	37.9245345	-15.962267	3	4	0.044189007
	7	37.9245345	-15.962267	3	4	0.044189007
	8	37.9245345	-15.962267	3	4	0.044189007
	9	37.9245345	-15.962267	3	4	0.044189007
	10	39.9245345	-15.962267	4	6	0.016256227
Scinax curicica	1	36.51198	-17.256	1	0	0.326515
	2	38.51198	-17.256	2	2	0.120118
	3	38.51198	-17.256	2	2	0.120118
	4	38.51198	-17.256	2	2	0.120118
	6	38.51198	-17.256	2	2	0.120118
	5	40.511975	-17.255988	3	4	0.044189007
	7	40.511975	-17.255988	3	4	0.044189007
	8	40.511975	-17.255988	3	4	0.044189007
	9	40.511975	-17.255988	3	4	0.044189007
	10	42.511975	-17.255988	4	6	0.016256227
Thoropa megatympanum	1	37.13571	-17.5679	1	0	0.326515
	2	39.13571	-17.5679	2	2	0.120118
	3	39.13571	-17.5679	2	2	0.120118
	4	39.13571	-17.5679	2	2	0.120118
	6	39.13571	-17.5679	2	2	0.120118
	5	41.1357091	-17.567855	3	4	0.044189007
	7	41.1357091	-17.567855	3	4	0.044189007
	8	41.1357091	-17.567855	3	4	0.044189007
	9	41.1357091	-17.567855	3	4	0.044189007
	10	43.1357091	-17.567855	4	6	0.016256227

Anexo

Produção relacionada

Magalhães, R. F.; Lemes, P.; Santos, M. T. T.; Mol, R. M.; Ramos, E. K. S.; Oswald, C. B.; Pezzuti, T. L.; Santos, F. R.; Brandão, R. A.; Garcia, P. C. A. (2021). Evidence of introgression in endemic frogs from the *campo rupestre* contradicts the reduced hybridization hypothesis. *Biological Journal of the Linnean Society 133* (2): 561–576. https://doi.org/10.1093/biolinnean/blaa142

Biological Journal of the Linnean Society, 2021, **133**, 561–576. With 5 figures.

Evidence of introgression in endemic frogs from the *campo rupestre* contradicts the reduced hybridization hypothesis

RAFAEL F. MAGALHÃES[1,2,3*], PRISCILA LEMES[4], MARCUS THADEU T. SANTOS[5], RAFAEL M. MOL[2], ELISA K. S. RAMOS[6], CAROLINE B. OSWALD[2], TIAGO L. PEZZUTI[2], FABRÍCIO R. SANTOS[2,3], REUBER A. BRANDÃO[7] and PAULO C. A. GARCIA[2]

[1]*Departamento de Ciências Naturais, Universidade Federal de São João del-Rei, São João del-Rei, Minas Gerais, Brazil*
[2]*Programa de Pós-Graduação em Zoologia, Departamento de Zoologia, Universidade Federal de Minas Gerais, Belo Horizonte, Minas Gerais, Brazil*
[3]*Laboratório de Biodiversidade e Evolução Molecular, Departamento de Genética, Ecologia e Evolução, Universidade Federal de Minas Gerais, Belo Horizonte, Minas Gerais, Brazil*
[4]*Laboratorio de Ecologia e Conservação, Departamento de Botânica e Ecologia, Instituto de Biociências, Universidade Federal do Mato Grosso, Cuiabá, Mato Grosso, Brazil*
[5]*Programa de Pós-Graduação em Zoologia, Instituto de Biociências, Universidade Estadual Paulista (UNESP), Rio Claro, São Paulo, Brazil*
[6]*Programa de Pós-Graduação em Genética e Biologia Molecular, Departamento de Genética, Evolução, Microbiologia e Imunologia, Universidade Estadual de Campinas, Campinas, São Paulo, Brazil*
[7]*Laboratório de Fauna e Unidades de Conservação, Departamento de Engenharia Florestal, Universidade de Brasília, Brasília, Distrito Federal, Brazil*

Received 22 June 2020; revised 13 August 2020; accepted for publication 18 August 2020

The *campo rupestre* ecosystem is considered an old, climatically buffered, infertile landscape. As a consequence, long-term isolation is thought to have played an important role in the diversification of its biota. Here, we tested for hybridization between two endemic leaf frogs from the *campo rupestre*. We used sequence markers and coalescent models to verify haplotype sharing between the species, to test the existence and direction of gene flow, and to reconstruct the spatiotemporal dynamics of gene flow. Additionally, ecological niche modelling (ENM) was used to assess for potential co-occurrence by overlapping the climatic niche of these species since the middle Pleistocene. We found haplotype sharing and/or lack of differentiation in four nuclear fragments, one of them associated with introgression. The coalescent models support introgressive hybridization unidirectionally from *Pithecopus megacephalus* to *P. ayeaye*, occurring ~300 kya. ENM corroborates this scenario, revealing areas of potential environmental niche overlap for the species at about 787 kya. These results contradict the expectation of reduced hybridization, while ENM suggests climatic fluctuation rather than stability for the two species. The reduced hybridization hypothesis needs to be further investigated because our results suggest that it may have unrealistic premises at least for animals.

ADDITIONAL KEYWORDS: climate instability – ecological niche modelling – phylogeographical diffusion – *Pithecopus ayeaye* – *Pithecopus megacephalus* – sky islands.

INTRODUCTION

Mountains are among the most important physiographic elements in the generation and maintenance of terrestrial biodiversity (Körner *et al.*, 2017;

*Corresponding author. E-mail: rafaelmagalhaes@ufsj.edu.br

Antonelli *et al.*, 2018; Perrigo *et al.*, 2020). These landforms cover more than one-tenth of continental surfaces and host nearly one-quarter of terrestrial species richness, including many endemic species (Körner *et al.*, 2017). This high diversity and endemism can be explained by the interaction between abiotic and biotic factors (Hopper, 2009; Antonelli *et al.*, 2018). Geodynamics and cyclical climate changes, for instance, have resulted in the emergence, differentiation and 'flickering' connectivity of habitats, accelerating speciation rates, forcing populations to change their geographical distributions or causing extinctions (Antonelli *et al.*, 2018; Flantua & Hooghiemstra, 2018). How each species responds to this dynamism depends on its adaptive potential, physiological tolerances and vagility (Flantua & Hooghiemstra, 2018; Polato *et al.*, 2018; Perrigo *et al.*, 2020).

The climate changes of the Pleistocene influenced the biological diversification of mountain systems through four main processes: fragmentation of species ranges, colonization of new areas, intermixing of previously isolated biotas and hybridization (Flantua & Hooghiemstra, 2018). Each mountain belt has a particular fingerprint with regard to the relative effects of these mechanisms on its biota (Flantua & Hooghiemstra, 2018). Although Pleistocene climate oscillations have been identified as an important factor shaping mountain diversification (Baker, 2008; McCormack *et al.*, 2009), some highland regions exhibited greater climatic stability during this epoch (Hopper, 2009; Hopper *et al.*, 2016). Such regions, with nutrient-poor soils, prolonged weathering and non-deposition, were classified by Hopper (2009) as 'old, climatically buffered, infertile landscapes' (OCBILs), many of them being archipelagos of sky islands (Silveira *et al.*, 2020). As stated by Hopper (2009), the relatively higher stability in these landscapes would generate a kind of mountain fingerprint in which long-term fragmentation would be the most relevant biogeographical process, especially for plants, as evidenced by high numbers of older evolutionary radiations (Hopper, 2009; Hopper *et al.*, 2016). Consequently, the biota of OCBILs should show overall reduced hybridization, because interspecific genetic exchange is a more common process in fluctuating environments such as 'young, often disturbed, fertile landscapes' (YODFELs; Hopper, 2018). This hypothesis posits that small fragmented populations in OCBILs evolved mechanisms for the retention of heterozygosity as a means to avoid the deleterious effects of inbreeding (Hopper, 2009), resulting in strong post-mating barriers as a by-product (Hopper, 2018). However, one cannot rule out the hypothesis that reproductive isolation evolves more slowly in allopatric populations, leading to expectations contrary to those of the reduced hybridization hypothesis (Hopper, 2018).

The Brazilian Shield highlands include several mountain systems such as the Serra do Mar, Mantiqueira, Canastra and Espinhaço ranges (Körner *et al.*, 2017; Guedes *et al.*, 2020). The summit ecosystem of the more inland portion of the Brazilian Shield highlands is the *campo rupestre*, consisting of grasslands associated with shallow and nutrient-poor soils and outcrops of quartzite, arenite or ironstone (Silveira *et al.*, 2016). Furthermore, this environment was climatically buffered during the Pleistocene (Barbosa & Fernandes, 2016) and subject to long-term geological stability (Silveira *et al.*, 2016, 2020), and as such has been recently identified as an OCBIL (Hopper *et al.*, 2016; Silveira *et al.*, 2016). The core of the *campo rupestre* is the Espinhaço mountain range, which extends for ~1100 km (from 20.35°S to 11.11°S) and is 75 km wide, and is subdivided into three main regions: Quadrilátero Ferrífero at the southern end of the range, Espinhaço Meridional mainly in Minas Gerais state and the northernmost Espinhaço Setentrional in Bahia state (Carvalho *et al.*, 2014; Guedes *et al.*, 2020). The *campo rupestre* also occurs on isolated mountain islands in central Brazil (Fernandes *et al.*, 2014; Barbosa & Fernandes, 2016; Silveira *et al.*, 2016). This ecosystem hosts disproportionately high levels of diversity and endemism for its relatively restricted area (Silveira *et al.*, 2016, 2020).

Most endemic species of the *campo rupestre* are restricted to very small geographical ranges, including many plants (e.g. Versieux *et al.*, 2010; Echternacht & Trovó, 2015), birds (e.g. Gonzaga *et al.*, 2007), mammals (e.g. Pardiñas *et al.*, 2014) and frogs (e.g. Santos *et al.*, 2020a). Furthermore, genetic assessments of endemic plants and some amphibians have indicated reduced gene flow between fragmented populations in this ecosystem (e.g. Fiorini *et al.*, 2019; Santos *et al.*, 2020b; Silva *et al.*, 2020; Silveira *et al.*, 2020). These lines of evidence corroborate the premise of reduced dispersability and increased local endemism in OCBILs (Hopper, 2009; Hopper *et al.*, 2016). The reduced hybridization hypothesis (Hopper, 2018), if corroborated, would reinforce the role of natural fragmentation on the evolution of communities of this OCBIL ecosystem. However, studies specifically developed to test this hypothesis for elements of the *campo rupestre* biota are scarce (Silveira *et al.*, 2020).

Anurans are good models for testing hypotheses relating to OCBILs because they generally exhibit low dispersal abilities (Smith & Green, 2005) and show high endemism in mountains (Guedes *et al.*, 2020), which is consistent with the premise of strongly differentiated population systems in OCBILs (Hopper, 2009). On the other hand, they are able to shift their ranges under climate change (Kusrini *et al.*, 2017), which may promote contact between previously isolated populations. Consequently, hybridization may

be a common phenomenon in anurans, including events between distantly related species (Chen *et al.*, 2018), so hybridization may have occurred if two previously isolated species came into contact during the climate cycles of the Pleistocene (Flantua & Hooghiemstra, 2018).

Here we investigated the phylogeography of two leaf frogs endemic to the *campo rupestre*: *Pithecopus ayeaye* B. Lutz, 1966 and *P. megacephalus* (Miranda-Ribeiro, 1926) (Hylidae, Phyllomedusinae). Although these frogs are not sister taxa, molecular phylogenetic analysis has shown that they are closely related (Faivovich *et al.*, 2010). Both species present several biological characteristics in line with the expectations for hypotheses relating to OCBILs. They show genetic structure associated with isolation on sky islands (Magalhães *et al.*, 2017; Ramos *et al.*, 2018). Also, the speciation of leaf frogs in the *campo rupestre* was accompanied by changes in reproductive mode, colour pattern, and modification from r- to K-selection (Faivovich *et al.*, 2010; Oliveira, 2017). These features represent putative adaptations to an OCBIL environment related to breeding in water bodies associated with rock outcrops (Magalhães *et al.*, 2017; Ramos *et al.*, 2018).

Pithecopus ayeaye and *P. megacephalus* are currently allopatric (Brandão *et al.*, 2012; Magalhães *et al.*, 2017; Ramos *et al.*, 2018), although Magalhães *et al.* (2017) identified an area of high climatic suitability for *P. ayeaye* in the southern limit of the geographical range of *P. megacephalus* in the southern Espinhaço Meridional. Here, we tested the reduced hybridization hypothesis, as expected by OCBIL theory (Hopper, 2018), vs. the presence of hybridization. We used hybridization in its broad sense, considering recent or past interbreeding (Joly *et al.*, 2012; Harrison & Larson, 2014). We also used ecological niche models (ENMs) to evaluate the role of Pleistocene climate cycles on the geographical distribution of *P. ayeaye* and *P. megacephalus*.

MATERIAL AND METHODS

Data sampling and editing

We used 86 samples of *P. ayeaye* from nine locations, and 55 samples of *P. megacephalus* from ten localities (Supporting Information, Table S1). For both species, we covered almost the entirety of their known geographical ranges. Moreover, we added sequences of a *Pithecopus rohdei* (Mertens, 1926) lineage that includes individuals from the type locality (Ramos *et al.*, 2019), which were specifically used in *BEAST analysis (see below). Our matrix included sequences of one mitochondrial DNA (mtDNA) marker, cytochrome b (cyt-*b*), and six nuclear DNA (nDNA) markers, including intron 1 of fibrinogen A α-polypeptide (Afib-int1), intron 7 of β-fibrinogen (*β*fib-int7), intron 5 of ribosomal protein L3 (RPL3-int5), and partial exons of proto-oncogene cellular myelocytomatosis (c-*myc*), proopiomelanocortin A (POMC) and tensin 3 (TNS3). We used sequences generated by Magalhães *et al.* (2017) and Ramos *et al.* (2018, 2019), and complemented them with newly acquired sequences of Afib-int1 (primers MVZ47 and MVZ 48: Bell *et al.*, 2011), *β*fib-int7 (primers FIB-B17U and FIB-B17L: Prychitko & Moore, 1997), c-*myc* (primers cmyc1U and cmyc-ex2eR: Crawford, 2003; Wiens *et al.*, 2005) and TNS3 (primers WL421 and WL423: Smith *et al.*, 2007). DNA extraction, PCR and sequencing protocols followed Magalhães *et al.* (2017), except for PCR melting temperatures and times which varied between fragments (i.e. 55 °C for 60 s for Afib-int1; 56 °C for 60 s for *β*fib-int7 and TNS3; 54 °C for 60 s for c-*myc*). The electropherograms obtained from the automated sequencer were checked, edited, and assembled using the sequence editing software SEQSCAPE 2.6 (Applied Biosystems). GenBank accession numbers and voucher information are given in Table S1.

We performed independent sequence alignments for each marker using the MUSCLE algorithm under default parameters (Edgar, 2004) implemented in ALIVIEW v.1.19 (Larsson, 2014). We then used the PHASE v.2.1.1 software (Stephens *et al.*, 2001), and the SeqPHASE input/output interconversion tool (Flot, 2010) to solve the haplotype gametic phases of nuclear markers, under a threshold of 0.7 posterior probability (PP). We found one individual heterozygous for insertion/deletion in Afib-int1, which was phased using the INDELLIGENT 1.2 web tool under default parameters (Dmitriev & Rakitov, 2008).

Gene flow analyses and testing

We first constructed haplotype networks to check for haplotype relatedness and sharing between *P. ayeaye* and *P. megacephalus* in each sampled fragment. For this, we estimated maximum likelihood (ML) gene trees through the new rapid hill-climbing algorithm using RAXML v.8.2.10 (Stamatakis *et al.*, 2007; Stamatakis, 2014) under the GTRGAMMA model, with 50 independent searches for the best gene trees. We assumed that each indel in intronic fragments must be the result of a single mutational event. Hence, the long indels in Afib-int1, *β*fib-int7 and RPL3-int5 fragments were represented as 1-bp indels to avoid overestimating mutational steps in networks. These trees were converted into haplotype networks through HAPLOVIEWER software (Salzburger *et al.*, 2011).

To check for the presence of putative hybrid individuals in nDNA data (Joly & Bruneau, 2006), we built a multigenic distance matrix using the *genpofad*

algorithm implemented in POFAD v.1.07 (Joly *et al.*, 2015). This matrix was converted into a network using the *NeighborNet* algorithm implemented in SPLITSTREE v.4.14.8 (Bryant & Moulton, 2004; Huson & Bryant, 2006).

We also tested between hybridization and incomplete lineage sorting (ILS) for fragments that exhibited shared haplotypes between *P. ayeaye* and *P. megacephalus* or no clear differentiation in exclusive haplogroups. We first generated a species tree using *BEAST from BEAST v.1.8.4 (Drummond *et al.*, 2012). The substitution models for each fragment were estimated in PARTITIONFINDER v.2.1.1 (Lanfear *et al.*, 2017) and the best models were selected using the corrected Akaike information criterion, these being HKY+I, GTR+I+Γ, HKY+I, GTR+Γ, HKY+I, K80+I+Γ and GTR+I+Γ for Afib-int1, *β*fib-int7, c-*myc*, cyt-*b*, POMC, RPL3-int5 and TNS3, respectively. The clocks were set as strict for all fragments, with the substitution rate for cyt-*b* fixed at 1 and the rates of the other fragments estimated relative to it. The Yule speciation-process prior and the piecewise constant size model were set for the species tree estimation. These settings were chosen following the assumptions of Joly (2012, 2017). The analysis was run in two independent replicates, with 5×10^8 generations, 5×10^4 thinning and 10% burn-in each. The minimal effective sample sizes (ESS > 200) and the convergence between runs were checked with TRACER v.1.7.1 (Rambaut *et al.*, 2018). We combined the trees and log files from the runs using the LOGCOMBINER v.1.8.4 post-processing tool (Drummond *et al.*, 2012), discarding the burn-in.

The test of hybridization per se was made using the software JML v.1.3.1 (Joly, 2012), simulating sequences for each fragment from a sample of 1×10^4 species trees from *BEAST runs, at a *P*-value threshold of 0.05. The model assumes neutrality and no recombination in the fragments of interest (Joly *et al.*, 2009). We therefore tested departures from neutrality through Tajima's *D* (Tajima, 1989) implemented in DNASP v.6.12.01 (Rozas *et al.*, 2017) and we performed Φ-tests of recombination (Bruen *et al.*, 2006) in SPLITSTREE 4 (Huson & Bryant, 2006). The parametric model implemented in JML tests whether the minimum distance between sequences of species pairs is smaller than in a scenario of ILS (i.e. the null model; Joly *et al.*, 2009). Additionally, it calculates the null distributions for the test statistic through comparisons between sequences simulated under ILS from a sample of species trees and the observed sequences (Joly *et al.*, 2009; Joly, 2012).

Additionally, we performed an independent test of gene flow using the Bayesian algorithm of MIGRATE-N v.3.7.2 (Beerli, 2006; Beerli & Palczewski, 2010) implemented in the online CIPRES Science gateway portal (Miller *et al.*, 2010). We tested between four models: (1) isolation between *P. ayeaye* and *P. megacephalus* (i.e. equivalent to the null model tested in JML analyses); (2) unidirectional gene flow from *P. ayeaye* to *P. megacephalus*; (3) unidirectional gene flow from *P. megacephalus* to *P. ayeaye*; and (4) bidirectional gene flow. To estimate each model, we applied empirical transition–transversion ratios ($R_{\text{cyt-}b} = 6.73$; $R_{\text{Afib-int1}} = 1.60$; $R_{\beta\text{fib-int7}} = 1.18$; $R_{\text{c-}myc} = 0.83$; $R_{\text{POMC}} = 1.51$; $R_{\text{RPL3-int5}} = 1.30$; $R_{\text{TNS3}} = 0.50$) estimated under the K80 model in MEGA X v.10.0.5 (Kimura, 1980; Kumar *et al.*, 2018). Additionally, we set the relative mutation rates among loci using the means obtained in *BEAST analysis as above (i.e. 1, 0.119, 0.506, 0.139, 0.125, 0.489 and 0.085 for cyt-*b*, Afib-int1, *B*fib-int7, c-*myc*, POMC, RPL3-int5 and TNS3, respectively). We assumed uniform and exponential distributions for the gene flow parameter ($M = m/\mu$) and mutation-scaled effective population sizes (θ), respectively. Initial values for M and θ were derived from F_{ST} estimates, and the prior distributions were adjusted after exploratory analyses. Each analysis was made in two parallel replicates, using one long and 14 short chains heated under the thermodynamic static strategy. The heating was made with the cold chain equal to 1, the hottest chain equal to 1×10^6, and the remaining chains growing at a cumulative exponential scale of $x^{1.3}$, starting from 1.5. The run-length was set with a burn-in period of 1×10^7, 1×10^8 generations and thinning of 100. Convergence between replicates was accessed through the *pairs* strategy, and mixing was evaluated using ESSs plus update rates of the chains. Selection between the four aforementioned models was made using a Bayes factor test, using Bezier's approximation scores calculated for each model (Beerli & Palczewski, 2010).

Phylogeographical dynamics

As we identified the gene fragment involved in the introgression between *P. ayeaye* and *P. megacephalus* (i.e. RPL3-int5; see Results), we used a Cauchy relaxed random walk (RRW; Lemey *et al.*, 2010) implemented in BEAST v.1.10.4 (Suchard *et al.*, 2018) to reconstruct its spatiotemporal dynamics. After exploratory analyses, we selected only one copy of each haplotype by locality to facilitate calculations in the Markov chain. A new run of PARTITIONFINDER (Lanfear *et al.*, 2017) was made to select the best substitution model for this subset of sequences (i.e. TrNef+I+Γ). We set a jitter of 0.1 to create noise in identical coordinates. We used a substitution rate of 8.7×10^{-3} substitutions per lineage per million years as estimated by Magalhães *et al.* (2017) and the

clock was set as uncorrelated log-normal (Drummond *et al.*, 2006). Concomitantly, we used the Bayesian skyline coalescent method (Drummond *et al.*, 2005) to estimate the demographic dynamics through the time of RPL3-int5. The analysis was run three times, with 5×10^8 generations, 5×10^4 thinning and 20% burn-in each, and the ESS and convergence were checked as above. The trees and log files from the runs were combined using LOGCOMBINER v.1.10.4 (Suchard *et al.*, 2018), discarding the burn-in. The maximum clade credibility (MCC) gene tree was computed with the TREEANNOTATOR v.1.10.4 post-processing tool (Suchard *et al.*, 2018). We used this MCC gene tree to reconstruct the spatiotemporal dynamics using the SPREAD v.1.0.7 software (Bielejec *et al.*, 2011). The variation in diffusion rate over time was summarized using the TimeSlicer tool (Lemey *et al.*, 2010) while the Bayesian skyline plot was produced in TRACER v.1.7.1 (Rambaut *et al.*, 2018).

Ecological niche modelling (ENM)

First, we spatially thinned the occurrence localities (Supporting Information, Table S2) by 10 km to minimize a clustering of records due to biased sampling by using *thin*() available in the package *spThin* v.0.2.0 (Aiello-Lammens *et al.*, 2015) within R v.4.0.0 (R Core Team, 2020). Some of these occurrences are unpublished and were obtained from field expeditions made after Magalhães *et al.* (2017) and Ramos *et al.* (2018) (Magalhães *et al.*, 2020). We gathered 22 occurrence records for *P. ayeaye* and 20 for *P. megacephalus* after data cleaning. We used 14 bioclimatic variables as current candidate predictors with a spatial resolution of 0.08333° (~10 km) from the global dataset of PaleoClim (Brown *et al.*, 2018). It is important to note that five variables related to monthly maximum and minimum temperatures were not available in these simulations (see Brown *et al.*, 2018). To avoid problems associated with multicollinearity, the candidate normalized predictors were selected by the variance inflation factor (VIF; Zuur *et al.*, 2010), and we retained only those variables with VIF < 10 (Dormann *et al.*, 2012) using the function *vifstep*() from the R package *sdm* v.1.0–92 (Naimi *et al.*, 2014; Naimi & Araújo, 2016). For each species, we kept a distinct environmental dataset used for calibrating the ENMs (Fig. S1). To characterize past climate conditions for each species, we used the same current environmental dataset projected to Marine Isotope Stage 19 (MIS19) in the Pleistocene (~787 kya), the Last Interglacial (LIG, ~130 kya), the Last Glacial Maximum (LGM, ~21 kya) and Mid-Holocene (MH, ~8.326–4.2 kya), all global climate slices that are available on PaleoClim (Brown *et al.*, 2018).

The spatial distribution records were associated with climatic data to characterize environmental conditions experienced by species to predict their geographical distribution. We used the *sdm* package (Naimi & Araújo, 2016) to develop the ensemble forecasting (Araújo & New, 2007) of ENM (Peterson & Soberón, 2012), and the output models were combined to generate a single prediction. For each species, we calibrated models using presence-only and presence–absence methods, as follows: bioclim, domain, MaxLike, random forest and boosted regression trees, and we used these methods from the *sdm* package (Naimi & Araújo, 2016). Because some methods require absence records, we generated pseudo-absences by taking a random sample of 10 000 sites. We used a bootstrapping method due to the small number of presence records for both species (Liu *et al.*, 2011). Models were parameterized using default options of the *sdm* package (Naimi & Araújo, 2016).

We used the area under the curve (AUC) of the receiver operating characteristic (ROC) to assess the accuracy of ENMs (Fielding & Bell, 1997). An ROC curve estimates the proportion of omission and commission errors across all possible thresholds between 0 and 1 (Jiménez-Valverde, 2012). AUC values of 0.5–0.7 correspond to low accuracy, 0.7–0.9 indicate good accuracy, and values > 0.9 indicate high accuracy (Swets, 1988). The true skill statistic (TSS) is calculated as sensitivity + specificity − 1 (Allouche *et al.*, 2006) and ranges from −1 to +1. For each species, we generate ensemble forecasting using the output models for each time slice. We classified continuous predictions into presence and absence maps based on maximizing TSS values (Allouche *et al.*, 2006). The consensual maps were weighted by TSS values. Further, we assembled the binary maps by simple mean values for each species from single methods under current and past climate conditions. Also, we evaluated the relative variable importance (Murray & Conner, 2009) and plotted the predicted response curves (Elith *et al.*, 2005) to infer the relationship between the environmental variables and predicted habitat suitability.

Areas of potential co-occurrence were calculated by superimposing the presence and absence maps of the both species using the *raster* package v.3.0–12 of the R software (Hijmans, 2020). Potential co-occurrence therefore indicates areas that host environmental conditions that are considered suitable for both species (Araújo *et al.*, 2011). Finally, we used the binary maps to define areas of long-term climate stability for both species. If a species was predicted to occur in a given cell in different periods (MIS19, LIG, LGM, MH and current), then this cell was considered climatically stable. Therefore, the proportion of presence over time expresses the relative climatic stability.

RESULTS

Gene flow

The mtDNA network revealed that *P. ayeaye* and *P. megacephalus* are distinguished by 102 mutational steps (Fig. 1A). Regarding the nDNA networks, only *β*fib-int7 and c-*myc* exhibit two well-differentiated haplogroups representing the two distinct species (Fig. 1B, G). The fragment POMC shows no clear haplogroup differentiation (Fig. 1F), while Afib-int1, RPL3-int5 and TNS3 each show a shared haplotype between the two species (Fig. 1C, D, E). Despite more than half of the nDNA fragments showing no exclusive and/or well-differentiated haplogroups, there is no evidence of hybridization over a few generations between the species, as revealed by the lack of individuals mixed in distinct clusters or represented in the 'torso' of the multigenic nuclear network (Fig. 2A).

There is no evidence of deviation from neutrality or recombination within the fragments Afib-int1, POMC, RPL3-int5 and TNS3 (Table 1). The null model of ILS was not rejected for the fragments Afib-int1, POMC and TNS3. On the other hand, the result of JML analysis supports nDNA introgression in the fragment RPL3-int5 (Table 1). There were seven haplotypes whose pairwise distances between *P. ayeaye* and *P. megacephalus* were shorter than expected in the ILS scenario ($P < 0.05$), one of them being very abundant and well distributed in all localities with evidence of introgressive hybridization (Fig. 3).

The MIGRATE-N results show that the model with unidirectional gene flow from *P. megacephalus* to *P. ayeaye* has the highest probability (PP = 0.994, Table 2), supporting unidirectional introgressive hybridization in the past. For this scenario, parameter estimates are presented in the Supporting Information Table S3. On the other hand, the model with isolation between the species has the lowest probability (PP < 0.001, Table 2), reinforcing the scenario of introgression.

Phylogeographical dynamics

The haplotypes of RPL3-int5 coalesced around 5.68 Mya [95% highest posterior density (HPD): 1.68–15.90 Mya) (Supplementary File 1). Past population dynamics of this gene show effective size increased at about ~150 kya (Fig. 4A). The mean diffusion rate for the data was ~137.4 km/Myr (= 0.137 m/year; 95% HPD: 0.073–0.204 m/year). Variation in the diffusion rate through time indicated an acceleration between 780 and 340 kya, and other accretion in the rate from 100 kya until the present (Fig. 4B). The haplotypes showing a sign of introgression coalesced at ~541 kya (95% HPD: 255–980 kya), with the estimated node in the northern distribution of *P. megacephalus* (Fig. 4C). The diffusion from *P. megacephalus* to *P. ayeaye* was estimated to have occurred at ~300 kya (95% HPD: 119–561 kya), concomitantly with the highest diffusion rate during a cold period in the Middle Pleistocene (Fig. 4B, C). We found no relationship between the main diffusion events for the haplotypes with the trace of introgression and the increase in the effective size based on RPL3-int5 (Fig. 4A, C).

Ecological niche modelling

Four variables presented VIF < 10 for each species (Supporting Information, Fig. S1). The predictive accuracies of the models were relatively high for both species with an AUC of 0.965 (SD = 0.015) (Table S4). The response curves showed that the probability of occurrence of both species is fundamentally limited by precipitation (Fig. S1). The probability of occurrence of *P. ayeaye* followed an optimum curve with high probability between 500 and 1000 mm or up to 2000 mm for precipitation of the warmest quarter (BIO18), while *P. megacephalus* showed a high probability of occurrence in areas that have an abrupt decline in precipitation of the driest month (BIO14), suggesting that this species prefers drier areas (Fig. S1). Using the binary maps (TSS = 0.920, SD = 0.020), the results show climatically stable areas for *P. ayeaye* covering the southern *campo rupestre* over time, in addition to a part of the Mantiqueira range. For *P. megacephalus*, climate stability has been extended to the core of the *campo rupestre*, in Espinhaço Meridional (Fig. 5A).

The models predict different areas of co-occurrence by overlapping the climatic niches between the two species over time, and which were inferred to be established in the Espinhaço range under the current scenario (Fig. 5B). For both species, there was a contraction in areas of suitability during the LIG (Fig. 5B; Supporting Information, Fig. S2). Moreover, the results of habitat suitability modelling showed a marked range contraction for *P. ayeaye* during the LGM, followed by an expansion during the MH until the present (Fig. 5B; Fig. S2). For *P. megacephalus*, a huge range expansion northwestward was inferred during the LGM, with a subsequent increase in habitat suitability at the core of the *campo rupestre* during the MH and at present (Fig. 5B; Fig. S2).

DISCUSSION

Our JML, MIGRATE-N and RRW analyses independently support introgressive hybridization involving *P. megacephalus* and *P. ayeaye*. Although our geographical sampling was heterogeneous (Supporting Information, Table S1), it is possible to state that introgressed haplotypes are more common at the

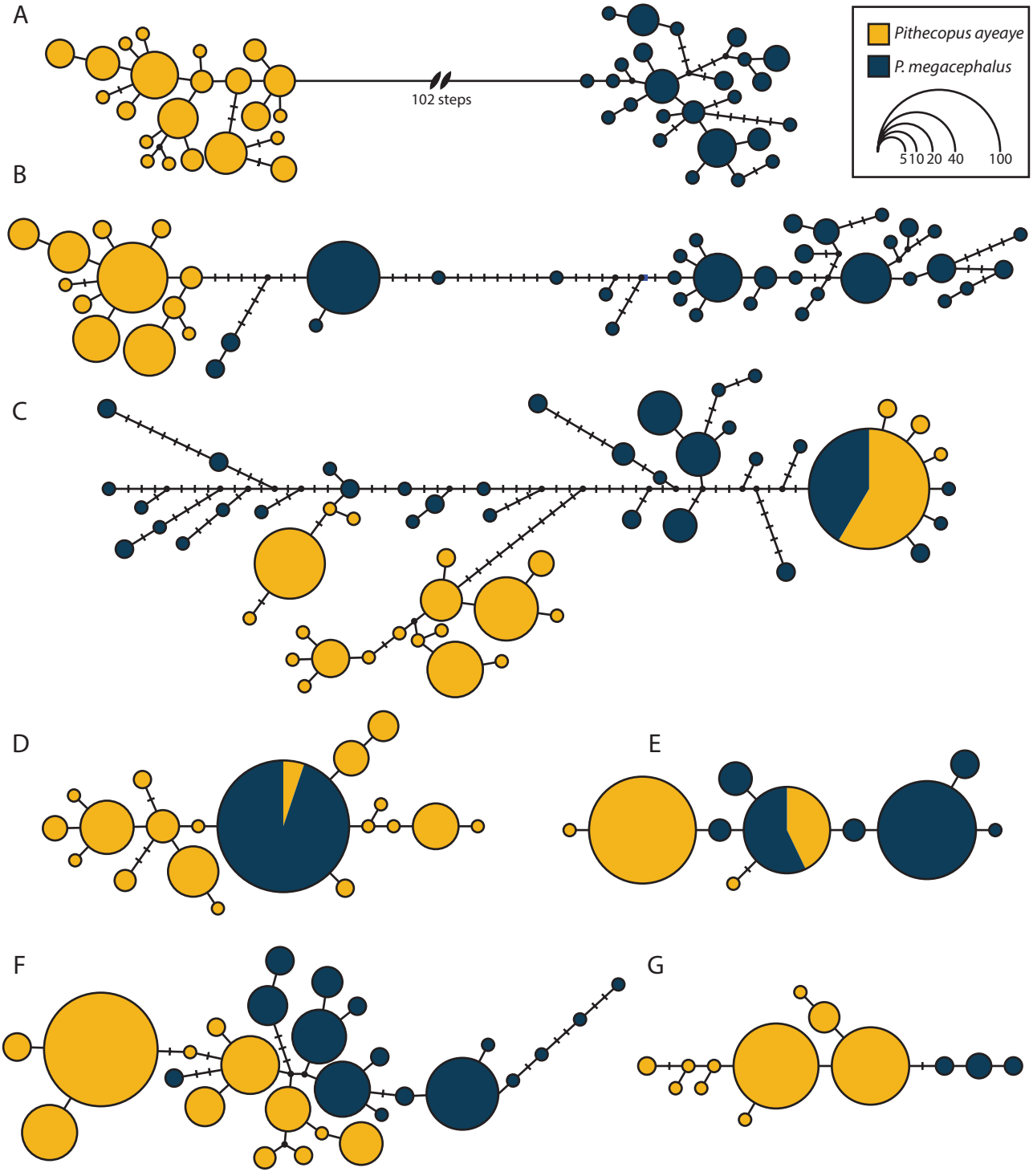

Figure 1. Haplotype networks for the markers cytochrome b (A), intron 7 of β-fibrinogen (B), intron 5 of ribosomal protein L3 (C), intron 1 of fibrinogen A α-polypeptide (D), tensin 3 (E), proopiomelanocortin A (F) and proto-oncogene cellular myelocytomatosis (G) according to their maximum likelihood gene trees. Dashes correspond to mutational steps and black dots represent unobserved haplotypes and potential intermediates.

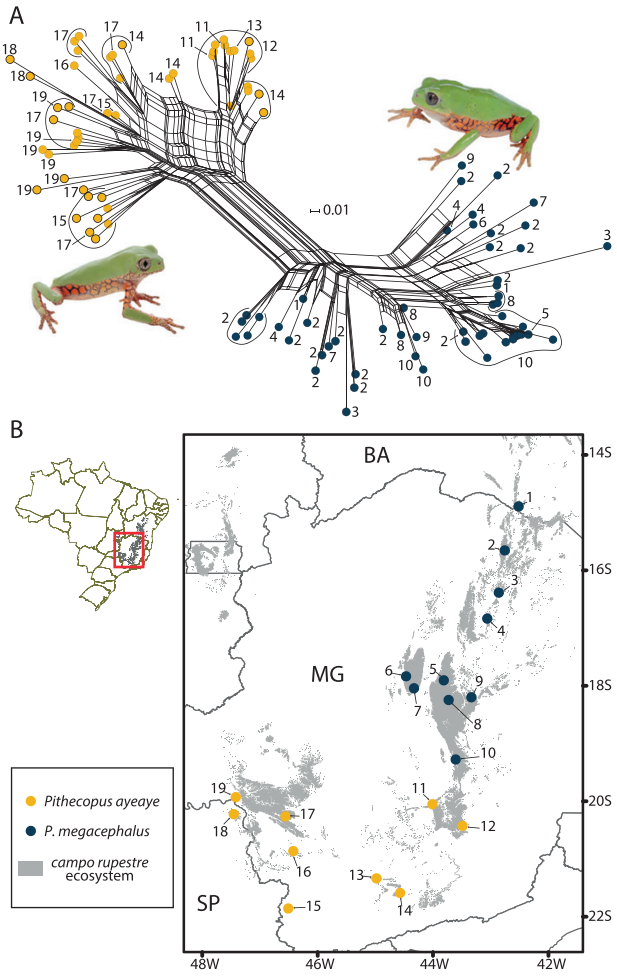

Figure 2. A, neighbour-net representation of *genpofad* multilocus nuclear distances; and B, sampling localities of *Pithecopus ayeaye* and *P. megacephalus*. Scale bar representes standardized genetic distances for the net. Numbers in A and B refer to the following localities (municipality, state): 1: Jacaraci, BA; 2: Rio Pardo de Minas, MG; 3: Grão Mogol, MG; 4: Botumirim, MG; 5: Buenópolis, MG; 6: Lassance, MG; 7: Augusto de Lima, MG; 8: Diamantina, MG; 9: São Gonçalo do Rio Preto, MG; 10: Santana do Riacho, MG; 11: Nova Lima, MG; 12: Ouro Preto, MG; 13: Lavras, MG; 14: Minduri, MG; 15: Poços de Caldas, MG; 16: Alpinópolis, MG; 17: São Roque de Minas, MG; 18: Pedregulho, SP; 19: Sacramento, MG. For geographical coordinates, refer to Table S1. Brazilian state acronyms: BA, Bahia; MG, Minas Gerais; SP, São Paulo. Limits of the *campo rupestre* are modified from Fernandes *et al.* (2014). Photos of *Pithecopus ayeaye* (left) and *P. megacephalus* (right) by T.L.P.

southern limit of the distribution of *P. megacephalus* (Southern population *sensu* Ramos *et al.*, 2018) and the north-eastern limit of the distribution of *P. ayeaye* (Quadrilátero evolutionarily significant unit *sensu* Magalhães *et al.*, 2017). Additionally, the ENMs predicted co-occurrence by overlapping the climatic niches between *P. ayeaye* and *P. megacephalus* at the limits of their geographical ranges in all projections except for the LGM. The suitable areas of co-occurrence were quite discrete in the LIG, coinciding with range contraction for both species. In general, the ENMs are in accordance with the genetic models, suggesting that Pleistocene climate dynamics may have promoted contact between the two species, assuming that precipitation is highly related to their geographical distribution. This scenario is likely because the two species breed synchronously and in the same kind of environment (Oliveira *et al.*, 2012; Nali *et al.*, 2015; Oliveira, 2017), which would facilitate reproductive syntopy and synchrony between them.

The sign of introgression has an impact on the conservation and systematics of these species. Magalhães *et al.* (2017) used three genetic markers (cyt-*b*, POMC and RPL3-int5) to investigate diversification within *P. ayeaye*. They found three evolutionarily significant units (ESUs), one of which, the Quadrilátero ESU, corresponded exactly to the area where we found haplotypes introgressed from *P. megacephalus*. Because Magalhães *et al.* (2017) worked with a limited sampling of markers, including RPL3-int5, the novel haplotypes incorporated from *P. megacephalus* in the Quadrilátero ESU may have influenced the observed pattern of genetic structure. Despite this, we do not rule out that the number of ESUs has been overestimated for *P. ayeaye* due to the use of RPL3-int5, especially if the introgression signature is limited to a small amount of the genome. Therefore, an assessment of genome-wide markers is necessary to evaluate the extent of genome exchanged between these species and its influence on their genetic structures.

In accounting for gene flow, molecular systematics represents another challenge with regard to these leaf frogs. The amount of the genome involved in reproductive isolation between two species tends to increase with time (Harrison & Larson, 2014). It is noteworthy that although *P. ayeaye* and *P. megacephalus* are not sister species (Faivovich *et al.*, 2010), we found signs of introgression. It is therefore reasonable to expect that the number of introgressed genes among sister species of *Pithecopus* will be greater than between *P. ayeaye* and *P. megacephalus*, but this hypothesis remains to be tested. High gene tree discordance has been reported for some *Pithecopus* species, which resulted in species trees with poorly supported nodes, as described for *P. megacephalus* and the *P. rohdei* complex (Ramos *et al.*, 2019) and observed for the complex that includes *P. ayeaye*, *P. centralis* and *P. oreades* (R. F. Magalhães *et al.*, unpublished data). Although this discordance can be explained in part

by ILS, gene flow may also contribute to topological incongruences (Ramos *et al.*, 2019). Additionally, mtDNA genetic distances between these species are exceedingly small (Faivovich *et al.*, 2010), which can also result from the influence of gene flow during their evolutionary histories (Harrison & Larson, 2014). Our results reinforce the idea that hybridization and introgression are common phenomena driving the diversification of phylomedusines (Haddad *et al.*, 1994; Gray, 2011; Brunes *et al.*, 2014). Thus, phylogenetic methods that take gene flow into account (e.g. Zhang *et al.*, 2017; Hey *et al.*, 2018; Jones, 2019) are probably more appropriate for the reconstruction of the evolutionary history of *Pithecopus* species.

The reduced hybridization hypothesis proposed by Hopper (2018) implies that introgression and hybridization are less common in OCBILs than in YODFELs. Nevertheless, our results reveal introgression in low-vagility organisms (Smith & Green, 2005) that are not strictly soil-dependent, contradicting the premise that fragmentation and long-term isolation are the most important processes related to diversification in the *campo rupestre*, at least for some animals. In contrast to plants, whose seed dispersal from a parental habitat results in a high risk of landing on inappropriate soils (Hopper, 2009; Hopper *et al.*, 2016), vagile animals can actively search for an ideal environment at most stages of their lives. In this sense, if the climatic fluctuations of the Pleistocene made valleys environmentally suitable for organisms from mountain tops, it is to expected that some animals changed their altitudinal range (Flantua & Hooghimstra, 2018) while plants remained restricted to the soils to which they are adapted (Silveira *et al.*, 2020). These range dynamics may have promoted contact between previously isolated populations or species, as appears to be the case of *P. ayeaye* and *P. megacephalus*.

Table 1. Neutrality, recombination and introgression tests for the nuclear DNA fragments without haplogroup differentiation or with haplotype sharing between *Pithecopus ayeaye* and *P. megacephalus*. Numbers in bold are significant at the 95% confidence limit. Tajima's *D* values were not significant

Fragment	Tajima's *D*	ϕ-Test *P*-value	JML test	
			Minimum distance	*P*-value
Afib-int1	−0.853	0.082	0	0.413
POMC	0.030	0.386	0.005	0.872
RPL3-int5	0.725	0.556	**0**	**0.026**
TNS3	0.226	0.841	0	0.615

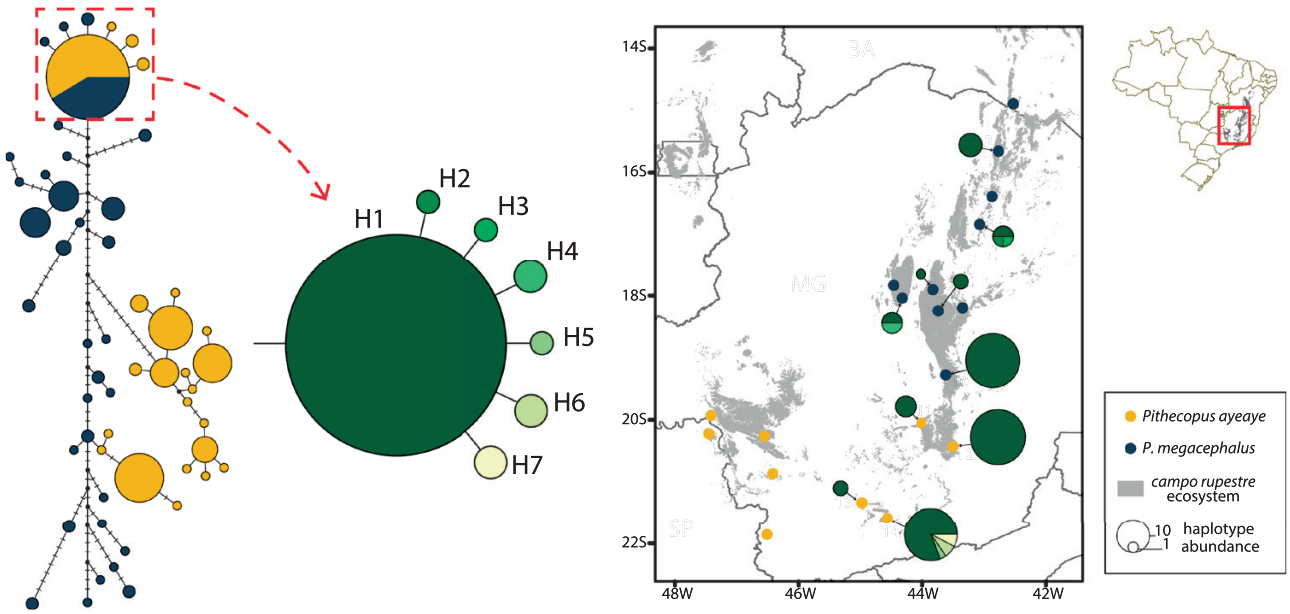

Figure 3. Haplotype network of intron 5 of ribosomal protein L3 highlighting (dashed red square and arrow) the haplogroup with potentially introgressed haplotypes. On the right is the geographical distribution of these haplotypes. Numbers in the map refer to the following localities (equivalent to those in Fig. 2, all in the state of Minas Gerais): 2: Rio Pardo de Minas; 4: Botumirim; 5: Buenópolis; 7: Augusto de Lima; 8: Diamantina; 10: Santana do Riacho; 11: Nova Lima; 12: Ouro Preto; 13: Lavras; 14: Minduri. Limits of the *campo rupestre* are modified from Fernandes *et al.* (2014).

Table 2. Model selection with MIGRATE-N. Parameter estimates for the best model are presented in Table S3

Model	Bezier's approximation score	PP	Weight
P. ayeaye → *P. megacephalus*	−10 973.22	0.006	0.006
P. ayeaye ← *P. megacephalus*	−10 968.08	0.994	1.000
P. ayeaye ↔ *P. megacephalus*	−10 976.51	<0.001	<0.001
Isolation	−11 333.60	<0.001	<0.001

PP, posterior probability.

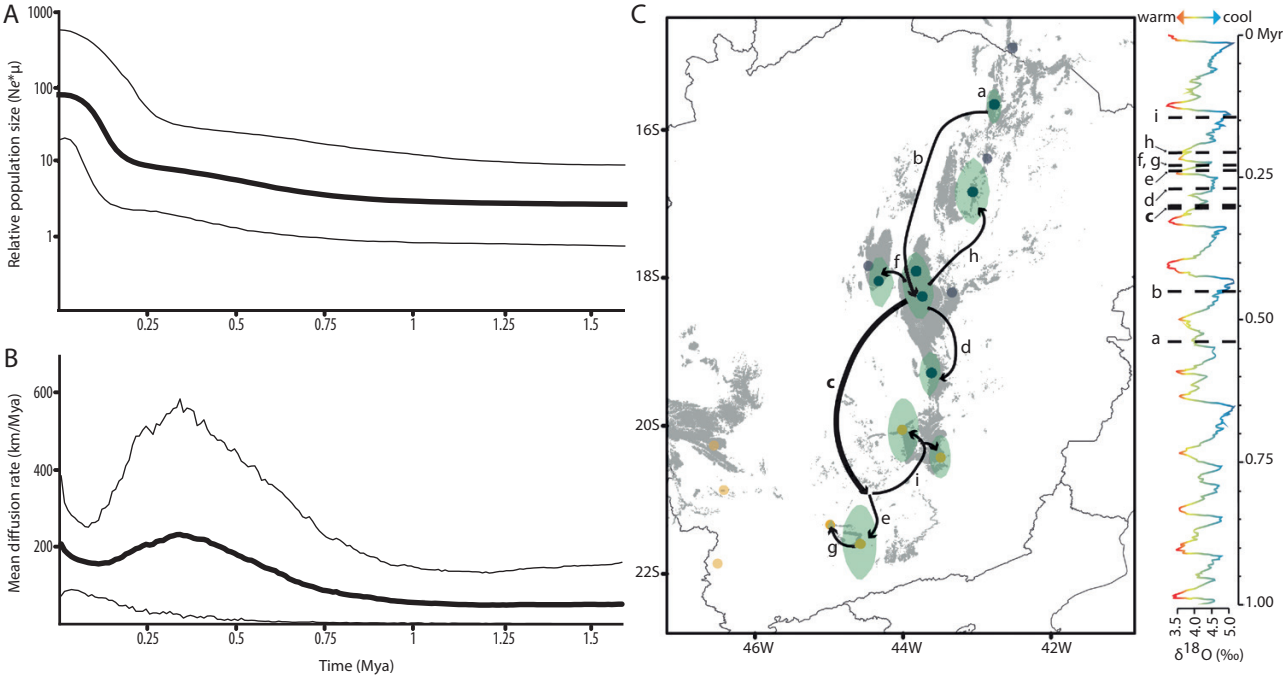

Figure 4. Variation through time in effective population size based on Bayesian skyline (A) and diffusion rate based on Cauchy RRW analyses (B) for intron 5 of ribosomal protein L3 (RPL3-int5). Thick lines represent the means and thin lines are the 95% HPD credibility interval. C, schematic representation of the spatio-temporal dynamics of haplotypes that show pairwise distances smaller than expected by the model of incomplete lineage sorting in RPL3-int5 (the complete reconstruction is available as a KML file in Supplementary File 1). Green polygons in the map represent the 80% HPD interval of uncertainty in the location of ancestral branches. The coalescence of these haplotypes (a) and the colonization routes (b–i) are representations of the nodes of each event, whose mean times are indicated in the $\delta^{18}O$ curve (i.e. the composite benthic stable oxygen isotope ratios; modified from Lisiecki & Raymo, 2005). The estimated route and time for introgression from *P. megacephalus* to *P.ayeaye* (c) are highlighted in bold on the map and the $\delta^{18}O$ curve. Limits of the *campo rupestre* are modified from Fernandes *et al.* (2014).

The assumption of reduced hybridization in OCBILs comes from the idea that genetic exchange in fluctuating environments is greater than in stable environments (Hopper, 2018). At this point, our ENM results do not support the historical stability predicted for the *campo rupestre* over the past 20 kyr (Barbosa & Fernandes, 2016), suggesting climatic instability at least for precipitation patterns (Fig. 5; Supporting Information, Fig. S1). As with Magalhães *et al.* (2017), we found suitable areas for the co-occurrence of species, although there is no record of sympatry at present. This could be explained by competition or historical contingency (Magalhães *et al.*, 2017), but we do not rule out the hypothesis that *P. ayeaye* and *P. megacephalus* may be found together in some poorly sampled locations between northern Quadrilátero Ferrífero and southern Espinhaço Meridional, where some small mountains are found.

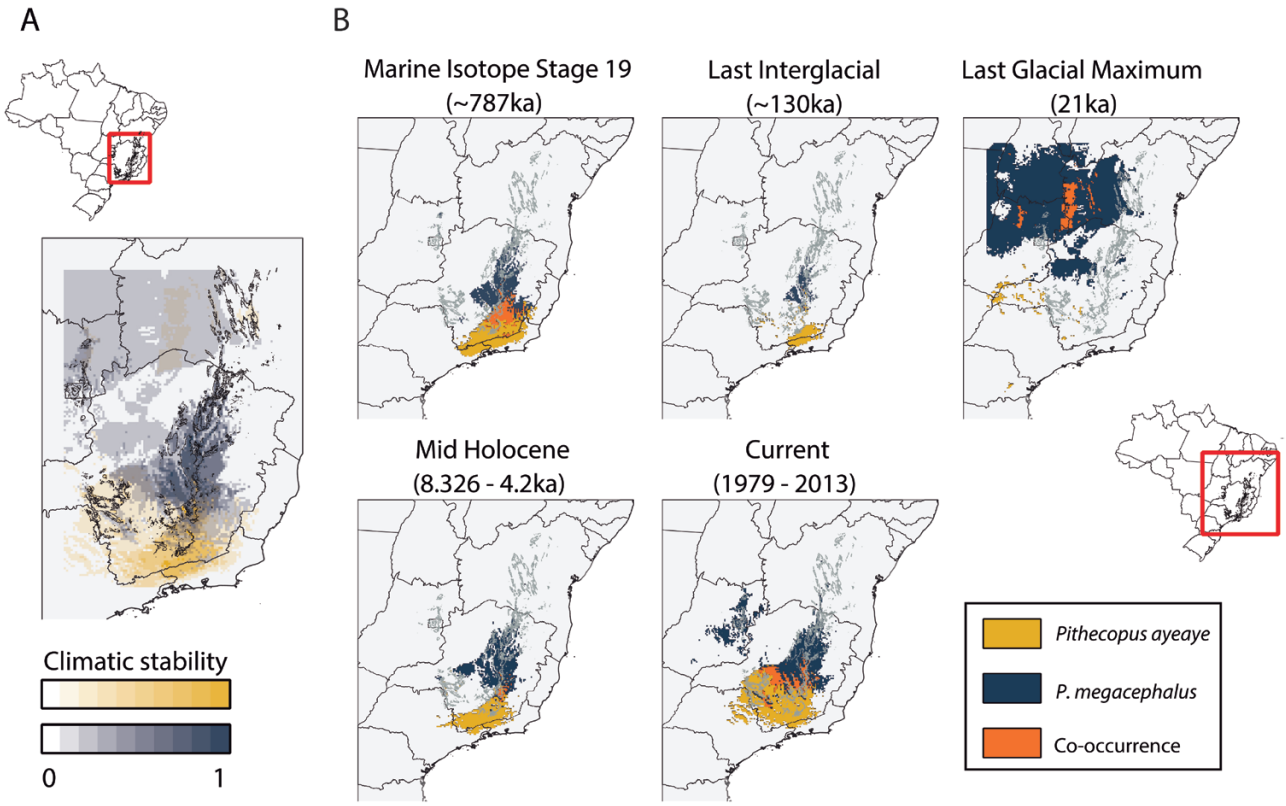

Figure 5. Maps of ecological niche models for *Pithecopus ayeaye* and *P. megacephalus* that represent the relative climatic stability for both species over time (A), and binary maps with inferred co-occurrence areas in orange (B). Limits of the *campo rupestre* (in grey) are modified from Fernandes *et al.* (2014).

Our ENM results for the LGM show a marked range expansion for *P. megacephalus*, following the expansion of a plateau climate and range contraction of a valley climate in central Brazil (Vidal *et al.*, 2019). However, our projection reveals a displacement of suitable climate to the north-west of Espinhaço Meridional, in two main disjunct areas, a smaller one in north-western Minas Gerais and a much bigger area including western Bahia, southern Tocantins, northern Goiás and north-eastern Mato Grosso states (Fig. 5B). A complete range shift for the species is a biologically unlikely scenario, as it would imply the crossing of important barriers, such as the São Francisco River valley. Werneck *et al.* (2012) reported a decrease in precipitation of the driest month (BIO14) in central Brazil during the LGM, which may have generated inappropriately drier climates for *P. megacephalus* in Espinhaço Meridional. Thus, it is more credible that *P. megacephalus* has remained restricted to microrefugia in the *campo rupestre*, rather than has shifted its geographical range towards central Brazil. For *P. ayeaye*, the contraction plus displacement of suitable climates during the LGM (Fig. 5B) also suggests a scenario of restriction to microrefugia.

Although Barbosa & Fernandes (2016) have suggested general climatic stability for the *campo rupestre*, they reported contractions at the borders of its core areas, supporting a scenario of cyclical isolation and contact between the limits of distinct mountains. In this regard, the potential contact areas observed for *P. ayeaye* and *P. megacephalus* during MIS19, the MH and at present, plus their reciprocal isolation during the LIG and LGM, suggest that the region between the northern Quadrilátero Ferrífero and Southern Espinhaço Meridional may be a hotspot for hybridization, intermixing, and colonization for organisms whose distribution is driven by precipitation. This pattern has already been reported, at least for amphibians, with evidence of biota intermixing between this region and the Mantiqueira range (Silva *et al.*, 2018). Moreover, the distribution of other frogs suggests a scenario of recent colonization. *Bokermannohyla saxicola* (Bokermann, 1964), for instance, has most of its distribution recorded in the Espinhaço Meridional (Leite *et al.*, 2008). A population of the species was recently recorded in the extreme northern Quadrilátero Ferrífero, belonging to a lineage that has diversified very recently in the history of the

species (Nascimento *et al.*, 2018). The opposite seems to occur with *Phasmahyla jandaia* (Bokermann & Sazima, 1978), which is mainly distributed in the Quadrilátero Ferrífero, but also occurs at the southern end of the Espinhaço Meridional (Leite *et al.*, 2008).

For plants, long-term isolation in the *campo rupestre* has been widely demonstrated through population genetics and phylogeographical studies (Silveira *et al.*, 2020). However, our results suggest that climate fluctuations of Pleistocene may have resulted in a far more dynamic mountain fingerprint than expected by OCBIL theory (Hopper, 2009), and this should be further investigated for other animals. The diversity in Brazilian highlands is related to a multitude of factors that influence their degree of connectivity, including topography and climate changes (Vidal *et al.*, 2019). In this sense, OCBIL theory would benefit from incorporating more holistic models than its fixed premises, such as the flickering connectivity system (FCS) proposed by Flantua & Hooghiemstra (2018). The FCS evaluates the relationship between Pleistocene climate changes and biodiversity dynamics in mountains from population to community levels. Thus, the focus of hypothesis testing in OCBIL theory would change from isolation, as demonstrated for plants (Silveira *et al.*, 2020), to the relative role of fragmentation, colonization, intermixing or hybridization in shaping the biodiversity patterns in these areas (Flantua & Hooghiemstra, 2018), especially for more vagile organisms such as animals. The advantage of the FCS is that it assumes that each mountain system has a unique evolutionary history, namely its own mountain fingerprint with regard to the above processes (Flantua & Hooghiemstra, 2018). Its adoption would avoid the ad-hoc adjustments that are often made regarding the premises of OCBIL theory for each mountain range (Hopper *et al.*, 2016; Silveira *et al.*, 2020).

The mountain fingerprint expected for the *campo rupestre* through OCBIL theory seems to be unrealistic for vagile organisms because evidence suggests that recent colonization and intermixing of biota may have been important processes in the diversification of this ecosystem, at least for anurans (Nascimento *et al.*, 2018; Silva *et al.*, 2018). Despite this being a small-scale study, our findings highlight that hybridization may also have influenced diversification patterns. Given the lack of studies on this subject, further investigations should explicitly test the reduced hybridization hypotheses for the *campo rupestre* biota.

ACKNOWLEDGEMENTS

This study was conducted in a time of extreme difficulties for researchers, teachers and environmental professionals in Brazil. We express our displeasure with the government that has dismantled public policies that had improved for decades and brought advances in research and environmental protection. We thank Fernanda Werneck, Suzette Flantua, Arley Camargo, Philippe Lemey and Simon Joly for resolving problems or giving suggestions. We are grateful to Diogo Provete and an anonymous reviewer for their valuable criticisms that helped to improve the manuscript. We also thank Fernando Silveira for inviting us to submit this paper as a contribution to *OCBIL Theory: A new science for old ecosystems*, a special issue of the *Biological Journal of the Linnean Society*. R.A.B., R.F.M., T.L.P. and F.R.S. are grateful to the Critical Ecosystem Partnership Fund and Instituto Internacional de Educação do Brasil for financial support through the project 'Conservação de *Pithecopus ayeaye*, espécies relacionadas e seus ecossistemas'. We thank FAPEMIG for financial support (grant APQ-01998-17). R.F.M., R.M.M. and T.L.P. thank CNPq/CAPES for their PROTAX fellowships (grant 440665/2015-9). T.L.P. was also supported by a CAPES fellowship (grant 88887.468027/2019-00). P.L. was supported by FAPESP (grant 2014/22344-6) and M.T.T.S. was supported by CAPES fellowships (grants 88881.189822/2018-01 and 88882.434124/2019-01). F.R.S. and P.C.A.G. thank CNPq for their research fellowships. Collection permits were provided by ICMBio/SISBIO (licence 37435-6). The authors declare that there is no conflict of interest.

REFERENCES

Aiello-Lammens ME, **Boria RA**, **Radosavljevic A**, **Vilela B**, **Anderson RP. 2015.** spThin: an R package for spatial thinning of species occurrence records for use in ecological niche models. *Ecography* **38:** 541–545.

Allouche O, **Tsoar A**, **Kadmon R. 2006.** Assessing the accuracy of species distribution models: prevalence, kappa and the true skill statistic (TSS). *Journal of Applied Ecology* **43:** 1223–1232.

Antonelli A, **Kissling WD**, **Flantua SGA**, **Bermúdez MA**, **Mulch A**, **Muellner-Riehl AN**, **Kreft H**, **Linder HP**, **Badgley C**, **Fjeldså J**, **Fritz SA**, **Rahbek C**, **Herman F**, **Hooghiemstra H**, **Hoorn C. 2018.** Geological and climatic influences on mountain biodiversity. *Nature Geosciences* **11:** 718–725.

Araújo MB, **New M. 2007.** Ensemble forecasting of species distributions. *Trends in Ecology and Evolution* **22:** 42–47.

Araújo MB, **Rozenfeld A**, **Rahbek C**, **Marquet PA. 2011.** Using species co-occurrence networks to assess the impacts of climate change. *Ecography* **34:** 897–908.

Baker AJ. 2008. Islands in the sky: the impact of Pleistocene climate cycles on biodiversity. *Journal of Biology* **7:** 32.

Barbosa NPU, **Fernandes GW. 2016.** Rupestrian grassland: past, present and future distribution. In: Fernandes GW, ed. *Ecology and conservation of mountaintop grasslands*

in Brazil. New York: Springer International Publishing, 531–544.

Beerli P. 2006. Comparison of Bayesian and maximum-likelihood inference of population genetic parameters. *Bioinformatics* **22:** 341–345.

Beerli P, **Palczewski M. 2010.** Unified framework to evaluate panmixia and migration direction among multiple sampling locations. *Genetics* **185:** 313–326.

Bell RC, **MacKenzie JB**, **Hickerson MJ**, **Chavarría KL**, **Cunningham M**, **Williams S**, **Moritz C. 2011.** Comparative multi-locus phylogeography confirms multiple vicariance events in co-distributed rainforest frogs. *Proceedings of the Royal Society of London Series B: Biological Sciences* **279:** 991–999.

Bielejec F, **Rambaut A**, **Suchard MA**, **Lemey P. 2011.** SPREAD: spatial phylogenetic reconstruction of evolutionary dynamics. *Bioinformatics* **27:** 2910–2912.

Brandão RA, **Leite FSF**, **Françoso RD**, **Faivovich J. 2012.** *Phyllomedusa megacephala* (Miranda-Ribeiro 1926) (Amphibia, Anura, Hylidae, Phyllomedusinae): distribution extension, new state record and map. *Herpetology Notes* **5:** 535–537.

Brown JL, **Hill DJ**, **Dolan AM**, **Carnaval AC**, **Haywood AM. 2018.** PaleoClim, high spatial resolution paleoclimate surfaces for global land areas. *Scientific Data* **5:** 180254.

Bruen TC, **Philippe H**, **Bryant D. 2006.** A simple and robust statistical test for detecting the presence of recombination. *Genetics* **172:** 2665–2681.

Brunes TO, **Alexandrino J**, **Baêta D**, **Zina J**, **Haddad CFB**, **Sequeira F. 2014.** Species limits, phylogeographic and hybridization patterns in Neotropical leaf frogs (Phyllomedusinae). *Zoologica Scripta* **43:** 586–604.

Bryant D, **Moulton V. 2004.** NeighborNet: an agglomerative algorithm for the construction of planar phylogenetic networks. *Molecular Biology and Evolution* **21:** 255–265.

Carvalho F, **Godoy EL**, **Lisboa FJG**, **Moreira FMS**, **Souza FA**, **Berbara RLL**, **Fernandes GW. 2014.** Relationship between physical and chemical soil attributes and plant species diversity in tropical mountain ecosystems from Brazil. *Journal of Mountain Science* **11:** 875–883.

Chen J, **Luo M**, **Li S**, **Tao M**, **Ye X**, **Duan W**, **Zhang C**, **Qin Q**, **Xiao J**, **Liu S. 2018.** A comparative study of distant hybridization in plants and animals. *Science China Life Sciences* **61:** 285–309.

Crawford AJ. 2003. Huge populations and old species of Costa Rican and Panamanian dirt frogs inferred from mitochondrial and nuclear gene sequences. *Molecular Ecology* **12:** 2525–2540.

Dmitriev DA, **Rakitov RA. 2008.** Decoding of superimposed traces produced by direct sequencing of heterozygous indels. *PLoS Computational Biology* **4:** e1000113.

Dormann CF, **Elith J**, **Bacher S**, **Buchmann C**, **Carl G**, **Carré G**, **Marquéz JRG**, **Gruber B**, **Lafourcarde B**, **Leitão PJ**, **Münkemüller T**, **McClean C**, **Osborne PE**, **Reineking B**, **Schröder B**, **Skidmore AK**, **Zurell D**, **Lautenbach S. 2012.** Collinearity: a review of methods to deal with it and a simulation study evaluating their performance. *Ecography* **36:** 27–46.

Drummond AJ, **Ho SYW**, **Phillips MJ**, **Rambaut A. 2006.** Relaxed phylogenetics and dating with confidence. *PLoS Biology* **4:** e88.

Drummond AJ, **Rambaut A**, **Shapiro B**, **Pybus OG. 2005.** Bayesian coalescent inference of past population dynamics from molecular sequences. *Molecular Biology and Evolution* **22:** 1185–1192.

Drummond AJ, **Suchard MA**, **Xie D**, **Rambaut A. 2012.** Bayesian phylogenetics with BEAUti and the BEAST 1.7. *Molecular Biology and Evolution* **29:** 1969–1973.

Echternacht L, **Trovó M. 2015.** *Paepalanthus serpens*, a new microendemic species of Eriocaulaceae from the Espinhaço Range, Minas Gerais, Brazil. *PhytoKeys* **48:** 43–49.

Edgar RC. 2004. MUSCLE: multiple sequence alignment with high accuracy and high throughput. *Nucleic Acids Research* **32:** 1792–1797.

Elith J, **Ferrier S**, **Huettmann F**, **Leathwick J. 2005.** The evaluation strip: a new and robust method for plotting predicted responses from species distribution models. *Ecological Modelling* **186:** 280–289.

Faivovich J, **Haddad CFB**, **Baêta D**, **Jungfer K**, **Álvares GFR**, **Brandão RA**, **Sheil C**, **Barrientos LS**, **Barrio-Amorós CL**, **Cruz CAG**, **Wheeler WC. 2010.** The phylogenetic relationships of the charismatic poster frogs, Phyllomedusinae (Anura, Hylidae). *Cladistics* **26:** 227–261.

Fernandes GW, **Barbosa NPU**, **Negreiros D**, **Paglia AP. 2014.** Challenges for the conservation of vanishing megadiverse rupestrian grasslands. *Natureza & Conservação* **12:** 162–165.

Fielding AH, **Bell JF. 1997.** A review of methods for the assessment of prediction errors in conservation presence/absence models. *Environmental Conservation* **24:** 38–49.

Fiorini CF, **Miranda MD**, **Silva-Pereira V**, **Barbosa AR**, **Oliveira U**, **Kamino LHY**, **Mota NFO**, **Viana PL**, **Borba EL. 2019.** The phylogeography of *Vellozia auriculata* (Velloziaceae) supports low zygotic gene flow and local population persistence in the campo rupestre, a Neotropical OCBIL. *Botanical Journal of the Linnean Society* **191:** 381–398.

Flantua SGA, **Hooghiemstra H. 2018.** Historical connectivity and mountain biodiversity. In: Hoorn C, Perrigo A, Antonelli A, eds. *Mountains, climate and biodiversity.* Oxford: Wiley Blackwell, 171–186.

Flot JF. 2010. SeqPHASE: A web tool for interconverting PHASE input/output files and FASTA sequence alignments. *Molecular Ecology Resources* **10:** 162–166.

Gonzaga LP, **Carvalhaes AMP**, **Buzzetti DRC. 2007.** A new species of *Formicivora* antwren from the Chapada Diamantina, eastern Brazil (Aves: Passeriformes: Thamnophilidae). *Zootaxa* **1743:** 25–44.

Gray AR. 2011. Notes on hybridization in leaf frogs of the genus *Agalychnis* (Anura, Hylidae, Phyllomedusinae). *arXiv* 1102.4039.

Guedes TB, **Azevedo JAR**, **Bacon CD**, **Provete DB**, **Antonelli A. 2020.** Diversity, endemism, and evolutionary history of montane biotas outside the Andean region. In:

Rull V, Carnaval AC, eds. *Neotropical diversification: patterns and processes*. New York: Springer International Publishing, 299–328.

Haddad CFB, **Pombal Jr JP**, **Batistic RF. 1994.** Natural hybridization between diploid and tetraploid species of leaf-frogs, genus *Phyllomedusa* (Amphibia). *Journal of Herpetology* **28:** 425–430.

Harrison RG, **Larson EL. 2014.** Hybridization, introgression, and the nature of species boundaries. *Journal of Heredity* **105:** 795–809.

Hey J, **Chung Y**, **Sethuruman A**, **Lachance J**, **Tishkoff S**, **Sousa VC**, **Wang Y. 2018.** Phylogeny estimation by integration over isolation with migration models. *Molecular Biology and Evolution* **35:** 2805–2818.

Hijmans RJ. 2020. *raster: geographic data analysis and modeling. Manual. R package version 3.0–12.* Available at: https://CRAN.R-project.org/package=raster.

Hopper SD. 2009. OCBIL theory: towards an integrated understanding of the evolution, ecology and conservation of biodiversity on old, climatically buffered, infertile landscapes. *Plant and Soil* **322:** 49–86.

Hopper SD. 2018. Natural hybridization in the context of Ocbil theory. *South African Journal of Botany* **118:** 284–289.

Hopper SD, **Silveira FAO**, **Fiedler PL. 2016.** Biodiversity hotspots and Ocbil theory. *Plant and Soil* **403:** 167–216.

Huson DH, **Bryant D. 2006.** Application of phylogenetic networks in evolutionary studies. *Molecular Biology and Evolution* **23:** 254–267.

Jiménez-Valverde A. 2012. Insights into the area under the receiver operating characteristic curve (AUC) as a discrimination measure in species distribution modelling. *Global Ecology and Biogeography* **21:** 498–507.

Joly S. 2012. JML: testing hybridization from species trees. *Molecular Ecology Resources* **12:** 179–184.

Joly S. 2017. *JML, version 1.3.1.* Manual. Montréal: Institut de recherche em biologie végétale, Université de Montréal & Montréal Botanical Garden.

Joly S, **Bruneau A. 2006.** Incorporating allelic variation for reconstructing the evolutionary history of organisms from multiple genes: an example from *Rosa* in North America. *Systematic Biology* **55:** 623–636.

Joly S, **Bryant D**, **Lockhart PJ. 2015.** Flexible methods for estimating genetic distances from single nucleotide polymorphisms. *Methods in Ecology and Evolution* **6:** 938–948.

Joly S, **McLenachan PA**, **Lockhart PJ. 2009.** A statistical approach for distinguishing hybridization and incomplete lineage sorting. *The American Naturalist* **174:** E54–E70.

Jones GR. 2019. Divergence estimation in the presence of incomplete lineage sorting and migration. *Systematic Biology* **68:** 19–31.

Kimura M. 1980. A simple method for estimating rate of base substitutions through comparative studies. *Journal of Molecular Evolution* **16:** 111–120.

Kumar S., Stecher G., Li M., Knyaz C., Tamura K. 2018. MEGA X: molecular evolutionary genetic analysis across computing platforms. *Molecular Biology and Evolution* **35:** 1547–1549.

Körner C, **Jetz W**, **Paulsen J**, **Payne D**, **Rudmann-Maurer K**, **Spehn EM. 2017.** A global inventory of mountains for bio-geographical applications. *Alpine Botany* **127:** 1–15.

Kusrini MD, **Lubis MI**, **Endarwin W**, **Yazid M**, **Darmawan B**, **Ul-Hasanah AU**, **Sholihat N**, **Tajalli A**, **Lestari V**, **Utama H**, **Nasir DM**, **Ardiansyah D**, **Rachmadi R. 2017.** Elevation range shift after 40 years: the amphibians of Mount Gede Pangrango National Park revisited. *Biological Conservation* **206:** 75–84.

Lanfear R, **Frandsen PB**, **Wright AM**, **Senfeld T**, **Calcott B. 2017.** PartitionFinder 2: new methods for selecting partitioned models of evolution for molecular and morphological phylogenetic analyses. *Molecular Biology and Evolution* **34:** 772–773.

Larsson A. 2014. AliView: a fast and lightweight alignment viewer and editor for large datasets. *Bioinformatics* **30:** 3276–3278.

Leite FSF, **Juncá FA**, **Eterovick PC. 2008.** Status do conhecimento, endemismo e conservação de anfíbios anuros da Cadeia do Espinhaço, Brasil. *Megadiversidade* **4:** 158–176.

Lemey P, **Rambaut A**, **Welch JJ**, **Suchard MA. 2010.** Phylogeography takes a relaxed random walk in continuous space and time. *Molecular Biology and Evolution* **27:** 1877–1885.

Lisiecki EL, **Raymo ME. 2005.** A Pliocene–Pleistocene stack of 57 globally distributed benthic $\delta^{18}O$ records. *Paleoceanography* **20:** PA1003.

Liu C, **White M**, **Newell G. 2011.** Measuring and comparing the accuracy of species distribution models with presence-absence data. *Ecography* **34:** 232–243.

Magalhães RF, **Gorgulho HF**, **Campello S**, **Domingos F**, **Freire I**, **Oswald CB**, **Santos DF**, **Pezzuti TL**, **Santos FR**, **Lemes P**, **Strüssmann C**, **Coelho ME**, **Colli GR**, **del Prette AC**, **Vasconcelos B**, **Brandão RA. 2020.** Conserving the poorly known and threatened monkey-frogs of the Brazilian Cerrado highlands. *Oryx* **54:** 440–441.

Magalhães RF, **Lemes P**, **Camargo A**, **Oliveira U**, **Brandão RA**, **Thomassen H**, **Garcia PCA**, **Leite FSF**, **Santos FR. 2017.** Evolutionarily significant units of the critically endangered leaf frog *Pithecopus ayeaye* (Anura, Phyllomedusidae) are not effectively preserved by the Brazilian protected areas network. *Ecology and Evolution* **7:** 8812–8828.

McCormack JE, **Huang H**, **Knowles LL. 2009.** Sky islands. In: Gillespie RG, Clague D, eds. *Encyclopedia of islands*. Berkeley: University of California Press, 839–843.

Miller MA, **Pfeiffer W**, **Schwartz T. 2010.** Creating the CIPRES Science Gateway for inference of large phylogenetic trees. *Proceedings of the Gateway Computing Environments Workshop* **2010:** 1–8.

Murray K, **Conner MM. 2009.** Methods to quantify variable importance: implications for the analysis of noisy ecological data. *Ecology* **90:** 348–355.

Naimi B, **Araújo MG. 2016.** sdm: a reproducible and extensible R platform for species distribution modelling. *Ecography* **39:** 368–375.

Naimi B, **Hamm NA**, **Groen TA**, **Skidmore AK**, **Toxopeus AG. 2014.** Where is position uncertainty a problem for species distribution modelling? *Ecography* **37:** 191–203.

Nali RC, **Borges MM**, **Prado CPA. 2015.** Advertisement and release calls of *Phyllomedusa ayeaye* (Anura: Hylidae) with comments on the social context of emission. *Zoologia* **32:** 263–269.

Nascimento AC, **Chaves AV**, **Leite FSF**, **Eterovick PC**, **Santos FR. 2018.** Past vicariance promoting deep genetic divergence in an endemic frog species of the Espinhaço Range in Brazil: the historical biogeography of *Bokermannohyla Saxicola* (Hylidae). *PLoS ONE* **13:** e0206723.

Oliveira FFR. 2017. Mating behaviour, territoriality and natural history notes of *Phyllomedusa ayeaye* Lutz, 1966 (Hylidae, Phyllomedusinae) in south-eastern Brazil. *Journal of Natural History* **51:** 657–675.

Oliveira FFR, **Nogueira PAG**, **Eterovick PC. 2012.** Natural history of *Phyllomedusa megacephala* (Miranda-Ribeiro, 1926) (Anura: Hylidae) in southeastern Brazil, with descriptions of its breeding biology and male territorial behaviour. *Journal of Natural History* **46:** 117–129.

Pardiñas UFJ, **Lessa G**, **Teta P**, **Salazar-Bravo J**, **Câmara EMVC. 2014.** A new genus of sigmodontinae rodent from eastern Brazil and the origin of the tribe Phyllotini. *Journal of Mammalogy* **95:** 201–215.

Perrigo A, **Hoorn C**, **Antonelli A. 2020.** Why mountains matter for biodiversity. *Journal of Biogeography* **47:** 315–325.

Peterson AT, **Soberón J. 2012.** Species distribution modeling and ecological niche modeling: getting the concepts right. *Natureza & Conservação* **10:** 102–107.

Polato NR, **Gill BA**, **Shah AA**, **Gray MM**, **Casner KL**, **Barthelet A**, **Messer PW**, **Simmons MP**, **Guayasamin JM**, **Encalada AC**, **Kondratieff BC**, **Flecker AS**, **Thomas SA**, **Ghalambor CK**, **Poff NL**, **Funk WC**, **Zamudio KR. 2018.** Narrow thermal tolerance and low dispersal drive higher speciation in tropical mountains. *Proceedings of the National Academy of Sciences of the United States of America* **115:** 12471–12476.

Prychitko TM, **Moore WS. 1997.** The utility of DNA sequences of an intron from the β-fibrinogen gene in phylogenetic analysis of woodpeckers (Aves: Picidae). *Molecular Phylogenetics and Evolution* **8:** 193–204.

R Core Team. **2020.** *R: a language and environment for statistical computing*. Vienna: R Foundation for Statistical Computing. Available at: https://www.r-project.org/.

Rambaut A, **Drummond AJ**, **Xie D**, **Baele G**, **Suchard MA. 2018.** Posterior summarization in Bayesian phylogenetics using Tracer 1.7. *Systematic Biology* **67:** 901–904.

Ramos EKS, **Magalhães RF**, **Marques NCS**, **Baêta D**, **Garcia PCA**, **Santos FR. 2019.** Cryptic diversity in Brazilian endemic monkey frogs (Hylidae, Phyllomedusinae, *Pithecopus*) revealed by multispecies coalescent and integrative approaches. *Molecular Phylogenetics and Evolution* **132:** 105–116.

Ramos EKS, **Magalhães RF**, **Sari EHR**, **Rosa AHB**, **Garcia PCA**, **Santos FR. 2018.** Population genetics and distribution data reveal conservation concerns to the sky island endemic *Pithecopus megacephalus* (Anura, Phyllomedusidae). *Conservation Genetics* **19:** 99–110.

Rozas J, **Ferrer-Mata A**, **Sánchez-DelBarrio JC**, **Guirao-Rico S**, **Librado P**, **Ramos-Onsins SE**, **Sánchez-Gracia A. 2017.** DnaSP 6: DNA sequence polymorphism analysis of large data sets. *Molecular Biology and Evolution* **34:** 3299–3302.

Salzburger W, **Ewing GB**, **von Haeseler A. 2011.** The performance of phylogenetic algorithms in estimating haplotype genealogies with migration. *Molecular Ecology* **20:** 1952–1963.

Santos MTT, **Magalhães RF**, **Ferreira RB**, **Vittorazzi SE**, **Dias IR**, **Leite FSF**, **Lourenço LB**, **Santos FR**, **Haddad CFB**, **Garcia PCA. 2020a.** Systematic revision of the rare bromeligenous genus *Crossodactylodes* Cochran 1938 (Anura: Leptodactylidae: Paratelmatobiinae). *Herpetological Monographs* **34:** 1–38.

Santos MTT, **Magalhães RF**, **Lyra ML**, **Santos FR**, **Zaher H**, **Giasson LOM**, **Garcia PCA**, **Carnaval AC**, **Haddad CFB. 2020b.** Multilocus phylogeny of Paratelmatobiinae (Anura: Leptodactylidae) reveals strong spatial structure and previously unknown diversity in the Atlantic Forest hotspot. *Molecular Phylogenetics and Evolution* **148:** 106819.

Silva ET, **Peixoto MAA**, **Leite FSF**, **Feio RN**, **Garcia PCA. 2018.** Anuran distribution in a highly diverse region of the Atlantic Forest: the Mantiqueira mountain range in Southeastern Brazil. *Herpetologica* **74:** 294–305.

Silva GAR, **Khan G**, **Ribeiro-Silva S**, **Aona LYS**, **Machado MC**, **Bonatelli IAS**, **Moraes EM. 2020.** Extreme genetic structure in a relict cactus genus from *campo rupestre* landscapes: implications for conservation. *Biodiversity and Conservation* **29:** 1263–1281.

Silveira FAO, **Dayrell RLC**, **Fiorini CF**, **Negreiros D**, **Borba EL. 2020.** Diversification in ancient and nutrient-poor neotropical ecosystems: how geological and climatic buffering shaped plant diversity in some of the world's neglected hotspots. In: Rull V, Carnaval AC, eds. *Neotropical diversification: patterns and processes*. New York: Springer International Publishing, 329–368.

Silveira FAO, **Negreiros D**, **Barbosa NPU**, **Buisson E**, **Carmo FF**, **Carstensen DW**, **Conceição AA**, **Cornelissen TG**, **Echternacht L**, **Fernandes GW**, **Garcia QS**, **Guerra TJ**, **Jacobi CM**, **Lemos-Filho JP**, **Le Stradic S**, **Morellato LPC**, **Neves FS**, **Oliveira RS**, **Schaefer CE**, **Viana PL**, **Lambers H. 2016.** Ecology and evolution of plant diversity in the endangered *campo rupestre*: a neglected conservation priority. *Plant and Soil* **403:** 129–152.

Smith MA, **Green DM. 2005.** Dispersal and the metapopulation paradigm in amphibian ecology and conservation: are all amphibian populations metapopulations? *Ecography* **28:** 110–128.

Smith SA, **Arif S**, **de Oca ANM**, **Wiens JJ. 2007.** A phylogenetic hot spot for evolutionary novelty in Middle American treefrogs. *Evolution* **61:** 2075–2085.

Stamatakis A. 2014. RAxML version 8: a tool for phylogenetic analysis and post-analysis of large phylogenies. *Bioinformatics* **30:** 1312–1313.

Stamatakis A, **Blagojevic F**, **Nikolopoulos DS**, **Antonopoulos CD. 2007.** Exploring new search algorithms and hardware for phylogenetics: RAxML meets the IBM cell. *The Journal of VLSI Signal Processing Systems for Signal, Image, and Video Technology* **48:** 271–286.

Stephens M, **Smith NJ**, **Donnelly P. 2001.** A new statistical method for haplotype reconstruction from population data. *The American Journal of Human Genetics* **68:** 978–989.

Suchard MA, **Lemey P**, **Baele G**, **Ayres DL**, **Drummond AJ**, **Rambaut A. 2018.** Bayesian phylogenetic and phylodynamic data integration using BEAST 1.10. *Virus Evolution* **4:** vey016.

Swets JA. 1988. Measuring the accuracy of diagnostic systems. *Science* **240:** 1285–1293.

Tajima F. 1989. Statistical method for testing the neutral mutation hypothesis by DNA polymorphism. *Genetics* **123:** 585–595.

Versieux LM, **Louzada RB**, **Viana PL**, **Mota N**, **Wanderley MGL. 2010.** An illustrated checklist of Bromeliaceae from Parque Estadual do Rio Preto, Minas Gerais, Brazil, with notes on phytogeography and one new species of *Cryptanthus*. *Phytotaxa* **10:** 1–16.

Vidal JD, **Souza AP**, **Koch I. Jr 2019.** Impacts of landscape composition, marginality of distribution, soil fertility and climatic stability on the patterns of woody plant endemism in the Cerrado. *Global Ecology and Biogeography* **28:** 904–916.

Werneck FP, **Nogueira C**, **Colli GR**, **Sites Jr JW**, **Costa GC. 2012.** Climatic stability in the Brazilian Cerrado: implications for biogeographical connections of South American savannas, species richness and conservation in a biodiversity hotspot. *Journal of Biogeography* **39:** 1695–1706.

Wiens JJ, **Fetzner JW**, **Parkinson CL**, **Reeder TW. 2005.** Hylid frog phylogeny and sampling strategies for speciose clades. *Systematic Biology* **54:** 778–807.

Zhang C, **Ogilvie HA**, **Drummond AJ**, **Stadler T. 2017.** Bayesian inference of species networks from multilocus sequence data. *Molecular Biology and Evolution* **35:** 504–517.

Zuur AF, **Ieno EN**, **Elphick CS. 2010.** A protocol for data exploration to avoid common statistical problems. *Methods in Ecology and Evolution* **1:** 3–14.

SUPPORTING INFORMATION

Additional Supporting Information may be found in the online version of this article at the publisher's website:

Table S1. Vouchers, geographical data and GenBank accession numbers for sequences used in the study.
Table S2. Occurrence points of *Pithecopus ayeaye* and *P. megacephalus* used in the ecological niche modelling. The novel records were obtained from field expeditions reported by Magalhães *et al.* (2020).
Table S3. MIGRATE-N distribution of parameters θ and *M* for the best model (i.e. unidirectional gene flow from *Pithecopus megacephalus* to *P. ayeaye*, Table 2). The percentages represent the quantiles of the 95% HPD.
Table S4. Model performance (accuracy) metrics given the observed and predicted values for *Pithecopus* species. AUC = area under the curve of the receiver operating characteristic; TSS = true skill statistic.
Figure S1. Relative importance and response curve for each predictor variable used to fit the ENM of *Pithecopus ayeaye* (A), and *P. megacephalus* (B). Bioclimatic variables evaluated were annual mean temperature (BIO1), temperature seasonality (BIO4), mean temperature of the wettest quarter (BIO8), mean temperature of the driest quarter (BIO9)***, mean temperature of the warmest quarter (BIO10), mean temperature of the coldest quarter (BIO11), annual precipitation (BIO12), precipitation of the wettest month (BIO13)**, precipitation of the driest month (BIO14)***, precipitation seasonality (BIO15), precipitation of the wettest quarter (BIO16)*, precipitation of the driest quarter (BIO17), precipitation of the warmest quarter (BIO18)***, precipitation of the coldest quarter (BIO19). Variables that show VIF < 10 for *P. ayeaye* (*), *P. megacephalus* (**) or for both species (***).
Figure S2. Potential distribution of *Pithecopus ayeaye* (A) and *P. megacephalus* (B) for both present and past climate conditions. Grey borders indicate limits of the *campo rupestre* (modified from Fernandes *et al.*, 2014).
Supplementary File 1. Spatial projection of the diffusion pattern through time, based on the maximum clade credibility (MCC) tree estimated with the Cauchy relaxed random walk.

SHARED DATA

The sequences are available in GenBank (accession numbers in Table S1). Occurrence records are available in Table S2. Post-processed data and raw results are available upon request.